# LATE PRECAMBRIAN AND CAMBRIAN CARBONATES OF THE ADELAIDEAN IN THE FLINDERS RANGES, SOUTH AUSTRALIA - A PETROGRAPHIC, ELECTRON MICROPROBE AND STABLE ISOTOPE STUDY

by

UPDESH SINGH

DEPARTMENT OF GEOLOGY AND GEOPHYSICS

UNIVERSITY OF ADELAIDE

Thesis submitted to the University of Adelaide
in fulfilment of the requirements for the
degree of Doctor of Philosophy

DECEMBER 1986

This thesis contains no material that has been accepted for the award of any other degree or diploma in any University and, to the best of my knowledge and belief, it contains no material previously written or published by another person or persons except where due reference is made in the text. I consent to this thesis being made available for photocopying and loan if applicable if accepted for the award of the degree.

## ACKNOWLEDGEMENT

facilities is acknowledged.

I am especially indebted to my parents for their support, patience and understanding and for making it all possible and to Pam for the companionship and motivation.

# ABSTRACT

A detailed study of the petrography, trace element chemistry and stable isotope composition was carried out on the Sturtian (Balcanoona Formation), Marinoan (Trezona Formation) and Ediacaran (Wonoka Formation) and the early Cambrian (Wilkawillina Limestone) units of the Adelaidean in the Flinders Ranges. Detailed petrographic study of the oolite units from these formations showsthat ooids with definite aragonite replacement textures occur in both the Late Precambrian and Early Cambrian units. These include neomorphic spar ooids, brick-texture ooids and ooid molds. Evidence for possible bimineralic ooids, i.e. with aragonitic and calcitic cortical layers, is present in all the units studied and include half-moon ooid fabrics and ooids with eccentrically displaced nucleii. Ooids with calcitic precursor mineralogy,i.e. radial calcite ooids, only appear in the Early Cambrian oolites. Micritic ooids are ubiquitous and their precursor mineralogy is difficult to interpret. Very large ooid sizes (maximum diameter, 16mm) are recorded from the Marinoan Trezona Formation.

Electron microprobe analyses recorded unusually high Sr concentrations (1000-4500 ppm Sr) in some ooids and cements from the Late Precambrian units. Some of the cements occur as blocky interparticle cements in ooid grainstones associated with calcitized ooids. Others occur as blocky calcite mosaics within sparry laminae of stromatolites or laminated limestones. Most of these strontium rich blocky calcite cements do not have the classical calcitization fabrics and their genesis remains uncertain. Some of these strontium rich cements, termed

poikilotopic cements, have neomorphic fabrics and could represent calcitized products.

Strontium isotope analysis of the Trezona Formation obtained a low marine 87Sr/86Sr ratio of 0.7071, while the 87Sr/86Sr ratio of the early Cambrian Wilkawillina Limestone ranged from 0.7085 to 0.7093.

The carbon isotope signature within each of the above units had a large scatter. However, there was a real and significant difference in the carbon signatures of some of the units. Carbon isotope analyses indicate a heavy carbon signature in the Sturtian Balcanoona Formation with a decrease to small positive or negative values in the Marinoan, Ediacaran and Early Cambrian. This carbon shift is broadly correlated with those recorded from other Late Proterozoic carbonate sequences. Depleted carbon signatures were recorded from the Marinoan and Early Cambrian diagenetic components. The Sturtian-Marinoan carbon isotope shift may have been due to glacially induced changes in oxygenation levels, causing changes in the Corg/Ccarb ratio. Unlike the carbon isotopes, oxygen isotopes of the Late Precambrian and Early Cambrian units studied had a more or less constant range of values and did not reveal any discernible trend.

The Precambrian-Cambrian boundary in this study did not record any significant changes apart from the appearance of definite calcitic precursors in the early Cambrian. A major change in the stable isotope chemistry of shallow marine environments appears to have occurred in the late Precambrian as revealed by carbon isotope profiles from this and previous studies.

# TABLE OF CONTENTS

## CHAPTER THREE: LATE PRECAMBRIAN BALCANOONA FORMATION

## CHAPTER FOUR: LATE PRECAMBRIAN WONOKA FORMATION

## CHAPTER FIVE: EARLY CAMBRIAN WILKAWILLINA LIMESTONE

PAGE PROOFS OF PUBLICATION

# LIST OF FIGURES

# CHAPTER ONE

## INTRODUCTION, AIMS AND METHODOLOGY

### 1.1: INTRODUCTION AND AIMS

The Precambrian-Cambrian boundary marks a major transition in geological history recording a change in the earth's biosphere with the advent of skeletal organisms where previously only soft-bodied and algal bacterial forms existed. This biotic "explosion" is well represented in the carbonate rock record with the appearance of archeocyathids at the base of the Cambrian. Skeletalization also brought about a change in the pattern of physical sedimentation and facies associations.

Compared to the large data base provided by numerous studies of Phanerozoic limestones, very little is known about Precambrian limestones. Part of the reason for this is due to the lack of preserved Precambrian limestones, since the majority of carbonates in the Precambrian are dolomites. The need to better understand Precambrian carbonate environments has gained impetus with the appearance of studies suggesting changes in carbonate environments and mineralogy through the Phanerozoic [ Sandberg 1983; Mackenzie and Piggot 1981 ]. In addition, recent research has recorded changes in carbon isotope trends across the Precambrian-Cambrian transition [ Tucker 1986; Magaritz 1986; Knoll et al.1986 ]. These changes in carbonate environments and the isotopic record have been attributed to plate tectonically induced changes in the atmosphere/hydrosphere, climatic changes, and to evolution of new biota.

It had been widely accepted that the abundant aragonite in Holocene sediments has mirrored the formation of

1

carbonates in the geological past. Beginning with Sandberg [1975] these conventional ideas have increasingly been questioned. His work suggested that carbonate mineralogy through geologic time may not have remained constant and he concluded that Paleozoic non-skeletal carbonates were mainly calcitic, and that aragonite became abundant only in the Cenozoic. Later work by Mackenzie and Piggot [1981] showed essentially similar trends. There was however, disagreement on the placement of the transition from calcite dominance to aragonite dominance. Sandberg [1975] placed the transition during the early to middle Cenozoic, whereas Mackenzie and Piggot [1981] placed it during the Carboniferous. However, later work by Sandberg [1983] has suggested a cycle of varying carbonate mineralogies through the Phanerozoic.

Recent studies suggest the coexistence of aragonite and calcite non-skeletal components during deposition of ancient carbonates. Studies by James and Klappa [1983], Sandberg [1983], Rich [1982], Wilkinson, Buczynski and Owen [1984], Grotzinger and Read [1983] and Tucker [1984] have put forth evidence for the coprecipitation of aragonite and calcite components during carbonate deposition of Precambrian (midProterozoic), Cambrian, Mississippian,and Pennsylvanian age.

Numerous studies have recorded changes in the oxygen and carbon isotopic compositions of the carbonates as well as in the mineralogy of the precursors [ Veizer and Hoefs 1976 ; Sandberg 1983 ]. The carbon isotope record shows a shift towards heavier values at the Precambrian-Cambrian boundary and carbonates with abnormally heavy carbon isotope compositions have been documented from some Precambrian

2

sequences [Veizer and Hoefs 1976; Schidlowski et al.1975 ]. The predominance of fine-grained "primary" dolomite in the Precambrian has prompted suggestions of differences in chemistry of those times from that of modern marine waters [ Tucker 1982 ]. Most isotopic studies have concentrated on the Phanerozoic carbonate record with comparatively little information being available from the Precambrian. It was therefore decided to investigate a section through the Precambrian-Cambrian boundary for possible changes in the nature of carbonate mineralogy as well as record any carbon and oxygen isotope trends.

The Precambrian carbonates investigated commonly comprise ooids, stromatolites, intraclasts and micrites. Stromatolites have been extensively studied in the Precambrian as aids to environmental interpretations and in stratigraphic correlations [ Walter 1976; Preiss 1977]. In the course of the present study the environmental significance of the microstructure of some of the stromatolites (in the Trezona Formation ) was investigated. Since the macrostructure of the stromatolites is largely a reflection of the environment, it was argued that specific environments would have certain specific blue-green algae and bacteria which would generate distinct microstructures. However, the distinction between the original microstructure and the diagenetic overprint was hard to resolve with the techniques at hand.

The study of intraclasts and micrites has been largely ignored and overlooked mainly because they are seemingly homogeneous and textureless under light microscopy and therefore little understood.  Lasemi and Sandberg [1980]

provide an insight into what can be achieved by SEM studies of micrites, and highlight the possibility of their increased use in future work.

The study of ooids has been increasingly popular in the past few years and has provided the basis for some of the secular trends recognised in the Phanerozoic [ Sandberg 1983 ; Mackenzie and Piggot 1981 ]. In comparision, Precambrian ooids have been relatively neglected, with only a few studies involved in documenting fabric details [ Radwanski and Berkenmajer 1977; Tucker 1983; 1984 ]. With the absence of skeletal components in the Precambrian, ooids provide important elements with which to study Precambrian marine chemistry and precursor mineralogy. Also, the large amount of data provided by Phanerozoic ooid studies serves as a valuable source of information with which to compare Precambrian ooids.

One of the aims of this thesis is to decipher the precursor carbonate mineralogy of some late Precambrian and early Cambrian marine limestones by means of detailed petrographic and geochemical analyses. The geochemical analysis involved trace element determination under the electron microprobe in addition to oxygen and carbon isotope and strontium isotope analysis. A further aim is to enhance our understanding of global marine evolution by a study of the oxygen and carbon isotope composition of the carbonates and comparing them with those of other studies. The present study focuses on a section of Late Precambrian and early Cambrian carbonates of the Flinders Ranges in South Australia and specifically on their oolitic units. These carbonates are relatively unmetamorphosed and provide a rare opportunity for

4

investigating the nature of carbonate precipitation across this crucial part of geological history. There are few areas in the world where Precambrian limestones are preserved. The present study is significant for two reasons. Firstly, it looks at a section of ancient oolitic carbonates from which, compared to Phanerozoic ooids, very little is known. Secondly, it is the first such study of an Australian Precambrian carbonate sequence and should add to our understanding of Precambrian carbonate environments and in the reconstruction of global evolution and environmental history.

## 1.2: LOCAL STRATIGRAPHY AND GEOLOGICAL SETTING

Sprigg [ 1952 ] first used the term " Adelaide Geosyncline " for the thick sequence of Late Proterozoic and Cambrian sediments lying to the east of the Sturt Shelf and separated from it by the Torrens Hinge zone [ Thomson 1969;1970 ] (Fig.1.1). These sediments may have been continuous with the Amadeus and Officer basins of central Australia  They were deformed by the Cambro-Ordovician Delamerian orogeny. The tectonics of sedimentation with regard to the plate tectonics model is improperly understood and various ideas have been proposed. These vary from it being a miogeosynclinal wedge across a passive plate margin [ Sprigg 1952 ], an aulacogene [ Rutland 1973; Scheibner 1973 ] or the result of rifting and drifting during the Cambrian [ Veevers and McElhinny 1976 ]. Penecontemporaneous faulting and diapirism has had a strong local influence on sedimentation [ Coats 1965; Lemon 1985 ].

The Adelaidean sediments were originally divided into

four major stratigraphic units; the Willouran, Torrensian, Sturtian and Marinoan [ Mawson and Sprigg 1950; Sprigg 1952 ]. A further lithostratigraphic subdivision of the sequence was proposed by Thomson et el. [1964]. The various subdivisions of the units and their occurrence and relationships are shown in Figure 1.2 together with the carbonate units that were included in this study, namely the Late Precambrian Balcanoona, Trezona and Wonoka Formations and the early Cambrian Wilkawillina Limestone of the Hawker Group. This stratigraphic subdivision was recently updated and a new division added, the Ediacaran, representing the terminal stage of Late Precambrian sedimentation [ Jenkins 1981 ]. Figure 1.3 shows this updated division of the Adelaidean sequence.

Geochronological data on the Adelaidean is rather scarce and inconclusive. Based on stromatolite biostratigraphy, a broad correlation was made with the Riphean and Vendian of the USSR [ Preiss 1977 ]. The Willouran and Torrensian stromatolites correlate with Early and Mid-Riphean forms respectively. The Sturtian and Marinoan stromatolites are close to the Riphean-Vendian boundary. Accurate and reliable radiometric dates have been difficult to obtain due to lack of datable samples, uncertain basement-cover relationships and overprinting by orogenic events [ Webb et al. 1983 ]. Compston et al. [1966] and Cooper [1975] obtained Rb-Sr ages of 830 Ma for the Willouran Wooltana volcanics although these have been correlated with the 1300 Ma Roopena volcanics of the Sturt Shelf [ Thomson 1966 ]. Recently obtained single and multiple grain U-Pb dates indicate an age of 802 ±10 Ma for the Early Adelaidean Rook Tuff of the Willouran Ranges [

Fanning et al. 1986 ]. This age is in broad agreement with
Rb-Sr total rock age for the Wooltana volcanics [ op. cit. ].
Mason et al. [1978] correlated the Wooltana volcanics to the
Beda volcanics which have given ages of 1076 ±34 Ma [ Thomson
1980 ]. The age of the pre-Torrensian basement is 849 ±31 Ma
[ Cooper and Compston 1971 ]. With the present data it is
probable that the Adelaidean sedimentation commenced between
1100 and 800 Ma ago with platform sedimentation in the Stuart
Shelf being initiated prior to sedimentation in the Adelaide
Geosyncline [ Rutland 1977 ].

## 1.3: METHODOLOGY

The study of carbonates and their diagenesis has
undergone some significant changes with the development of
new techniques and concepts over the years. From the
conventional textural studies using light microscopes,
increasing use is being made of geochemical data in the form
of trace element, stable isotope and fluid inclusion
analysis. They are used as complimentary studies in an
integrated approach to the study of carbonates and their
diagenesis.

Whole rock analysis can serve as a source of basic data
but is frequently inadequate in providing answers about the
genesis of particular components and their diagenetic
history. The secular trends of carbon and oxygen isotopes
obtained by whole rock analysis have a large error limit and
mainly indicate broad or gross perturbations in geologic
history [ Keith and Weber 1964; Veizer 1976 ]. Such data is a
composite of both primary and secondary signatures. Further
refinement of the data is required to pick out the primary or
original compositions. This can only be done by sampling

individual components. Only by understanding the diagenetic trends and history of a sample can one hope to obtain information pertaining to it's original or precursor state. In the present study, textural data from petrographic studies have been integrated with geochemical data from trace element studies. The petrographic textures form the basis for the interpretations with the geochemical data being used to provide constraints on the types of diagenetic changes that took place. By itself geochemical data can be inconclusive, but in combination with textural data it can be crucial in understanding the nature of precursors and the chemistry of past environments.

Calcitic components, being relatively stable, retain their original fabrics during diagenesis. Metastable aragonitic components fail to retain any original fabrics during their transformation to stable calcite. Based on the diagenesis of skeletal and non-skeletal aragonitic components, a set of criteria has developed for evaluating original aragonitic mineralogy [Sandberg 1985]. This includes the presence of coarse (relative to original aragonite) calcite mosaics irregularly cross-cutting original structure and containing relic inclusions, presence of aragonite relics, brownish nature of replacement spar and elevated Sr content of replacement calcites. High-Mg calcite and low-Mg calcite components generally display little change during diagenesis, apart from possible increase in size or loss of Mg. However, recent studies have shown that aragonite has the same solubility as calcite with 12.5 mole % $MgCO_3$ [Walter 1985]. The study by Walter [1985] also showed that under certain diagenetic settings, the microstructure can override

8

the mineralogy and aragonite dissolution can precede the less stable Mg-calcite. Evaluation of original ooid mineralogy based purely on fabric criteria is therefore fraught with uncertainty. A combination of fabric and geochemical data can make this task a little easier.

Chemical diagenetic trends in carbonates have been the subject of a number of studies over the years [eg Pingitore 1976;1978; Brand & Veizer 1980]. Based on the above cited studies, it is found that Sr and Na concentrations decrease and Mn and Fe concentrations increase with increasing diagenetic modification. Mg can increase or decrease depending on the precursor mineral. Magnesium concentration of high Mg-calcite precursors decreases with increasing diagenesis. In spite of diagenesis, carbonate components can still retain some of their original geochemical signatures. This heterogenous distribution of trace elements amongst the various components is used as an aid in evaluating diagenetic history and precursor mineralogy.

1.3.1: TEXTURAL ANALYSIS

The range of textures displayed by marine carbonates is very large [ Bathurst 1975; Bricker 1971 ]. Since the dominant minerals in modern marine carbonates are either aragonite or Mg calcite, the diversity of textures present must indicate a strong environmental control aside from the mineralogical control. In fact, in fossil carbonates the metastable aragonite and Mg calcite reverts to calcite and the dominant mineralogy is therefore only calcite. Dolomite does exists in limestone sequences, normally as a late diagenetic component, but it's textures and genesis are

beyond the scope of the present study.

The type of textures that result and the nature of transformation during the diagenesis of a limestone are dependent on the precursor mineralogy and the diagenetic environment. Through the increasing number of studies on diagenesis of ooids and cements, attempts have been made to relate the textures to it's precursor mineralogy. Until recently, all fossil ooids were considered to have had an aragonite precursor. This was based on modern correlatives of the ooids, which were aragonitic. It was therefore assumed that the nature of carbonate precipitation had not changed, at least since the Phanerozoic.

Since the appearance of Sandberg's [1975] landmark paper on ooids, there has been a change in this type of thinking. Other studies have appeared that indicate that indeed there have occurred changes in carbonate precipitation through geologic history [ Mackenzie and Piggot 1981; Sandberg 1983 ]. Sorby [ 1879 ] put forth evidence for primary precipitation of radial ooids almost 100 years before Sandberg [1975]. The nature of the precursor is therefore evaluated on more secure textural evidence rather than on modern analogy. Such studies have exposed some of the limitations of modern examples as ancient analogues.

ARAGONITE REPLACEMENT

The reevalution of knowledge on ooid and cement genesis has resulted in the establishment of certain criteria for recognition of ancient aragonites [ Fig.1.4 and Sandberg 1985 ]. The major distinguishing feature of aragonite-calcite transformation is the textural and optic disruption that occurs. Since the transformation involves a change in crystal

10

habit from orthorhombic aragonite to hexagonal calcite, the process has to completely breakdown the aragonite crystal and rebuild a calcite crystal. This transformation of aragonite to diagenetic calcite takes place by dissolution-reprecipitation events along reaction zones variously named thin-films, chalky zones [ Pingitore 1976 ], or messenger-films [ Brand and Veizer 1980; Katz and Matthews 1977 ].

The alteration of an aragonite ooid can occur either by complete dissolution and void formation, subsequently being filled by sparry calcite, or by calcitization. In the latter process, the resulting calcite is neomorphic in origin and may have relics of the precursor aragonite preserved. Both the above alterations involve a " wet " transformation, with dissolution and reprecipitation events, and differ only in the scale of the intervening void. They could therefore be viewed as part of a continuum involving the transformation of aragonite to diagenetic calcite. The factors that favour one process over the other and the type of diagenetic environment neeeded are not clearly understood. Calcitization of aragonite can apparently occur in near surface meteoric environments, in burial conditions [ Sandberg and Hudson 1983 ], in rocks with low permeability as well as in porous grainstones [Sandberg 1985].

Therefore, while one may be able to reasonably interpret an aragonite precursor based on fabrics, it is difficult to get an insight into the type of diagenetic environment based solely on textures. It appears that the fabrics of aragonite transformations are process controlled rather than environment controlled [ Sandberg and Hudson 1983,p.887 ]. Pingitore [ 1976 ] observed two modes of alteration of

aragonite corals. The vadose environment produced fabric selective alteration with small crystal sizes involving dissolution-reprecipitation along thin-film fronts. The phreatic transformation produced poor preservation of original fabrics, with a cross-cutting mosaic of crystals involving alteration along broader chalky reaction fronts.

Increasing evidence from carbonate diagenetic work has shown that undolomitized limestones do not undergo repeated dissolution-reprecipitation [ Sandberg 1983; Hudson 1977; Hudson and Coleman 1978 ]. Once a stable diagenetic calcite phase is precipitated little transformation or alteration occurs. The presence of aragonite relics in fossil limestones of Jurassic age within coarse neomorphic calcites suggest that the aragonite-calcite transformation was probably a rapid one-step process [ Sandberg and Hudson 1983 ]. Supporting evidence in the form of stable isotope and trace element compositions is further proof of the validity of such an interpretation [Hudson and Coleman 1978; Walls et al.1979].

## MG-CALCITE REPLACEMENT

In contrast to aragonite replacement, Mg calcite replacement is essentially less disruptive on the original precursor fabrics and largely involves loss of magnesium and crystal enlargement [Steinen 1978; Towe and Hemleben 1976]. The transformation preserves optic orientation and any textural modification is hard to detect under light microscopes [Friedman 1964; Schneidermann 1970; Sandberg 1975]. Until recently it was thought that Mg calcite had a greater solubility than aragonite in dilute waters. Walter [ 1985 ] has shown however, that in normal diagenetic pore-

12

waters, the solubility can be strongly controlled by the microstructure rather than the mineralogy. Therefore an interpretation of precursor mineralogy cannot be made based on the timing of dissolution textures during early diagenesis. Ooid molds occupied by void-filling calcite cements could indicate either an aragonite or Mg calcite precursor [ Sandberg 1983 ]. Definite aragonite replacement textures have to be found to make a proper interpretation. The converse is not necessarily true, i.e. the absence of aragonite replacement textures does not preclude an aragonite precursor.

Fibrous calcites have been the focus of numerous studies on carbonate diagenesis [ see Mazzullo 1980 for brief review ]. Inspite of this there remains a number of uncertainties regarding precursor mineralogy and replacement processes. In some studies it was possible to interpret the precursor with some reliability based on stable isotopes and trace element compositions, and on microdolomite inclusions [ Davies 1977; Lohmann and Meyers 1977 ]. Radiaxial fibrous calcites ( RFC ) and fascicular optic calcites ( FOC ) have received particular attention as replacements of marine acicular cements [ Kendall and Tucker 1973; Kendall 1977 ]. The precursor mineralogy of RFC and FOC remained uncertain and suggestions of possible aragonite and Mg calcite precursors were made based on recent analogues. However, with present day reevaluation of aragonite diagenesis and an understanding of it's replacement textures, the evidence indicates that RFC and FOC are probably original precipitates [ Kendall 1985; Sandberg 1985 ].

13

## 1.3.2: TRACE ELEMENT ANALYSIS

The application of minor element concentrations in the study of carbonate diagenesis is a relatively new field. Although being increasingly used nowadays, especially as a complimentary tool to textural and stable isotopic studies, there remains a lack of understanding of it's basic principles and theoretical concepts. Admittedly, trace element data viewed in isolation does not provide solutions to diagenetic problems. It is used mainly as a complementary tool to the better understood textural studies. A summary of the theoretical concepts and results of empirical studies will be outlined below. A good outline of it's basic principals and examples of it's application is found in Veizer [ 1983 ].

The mineralogy of the carbonate controls to a large extent the concentration of a trace element within it. The trace elements can be incorporated into the carbonate mineral in a number of ways ; (i) substitution for Ca2+ in the CaCO3 lattice, (ii) in the interstices between lattice planes, (iii) occupy defective lattice positions, (iv) by adsorbtion due to remnant ionic charges, (v) in non-carbonate inclusions, such as silicates and fluid inclusions [ McIntire 1963; Zemann 1969 ]. The orthorhombic aragonite lattice is able to hold trace elements with large ionic radii ( Sr,Ba,Na,U ) whereas the rhombohedral calcite lattice incorporates smaller cations ( Mg,Fe,Mn,Zn ). Little is known about the other factors ( ii to v ) and if dominant can contribute to erroneous results and interpretations. With the advent of microsampling techniques and point analysers such errors should be greatly reduced.

The concentration of a trace element incorporated in a carbonate lattice during precipitation depends on the partition coefficient or distribution coefficient (D). Distinction has to be made between the distribution coefficient during homogeneous precipitation (D) and during heterogeneous precipitation ( $\lambda$ ). Presence of zoned crystals and results of experimental studies [ Katz et al. 1972; Kinsman and Holland 1969 ] favours heterogeneous precipitation as the prevalent process in diagenesis. Homogenous precipitation occurs in crystals precipitating from large solution reservoirs. For values of $\lambda < 1$, the precipitating carbonate phase is depleted in that trace element compared to the concentration in the ambient water or precursor. For values of $\lambda > 1$, there is an enrichment of the trace element in the carbonate phase relative to that in the pore-waters or the precursor.

The exact values of $\lambda$ or D are not precisely known and depend on factors such as rate of precipitation and temperature [ Lorens 1981; Kinsman 1969 ]. Precise information on pore-water chemistry is therefore not obtainable given our state of knowledge on partition coefficients. Since the best we can do at present is knowing the order of magnitude of the partition coefficient, only crude estimates of the pore-water chemistry are possible. This information is sufficient however for working out the chemical diagenetic trends and their relative magnitude. Studies have shown that such information, when combined with textural data, can be an aid in deciphering the nature of diagenetic environments and precursor mineralogy of components [ Brand and Veizer 1980 ].

The model put forth by Brand and Veizer, [1980] is based on the distribution of Sr and Mn, since their vastly different distribution coefficients and concentrations in marine and meteoric waters results in opposing chemical diagenetic trends. Other elements commonly used are Mg and Zn [ Pingitore 1978 ]. Based on the nature of these chemical diagenetic trends, the diagenesis has been called either "open" or "closed" [ Kinsman 1969 ]. The depletion of Sr that is commonly observed during diagenesis is generally attributed to flushing by meteoric waters. However, there have been studies where there is no evidence of such Sr depletion by meteoric waters. Rather it was argued that Sr depletion can occur in seawater [ Katz et al. 1972; Land 1979;1980 ].

## 1.3.3: OXYGEN AND CARBON ISOTOPES

Ever since the foundations of stable isotope geochemistry were established by Urey and associates in the 1940s and 1950s, their application by carbonate sedimentologists has gained increasing use. The most commonly used stable isotopes are those of oxygen and carbon. Present day studies on carbonate diagenesis routinely employ oxygen and carbon isotope analysis. With the use of data on the oxygen and carbon isotope compositions of the carbonates, it has been possible to quantify interpretations on diagenetic processes to some extent. Reasonable interpretations can be made on the origin of pore-waters, the temperature of diagenetic processes and on the isotopic composition of palaeocean waters.

The range of oxygen and carbon isotope compositions in

carbonate sediments is shown by Figure 1.5. The factors that control their isotopic composition are also listed. Both the oxygen and carbon isotopes are represented with reference to the PDB standard (Pee Dee Belemnite) and represented as "Del" values. Present day marine waters have oxygen and carbon values of 0 per mil. Most marine carbonates have PDB values close to zero per mil, normally small positive or negative numbers. The isotopic composition of water is represented with reference to the SMOW ( Standard Mean Ocean Water ) standard. The oxygen isotopic composition of SMOW is -30.4 on the PDB scale, and at approximately 16.5 C the oxygen isotope values on the SMOW and PDB scales are both zero.

The small variation in marine carbon isotope compositions represents a well mixed carbon reservoir. In contrast, non-marine carbonates have large variations in carbon due mainly to factors such as exchange with atmospheric $CO_2$, input of dissolved carbonates in ground-waters, $CO_2$ production of organic decomposition and photosynthesis [ Fritz and Poplawski 1974 ]. The near surface carbon cycle has 18% of it's carbon bound in sedimentary-cum-biological reservoirs as reduced carbon. The rest comprises the carbonate reservoir. Studies have shown that the carbon cycle has apparently remained stable for most of geological history [ Schidlowski et al.1975 ].

Most of the variation in carbon isotope compositions are caused by involvement of organic carbon. Organic carbon is greatly depleted in C13 and has a carbon isotope value of -25 permil. There are various processes responsible for input of organic carbon into the carbonate record, each having it's distinct carbon isotopic signature. Irwin et al.[1977]

17

outlined a few of these that operate during progressive burial of carbonate sediments rich in organic carbon. Aerobic oxidation of carbon is one of the earliest processes to operate and the evolved $CO_2$ that is incorporated into any precipitating $CaCO_3$ phase has carbon isotope compositions approaching that of organic carbon (-25 permil). Anaerobic oxidation, involving also biological reduction of sulphates also generates carbon isotopic composition similar to organic carbon. During fermentation of organic carbon, methane is generated. This methane is enriched in $C12$ and therefore any residual $CO_2$ has an extremely heavy carbon isotope signature (+15 permil), that may subsequently be recorded in late diagenetic cements. Further organic reactions do occur that are complex in nature and include decarboxylation which can generate carbon isotope values of between -10 permil to -25 permil.

The contribution of soil $CO_2$ to the isotopic signature of various carbonate cements has been one of the better studied and documented aspects of stable isotope geochemistry in carbonates [ Gross 1964; Allan and Matthews 1977 ]. The $CO_2$ generated in the vadose zone is depleted in $C13$ and the carbon isotope signature of the resulting cements precipitated by soil $CO_2$ charged meteoric waters is isotopically light (-12 permil). Generally, further reaction of this soil $CO_2$ with atmospheric $CO_2$ generates a slightly heavier carbon isotope value and therefore freshwater limestones have a range of carbon isotope compositions between -12 permil and +3 permil [ Keith and Weber 1964 ]. Such isotopically light carbon isotope values have been encountered in carbonates as old as the Precambrian and help

18

distinguish fossil "hardgrounds" of subaerial genesis from those of subaqueous marine genesis [Beeunas and Knauth 1985].

Large perturbations of isotopically light carbon are rare in the carbonate rock record, with the carbon isotope compositions quickly equilibrating with the rock carbon values. This tendency for the carbon isotope record to remain fairly close to the rock carbon value is due to the highly discordant sizes of the water and rock reservoirs. The rock carbon reservoir, being dominant, controls the isotopic signature during rock-water interactions [ Meyers and Lohmann 1985 ]. Whatever local perturbations due to, say light soil $CO_2$, is only a transient phase. With continued diagenesis the rock carbon signature reimposes it's dominance on the carbon isotope record. The carbon isotope record of carbonates is therefore a fairly reliable indicator of original rock carbon values and shows only small local variations.

The oxygen isotopic composition of a marine carbonate is strongly controlled by the isotopic values of the marine waters and the temperature [ Epstein 1959 ]. Like the carbon isotope composition, the oxygen isotope compositions of present-day marine waters has a narrow range, clustered around the zero per mil PDB. Variations occur in meteoric waters mainly due to various fractionating processes that operate on the marine waters, from which most meteoric water is derived. The ultimate oxygen isotope composition of meteoric waters depends on climate, distance from marine source and changes in composition of the marine source. Climate is important since oxygen isotopes are strongly dependant on temperature. With increasing distance from the

marine source, meteoric water undergoes increased
fractionation by repeated evaporation-precipitation. The
oxygen isotope composition of the meteoric water therefore
gets more and more O18 depleted. Changes in oxygen isotope
compositions of marine waters can occur during glacial
events. The marine waters would then be enriched in O18 since
glacial ice locks up the O16 fraction. In general then, the
non-marine waters are isotopically much lighter in their
oxygen isotope compositions compared with the marine waters.
The result of repeated diagenetic modifications by meteoric
pore-waters is therefore to produce increasingly light oxygen
isotope products. This evolving pore-water isotope chemistry
can be recorded in successive cement precipitates in some
cases [ Dickson and Coleman 1980; Marshall 1982 ].

Unlike the carbon isotope record, the oxygen isotopic
composition is strongly controlled by the water reservoir.
The rock reservoir signature is easily overprinted and erased
by diagenetic pore-waters. Increasing importance is being
given to the burial diagenetic environment and it's imprint
on the carbonate sediments [ Dickson 1985 ]. Presumably the
burial cements should have isotopically light values since
the temperature  of precipitation would be higher than near-
surface processes. However, the interpretation of stable
isotope data are certainly not clear cut and conflicting views
have arisen based on similar data [ Moore and Druckman 1981;
Wagner and Matthews 1982 ].

FIG.1.1: Map showing the distribution of sediments of the
Adelaide Geosyncline. The Torrens Hinge Zone (THZ)
separates the geosyncline from the Stuart Shelf on the
west.

QLD.

N.S.W.

VIC.

THZ

Lake Torrens

STUART
SHELF

STUDY
AREA

Lake Frome

GAWLER
CRATON

ADELAIDE
GEOSYNCLINE

ADELAIDE

0        100       200
KILOMETRES

FIG.1.2: Summary of the stratigraphy within the Flinders Ranges and adjacent areas. From Rutland et al.[1981] and based on data of the South Australian Department of Mines and Energy.

| | ADELAIDE REGION | STUART SHELF | SOUTH FLINDERS RANGES WESTERN FACIES | SOUTH FLINDERS RANGES EASTERN FACIES | NORTH FLINDERS RANGES | |
|---|---|---|---|---|---|---|
| € | NORMANVILLE GROUP | HAWKER GROUP EQUIVS. | HAWKER GROUP | | HAWKER GROUP | |

Chart column headings (right margin, top to bottom): WILPENA GROUP, UMBERATANA GROUP, BURRA GROUP, CALLANNA BEDS

Age column (left margin): €, MARINOAN, STURTIAN, TORRENSIAN, WILLOURAN

**WILPENA GROUP**

Pound [w/t] — Subgroup — Billy Springs Beds [gn]
Wonoka [gy] — Formation
Bunyeroo [r] — Formation

**MARINOAN**

ABC Range Qte equiv [w] — Arcoona Quartzite Mem [w] — ABC Range Quartzite [w] — Ulupa Siltstone — ABC Range Qte [w]
[r] Corraberra Sandstone Mem — Ulupa Siltst [gn]
Brachina Fm. equiv. [r] — Woomera Shale Mem. [r] — Brachina Formation [r] — Brachina Fm [r]
Seacliff Sandstone Mem — Nuccaleena Fm equiv — Nuccaleena [p] Formation — Nuccaleena Fm
Reynella Siltstone Mem. [r] — Reynella Siltstone Mem. equiv [r] — unnamed tillite & Reynella Siltstone Mem. — Grampus Qte., Pepuarta Tillite and Gumbowie Arkose [gy] — Yerelina Subgroup [gy]
& Whyalla Sandstone — Elatina Formation [w] [r]
Willochra Subgroup equivalents [r] — Willochra [r] — Trezona Fm [r] — Trezona Formation [r]
Marino Arkose — Yudnapinna Beds [r] — Enorama — Shale [gn] — Amberoona [r]
Subgroup — Etina Fm [r] — Etina Fm [r] — Angepena Formation
Tarcowie Siltstone [gy]

**UMBERATANA GROUP**

Brighton Limestone [b/gy] — Brighton [b/gy] — Limestone — Balcanoona Fm [b/gy]
Tapley Hill [gy] [bk] — Woocalta Dolomite — Formation

**STURTIAN**

Sturt Tillite [gn] [gy] — McLeay Beds / Appila / Tillite [gy] [gn] — Wilyerpa Formation [gn] — Merinjina Tillite [r]
Benda Siltstone [gy] — Yudnamutana Subgroup [gy]
Braemar Iron Formation facies
Pualco Tillite [gy]

**BURRA GROUP**

Belair Subgroup [w] [gy] — Belair Subgroup [w] [gy]
Glen Osmond Slate [gy] [gn] — Saddleworth Formation [gy]
Beaumont Dolomite & "upper phyllites" [gy] — Watervale Sandstone Mem — Auburn Dolomite [gy]

**TORRENSIAN**

Stonyfell Quartzite [w] — Undalya Quartzite [w] — Myrtle Springs Formation [gn]
Woolshed Flat Shale equiv [gy] — Woolshed Flat Shale [gy]
Castambul [w] & Montacute [gy] Dols [bk] — Skillogalee [Mg] Dolomite [gy] — Skillogalee [Mg] Dolomite
Emeroo Bungaree & Yednalue Quartzites [w] — Copley & Wortupa Quartzites [w]
Aldgate Sandstone [hv] — Wirrabara Fm. [r] [gy] / River Wakefield Subgroup [gy] — Opaminda Formation [gy]
Quartzite Rhynie Sandstone [hv] — Blue Mine Conglomerate [gy]
Woodnamoka Phyllite [gy]
Humanity Seal Fm [hv]

**CALLANNA BEDS**

River Broughton Beds

**WILLOURAN**

Beda Volcanics & Backy Point Beds — Depot Creek Volcanics — Wooltana Volcanics
Sequences of carbonates, immature clastics, volcanics and replaced evaporites, largely in disrupted contexts — Wywyana Formation
red siltstone — Paralana Quartzite
Pandurra Formation [r]

Barossa Complex pre-Adelaidean metamorphics

pre-Adelaidean basement, volcanics

Mount Painter Complex pre-Adelaidean metamorphics

Drn B D W

79-61 SA Department of Mines and Energy

FIG.1.3: Simplified stratigraphy and radiogenic ages of
the Adelaidean in the Flinders Ranges with an updated
division and addition of the Ediacaran period (After
Jenkins [1986]).

STRATIGRAPHY OF ADELAIDE FOLD BELT

| EON | SYSTEM/PERIOD | STAGE/EPOCH | SOUTHERN | NORTHERN |
|-----|---------------|-------------|----------|----------|

| | | | | |
|---|---|---|---|---|
| PHANEROZOIC | CAMBRIAN | EARLY | KANMANTOO GP | HAWKER GROUP |
| | | | NORMANVILLE GP | |

LATE PROTEROZOIC

ADELAIDEAN

Ediacaran — LATE / EARLY
Marinoan
Sturtian
Torrensian
Willouran

WILPENA GROUP
UMBERATANA GROUP
BURRA GROUP
CALLANNA BEDS

URATANNA FM
POUND SUB GP · BILLY CREEK BEDS · gy
WONOKA FM · gy
BUNYEROO FM-r — 588±35
ABC RANGE QTZ · 609±64
BRACHINA FM r k
WILLOCHRA gy r · YERELINA SUBGP
SUBGP r 675±54
TAPLEY HILL FM 750±53 gy
b
STURT FM · WILYERPA FM gy
BENDA SS Fe
PUALCO TILLITE gy
YUDNAMUTANA SUBGROUP

gy
k
b
RIVER WAKEFIELD SUBGP
b gy
r gn

metres
4000
3000
2000
1000
0

gy
gy
gn
gy
802±10
r
830±50
gn r
v v v

PRE-BURRA BASEMENT
849 ± 32

| gy - grey | k - khaki | r - red |
|-----------|-----------|---------|
| gn - green | b - black | Fe - iron formation |

FIG.1.4: Table listing criteria for the recognition of aragonite precursors (After Sandberg [1985]).

1. *Still aragonite.* Encountered in quite old rocks (Figs. 3A–D).

2. *Mosaic of generally irregular calcite spar containing oriented aragonite relics.* Crystal boundaries commonly cross-cut original structure defined by organic or other inclusions. Replacement crystals normally $10 - 10^3$ times larger than replaced aragonite crystals (Fig. 5).

3. *Calcite mosaic as for Criterion 2, but without aragonite relics.* Original aragonite mineralogy supported by elevated $Sr^{2+}$ content, relative to levels reasonably expected in dLMC resulting from alteration of originally calcitic constituents.

4. *Calcite mosaic as for Criterion 3, but $Sr^{2+}$ not elevated, or not measured.* Differing $Sr^{2+}$ content in the resulting calcites can reflect differing degrees of openness of the diagenetic system.

5. *Mold or subsequently calcite-filled mold.* Common for aragonitic consituents, but equivocal because observed for non-aragonitic constituents (e.g., miliolid foraminifera, Schroeder, 1979) in undolomitized limestone.

*Note:* Constituents preserving regularity both in texture and in optical orientations are sometimes suggested as products of pseudomorphic or paramorphic calcitization of aragonite. Not supported by observations on diagenesis of known aragonites. Even the unusual hot spring alteration of some aragonite ooids reported by Richter and Besenecker (1983, fig. 4) produces a 10–50 fold increase in crystal size and leaves aragonite relics (Sandberg, unpublished).

[1]Arranged in order of decreasing reliability. from Sandberg (1983).

FIG.1.5: Range of oxygen and carbon isotope compositions of carbonates and the controlling factors (After Hudson [1977]).

Heavy carbon diagenetic cements

Range common marine limestones

Late cements (Jurassic)

Chalks

Shallow cements

Average marine lsts

Deep limestones

Average freshwater limestones

Soil calcites Europe

Secondary calcites Bermuda

Early diagenetic concretions

Methane derived cements

Dilution ←—— Sea —— → Evaporation
water

Copenhagen    Bermuda

Rainwater
(Latitude dependent)

To-20    Subsurface waters (formation waters) generally
isotopically heavier with temp. and concentration

Temperature dependence for isotopic equilbrium
precipitation of calcite from water. Temperatures
assuming δO¹⁸ water = O for illustration.

Heavy carbon equilibrium with methane or residual from biological methane generation.

Solution — precipitation

Marine carbon

Soil weathering. Ca(H CO₃)₂

Non-equilibrium oxidation (soil; marine anaerobic)

Sedimentary organic matter

Biochemical CH₄

Light carbon oxidation of methane

Thermochemical C H₄—CO₂ equilibrium in natural gases

High temperature

Low temperature

# CHAPTER TWO

# LATE PRECAMBRIAN TREZONA FORMATION

## 2.1: INTRODUCTION

The Trezona Formation constitutes part of the Umberatana Group of glacigene and interglacial sediments. These sediments form part of a thick sequence of sedimentary rocks, ranging from Late Precambrian (Adelaidean) to Cambrian in age, that make up the Adelaide "Geosyncline" [Rutland 1981]. The glacigene sediments mark both the start and end of sedimentation during this interval of the Adelaidean. Based on radiometric data, the upper (Marinoan) glaciation is estimated to have occurred later than 724 Ma ago [Webb et al. 1983]. The interglacial sediments are dominantly siltstones with local development of shallow water carbonates formed around diapiric structural highs [Lemon 1985]. The Trezona Formation is such a sequence of shallow water carbonates developed in the central Flinders Ranges.

The area chosen for this study is south of Blinman because the Trezona Formation is thickest and best developed here, and the sediments are relatively undeformed. Samples were collected from sections at Werta, Bulls Gap and Enorama Creek ( Fig.2.1). The carbonate environments varied from subtidal barrier complexes to lagoonal and intertidal flats with extensive development of stromatolites [Preiss 1971]. Ooid shoal bodies occur in all the sections studied, but are best developed adjacent to the diapiric structure at Bulls Gap. The environment of carbonate deposition became increasingly restricted during deposition of the Trezona Formation, and terminated with the onset of glacial and fluvio-glacial conditions shown in the Elatina Formation.

## 2.2: PETROGRAPHY

### 2.2.1: OOIDS

There is a large range of fabrics and sizes displayed by the ooids. Ooid diameters vary from 0.3mm to 1.0mm for the small ooids, and upto 10mm or more (max. 16mm) for the large ooids (pisoids). The types of fabrics observed are shown in Figures 2.2 to 2.3. The large ooids have nucleii varying from 0.3mm to 2mm in diameter, with well developed concentric cortical fabrics of micrite and microspar (Fig.2.2a). The interiors of the large ooids are commonly made of clear blocky ferroan calcite filling a void into which fragments of the micritic cortex sometimes collapsed and are preserved (Fig.2.2b). The shapes of these large ooids generally tend to be elongate and asymmetrical, although occasionally spherical and symmetrical ooids are present (Figs.2.2c & 2.2a). Some of the cortical layers are sparry and made of equant to subequant calcite crystals with a brick-like fabric (Figs.2.2d & 2.2e). Each "brick" in the fabric corresponds to an individual component calcite crystal.

Small ooids have some of the fabrics displayed by the large ooids and also some fabrics that are unique. The small ooids are commonly micritic with sparry cores or occur as oomolds with blocky ferroan calcite infills (Figs.2.2g, 2.3b & 2.4c). Some oomolds clearly show an earlier generation of medium crystalline calcite cement that lines the inner ooid margins, and a later generation of coarsely crystalline calcite cement in the ooid centers (Fig.2.3b). These spar-filled oomolds also display some irregular shapes with trunk-to-tail elephantine chains (Fig.2.3f). The sparry calcite of micritic ooid cores has irregularly distributed rhomb-shaped

22

inclusions not found in the clear calcite in oomolds
(Fig.2.2g). Some small ooids are totally micritic with no
discernible cortical laminations. In contrast, some ooids
display neomorphic fabrics with sparry cortices of coarse
calcite with concentric cortical laminations preserved as
inclusions (Fig.2.2h). The calcite crystals of these sparry
neomorphic fabrics have a brownish colour. Fibrous non
ferroan isopachous calcite mosaics are found infilling some
small oomolds and are succeeded by blocky ferroan calcites at
ooid centers (Fig.2.4d). Half-moon ooid fabrics with their
micritic lower halves and sparry upper halves are present but
rare (Fig.2.3h). The various ooid fabrics have been
summarised in Figure 2.7. In all ten different ooid fabric
types, I to X were identified. The following section on ooid
geochemistry makes reference to these ooid types described in
Figure 2.7.

## 2.2.2: CEMENTS

Based on fabrics, spatial distribution, and ferroan non-
ferroan nature,five different groups of cements are
recognised.

Type A: Isopachous fibrous fringing cements around
depositional grains are non-ferroan and record the earliest
stage of cementation.(Fig.2.3a). They are the dominant
interparticle cement around ooids and intraclasts in
intercolumnar areas of stromatolite biostromes. In the ooid
grainstones proper, however, they comprise less than 10% of
the total interparticle cements.

Type B: This cement is also non-ferroan and occurs as a
bladed to granular form with anhedral crystal shapes. It is

the dominant cement in the interparticle spaces (Fig.2.3c).
It generally has a brownish appearance similar to the calcite
in type I and X ooid fabrics. The shape of these calcites
varies from bladed to granular forms (Fig.2.3b). Crystals
vary from 50um-200um in size and are inclusion free. In some
ooids this cement forms drusy calcite mosaics.

Type C: This cement is a blocky ferroan calcite spar.It is
the dominant component filling oomolds (Fig.2.2c, 2.2g &
2.3b) and is composed of well developed subhedral to euhedral
crystals, 1mm-0.13mm in size. In interparticle spaces it
represents the pore-occluding stage of cementation after Type
A or B cements. In ooids with Type III and IV fabrics, the
blocky ferroan calcite has microdolomite inclusions. Blocky
calcite is also present in fractures and veins and cross-cuts
earlier cement phases. In ooid grainstones with large
intraclastic populations fenestral voids are commonly filled
with this blocky cement and are termed fenestral cements
(Fig.2.5). In such cases the earlier cement is ferroan with
non-ferroan cement occupying pore centers.

Type D: This cement is typically cloudy subequant or bladed
calcite crystals. It is restricted to ooid grainstones that
have Type III and IV ooid fabrics (Fig.2.3d & 2.6). This
cement is non-ferroan when stained but has occasional iron
rich phases within it. In large pores,this cement is followed
by the pore-occluding Type C cement.

Type E: This is a coarsely crystalline non-ferroan calcite
mosaic containing relict ooids and peloidal grains (Fig.2.3e
& 2.4b). It has a characteristic brownish appearance similar
to the type B cements.There is no regular spatial
relationship between the position of ooids and peloids and

the crystal margins of the calcite mosaic. In some cases the peloidal grains occur in centers of calcite crystals, with the calcite resembling syntaxial growths around peloids. In others the crystal margins cut across the peloids. Unlike the other cement fabrics described thus far, type E cements occur in association with a laminated limestone facies and not with ooid grainstones. This laminated limestone facies consists of alternating dark sparry layers and light micritic layers ( type E cements ). The various cement fabrics are summarised in Figure 2.8.

## 2.3: TRACE ELEMENT CHEMISTRY

The trace element data are generated from the analyses of 43 separate components totalling from 430 to 860 individual microprobe analyses.

## 2.3.1: OOIDS

The trace element chemistry of the various ooid and cement fabrics, when plotted, fall into distinct fields with few overlaps (Figs.2.9,2.10 & 2.11). Ooid fabrics Type I and X have elevated Sr concentrations that are higher by an order of magnitude than Type II, III and IV fabrics (Fig.2.10). Type I fabric has the highest Sr and lowest Mg concentration, with an Fe concentration comparable to the blocky ferroan calcites of Type II fabrics. The sparry Type X ooid fabric has a lower Fe content, similar to that of the micritic Type VII fabric. The trace element chemistry of Type II, III and IV fabrics cluster with large overlaps. In general terms, the trace element chemistry of Type I and that of Types II, III, IV and VII fabrics represent two end members with chemistry of Type X fabrics being intermediate.

25

## 2.3.2: CEMENTS

The cements can also be separated into distinct groups based on trace element chemistry (Fig.2.11). Type E cement fabrics, with the highest Sr and lowest Mg concentration fall in the same field as Type I ooid fabrics. The similarity in the fields of Type C cements and Type II ooid fabrics is because the blocky ferroan calcites form the spar-filled Type II ooid fabrics. The Type A fibrous isopachous cements and the inclusion-rich Type D cements have the same trace element chemistry, but Type D cements have a very large Fe and Mg variation. Type B cements fall into an intermediate field, with a large range in Sr concentrations.

## 2.4: OOID INTERPRETATION

Most of the ooid fabrics have been described by other workers studying Phanerozoic ooids [Sandberg 1975; Wilkinson et.al. 1984] and Precambrian ooids [Tucker 1984]. Type I ooid fabrics representing calcitized ooids of neomorphic spar and the brick-like Type X fabrics are inferred to have been originally aragonitic. In type I fabrics the preservation of original concentric cortical laminae as inclusions implies a neomorphic fine-scale replacement process. The replacement spar comprises coarse interlocking calcite crystals and has a brownish colouration. These fabrics have been described by Sandberg [1985] and are typical in calcite replacement of skeletal aragonite. In addition, the type I ooid fabrics have elevated Sr concentrations, supporting the inference of aragonite replacement.

The Type X fabrics may result from the neomorphic alteration of an aragonite precursor and are identical to

26

those described by Tucker [1984] and Assereto and Folk [1976]. These type X ooid fabrics also have elevated Sr concentrations although not as high as those of the type I fabrics. In both the type I and X ooid fabrics, there is preservation of precursor relics, i.e. inclusions in type I fabrics and concentric cortical boundaries in type X fabrics.

Type I and X ooid fabrics can normally be found within the same thin-section and would therefore have been subjected to the same diagenetic environment. The reasons for generation of such different fabrics under essentially similar diagenetic conditions are unclear. The difference in the Sr content of these two calcitization fabrics may have been a reflection of the degree of interaction between the solution-films at reaction zones (calcitization fronts) and the pore-waters proper. This concept is explained in Pingitore [1976] and Brand and Veizer [1980]. A "closed" diagenetic environment is one brought about by the presence of thin solution films across diagenetic fronts in static water settings (vadose) [Pingitore 1976]. The "open" diagenetic system results in mobile pore-water settings (phreatic) were there is a high degree of interaction between the reaction fronts and the main pore-water body. The higher Sr and Fe of type I ooids compared to type X ooids would seem to suggest that type X ooids may have been generated in shallow meteoric settings and type I ooids in deep burial environments. However, Sandberg and Hudson [1983] found no difference in the calcitization fabrics in either of these two environments. At this stage the reasons are purely speculative in nature until more empirical work on these calcitization fabrics becomes available.

27

In some cases ooid fabrics have a composite fabric in which the central cortical parts are composed of blocky ferroan calcite, similar to type II ooids and the remaining cortical envelope comprises the brownish neomorphic spar of type I ooids. The chemistry of these two calcite types is also different, with the brownish neomorphic spar falling in the field of type E cements and the void-filling blocky calcites in the field of type C cements (Fig.2.11).

Type II ooid fabrics composed of oomolds filled with clear blocky ferroan calcite cements represent void-fill calcites. The lower Sr content of the type II ooid fabrics suggest a "open" diagenetic environment. This "open" setting was the result of the voids in the form of oomolds that were subsequently filled by the blocky ferroan calcites. These voids would have had relatively mobile pore-water flow conditions which allowed easy exchange of cations during calcite precipitation [ Pingitore 1976 ].Some of these spar-filled molds are deformed into irregular shapes and are similar to those described by Kettenbrink and Manger [1971] and Conley [1977]. They result from the early dissolution of the aragonite in ooids and subsequent collapse during burial. They normally have an outer rim of early calcite cements thereby retaining the gross shape of the ooid subsequent to deformation.

There are some ooid fabrics that indicate presence of bimineralic cortices,i.e. calcite and aragonite. These ooids, called half-moon ooid fabrics, have been interpreted by Carozzi [1963] as resulting from the dissolution of soluble or metastable elements in the ooid cortex and the collapse of the stable elements onto the ooid floor. The remaining cavity

28

being later filled by calcite cement. The half-moon ooids in this study have probably formed in a similar fashion with the dissolution of aragonitic layers in the cortex.

Inference of the precursor mineralogy of the micritic and microsparitic Type V,VI & VII ooid fabrics is problematic. Wilkinson,Owen & Carroll [1985,p.175] classified micritic and microsparitic ooid fabrics as of ambiguous origin. Those fabrics can represent original equant calcitic nannograins forming ooid cortices or micritized aragonitic or calcitic ooids. In view of these two possibilities, Type VI ooid fabrics are interesting. The cortical laminae of the ooids include both sparry brick-like calcite ( equivalent to type X ooids ) and micrite. The generation of the micritic cortical fabrics by micritization is unlikely because of the patchy and discontinous distribution of individual micritic laminae.The sparry fabrics in such ooids have calcites with elevated Sr concentrations similar to the type X ooid fabrics. The micritic laminae have comparatively lower Sr concentrations of between 600-1500ppm. Such high Sr calcites are unlikely to be derived from micritic calcitic ooids and are normally associated with calcites derived from transformation of aragonites [ Assereto and Folk 1976; Davies 1977; Sandberg and Hudson 1983 ]. One possibilty is the existence of both calcite and aragonite cortical layers and their alteration to generate the fabrics in type VI ooids. In such a case the sparry brick fabrics would represent the altered aragonite layers and the micritic fabrics the calcite layers. Alternatively if these ooids are inferred to have been originally aragonitic, then the micritic and sparry cortical fabrics represent two different replacement products

29

of aragonite. Such ooid fabrics have been described from Pleistocene marine oolites and from hot spring ooids [ Richter 1983; Richter and Besenecker 1982 ]. In these two settings, tangential-aragonitic ooids occur in various stages of transformation, from partially calcitized to completely calcitized and micritic/microsparitic forms. In both cases an aragonite precursor is inferred, either partially or totally making up the ooids. The brick-like fabric of some cortical layers and their high Sr content is evidence of this. Therefore, while it is not possible to adequately explain the type VI ooid fabrics, it seems probable that an aragonite precursor had a part in the genesis.

In type V and VII ooid fabrics, however, there is no such association of sparry and micritic cortical fabrics. In these two ooid fabrics, no clear evidence exists for determining the precursor mineralogy. The cortices are totally micritic. In both fabrics the micrites have comparatively low Sr concentrations, similar to the micrite in type VI ooids ( 600-1500ppm ). A precursor ooid made up of equant calcitic or Mg calcitic nannograins could generate such a fabric during diagenesis. However, algal micritization of original aragonite or calcite ooids can also generate similar fabrics. The void-fill calcite in some of the type V ooid cores suggests dissolution of a metastable element ( aragonite ) prior to precipitation of the ferroan calcite. In some cases however these sparry cores resemble sparry ferroan calcites within micritic cortical areas of similar ooids, possibly formed by aggrading neomorphism during burial diagenesis.

Ooid fabrics of type III and IV were probably originally calcitic with the replacement spar being the result of

30

aggrading neomorphism of the original micritic fabric. Such an interpretation is supported by the existence of ooids in various stages of neomorphism into spar, from some entirely micritic ooid fabrics to some entirely of sparry calcite. The comparatively high Mg content of these replacement calcites, with their microdolomite inclusions suggest Mg enriched pore-waters [ Lohmann and Meyers 1977 ]. The source of this Mg could have been either intragranular or from external sources. An external source of the Mg is discounted because of the distribution  of the microdolomite inclusions. They are confined to the ooids of type III and IV fabrics. No microdolomite inclusions are found in similar ferroan calcites in interparticle cements. The fabric specific occurrence of the microdolomite suggest some sort of local source for the Mg, probably a Mg calcite precursor. Also, ferroan calcites are common replacements of Mg calcite precursors [ Richter and Fuchtbauer 1978 ]. Lohmann and Meyers [1977] suggested the processes of solid-state exsolution and incongruent dissolution for the formation of microdolomite inclusions in calcite cements.

Solid-state exsolution results in formation of two stable phases, dolomite and calcite, by solid state diffusion. This process, however, proceeds at slow rates at diagenetic temperatures and was probably insignificant. Incongruent dissolution involves microscale dissolution of the precursor Mg calcite resulting in Mg enrichment of the solution film. This Mg enrichment presumably requires some sort of closed to semi-closed diagenetic environment. The processes involved and the factors responsible in this closure are not known. It is possible that local

microstructural differences may have aided in the formation
of microdolomites and the large variation in Mg observed in
these recrystallized ooids. Videtich [1985], in her study of
Mg distribution during diagenesis, found that inclusion-rich
areas had lower Mg than inclusion-rich areas of
recrystallized limestones. This was attributed to the
presence of higher microporosity and permeability in
inclusion-rich areas and their subsequent faster dissolution-
reprecipitation.

The Mg rich inclusion-free areas however, might undergo
closed system diagenesis resulting in formation of
microdolomites. It is not clear which mechanism was
responsible for the microdolomite in the present study.

Amongst the type III and IV ooids are occasionally found
type IX ooids made up of fibrous calcite mosaics with
micritic envelopes. The difference in the fabrics of these
associated ooids probably indicates difference in original
mineralogy. The lack of collapse features amongst these type
IX ooids,despite evidence of pressure solution indicates
stabilization before significant burial. The non-ferroan
calcites of these ooid fabrics suggest absence of burial
depths, which normally produce ferroan calcites. It is
inferred, therefore that the fibrous calcites of type IX
ooids were formed at shallow depths, probably by dissolution
of a metastable component (? aragonite). Their association
with type III and IV ooids implies the existence of both
originally calcitic and aragonitic components,with the
calcitic being dominant in these oolite units. Type IX ooids
form a very small percentage of the total ooid population
(less than 5%).The micritic envelopes in the type IX ooids

may have existed as original calcitic envelopes or as micritized aragonitic ooids. The essentially isopachous nature of this cement would indicate a vadose type environment although there was no evidence of vadose interparticle cements. Possibly they were present but have been overprinted by later phreatic cements. The clear ferroan cements found in the centers of some of these type IX ooids represents the pore occluding cementation stage during burial. The various ooid fabrics and their infered precursor mineralogy is schematically represented in Figure 2.12.

2.5: CEMENT INTERPRETATION

The cements associated with the oolite units record a range of diagenetic environments, from marine phreatic to meteoric phreatic and deep burial. The type A cements with their fibrous form and relatively Mg enriched chemistry are inferred to represent marine phreatic precipitates. Mosᴜ modern day marine cements form isopachous crust of acicular crystals of aragonite or Mg calcite [ Folk and Land 1975; Longman 1980; James and Choquette 1983 ]. Precipitation of the type A cements seems to be favoured in areas of active water circulation like the intercolumnar areas of stromatolitic buildups. The retention of a fibrous fabric and absence of a coarse calcite replacement fabric tends to discount the possibility of type A cements having an aragonite precursor. Both its fibrous form and high Mg content suggest that the precursor was Mg calcite.

Type D cements, with their bladed calcites and inclusion rich appearance are also interpreted as marine phreatic. Geochemically they encompass the field of the inferred marine

type A cements. The large variation in their Mg and Fe
contents is due to the presence of these inclusions. These
inclusions do not represent microdolomite phases but are
trapped solids including clays and iron oxides. Such
inclusion rich calcites of marine origin are described in
skeletal grainstones of Devonian reefs [ Walls and Burrowes
1985 ]. The clear blocky ferroan type C cements represent the
final phase of cementation and probably formed in the deep
phreatic burial environment.

The equant form and relatively clear appearance of the
type B and E cements is commonly interpreted to represent
precipitation from meteoric phreatic waters [ Folk and Land
1975 ] or a result of burial diagenesis. However, such a
relationship between crystal habit and pore-water chemistry
is not strictly valid. Equant high-Mg calcites are known to
form in Holocene shallow marine environments [ James and
Ginsburg 1979; Warme and Schneidermann 1983 ] and fibrous low
Mg calcites in meteoric vadose environments [ Braithwaite
1979; Kendall and Broughton 1978 ]. Also, equant blocky
calcites are reported to form marine cements in Upper
Jurassic [Wilkinson,Smith and Lohmann 1985 ], and Ordovician
limestones [Wilkinson et.al. 1982].

Type B and E cements however, also have a very high Sr
content (2000ppm-5000ppm) which is unlike normal diagenetic
calcite cements (400-700ppm) [Kinsman 1969]. Such high Sr
calcites have been inferred to represent aragonite
replacements in previous studies [Wardlaw 1978; Davies 1977].
But the fabrics of both type B and E cements are unlike those
commonly observed during calcitization [Sandberg 1985].
Although both the type E and B cements have high Sr content,

type B cements have a comparatively lower Sr content and are associated with ooid grainstones.

The constraints imposed by the geochemical and fabric data are of opposing nature. The geochemical data points to an aragonite precursor but is not supported by the fabric data. If there is an aragonite precursor involved, the fabrics of type B and E cements certainly do not represent normal aragonite calcite transformation. Could an aragonite precursor have been responsible in an indirect way for the high Sr content of these cements? The ooid-cement relationships does seem to suggest this for the type B cements.

## 2.6: OOID-CEMENT RELATIONSHIP

An interesting association of inferred aragonitic ooids with high Sr cements and calcitic ooids with low or "normal" Sr cements is found in the ooid grainstones. Whenever ooids with aragonite replacement fabrics were present, the interparticle cements are of type B described above. Where there was no evidence for the presence of aragonite replacement fabrics in ooids, the interparticle cement was of type D. It is common to find oolite units with both calcitic and aragonitic precursor ooids coexisting as well as those with only calcitic precursor ooids. The reasons for shifts in precipitation of Mg-calcite and aragonite in sea-water are unclear. Situations where both aragonite and Mg-calcite are precipitated in modern marine settings as cements and ooids are known [James and Ginsburg 1979; Land, Behrens and Frishman 1979]. The influence of organics and kinetic controls are possibly important [Given and Wilkinson 1985].

Possibly the coexistence of high Sr cements with inferred aragonitic ooids may be related to the diagenetic alteration of these ooids. During the transformation of the aragonite ooids, pore waters would have high Sr concentrations which could then result in the precipitation of high Sr cements similar to the type B cements. Such elevated Sr concentrations in pore-waters have been observed in modern oolites undergoing meteoric diagenesis [ Halley and Harris 1979 ]. Obviously such a diagenetic environment would have to be essentially a closed chemical system.

Such an explanation would not explain the type E cement fabrics since there is a lack of such aragonite replacement ooids with the type E cements. The type E cements are very similar to the calcite laminae fabrics described by Tucker [1983,p.301-303 and his Figs 8a and 8b] and Tucker [1986]. His cements are also associated with a laminated limestone facies which is organic rich. Based on the very high Sr content of his carbonates and the occurrence of ooid grainstones ( within the same formation ) with aragonite replacement fabrics, he inferred an aragonite precursor for the laminated limestone facies. Tucker [1983] made no mention of any calcitized fabrics or of textural evidence supporting aragonite replacement. Whilst the type B cement fabrics are unlikely to be replacements of aragonite, the type E cement fabrics certainly are not typical of calcite cements. Although type E cements are void-fill cements they do not have the typical features of crystal growth from pore margins and drusy crystal mosaics [Bathurst 1975]. With the evidence in hand a proper interpretation of the genesis of these cements is not possible. Although the geochemical data

36

suggest an aragonite precursor, this is not supported by the textural data. Alternatively it may be possible that the type E cement fabrics did have an aragonite precursor and the resulting fabrics are atypical of the commonly observed calcitization fabrics.

## 2.7: OXYGEN AND CARBON ISOTOPES

The carbon and oxygen isotope composition of 39 samples analysed are tabulated in Figure 2.13 and plotted in Figures 2.14 and 2.15. The oxygen and carbon isotope trend of the depositional (ooids) and diagenetic (cements) components differs from the commonly observed trend of lighter oxygen and carbon Del values with meteoric diagenesis. The cements have heavier oxygen and lighter carbon isotope compositions than the ooids. There is some overlap of the interparticle cement and ooid fields. The late diagenetic fenestral calcite cements are enriched in oxygen and depleted in carbon isotopes. The ooids and interparticle cements have similar carbon isotope values but differ in their oxygen values. The oxygen isotope composition of the ooids ranges from -9.5 permil to -15 permil. The interparticle cements are generally heavier in oxygen isotopes and range from -6.5 permil to -12 permil. With one exception both components have carbon isotope compositions with a comparatively narrow range; from -2 permil to -4 permil for the interparticle cements and -2.7 to -4 permil for the ooids. The exception is for interparticle cements comprising poikilotopic spar. These cements have been described in Singh [1986] and were referred to as Type E cements (section 2.2.2). The carbon values for these cements, ( approx. -7 permil ), indicate contributions

37

from an organic carbon source. The two data points for intraparticle cements ( ferroan calcites filling ooid molds),record oxygen isotope compositions ranging from -9.5 permil to -12 permil. Their carbon isotope composition is depleted in C13 and ranges from -4.5 permil to -7.5 permil. The fenestral calcites have comparatively narrow range of oxygen and carbon isotope compositions ; -6 to -6.5 permil for the oxygen and -6.5 to -8 permil for the carbon isotopes.

The oxygen and carbon isotope trends commonly observed in Phanerozoic marine limestones subjected to diagenesis with meteoric pore-waters involve a decrease in oxygen and carbon isotope compositions of the marine components, acquiring the lighter isotope values of meteoric waters. The carbon isotopes do not normally show as much of a shift as the oxygen isotopes during meteoric diagenesis. It is commonly a small positive or negative number in the case of modern marine limestones [ Hudson 1977 ]. However the shift in carbon isotopes can be large if an organic carbon source is present in the pore-waters, as in subaerial diagenesis involving soil gas $CO_2$. Various studies over the years have recorded such shifts in oxygen and carbon isotopic composition during meteoric diagenesis [ Magaritz 1983; Meyers and Lohmann 1985; Allan and Matthews 1982 ]. In the light of the above stable isotope trends established from previous studies, how does one interpret the carbon and oxygen trend of the Trezona limestones?

There are two aspects of the carbon and oxygen isotope signatures of the Trezona limestones that differ  from normal marine limestones and their diagenetic trends:

i) Apparent heavier oxygen isotope composition of

38

later precipitates (cements) compared to depositional components (ooids).

ii) Depleted carbon isotope composition of these later precipitates.

The ooids are the only marine components in the C-O plot of the Trezona limestones, and assuming no major diagenetic alteration, would represent the isotopic composition of the precipitating marine waters. However, oxygen isotope compositions of marine components are easily altered during diagenesis and the present isotopic compositions of the ooids are unlikely to be representative of original marine compositions. An important point to note when interpreting stable isotope data is that the depositional components will record the influence of varying pore-water chemistry. The diagenetic components on the other hand provide us with the isotopic composition of the various pore-waters involved in the diagenetic process. The large spread of oxygen isotope compositions in the ooids is probably the result of this overprinting of later diagenetic processes on their original marine composition.

Trace element composition of some ooids ( high Sr,low Mn and Fig.2.10 ) indicates limited equilibration with pore-waters. Inspite of the large range in oxygen isotopes of the ooids, the carbon isotope composition remains within a fairly narrow range. This is probably due to the fact that carbon isotope compositions are strongly rock controlled and equilibrate fairly rapidly [Meyers and Lohmann 1985; Magaritz 1983]. Magaritz [1983] showed that under similar diagenetic conditions, the carbon isotope record did not show large shifts from marine or rock values. In comparision the oxygen

isotope composition recorded large shifts. The Trezona ooids preserve a high minor element composition, with it's elevated Sr content indicating limited recrystallization with retention of precursor chemistry (?aragonite). It is inferred that the carbon isotope composition of the ooids would represent a good estimate of the original marine carbon isotope composition during deposition of the Trezona limestones.

The oxygen isotope composition of the ooids is unlikely to indicate original marine values. The trend towards lighter oxygen values with diagenesis is due to either an increase in temperature of pore-waters and/or isotopically depleted pore-waters. The present range of oxygen isotope compositions of the ooids (using Craig's (1965) expression) corresponds to calculated precipitation temperatures of between $62^{o}C$ and $102^{o}C$ from waters with oxygen compositions of -1.2 permil [pre-glacial value of Shackelton and Kennett 1975] or between $70^{o}C$ and $112^{o}C$ from waters with oxygen compositions of 0 permil [ present ocean waters with polar ice-caps]. These high temperatures indicate equilibration with pore-waters of burial environments. The relatively small variation in carbon isotopes of these ooids indicates high degree of rock-water interaction and equilibration with rock carbon values. There is ample evidence of pressure solution in the ooid grainstones with microstylolites, collapsed ooids and occasional sutured ooid contacts. The above explanation for the large negative oxygen isotope values of the ooids assumes a constant isotopic composition for the pore-waters. This is unlikely and the pore-waters would have been evolving with progressive rock-water interactions and introduction of

meteoric waters. The depleted oxygen isotope composition of the ooids is most probably the result of a combination of equilibration with high temperatures and light meteoric waters. Such lighter oxygen isotope composition of ooids compared to equant interparticle cements was also recorded by Moore and Druckman [1981] and they attributed this to later recrystallization of ooids in warmer temperatures.

The interparticle cements have similar carbon isotope compositions as the ooids and imply a common source, possibly marine. Although their oxygen isotope composition has a large overlap with the ooid composition, there is an apparent shift towards heavier oxygen isotope values. This heavier oxygen composition is considered to be an artifact of the large shift towards lighter oxygen isotope compositions recorded by the ooids from their original marine composition. These interparticle cements are interpreted as shallow subsurface phreatic precipitates. The pore-waters involved in the precipitation of these cements were essentially similar to those that caused depleted oxygen isotope compositions in the ooids.

The Type E interparticle cements have carbon isotope compositions that are depleted in C13, indicating organic carbon sources. Such excursions of the carbon isotope record from normal marine values is of local extent and rapidly equilibrates with the enclosing rock compositions [Meyers and Lohmann 1985]. Such excursions therefore indicate small degree of rock-water interaction. The high Sr content of these cements supports this and indicates diagenetic alteration analogous to the thin film/closed system of Pingitore [1976].

Void-filling or fenestral calcites with depleted carbon isotopes have very low Sr and high Mn content, probably the result of a relatively open system with involvement of meteoric pore-waters. These cements are enriched in O18 and record heavier oxygen compositions compared to the interparticle cements. This suggest that the pore-waters were either colder or had a heavier oxygen isotope composition than those involved in the genesis of the interparticle cements. These later precipitates would have formed in an environment which had stabilised, with absence of metastable components and the precipitation of the interparticle cements and alteration of the ooids. Therefore, there would have been limited rock-water interaction and any organic carbon source would be preserved in the resulting precipitates.

Dickson and Coleman [1980] in their study of diagenesis and oxygen and carbon isotope compositions found their first meteoric cements had heavier oxygen compositions than the enclosed skeletal grains. They suggested that the pore-waters were either heavier in their oxygen isotope compositions or there were colder waters involved. During glaciation, the locking up of waters in ice caps causes O18 enrichment of marine waters. Meteoric waters derived from such O18 enriched marine sources would also be comparatively enriched in the oxygen isotopes. Fairbanks and Matthews [1978] found that oxygen isotope composition of seawater increases by 0.11 permil for every 10 m fall in sealevel. The progressively heavier oxygen isotopes of later precipitates implies gradual enrichment of the meteoric waters, possibly from increasingly colder waters from the encroaching or expanding Marinoan glaciation. Also the cooler atmospheric conditions during

this low sea stand would have contributed towards the heavier oxygen compositions. The effect of glacial-interglacial events on the oxygen isotopes have been studied from both shallow water and basinal carbonates [ Fairbanks and Matthews 1978; Emiliani 1966; Shackelton and Kennett 1975 ]. These studies reveal shifts of between 1 permil to 1.65 permil in the oxygen isotope record due to glaciation.

Depleted carbon isotope signatures like those of the fenestral calcite cements and some interparticle cements normally indicate organic carbon source. These large negative carbon isotope compositions were also recorded by Veizer and Hoefs [1976,Appendix 1]. Similar depleted carbon compositions have been studied from Holocene and Pleistocene limestones and have been linked to subaerial exposure surfaces [Allan and Matthews 1982]. This enrichment in C12 has been attributed to contributions from soil gas $CO_2$ . These depleted carbon isotope values were also recorded from Paleozoic and Mesozoic limestones. However this unit is of Late Precambrian age and to suggest the involvement of soil gas $CO_2$ would imply that there were soil profiles of some sort present. There have been suggestions of such soil profiles in Precambrian environments from a recent study of carbonates [Beeunas and Knauth 1985].

Irwin et al. [1977] developed a model relating various organic matter degradation processes to the carbon isotope signature. They proposed a depth related variation in carbon isotopes of diagenetic carbonates in organic-rich sediments. Based on their study, it is possible to develop negative carbon isotope compositions in burial environments without resort to subaerial exposure and soil gas $CO_2$ contributions.

However, the present study does not reveal the systematic change of carbon isotopes with increasing burial noted by Irwin et al.[1977]. In fact the comparatively heavier oxygen isotope compositions of the diagenetic components does not support a burial environment.

Void-filling calcites with light carbon isotope signatures have been recorded in ammonite chambers by Marshall [1981]. These light carbon compositions occur in early calcites and shell replacement calcites, suggesting an early diagenetic source of organic carbon, possibly from bacterial reduction. In the Trezona limestones the light carbon isotopes were introduced during later diagenetic processes and probably prior to any significant burial.

With increased burial, the diagenetic environment becomes reducing, resulting in precipitation of ferroan cements. Such ferroan cements are found within molds and record depleted oxygen isotope compositions, probably reflecting the higher temperatures of burial. These cements also record negative carbon isotope compositions although there seems to be a trend towards heavier carbon isotopes. The large negative oxygen isotope compositions of the ooids from equilibration with light meteoric waters and/or burial diagenesis makes an estimation of the original marine oxygen composition difficult.

2.8: SUMMARY

Evidence for the precipitation of non-skeletal aragonite during the Late Precambrian is found in the Trezona Formation ooids. The ooids inferred to have been originally aragonitic are made of coarse interlocking mosaics of neomorphic
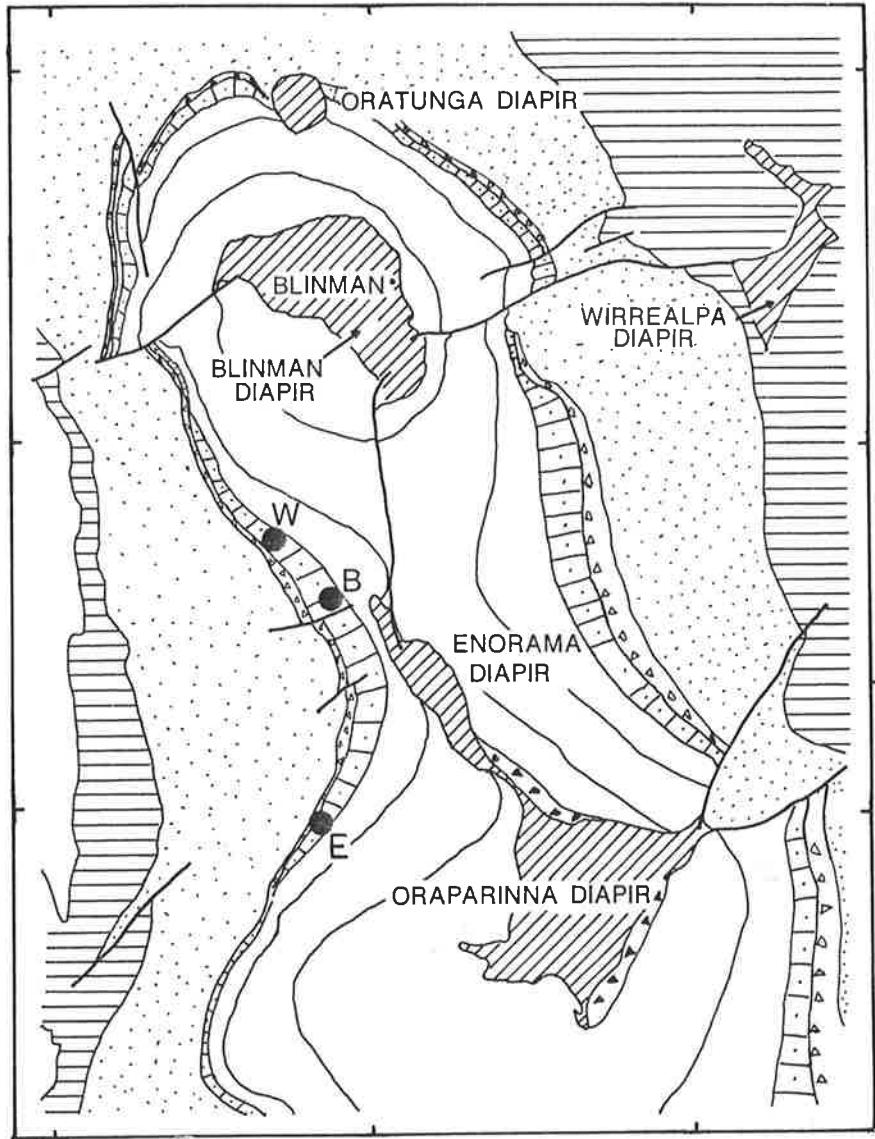
calcite, brick-textures and spar-filled ooid molds. Some of these coarse replacement calcites have cortical laminations preserved as inclusions. The neomorphic spar ooids have elevated Sr concentrations of between 3000ppm-5000ppm. Micritic ooid fabrics are ubiquitous and their original mineralogy is not known. However, some of the spar replacing the cores of some micritic ooids has high Mg concentration as well as microdolomite inclusions.

The cements associated with the ooids inferred to have been aragonitic have high Sr concentrations, varying from 2000ppm to 5000ppm. The textures of these strontium-rich cements do not support an aragonitic precursor and their genesis remains unclear. High Sr cements were also found in an associated laminated limestone facies. Texturally these strontium-rich cements comprise coarse poikilotopic calcites with neomorphic fabrics and could possibly have had aragonitic precursors. In contrast, cements associated with the ooids inferred to have been calcitic, have lower Sr concentrations of between 800-1200ppm.

The components of the Trezona formation limestone record unusual stable isotopic trends, compared to most Phanerozoic limestones. The heavier oxygen composition of the interparticle cements compared to the ooids may be an artifact of the large shift towards lighter values recorded by the ooids during burial diagenesis. The original oxygen composition of the ooids could not be therefore determined. Amongst the cements, there is a trend towards heavier oxygen and lighter carbon compositions with later precipitates (fenestral calcites). The lighter carbon isotopic composition could indicate involvement of organic carbon sources. There

45

were no subaerial exposure features associated with these depleted carbon isotope signatures. Such depleted carbon isotope compositions were recorded from correlatable late Proterozoic carbonates in Morocco and Svalbard and East Greenland by Tucker [1986] and Knoll et al.[1986]. This suggests that the depleted carbon isotopes could be the result of global fluctuations in the sea-water isotopic composition.

FIG.2.1: Location of study area and sample sites within the Trezona Formation. Modified after Lemon [1985]. Geology based on S.Aust.Dept. of Mines and Energy 1:250,000 Parachilna sheet.

ORATUNGA DIAPIR

BLINMAN

BLINMAN
DIAPIR

WIRREALPA
DIAPIR

W

B

ENORAMA
DIAPIR

E

ORAPARINNA DIAPIR

| 0 | 5 | 10 | 15 | 20 | 25 KM. |

| 0 | 5 | 10 | 15 MILES |

Cambrian(undifferentiated)

Wilpena Group

Upper glacials
Trezona Fm.
Undifferentiated
sediments
Lower glacials

Late Precambrian

Umberatana Group

Callana Group

Werta(W), Bulls Gap (B), Enorama Creek (E)
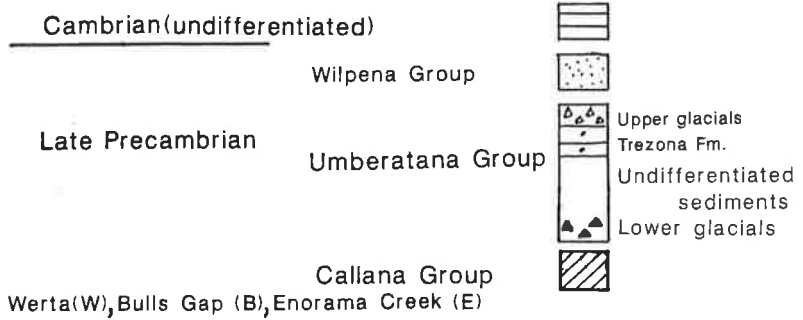
FIG.2.2a: Both large and small ooids with well developed micritic concentric cortical fabrics designated as type V and VII ooid fabrics. Large ooid in lower right has quartz grain with authigenic overgrowths as nucleus. The central cortical parts of some ooids have altered to coarse blocky ferroan calcite (type C cement of text).

FIG.2.2b: Large type V ooid with interior of blocky ferroan calcite and inward collapse of micritic cortical laminations.

FIG.2.2c: Large type IV ooids with a "groundmass" of type II ooids of void-fill calcite. Note asymmetrical shape of large ooid at bottom center.

FIG.2.2d: Large ooid with both sparry and micritic fabrics and blocky ferroan calcite core designated as type VI ooid fabrics.

FIG.2.2e: Type X ooids with cortices of sparry brick-like fabric made of brownish calcite and clear calcite in interparticle areas and ooid core. These ooid fabrics have elevated Sr content (ref.figure 2.10).

FIG.2.2f: Coated grain with the sparry brick-like fabric of type X ooids and micritic nucleus. Associated are type I ooids of neomorphic spar at bottom right and right.

FIG.2.2g: Type III ooid fabrics with spar-replaced interior. Note presence of rhomb-shaped inclusions in this replacement spar.

FIG.2.2h: Type I calcitized ooids of neomorphic spar under crossed nicols. Concentric cortical laminations are preserved as inclusions within the coarse calcite. Microprobe analysis revealed Sr content ranging from 3000-5000ppm.
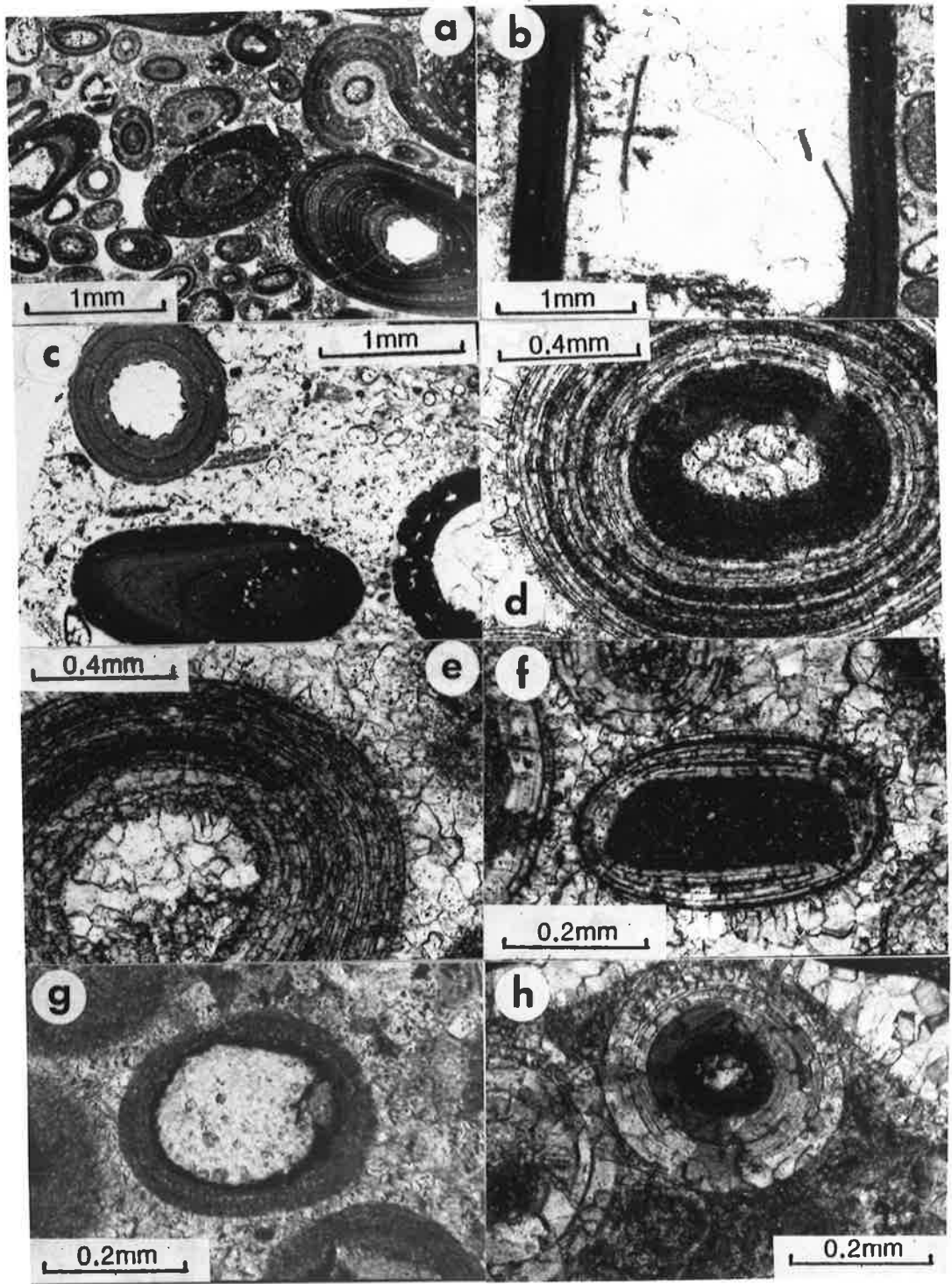
FIG.2.3a: Acetate peel of type A fibrous fringing cement and later generation type C blocky ferroan calcite cement.

FIG.2.3b: Interparticle type B cements with fringe of prismatic (p) cement around ooids. Ooid on right has been replaced by blocky ferroan calcite (type II ooid).

FIG.2.3c: Sparry type X ooids with clear type B non-ferroan blocky calcite in interparticle areas. This calcite cement has high Sr concentrations, ranging from 2000ppm-4000ppm.

FIG.2.3d: Type D calcite cement (IR) progressing into a inclusion-free (IF) phase. Generally associated with ooid grainstones having ooid fabrics suggesting calcitic precursors.

FIG.2.3e: Similar to figure 2.4b but with higher power objective.

FIG.2.3f: Distorted ooids with elephantine shapes associated with micritic ooids.

FIG.2.3g: Calcitized ooid of brownish calcite (type I) being replaced by clear blocky ferroan calcite. Note preservation of concentric cortical layers within the brownish calcite.

FIG.2.3h: Micritic and microsparitic ooids (type VII) with half-moon ooid fabrics (type VIII) in some (arrowed).

a

0.2mm

b

bl

bk

g

l

p

0.2mm

c

0.2mm

d

lF

0.2mm

e

0.2mm

f

1.4mm

g

0.2mm

h

1.4mm
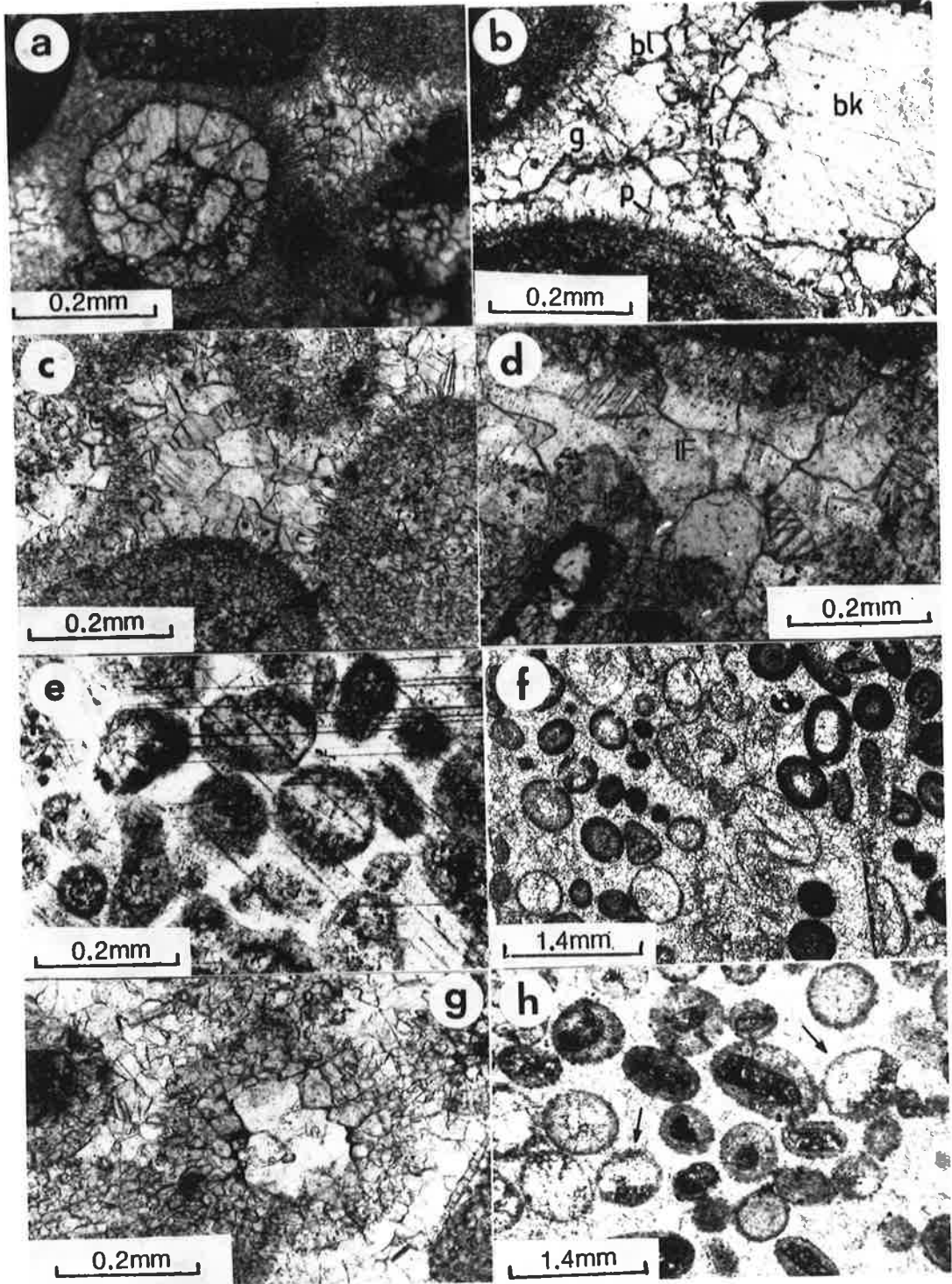
FIG.2.4a: Calcitized ooid of brownish calcite ( type I
ooid fabric ) adjacent to an ooid replaced by blocky
ferroan calcite ( type II ooid fabrics ). The
interparticle cement is of type B with it's elevated Sr
content (ref.figure 2.11).

FIG.2.4b: Type E poikilotopic calcite cement enclosing
peloids. This cement has Sr content between 2000-5000ppm.

FIG.2.4c: Stained acetate peel of type II and type X ooid
fabrics. The type II fabrics are ferroan as are the
nucleii of the type X ooids.

FIG.2.4d: Ooid grainstone comprising Type IX ooids ( arrow
) and type IV ooids.


FIG.2.5: Blocky calcite cement in a cavity, referred to as
fenestral cement. Note the Fe rich zoning and well
developed crystal terminations. Field of view is 4.4mm.


FIG.2.6: Interparticle cement in ooid-intraclast
grainstone with cloudy inclusion rich fringing cement
grading into a clear blocky calcite cement in pore center.
The cloudy fringing cement is referred to as Type D
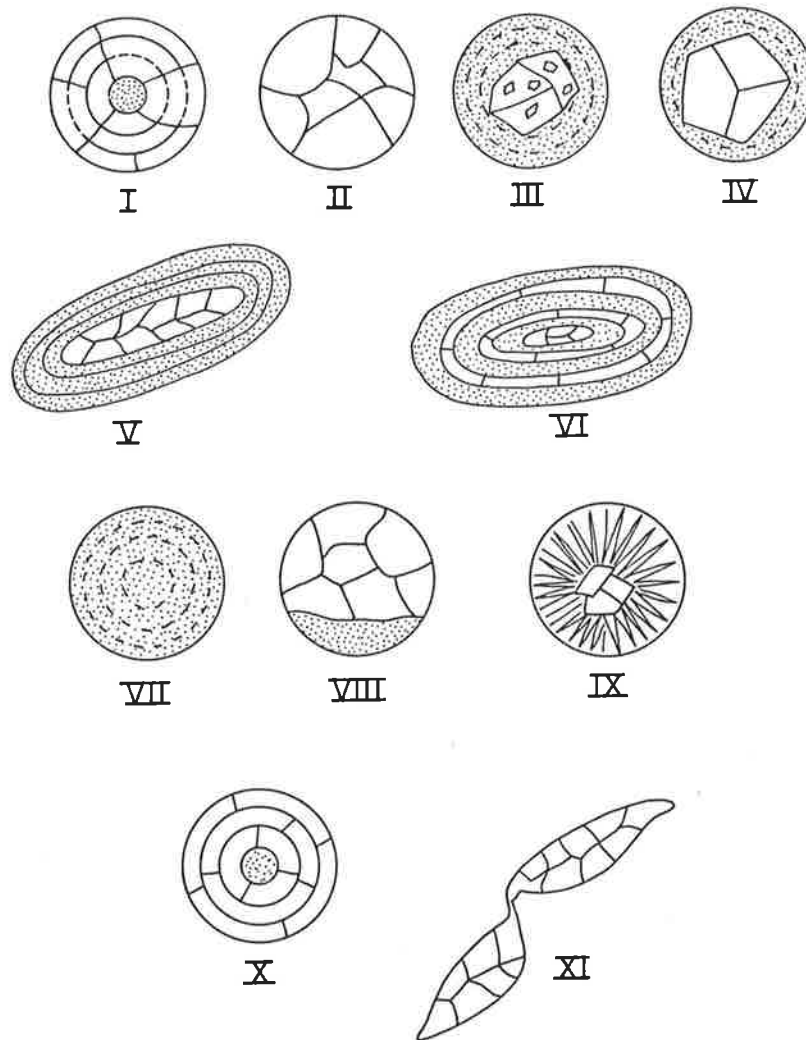cement. Field of view is 4.4mm.
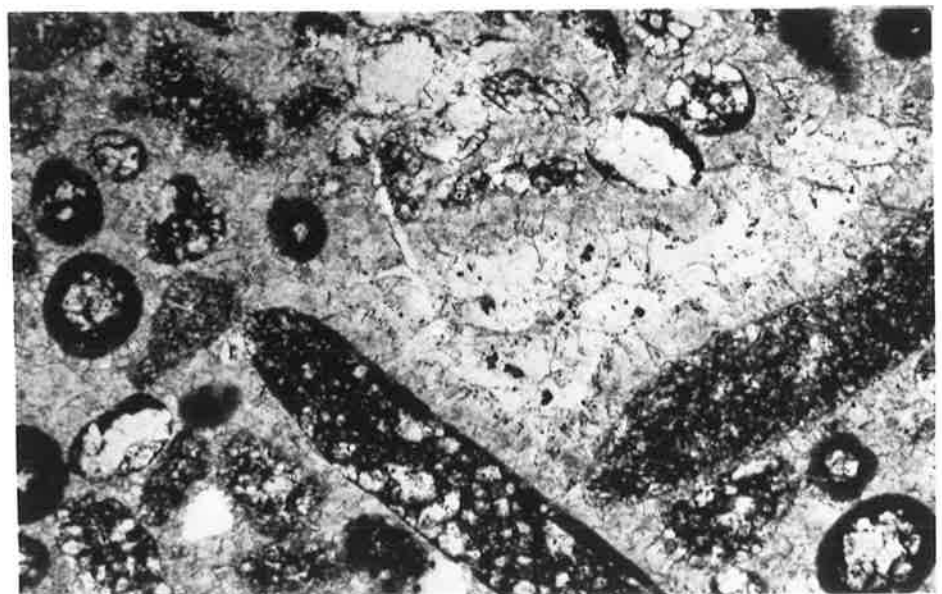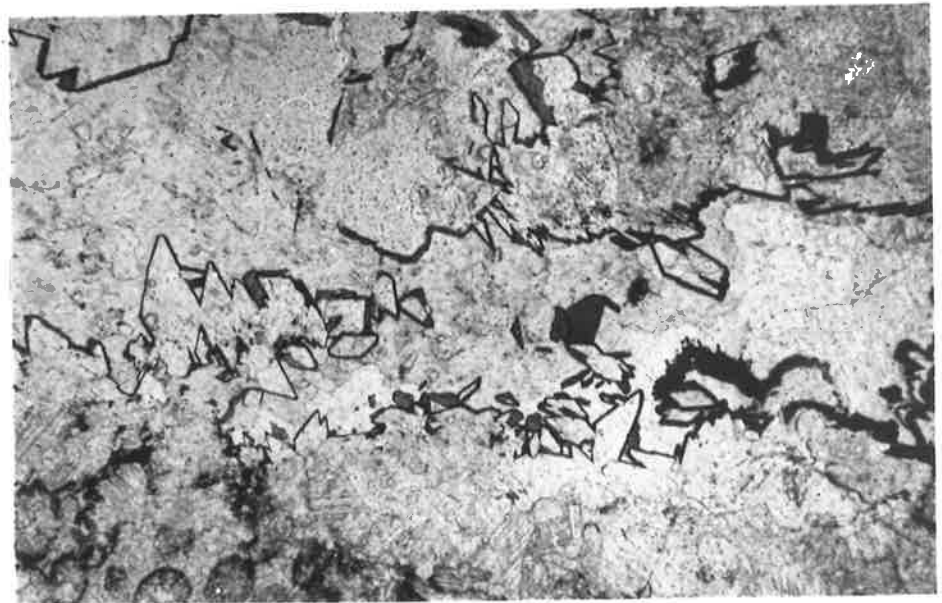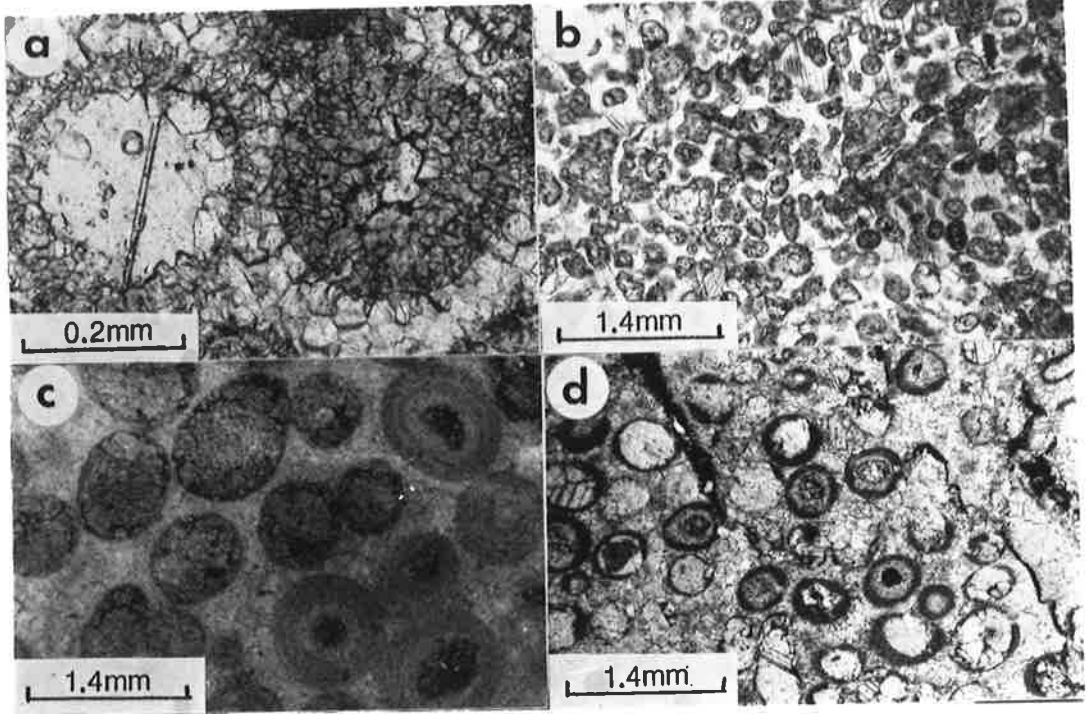
FIG.2.7: Summary of various ooid fabrics in the Trezona

Formation oolites.

I—Coarse neomorphic spar ooids with relict inclusions

II—Ooid molds with void-filling blocky ferroan calcite

III—Micritic ooids with ferroan calcite cores and microdolomite

IV—Micritic ooids with ferroan calcite cores

V—As type IV but with asymmetrical shapes

VI—Ooids with both sparry brick-like and micrite calcite

VII—Micritic ooids

VIII—Half-moon ooids with micritic floors and void-filling ferroan calcite

IX—Ooids in-filled with drusy calcite mosaics

FIG.2.8: Summary of cement fabrics in the Trezona
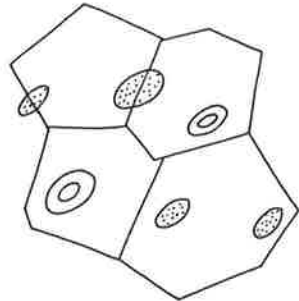Formation oolites.
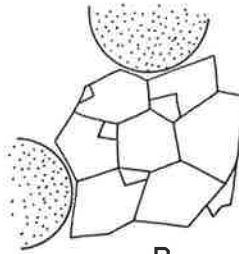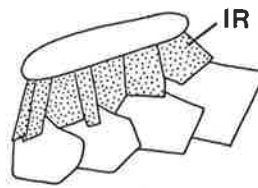
A-Fibrous isopachous cement

B-Non-ferroan equant calcite cement

C-Blocky ferroan calcite cement in oomolds

D-Inclusion rich(IR) subequant calcite cement
   grading into type C cement

E-Coarse non-ferroan calcite cement with
   included relicts of ooids and peloids

FIG.2.9: Trace element data of Trezona Formation components.
Reported values represent the means of between 10 and 20
microprobe analyses. Values in brackets refer to two standard
deviation from mean [2d].

| Sample | Description | Sr(ppm) | Mg(ppm) | Mn(ppm) | Fe(ppm) |
|--------|-------------|---------|---------|---------|---------|

**OOIDS**

| Sample | Description | Sr(ppm) | Mg(ppm) | Mn(ppm) | Fe(ppm) |
|--------|-------------|---------|---------|---------|---------|
| TBG10 | Neomorphic | 4580 (750) | 1310 (380) | b.d. | 3040 (560) |
| TBG17 | Brick-texture | 2770 (460) | 2140 (140) | b.d. | 1920 (420) |
| BG2 | " | 1409 (363) | 5048 (432) | 654 (143) | 1887 (188) |
| TB6 | Micritic | 1720 (300) | 2590 (110) | 280 (50) | 1520 (210) |
| TGC5 | " | 1078 (631) | 4250 (1016) | 258 (125) | 6908 (3136) |
| TB5 | " | 620 (120) | 2590 (90) | 850 (390) | 3550 (1470) |
| TBG17 | " | 1300 (200) | 1442 (76) | 203 (60) | 2492 (277) |
| TB4 | " | 470 (50) | 2820 (320) | 620 (190) | 1870 (200) |
| BG1 | " | 788 (185) | 3243 (638) | 255 (89) | 2339 (278) |
| T9 | " | 708 (272) | 2447 (311) | 557 (151) | 1953 (821) |
| T31 | " | 563 (238) | 4893 (1468) | 258 (180) | 4366 (5826) |
| T8 | " | 1170 (10) | 3110 (20) | 300 (10) | 2370 (130) |
| T16 | " | 1140 (200) | 4330 (1870) | 310 (180) | 2460 (470) |
| TB3 | " | 1280 (150) | 3140 (240) | b.d. | 1440 (90) |

**BOUNDSTONES**

| Sample | Description | Sr(ppm) | Mg(ppm) | Mn(ppm) | Fe(ppm) |
|--------|-------------|---------|---------|---------|---------|
| TB2 | | 3456 (2957) | 3045 (2064) | 367 (343) | 4246 (2742) |
| TAO | | 684 (227) | 3218 (336) | 872 (290) | 2161 (759) |

| Sample | Description | Sr(ppm) | Mg(ppm) | Mn(ppm) | Fe(ppm) |
|--------|-------------|---------|---------|---------|---------|
| **MICRITES** | | | | | |
| TG4 | | 1001 (14) | 3245 (313) | 247 (88) | 4111 (630) |
| TBG11 | | 523 (160) | 1199 (296) | 840 (80) | 6070 (3330) |
| TGC2 | | 3013 (71) | 2485 (618) | 176 (72) | 2368 (197) |
| **CEMENTS** | | | | | |
| TBG16 | Vein spar | 190 (99) | 1132 (369) | 2107 (344) | 2127 (354) |
| TB6 | Blocky inter-particle | 965 (685) | 2020 (10) | 303 (148) | 1495 (715) |
| TG6 | Poikilotopic | 3450 (1600) | 2310 (1010) | b.d. | 2722 (217) |
| BG2 | " | 350 (225) | 3652 (423) | 404 (180) | 2220 (535) |
| TB4 | " | 510 (266) | 2021 (1214) | 570 (685) | 1265 (1046) |
| TBG17 | " | 2203 (1118) | 2099 (802) | 432 (862) | 770 (800) |
| T9 | " | 566 (464) | 4106 (6464) | 628 (481) | 1016 (650) |
| TBG30 | " | 1706 (1731) | 3490 (624) | b.d. | 2520 (1425) |
| TBG11 | " | 703 (20) | 2359 (383) | 316 (92) | 4130 (819) |
| TG6 | Fenestral | 240 (100) | 2850 (920) | 520 (180) | 3850 (123) |
| TG10 | " | b.d. | 404 (106) | 475 (485) | 913 (635) |
| TGC3 | " | 416 (290) | 783 (367) | 467 (245) | 1492 (1250) |
| TBG11 | " | 341 (302) | 2413 (1169) | 976 (345) | 3850 (1013) |
| TGC2 | " | 245 (264) | 426 (197) | 421 (225) | 1612 (775) |

| Sample | Description | Sr(ppm) | Mg(ppm) | Mn(ppm) | Fe(ppm) |
|--------|-------------|---------|---------|---------|---------|
| TBG17 | Blocky intra-particle | 520 (410) | 1680 (480) | 380 (310) | 3340 (1480) |
| T9 | " | 239 (203) | 2127 (896) | 577 (133) | 3213 (2623) |
| TAO | " | 340 (62) | 4659 (408) | 1027 (669) | 4681 (288) |
| TB6 | " | 330 (140) | 1590 (230) | 3120 (270) | 4060 (410) |
| T8 | " | 600 (180) | 3780 (750) | 380 (130) | 3850 (510) |
| T16 | " | 180 (90) | 3660 (270) | 730 (110) | 2960 (400) |
| TB3 | " | 1470 (1250) | 1950 (450) | 310 (280) | 2470 (1380) |
| TB4 | " | 290 (80) | 2720 (660) | 680 (380) | 2800 (640) |
| TBG10 | " | 320 (160) | 3050 (540) | 300 (130) | 3660 (580) |
| TGC5 | " | 370 (213) | 2720 (990) | 468 (165) | 3439 (829) |

FIG.2.10A & B: Trace-element chemistry of the various ooid fabrics determined with the electron microprobe. The fields of the ooid fabrics are defined by two standard deviations from the mean (2d). The ooid fabric types correspond to those in figure 2.4. The number of analyses (N) for each field varied from 10 to 50.
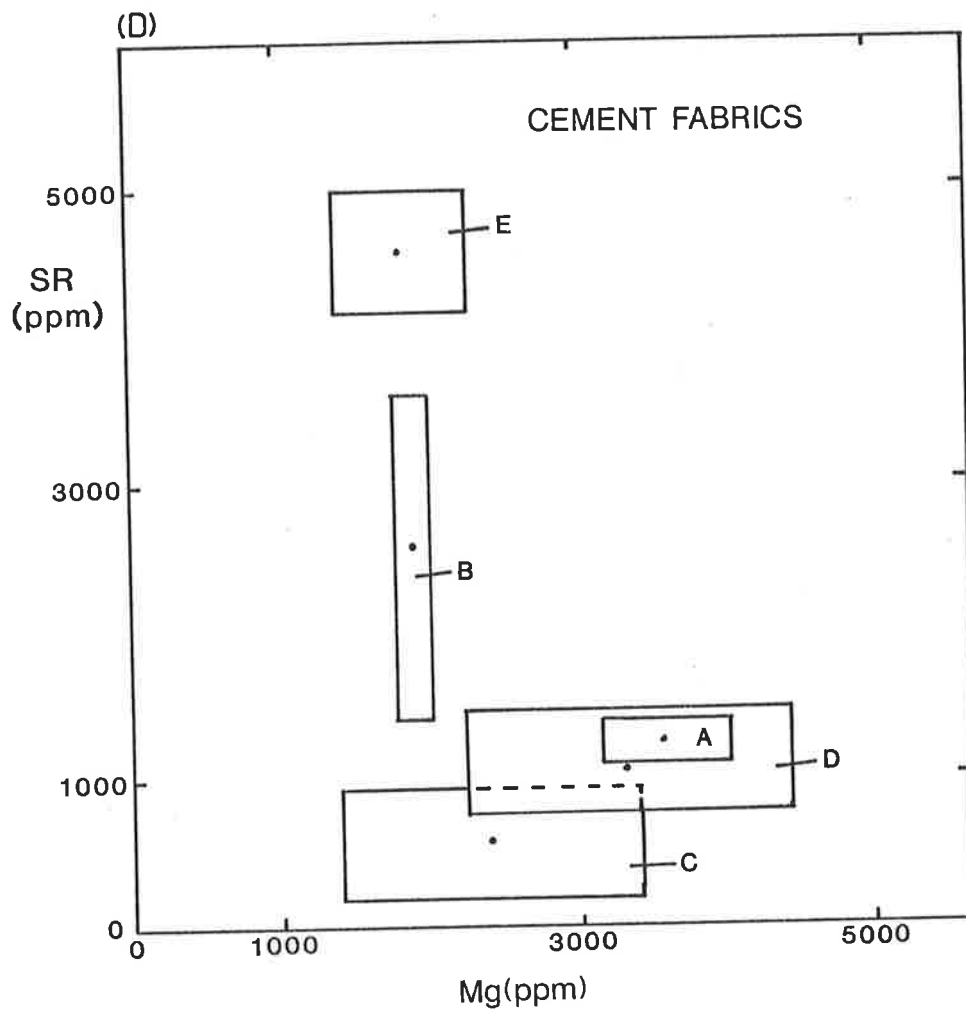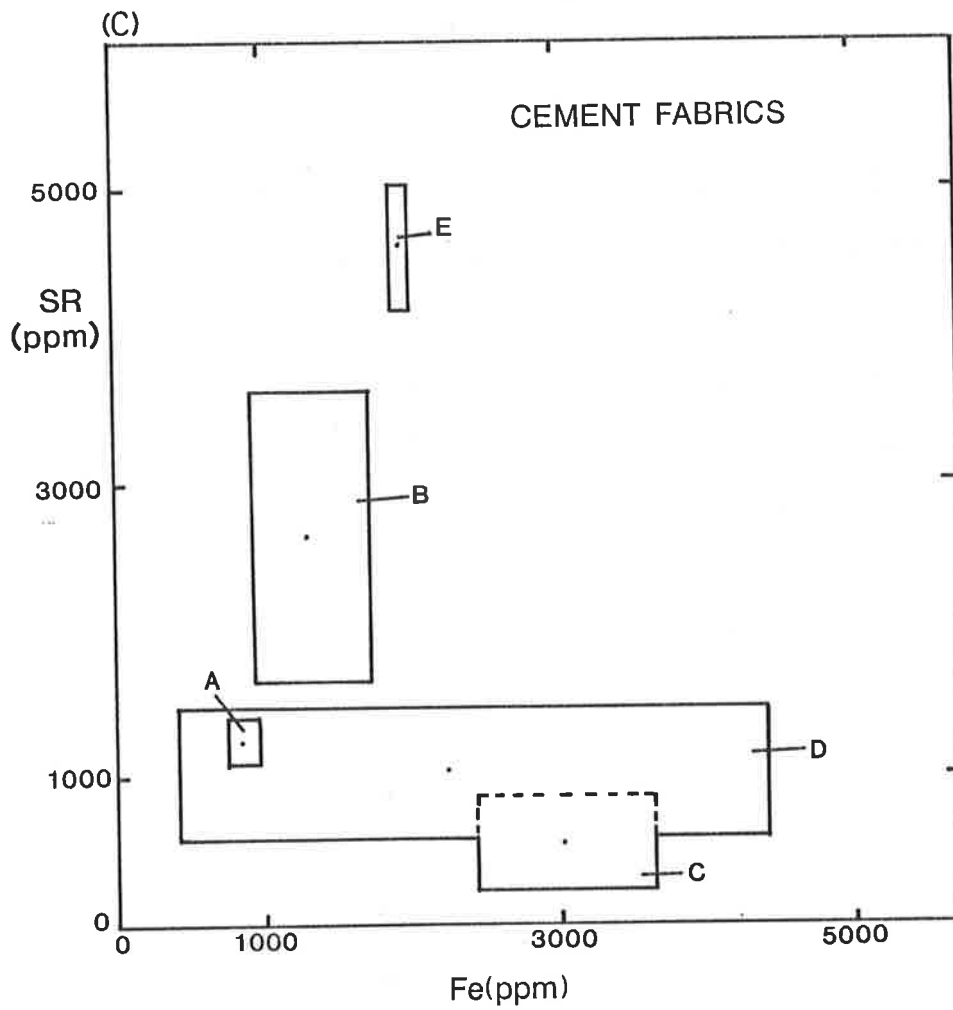
(A) OOID FABRICS

SR (ppm) vs Fe(ppm) plot showing fields I, X, VII, II, III & IV

(B) OOID FABRICS

SR (ppm) vs Mg(ppm) plot showing fields I, X, VII, II, III & IV
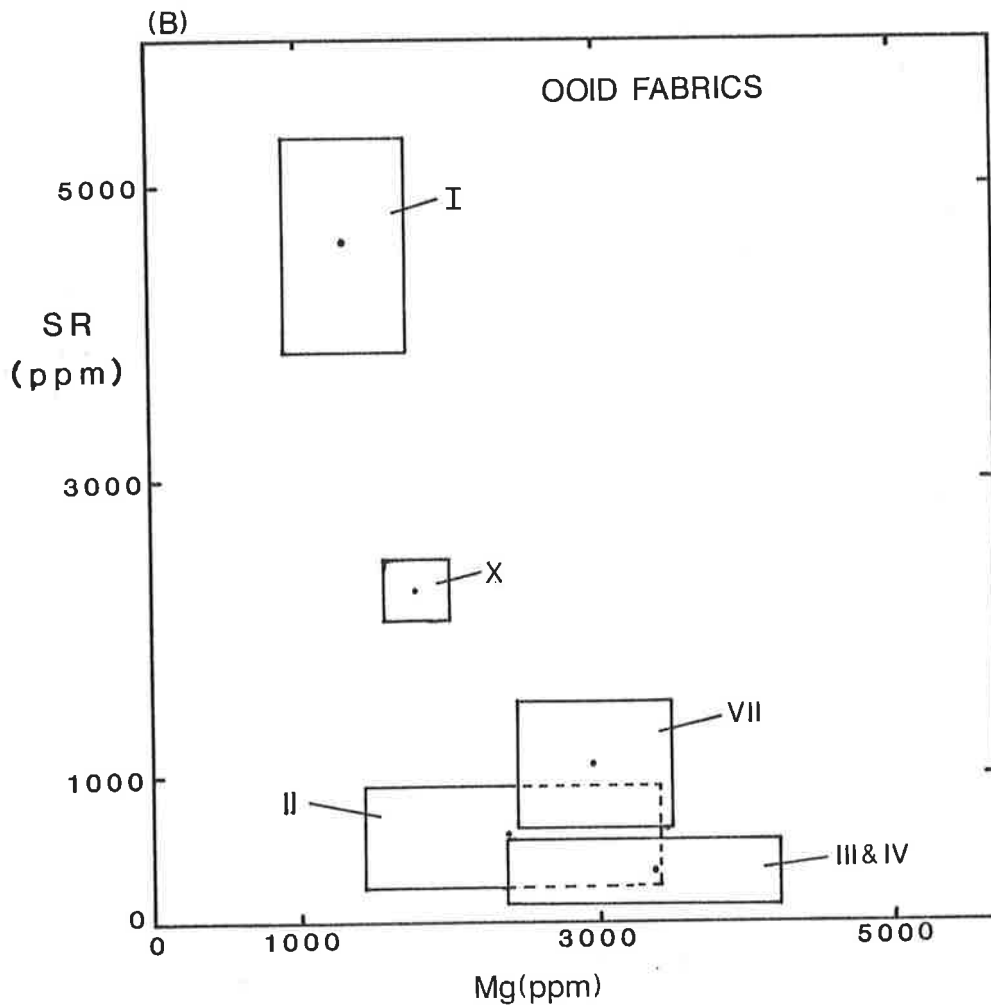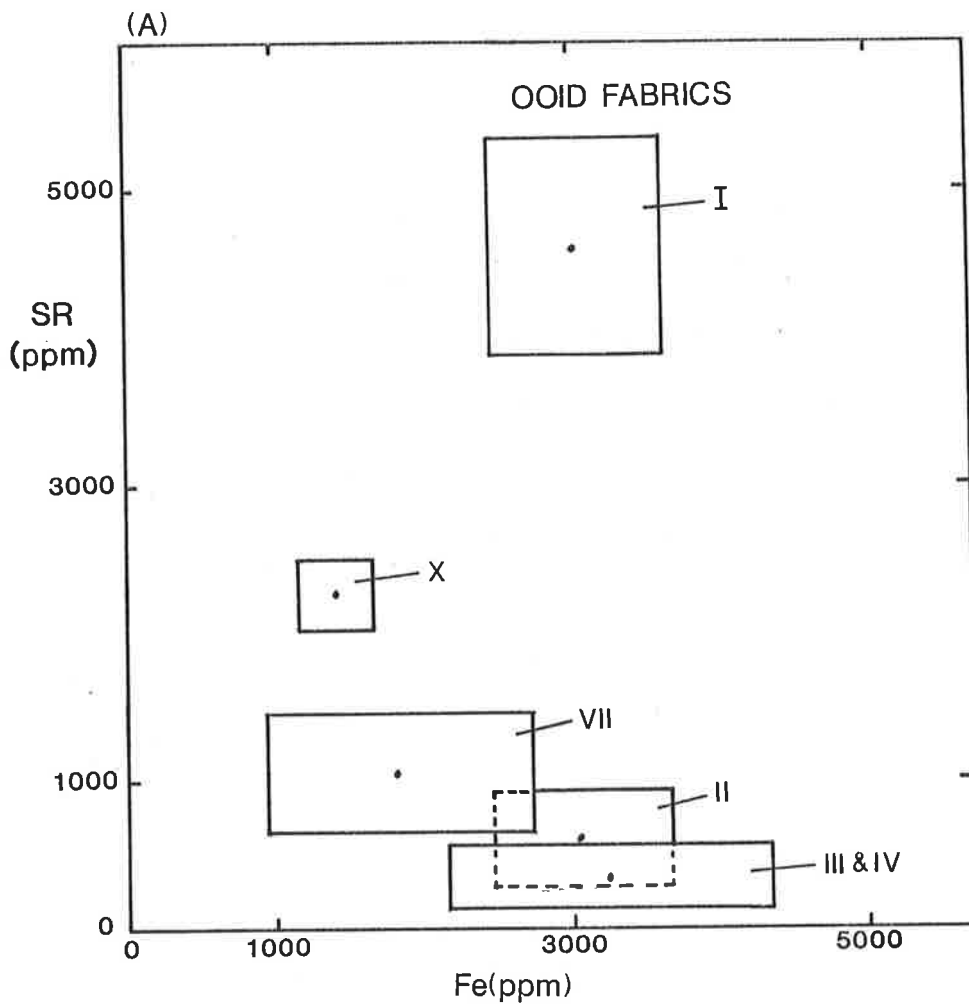
FIG.2.11C & D: Trace-element chemistry of the various cement fabrics determined with the electron microprobe. The fields of the cement fabrics are defined by two standard deviations from the mean (2d). The cement fabric types correspond to those in figure 2.6. The number of analyses (N) for each field varied from 10 to 50.

(C) CEMENT FABRICS

Plot of SR (ppm) versus Fe(ppm) showing labeled fields A, B, C, D, E.

(D) CEMENT FABRICS

Plot of SR (ppm) versus Mg(ppm) showing labeled fields A, B, C, D, E.

FIG.2.12: Schematic diagram of the inferred original ooid
mineralogies and their replacement fabrics.

Aragonitic Ooids    Bimineralic Ooids    Ambiguous

Calcitization

Dissolution-precipitation

VI    I    X    VIII    Microdolomite    III    IV

XI    II    IX

VII    V

Calcite
Aragonite
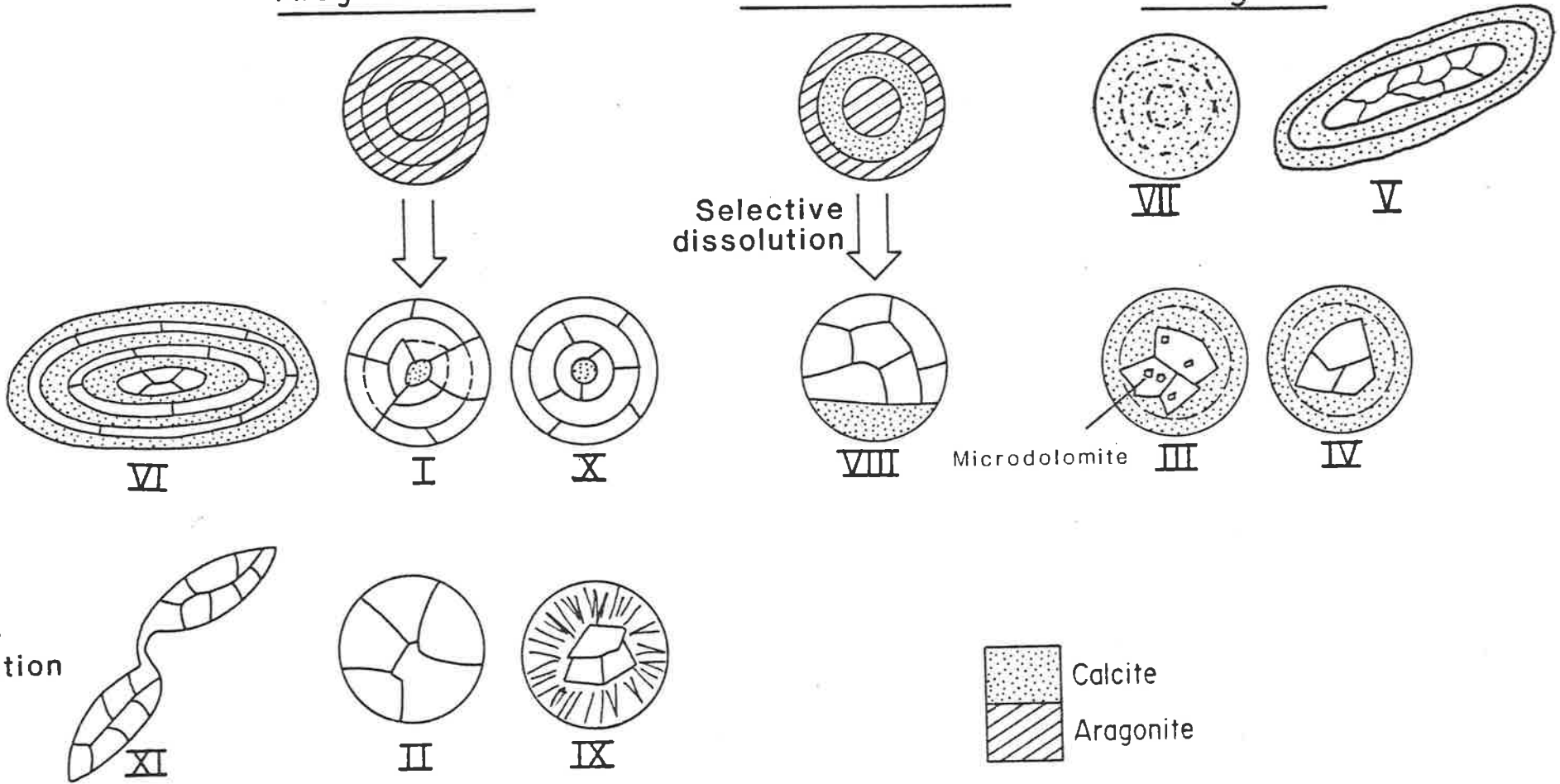
FIG.2.13: STABLE ISOTOPE DATA OF THE TREZONA FORMATION

| Sample | Description | Del O18 | Del C13 |
|--------|-------------|---------|---------|
| **OOIDS** | | | |
| TBG17 | Brick-texture + micritic fabric | -11.03 | -2.70 |
| TB5 | Micritic fabric | -13.89 | -2.90 |
| TBG17 | Micritic fabric | -11.26 | -2.81 |
| T9 | " | -14.74 | -3.96 |
| T31 | " | -9.85 | -3.84 |
| TB4 | " | -13.25 | -3.00 |
| BG1 | " | -10.67 | -3.89 |
| TB6 | " | -11.65 | -2.75 |
| **CEMENTS** | | | |
| TBG16 | Vein calcite | -16.96 | +2.36 |
| TB6 | Blocky inter-particle | -11.61 | -2.86 |
| TB4 | " | -11.33 | -2.29 |
| TBG17 | " | -10.57 | -2.60 |
| T9 | " | -9.76 | -4.14 |
| TBG30 | " | -6.96 | -4.04 |
| TG15 | " | -10.40 | -8.37 |
| TG6 | Poikilotopic cement | -8.73 | -7.04 |
| TG5 | " | -8.77 | -7.37 |
| TG6 | Fenestral cement | -6.48 | -7.66 |
| TG10 | " | -6.06 | -7.02 |
| TGC3 | " | -6.12 | -7.48 |
| TBG11 | " | -6.01 | -6.47 |
| T9 | Blocky intra-particle | -12.09 | -4.66 |
| TAO | " | -9.75 | -7.42 |

| Sample | Description | Del O18 | Del C13 |
|--------|-------------|---------|---------|
| TBG11 | Intermicritic cement | -10.25 | -6.64 |

**CEMENTS + OOIDS**

| Sample | Description | Del O18 | Del C13 |
|--------|-------------|---------|---------|
| T31 | | -9.45 | -5.51 |
| TBG30 | | -9.59 | -4.08 |

**BOUNDSTONES**

| Sample | Description | Del O18 | Del C13 |
|--------|-------------|---------|---------|
| TB2 | Domal stromatolite | -12.64 | -6.45 |
| TBG9 | Columnar stromatolite | -11.10 | -3.52 |
| TAO | " | -11.02 | -7.73 |

**MICRITES**

| Sample | Description | Del O18 | Del C13 |
|--------|-------------|---------|---------|
| TG10 | Micritic intraclast | -8.81 | -6.51 |
| TBG11 | | -11.59 | -6.46 |
| TGC2 | | -10.00 | -6.99 |

**WHOLE ROCKS**

| Sample | Description | Del O18 | Del C13 |
|--------|-------------|---------|---------|
| TGC5 | Ooid grainstone | -10.81 | -4.01 |
| TBG10 | " | -8.50 | -3.12 |
| TGC0 | Ooid intraclastic grainstone | -13.60 | -7.84 |
| TGC3 | " | -12.01 | -7.11 |
| TG10 | " | -8.38 | -7.23 |
| TGC1 | Cryptalgalaminite | -9.76 | -6.61 |
| TG4 | Mudstone | -11.06 | -7.35 |

FIG.2.14: Oxygen and carbon isotope plot of the Late
Precambrian Trezona Formation. Samples dominantly whole
rocks, implying composite isotopic compositions.

TREZONA (MARINOAN)
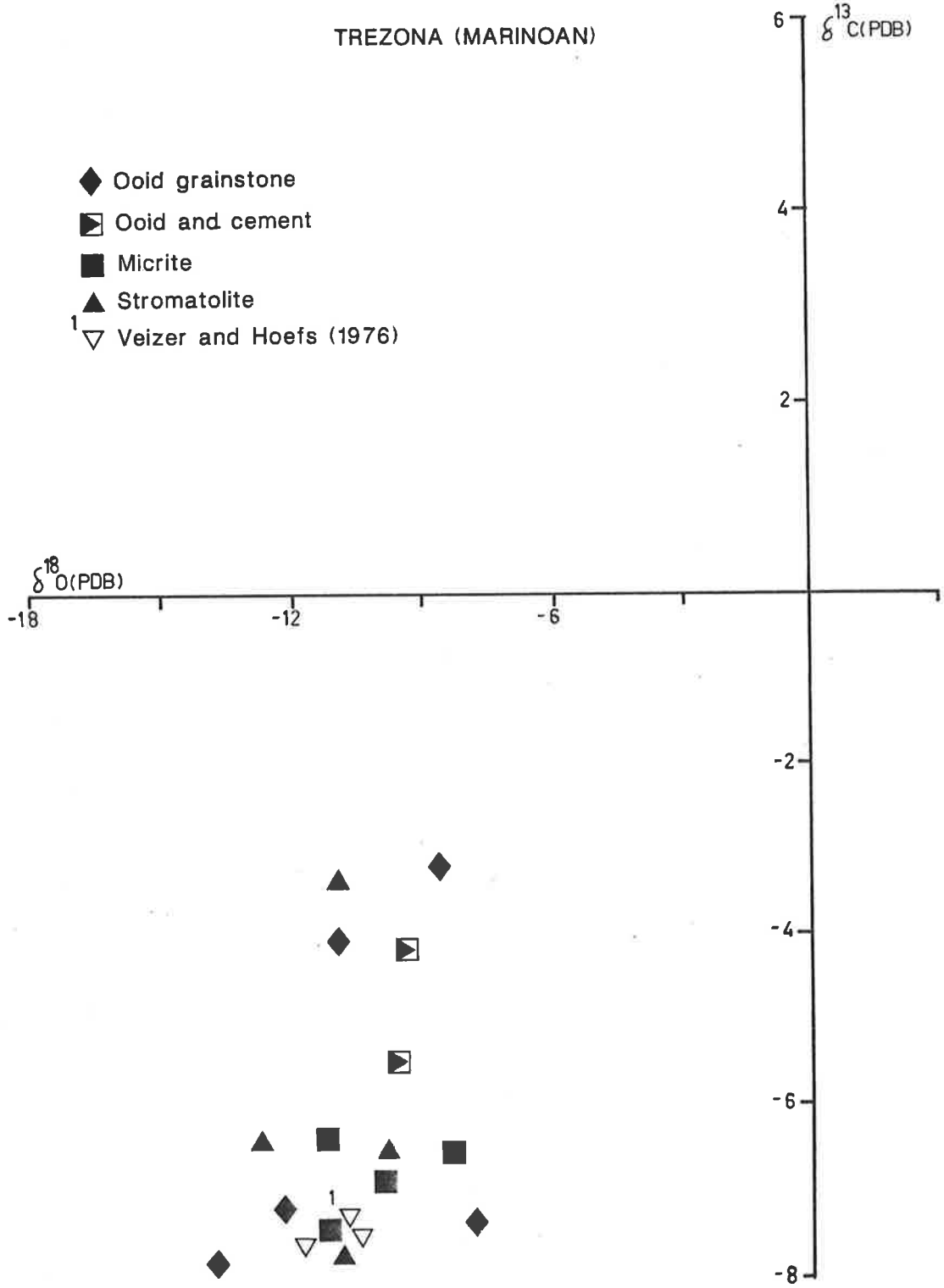
FIG.2.15: Oxygen and carbon isotope plot of the Late

Precambrian Trezona Formation. Samples are of individual

components.
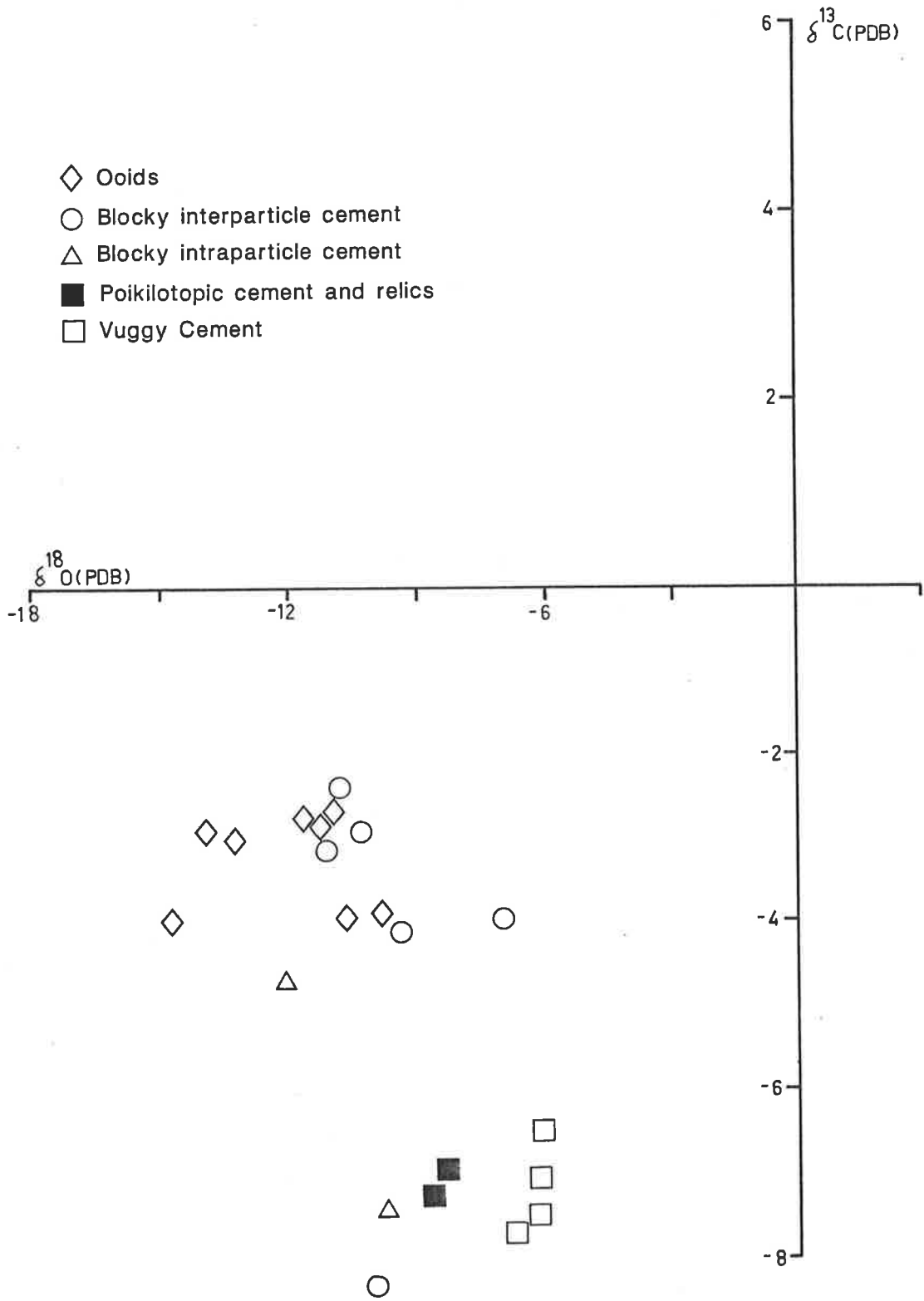
# CHAPTER THREE

## LATE PRECAMBRIAN BALCANOONA FORMATION

### 3.1: INTRODUCTION

The Balcanoona Formation constitutes a limestone-
dolomite sequence between the two Late Precambrian glacigene
formations that overlies the basinal shales of the Tapley
Hill Formation, and is the oldest unit investigated in this
study (Fig.1.2). Within the context of the stratigraphy of
the Adelaide Geosyncline, it represents the topmost unit of
Sturtian age. At it's type section in Nepouie Creek, the
Balcanoona Formation is reported to be approximately 450 ft
thick, but it's thickness is highly variable [ Coats and
Blisset 1971 ]. It thickens north of the type section and in
some areas syndepositional faulting results in thicknesses of
390m east of Arkaroola Homestead. Both it's lower and upper
contacts are transitional showing intertonguing relationships
with the underlying Tapley Hill Formation and the overlying
redbeds of the Angepena Formation. Although confined to the
Northern Flinders Ranges, the Balcanoona Formation has a
southern facies equivalent in the Brighton Limestone
(Fig.1.2).

The Balcanoona Formation consists of a massive, bedded,
dark grey limestone that is oolitic and stromatolitic. The
stromatolites vary from columnar and wavy forms to laterally
linked and laminar types [ Preiss 1971 ]. The top of the
Balcanoona Formation has the development of a buff coloured
fine-grained dolomite facies. The limestone of the Balcanoona
Formation is interpreted to have formed in shallow subtidal
to intertidal environments, with more restrictive supratidal
conditions forming the uppermost dolomite facies. Samples for

this study were obtained from a section in the Munyallina Valley area (Fig.3.1). The sampled horizons were mainly the oolite units although a few stromatolite samples were also studied.

## 3.2: PETROGRAPHY

### 3.2.1: OOIDS

The type of fabrics observed in the ooids of the Balcanoona Formation included half-moon ooids, brick-texture ooids, micritic to microsparitic ooids, sparry ooid molds and compound ooids. Ooid diameters ranged from 0.2mm to a maximum of 5mm, with no correlation between ooid size and fabric type being observed.

Half-Moon Ooids:

These ooids are well developed within the ooid grainstones with the ooid cores comprising characteristic micritic and microsparitic lower halves and coarsely crystalline blocky spar upper halves (Figs.3.2 & 3.3). There is a range of sizes of ooids with this half-moon ooid fabric, from 0.8mm to 2mm. The thickness of the micritic to microsparitic envelopes in these ooids also varies and commonly constitutes a minor proportion of the total ooid size. These envelopes in some cases have composite fabrics; inner cortical layers are darker, with a finer grain size compared to the lighter and larger crystals of the outer layers. There is a distinct difference in fabric of these cortical layers with inner micritic layers and outer brick-texture layers (Fig.3.6).

Brick-Texture Ooids:

This type of ooid refers to the fabric of the cortical

48

layers, which are made of a mosaic of calcite spar with rectangular shapes, resembling a layer of bricks (Figs.3.6 & 3.7). The concentric nature of the cortical layers is well developed. In some cases, the individual brick-like calcite crystals are not confined to single cortical layers but transect a few adjacent layers. Such brick-texture fabrics can comprise whole ooids or are developed in the outer parts of some ooid cortices, with the inner parts being micritic and having indistinct cortical laminations (Fig.3.6).

Micritic Ooids:

These ooids have cortical layers of randomly oriented micritic to microsparitic calcite. Most micritic ooids are homogenous with no distinct nucleus and vague cortical laminations (Fig.3.5). The nucleus, where discernible, comprises a sparry calcite mosaic. In some of the larger micritic ooids these cortical layers are more distinct. The sizes of these ooids range from 0.7mm to as large as 5mm in some cases. The larger ooids have less spherical shapes compared to the smaller micritic ooids.

Sparry ooid molds:

Some ooids are made of blocky ferroan calcite mosaics. The calcite spar has a void filling nature with its increasing crystal size from ooid margins to void center (Figs.3.4 & 3.5). These sparry ooid molds occur either with micritic envelopes, resembling superficial ooids, or comprise totally of blocky calcites.

Compound Ooids:

Occasionally two or more ooids are bound together with an envelope forming compound ooids (Fig.3.8). The diameters of these ooids can be as large as 3mm. The envelopes can be

micritic or sparry with a brick-texture fabric. The shapes of these compound ooids are normally asymmetrical.

### 3.2.2: CEMENTS

There are two types of calcite cements that were recognised in the ooid grainstones; fringing bladed cements and blocky cements. The bladed cements are rare and found fringing some ooids. The blocky cements are the dominant type and occur either as interparticle non-ferroan, blocky calcite cement or as intraparticle ferroan, blocky calcite cement (Figs.3.3 & 3.12). Some blocky calcites are associated with stromatolite laminae, where they form light sparry layers alternating with dark micritic layers (Fig.3.13). Replacement of ooid cores by dolomite is fairly pervasive in some ooid grainstones (Fig.3.10). The dolomite occurs as granular mosaics within ooids that show evidence of compaction with distorted shapes and grain-to-grain contacts. Occasionally ooid cores have large rhomb-shaped dolomite spar within a blocky calcite mosaic. The dolomite represents a late diagenetic phase and is associated with the intraparticle blocky ferroan calcites. The genesis and timing of dolomitization was not investigated and only the associated blocky calcite cements are discussed further.

Interparticle Cement:

These cements occupy the pore-spaces between ooids and other grains in the ooid grainstones. They are quite similar to the intraparticle cements texturally, but are non-ferroan and have a turbid to brownish appearance in plain light (Fig.3.12). There is generally a lack of any early fringing cements, since bladed cements are rare,  and this blocky

50

calcite spar seems to be the dominant cement generation between ooids (Fig.3.11).

Intraparticle Cement:

Their ferroan and clear, inclusion-free nature distinguishes them from the interparticle cements (Figs.3.3 & 3.12). Spatially they are generally confined within ooids and intraclast with the crystal size increasing from pore margins to centers. Some interparticle spaces do have this ferroan calcite spar occurring as a final pore-occluding stage, but this is rare.

## 3.3: TRACE ELEMENT CHEMISTRY

A total of 23 separate components involving 230 to 460 individual microprobe analysis were used to generate the trace element data.

### 3.3.1: OOIDS

The ooids have a large range of Sr contents, with the brick-texture ooids recording the highest Sr values ($\sim$ 1600 ppm ). Micritic ooids have Sr content that varies from 1300 ppm to 400 ppm (Fig.3.14). The Mn content of most of the ooids was below detection limits on the microprobe and appears to be independent of the Sr content (Fig.3.15). The Sr vs Fe plot, however, shows a negative correlation (Fig.3.16). The Mg content of the ooids ranges from 2000 ppm to 4200 ppm (Fig.3.17). The trace element fields for the ooid molds and the half-moon ooids are not represented because, comprising dominantly of blocky calcites, their trace element content is similar to that of the intraparticle cements (Figs.3.18 to 3.20). There was no discernible difference in the trace element chemistry of the micritic part of the half-moon ooid

51

fabric from that of the micritic ooids either.

## 3.3.2: CEMENTS

The trace element chemistry of the three major cement types i.e. blocky interparticle cements, blocky intraparticle cements and blocky cements associated with stromatolite laminae, define separate fields in terms of trace element concentrations (Figs.3.18 to 3.20).

The difference between the blocky interparticle cements and the intraparticle cements is in their Fe and Mn contents (Figs.3.18,3.19). Interparticle cements have lower amounts of Mn and Fe ( <200ppm to 300ppm Mn; 500ppm to 1100ppm Fe ) compared to the intraparticle cements ( 400ppm to 520ppm Mn; 1400ppm to 2600ppm Fe ). Their Sr content has a fairly similar range, varying from < 200ppm to 1000ppm. Although their Mg content is similar (Fig.3.20), the intraparticle cements have a larger spread of Mg values ( 1400ppm to 2700ppm ) compared to the interparticle cements ( 1800ppm to 2600ppm ) .

The blocky cements associated with stromatolite laminae record very high Sr ( 1700ppm to 4100ppm ) and Mg ( 3000ppm to 3600ppm ) contents. They are very low in Mn content, being below the detection limit on the microprobe ( < 200ppm ). Iron content shows a large spread ranging from about 1000ppm to 2900ppm.

## 3.4: OOID INTERPRETATION

All the ooid fabrics observed in the Balcanoona Formation oolites are also developed in the Trezona Formation oolites and their interpretion remains essentially the same as that discussed for the Trezona Formation ooids (section

52

2.4). Half-moon ooid fabrics are however, much more
extensively and better developed in the Balcanoona Formation
oolites.

Some of the ooid fabrics within the Balcanoona Formation
suggest the presence of aragonite precursors. The brick-
texture ooids are interpreted to have had an originally
aragonitic mineralogy, as discussed in the section on the
Trezona Formation oolites. They have been described by other
workers and have been similarly interpreted [ Assereto and
Folk 1976; Sandberg 1985; Tucker 1985 ]. Such an
interpretation is supported by the trace element chemistry,
with the brick-texture ooids recording high Sr content. This
retention of the original cortical layering and the high Sr
content implies limited recrystallization and the presence of
a relatively closed system [ Sandberg 1985; Wardlaw et
al.1978; Pinqitore 1976 ].

Half-moon ooids may have resulted from the preferential
dissolution of metastable aragonitic cortical layers with the
partial collapse of the ooid cortex, forming a cavity floored
by micritic/microsparitic sediment [Carozzi 1963]. The upper
half is later filled by blocky ferroan calcite. Such fabrics
could also develop from the dissolution of gypsum cortical
layers, but there is no evidence to suggest presence of
intense evaporitic conditions during deposition of the
Balcanoona Formation oolites.

The sparry ooid molds could represent original
aragonitic ooids, which were dissolved and replaced by blocky
ferroan calcite. Alternatively, such ooid fabrics could also
be generated from originally calcitic ooids, possibly under
burial conditions [ Sandberg 1983 ]. There is evidence of

burial diagenetic alteration with pressure-solution features and distorted and compacted ooids within the Balcanoona Formation oolites. Unlike in the Trezona Formation oolites, no composite ooid fabrics with both calcitized neomorphic spar and blocky calcite within the same ooid were found in the Balcanoona Formation. The original mineralogy of the sparry ooid molds therefore remains uncertain, although their close association with micritic ooids and the dichotomous diagenetic behaviour seems to favour an aragonitic mineralogy.

Micritic ooids remain ambiguous since they could be either micritized aragonitic ooids or originally calcitic ooids with a random micritic fabric [Wilkinson,Owen and Carrol 1985]. These possibilities were discussed in the section on the Trezona Formation oolites (section 2.4). If one interprets the original mineralogy of the micritic ooids as being calcitic, then there is a problem with the high Sr content of some of the micritic ooids (~ 1200 ppm ). Some micritic ooids seem to have a "micro" brick-texture which is hard to resolve under the light microscope. If these apparently micritic ooids do have a "micro" brick-texture, suggesting an original aragonitic mineralogy, then the high Sr content could be explained to some extent. The problem of the interpretation of the precursor mineralogy of the micritic ooids therefore remains unresolved.

## 3.5: CEMENT INTERPRETATION

Bladed fringing cements commonly coat grains in many shallow marine carbonates [Bricker 1971]. They can form either in marine environments or in the shallow subsurface

mixing or meteoric environments. These cements represent the first phase of cementation in the ooid grainstones and probably formed in diagenetic settings that had stronger marine influence compared to those resulting in the blocky cements.

The blocky interparticle calcite cements are interpreted as shallow subsurface phreatic precipitates and the blocky intraparticle calcite cements represent later precipitates in the deep burial environment. The later origin of the intraparticle cements is supported by the occurrence of blocky ferroan calcites, similar to the intraparticle cements, as pore-occluding phases within some interparticle areas. Also, the presence of ooid molds that have suffered compaction without affecting the in-filling intraparticle calcite cements suggests a deep burial origin for these cements.

These intraparticle calcite cements have a ferroan nature, probably from the reducing conditions found in burial environments. In contrast the interparticle calcite cements are non-ferroan, the result of precipitation from oxygenated pore-waters in the shallow subsurface environment. Although generally low in Mn, some of the interparticle calcite cements have high Mn contents, probably reflecting the ability of $Mn^{2+}$ to occur in more oxidizing waters than $Fe^{2+}$ [ Garrells and Christ 1965; Meyers and Lohmann 1980 ].

The Sr content of diagenetic blocky calcites is normally a few hundred ppm. The Sr content of some of the blocky interparticle cements is higher than normally found in diagentic calcites [ Kinsman 1969; Morrows and Mayers 1978; Veizer 1985 ]. The Sr content of the blocky calcites in

stromatolite laminae are even higher than those found in some of the interparticle calcite cements. Their genesis is not adequately understood and is discussed in section 7.4 in the concluding chapter. High Sr content in calcites can result from either precipitation in Sr enriched pore-waters or from neomorphic alteration of aragonitic precursors. There is a lack of calcitization fabrics within the interparticle calcite cements of the Balcanoona Formation oolites, discounting the possibility of an aragonite precursor. Incomplete understanding of the partition coefficients for Sr under varying diagenetic settings probably contributes to the problem of the interpretation of these strontium rich blocky calcites.

## 3.6: OXYGEN AND CARBON ISOTOPES

A total of 15 samples were analysed and the oxygen and carbon isotope plot of the Balcanoona Formation carbonates is distinctly different from that of the Trezona Formation in terms of their carbon signatures (Figs.3.21 & 3.22). The oxygen isotopes of the various components range from -4 permil to -12 permil. Carbon recorded a much larger range, from 1 permil to 9 permil. There is considerable scatter in both the oxygen and carbon isotopes, much like that obtained from the Trezona Formation. If one considers the oxygen and carbon signatures of the various components separately, however, they generally plot in fairly distinct fields.

The blocky interparticle cements show a trend of increasingly lighter oxygen with lighter carbon. This trend is a commonly observed one in carbonates, representing increasing diagenetic modification with meteoric pore-waters.

The blocky intraparticle cements are much lighter in both oxygen and carbon. Their lighter oxygen signature is probably the result of equilibration with either pore-waters of lighter isotopic composition and/or precipitation at higher temperatures with increasing burial. The higher precipitation temperatures would be consistent with the interpretation of a burial origin for these cements.

The oxygen and carbon compositions of the micritic ooids are distinctly different from those of the blocky cements. They are lighter in oxygen than the associated blocky interparticle cements, their oxygen composition being similar to the blocky intraparticle cements. They are significantly heavier in their carbon compositions compared to the intraparticle cements. The much lighter carbon composition of one ooid analysis was probably due to it's greater diagenetic alteration; it had the highest Fe content amongst the micritic ooids. The lighter oxygen composition of the ooids might be the result of recrystallization under burial conditions, after precipitation of the interparticle cements at shallow subsurface settings.

Such heavy carbon compositions are unusual and are normally associated with evaporitic environments [ Marowsky 1969; Harwood and Coleman 1983] or during anaerobic fermentation-decomposition of organic matter [ Irwin et al. 1977]. This heavy carbon excursion for the Balcanoona was also recorded by Schidlowski et al.[1975, Table XVI ] and Veizer and Hoefs [1976,Appendix 1]. Although Veizer and Hoefs [1976] did not record such large positive carbon values as those recorded from the ooids of this study, they did reveal a trend of heavy carbon in the Sturtian. Since they analysed

whole rock samples, it is possible their lower carbon values could be due to the incorporation of lighter diagenetic carbon.

Unusually heavy carbon carbonates are known from various Precambrian formations in different parts of the world [Schidlowski et al.1975]. These include the Lomagundi dolomites (Rhodesia), Karelian carbonates (Fennoscandia), Eleonore Bay Formation (East Greenland) and the Indian "Puranas". All of them have mean carbon values of +3 per mil to +5 per mil except the Lomagundi dolomites (+9.4 per mil = 2 per mil). Since the carbon isotopic composition is dependent on the contribution of carbon from the organic carbon and carbonate carbon reservoirs, the heavy carbon values reflect an increased Corg/Ccarb ratio. Increases in the burial rate or preservation of organic carbon will cause such increases in the Corg/Ccarb ratio. The increased burial rate could be due to increased organic productivity or increased preservation of organic carbon due to expansion in the oxygen minimum layer in ocean waters. The Phanerozoic carbonate record also has such heavy carbon excursions preserved in Permian and Cretaceous limestones [Holser et al.1986; Scholle and Arthur 1980 ].

It can be argued that the heavy carbon composition of the Balcanoona Formation is due to sedimentation in restricted to semi-restricted, possibly even lacustrine environments. Sedimentation of the Balcanoona Formation occurred in peritidal settings with possible supratidal conditions forming the upper dolomite facies. There was no evidence of any evaporites and the samples analysed for stable isotopes were dominantly from oolite units, formed in

comparatively open marine settings. The highest carbon compositions were recorded from these oolite units and the associated stromatolite and dolomitic units had much lower carbon compositions.

Moreover, there is evidence to suggest that restricted or evaporitic environments do not necessarily record unusually heavy carbon compositions. This has been argued by Magaritz et al. (1983) and in Holser et al.(1986), when explaining the Permian carbon anomaly. Although evaporitic sequences do record heavy carbon compositions, such excursions occur even in associated or underlying and overlying non-evaporitic sediments. Also, the non-evaporitic sediments normally record the heaviest carbon compositions in some Late Proterozoic sequences [Knoll et al. 1986; Tucker 1986].

Therefore, while heavy carbon compositions can and do occur in sediments deposited in restricted and evaporitic settings, sediments from non-restricted environments also record these heavy carbon compositions and they are normally heavier in these sediments. The validity of such heavy carbon compositions being of primary rather than secondary or diagenetic origin has gained support from some recent studies, where the associated organic carbon in the carbonates was analysed [Knoll et al. 1986]. It was shown that both the carbonate carbon and organic carbon recorded similar trends.

Based on the above facts then, it is inferred that the heavy carbon composition of the Balcanoona Formation carbonates is probably primary and related to the marine water chemistry and the Corg/Ccarb ratio in such waters

during Sturtian times (Balcanoona Formation). The question of whether this positive carbon anomaly in the Balcanoona Formation is of global or local extent is discussed in section 7.5 of the concluding chapter.

## 3.7: SUMMARY

The petrographic and geochemical investigations of the Balcanoona Formation oolites reveals a number of interesting features. Texturally, some of the ooids are well preserved with calcitized fabrics, indicative of an aragonitic precursor. This is evidenced by the presence of ooids with brick-texture cortical fabrics. In addition sparry ooid molds suggest leaching of the precursor carbonate (?aragonite). The presence of half-moon ooids could indicate possible bimineralic ooids. Unfortunately, the precursor mineralogy of the micritic ooids could not be determined with the same degree of confidence and remains uncertain.

Supporting evidence for an aragonitic precursor for the brick-texture ooids is found in their high Sr content. Some blocky calcite cements within the oolites record unusually high Sr content, as do sparry laminae within stromatolites. Although the high Sr content suggests the possibility of an aragonitic precursor for these cements, it is not supported by textural data. The genesis of these high Sr blocky calcites therefore is not understood and remains unresolved.

The oxygen and carbon stable isotope compositions of the Balcanoona Formation defines a fairly distinct field from that of the Trezona Formation. The carbon isotopes are significantly heavier than the Trezona Formation, recording positive values of between 1 permil and 9 permil. The oxygen

isotopes are fairly similar to the Trezona Formation and range from -4 permil to -12 permil.

FIG.3.1: Location map of the Munyallina Valley sample area for the Late Precambrian Balcanoona Formation (Based on Copley 1:250,000 sheet).

| CAMBRIAN | ⧄ | DIAPIR | ▦ | 0 | | 25km |
| PRECAMBRIAN | ⣿ | BASEMENT | + + + / + + + | | | |
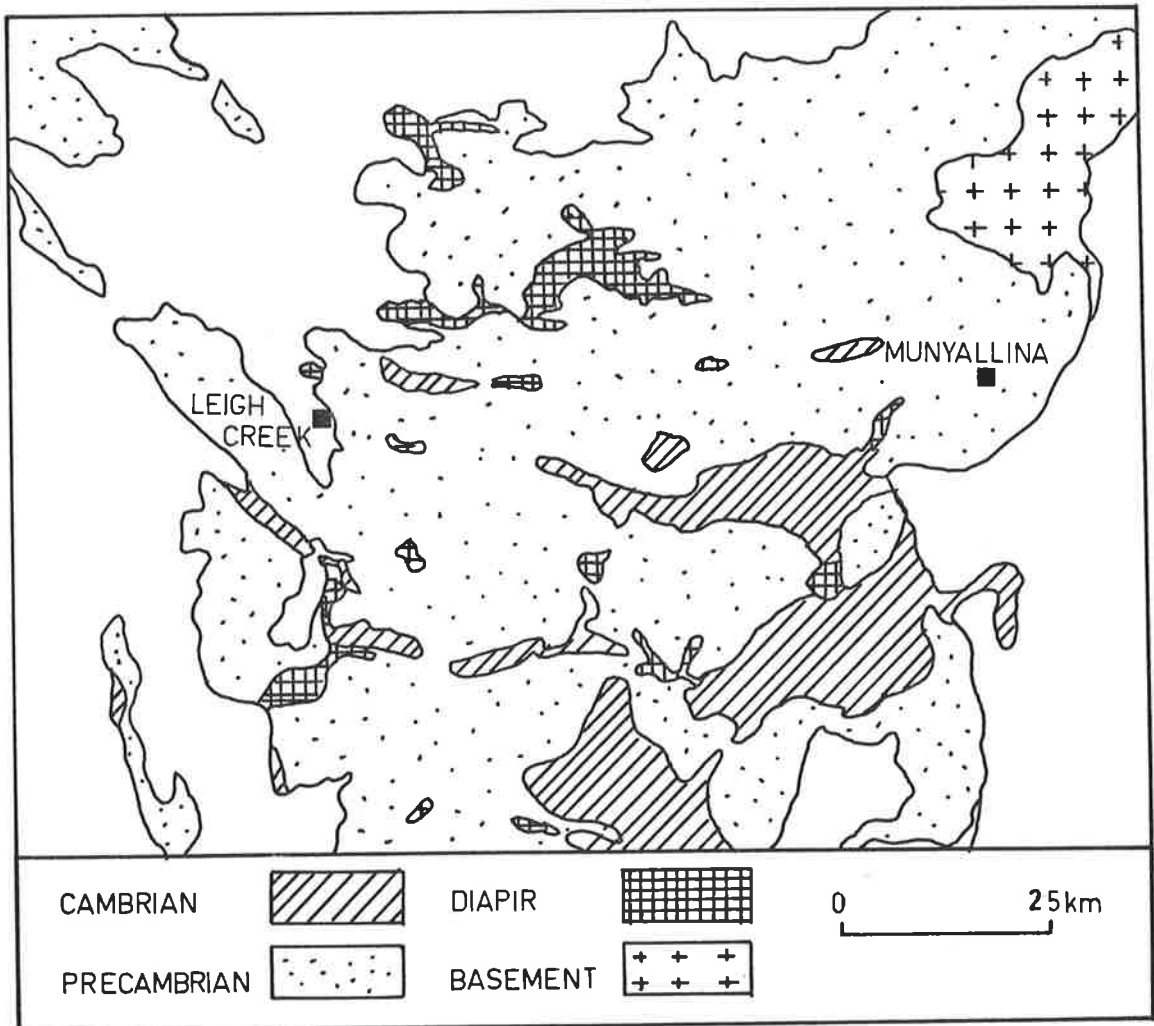
FIG.3.2: Half-moon ooids in the Balcanoona Formation with peloidal intraclast and interparticle micrite. Field of view is 4.4mm.

FIG.3.3: Close-up of half-moon ooid with sparry top and microsparitic bottom. Field of view is 1.1mm.

FIG.3.4: Micritic ooid with spar replaced center. Interparticle cement is of blocky calcite. Field of view is 1.1mm.
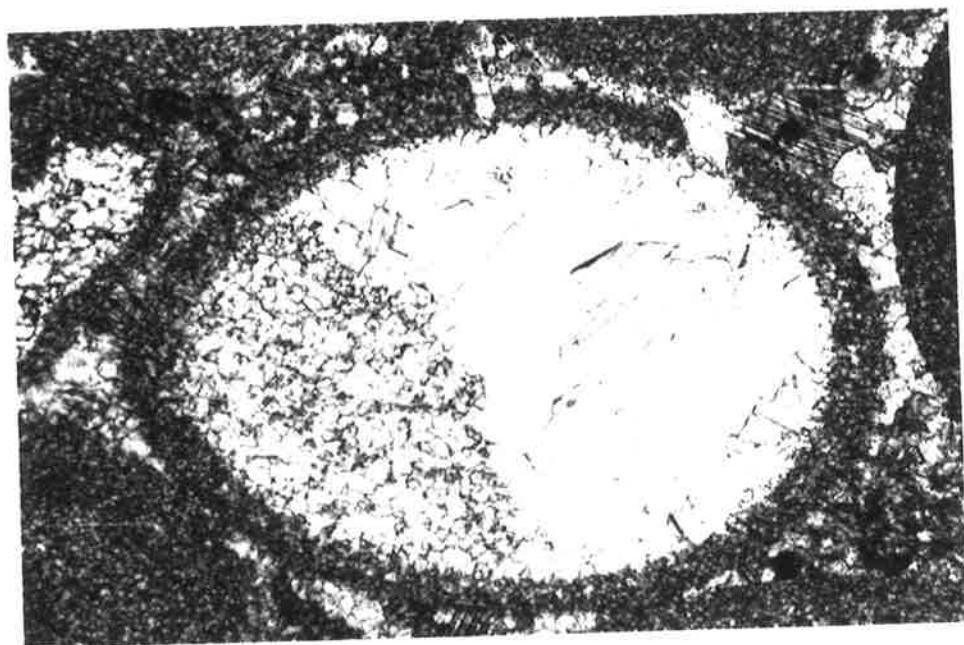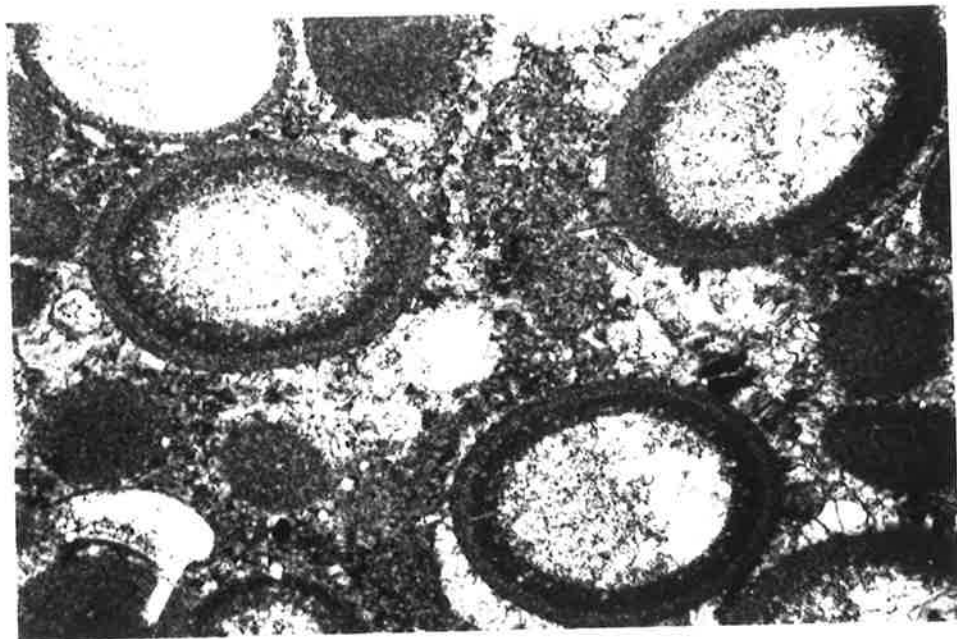
FIG.3.5: Micritic ooids with concentric cortical layers in the ooid at lower left. Some of the ooids are completely replaced by sparry calcite. Field of view is 4.4mm.

FIG.3.6: Ooid with a composite fabric comprising a inner micritic cortex and an outer brick-texture cortex. Ooid core has been replaced by blocky calcite. Field of view is 1.1mm.

FIG.3.7: Close-up of brick-texture cortical layers. Field of view is 1.1mm.
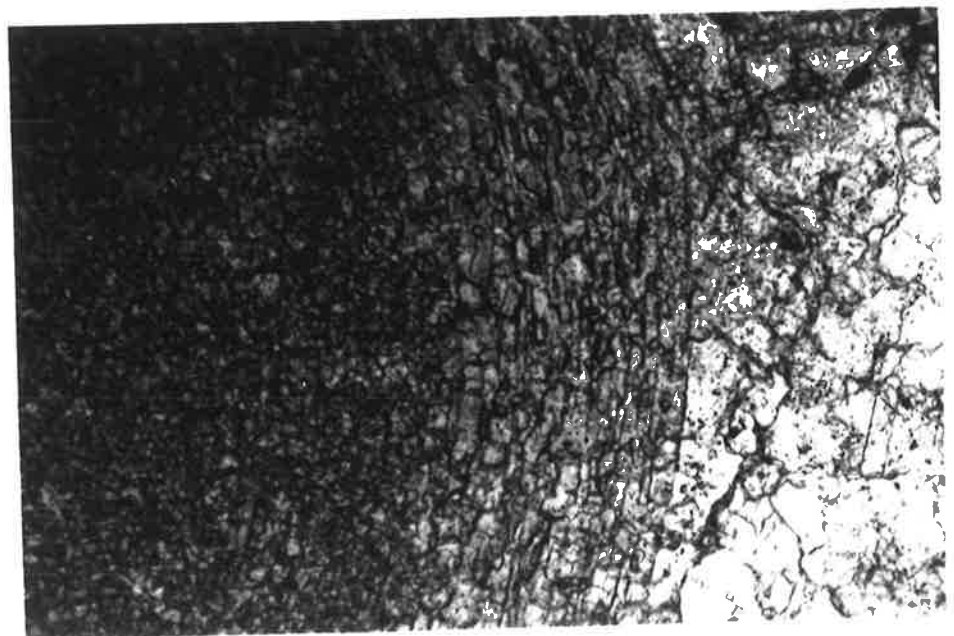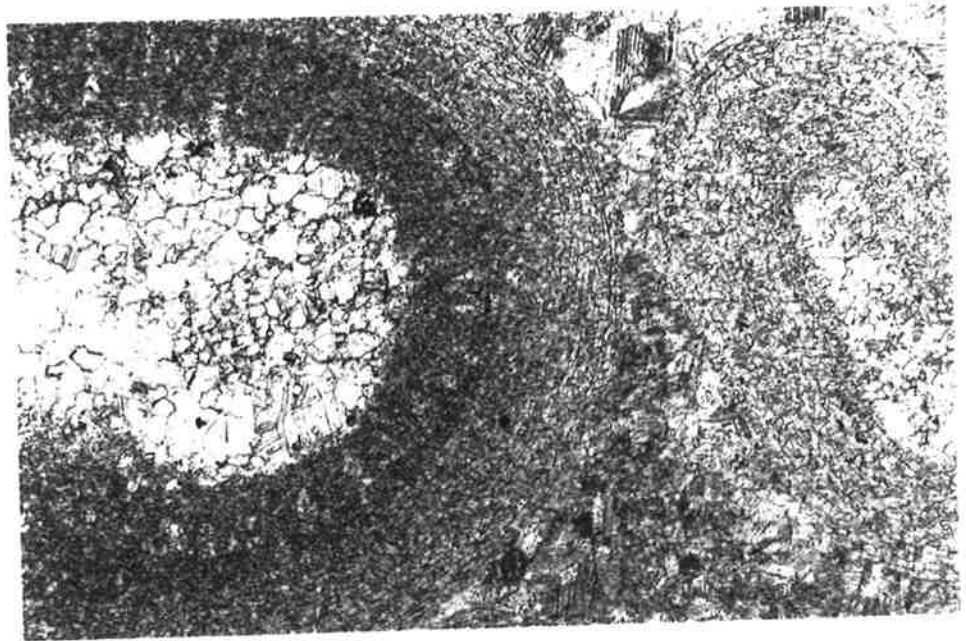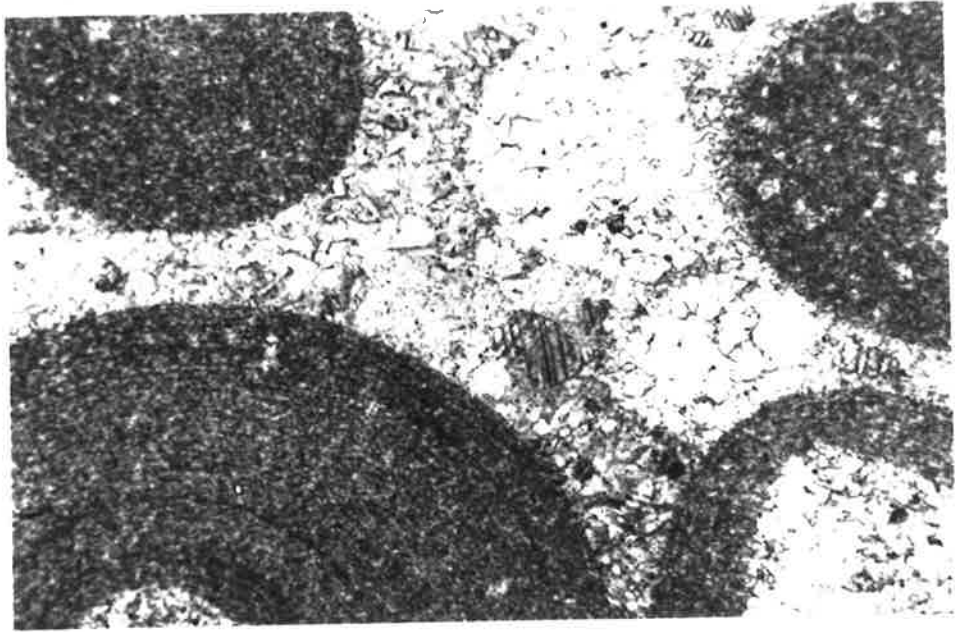
FIG.3.8: Compound ooid with brick-texture fabric. Ooid at top has been replaced by dolomite. Field of view is 4.4mm.

FIG.3.9: Brick-texture ooid with replaced core and inclusion rich interparticle cement. Field of view is 1.1mm.

FIG.3.10: Ooids with selectively dolomitized cores. Interparticle area has blocky calcite cement. Field of view is 4.4mm.
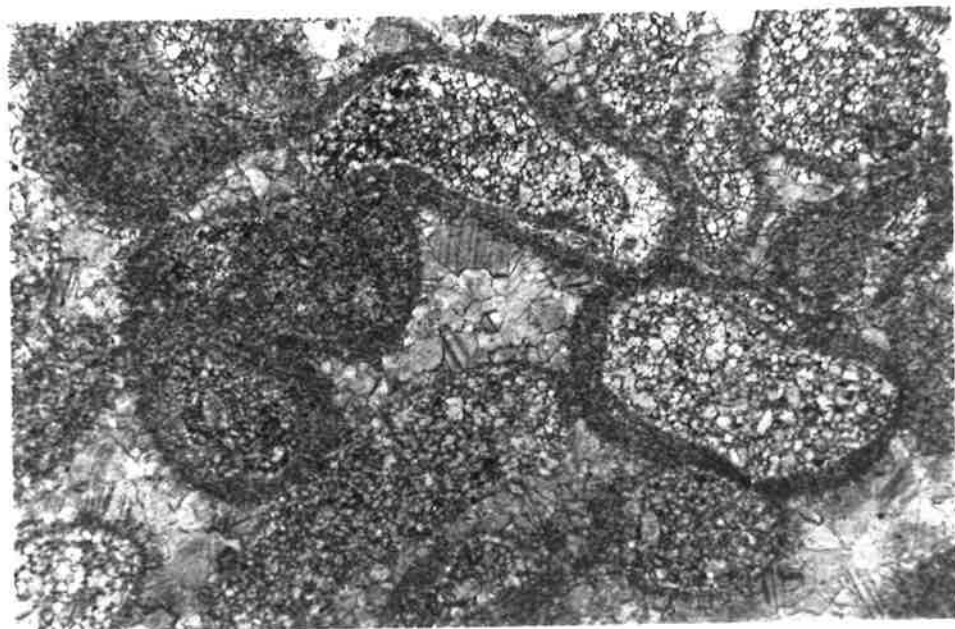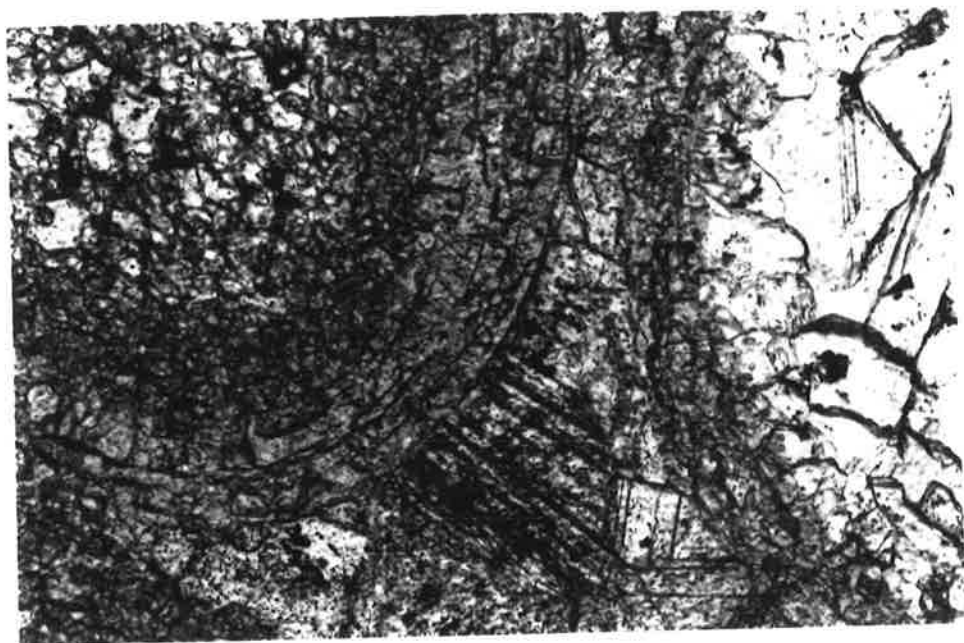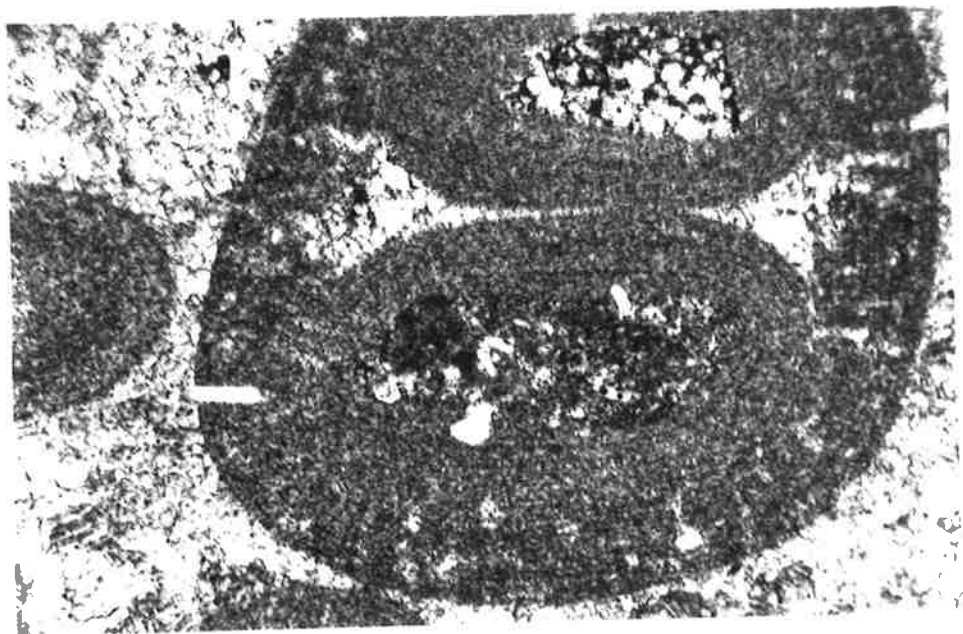
FIG.3.11: Clear calcite cement with irregular boundaries
and replacing ooid at left. Note relic concentric cortical
layers of replaced ooid. Field of view is 1.1mm.

FIG.3.12: Clear blocky calcite cement replacing ooids
contrasted with inclusion rich blocky calcite cement in
interparticle areas. Field of view is 1.1mm.

FIG.3.13: Blocky calcite layer in a stromatolite.
Microprobe analyses of this cement recorded elevated Sr
content. Field of view is 4.4mm.
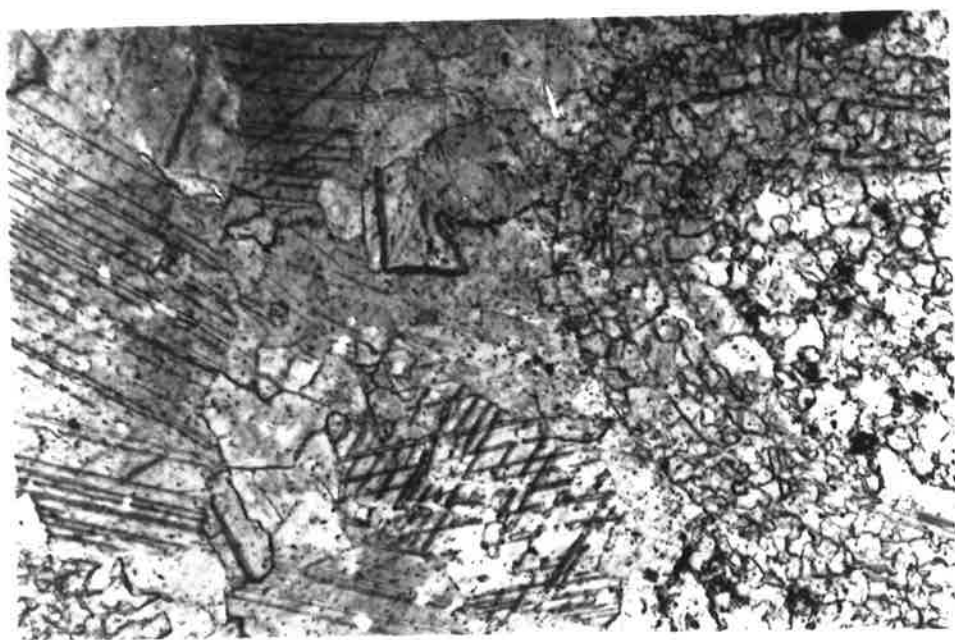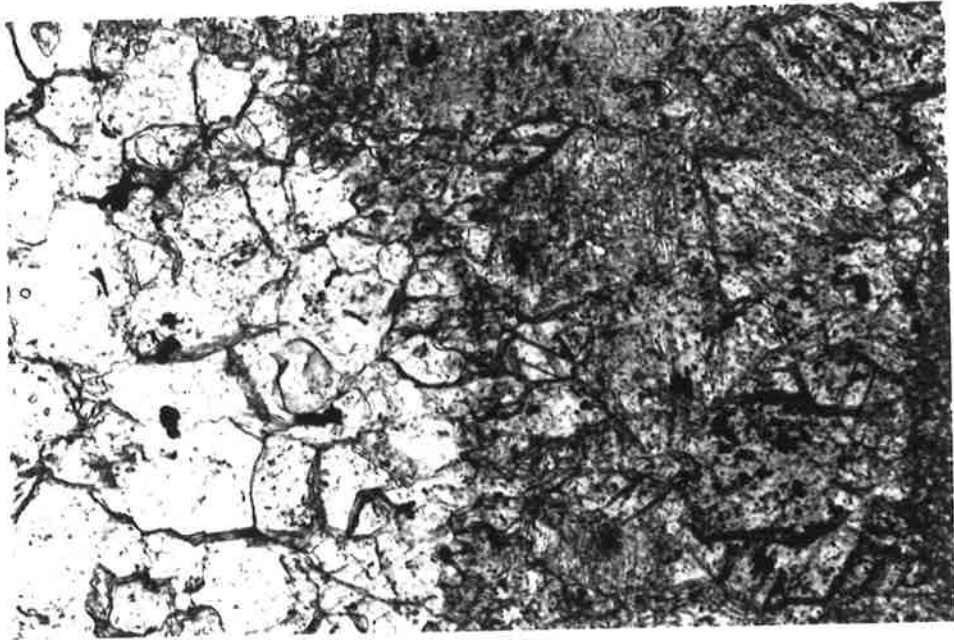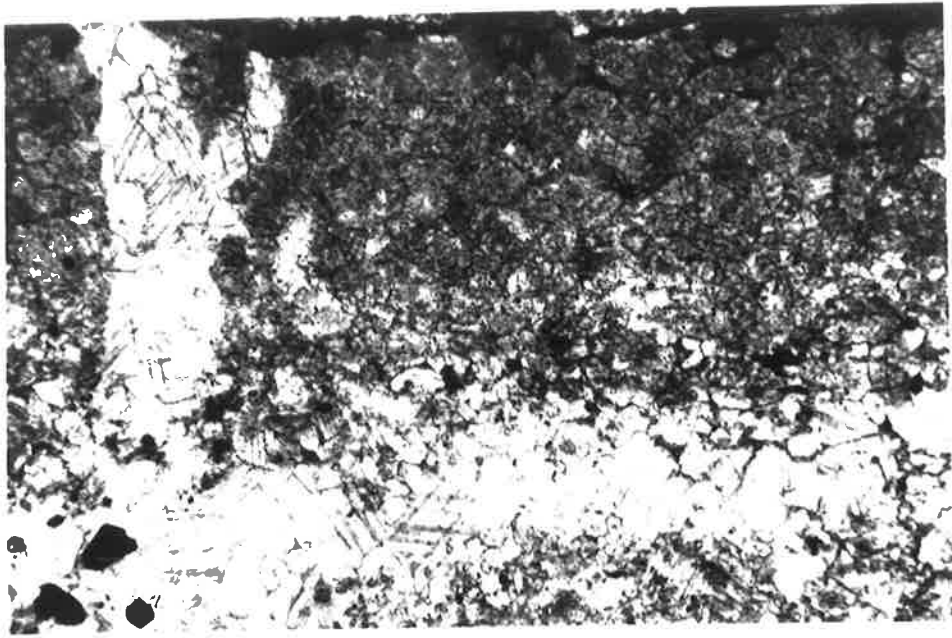
FIG.3.14: Trace element data of Balcanoona Formation components. Reported values represent the means of between 10 and 20 microprobe analyses. Values in brackets refer to two standard deviation from mean [2d].

| Sample | Description | Sr(ppm) | Mg(ppm) | Mn(ppm) | Fe(ppm) |
|---|---|---|---|---|---|
| **OOIDS** | | | | | |
| MV64 | Brick-texture | 1600 (980) | 3022 (1354) | b.d. | 311 (50) |
| MV61 | " | 1690 (330) | 2870 (620) | b.d. | 310 (190) |
| MV66(1) | Micritic | 1194 (454) | 2401 (401) | b.d. | 488 (601) |
| MV65 | " | 635 (302) | 2022 (494) | b.d. | 845 (230) |
| MV63 | " | 1332 (260) | 2590 (280) | b.d. | 501 (210) |
| MV66(2) | " | 390 (56) | 2085 (426) | 325 (74) | 1125 (637) |
| MV60 | Sparry ooids | 1271 (372) | 4193 (2721) | b.d. | 1950 (1587) |
| **CEMENTS** | | | | | |
| MV43 | Vein spar | 1794 (564) | 2617 (1193) | 412 (140) | 5936 (2312) |
| MV43 | Stromatolite spar | 4188 (3171) | 3079 (1634) | b.d. | 2436 (839) |
| MV43 | " | 1706 (1226) | 3657 (1472) | 149 (115) | 2782 (1344) |
| MV41 | " | 1660 (1031) | 2965 (1247) | b.d. | 867 (335) |
| MV60 | Interparticle spar | 1077 (544) | 2559 (699) | b.d. | 1126 (400) |
| MV66 | " | 1084 (894) | 2419 (1379) | 294 (386) | 508 (601) |
| MV64 | " | 378 (213) | 1859 (1267) | 447 (431) | 1119 (697) |
| MV65 | " | 540 (453) | 1974 (1483) | b.d. | 878 (719) |
| MV63 | " | 482 (206) | 1802 (540) | 180 (250) | 1121 (1213) |

| Sample | Description | Sr(ppm) | Mg(ppm) | Mn(ppm) | Fe(ppm) |
|--------|-------------|---------|---------|---------|---------|
| MV61 | Intraparticle spar | 850 (390) | 1920 (600) | 520 (160) | 2520 (720) |
| MV63 | " | 400 (150) | 1412 (200) | 510 (125) | 2035 (403) |
| MV64 | " | 603 (94) | 1382 (260) | 419 (115) | 2387 (564) |
| MV65 | " | 354 (151) | 2662 (2206) | 400 (224) | 1341 (635) |

MICRITE
--------

| | | | | | |
|--------|-------------|---------|---------|---------|---------|
| MV43 | | 4058 (2925) | 4056 (1726) | 197 (166) | 2608 (1299) |

DOLOMITE
--------

| | | | | | |
|--------|-------------|---------|---------|---------|---------|
| MV45 | Clear dolospar | 686 (207) | 13.40* (3520) | 243 (91) | 1.29* (8325) |
| MV45 | Fringing dolospar | 123 (102) | 13.25* (3688) | 261 (173) | 2480 (2812) |

* Weight percent Mg.

FIG.3.15: Trace element chemistry of ooids from the Late
Precambrian Balcanoona Formation, showing Sr vs Mn plot.
Each plotted sample represents the mean of between 10 to
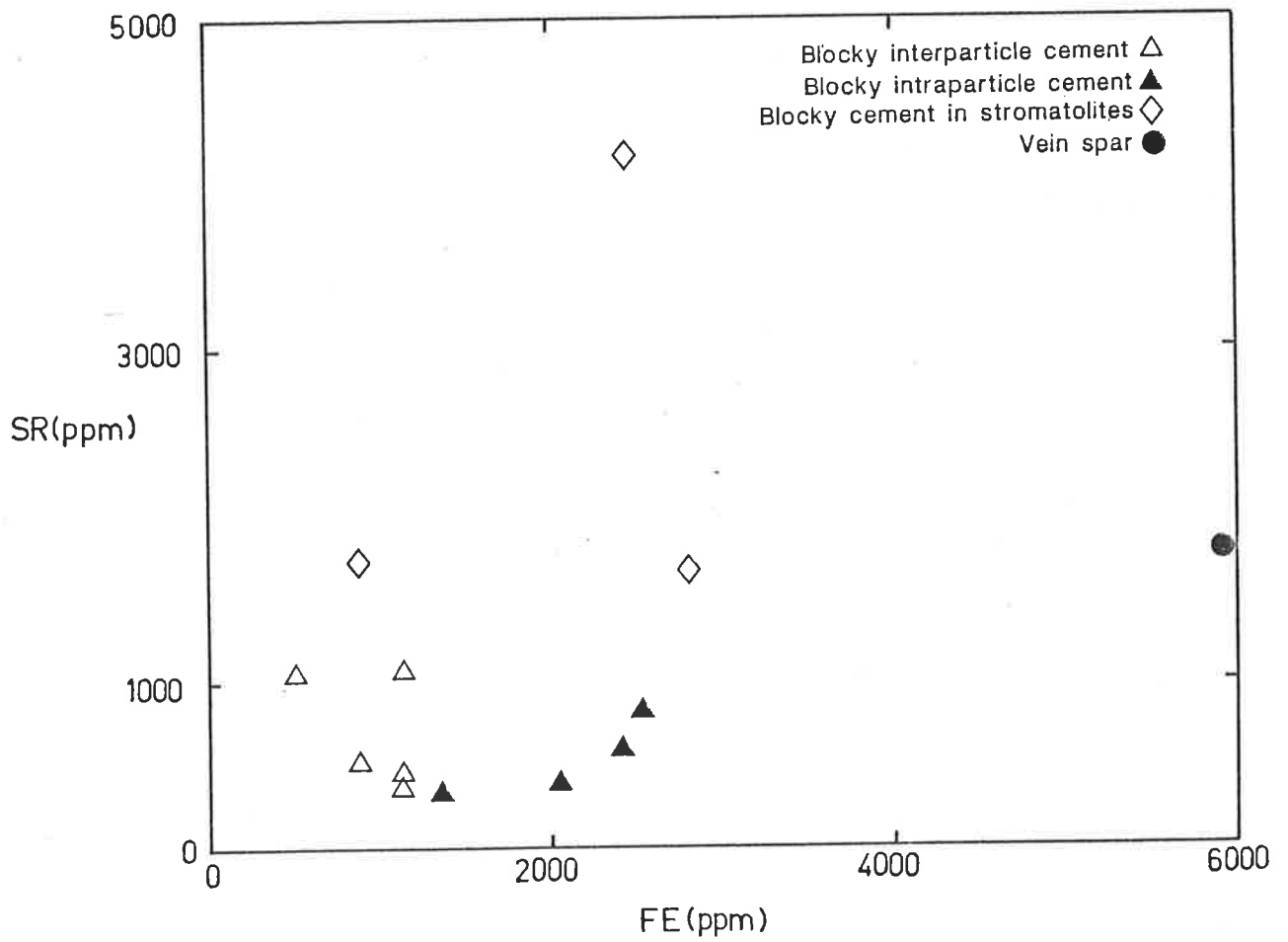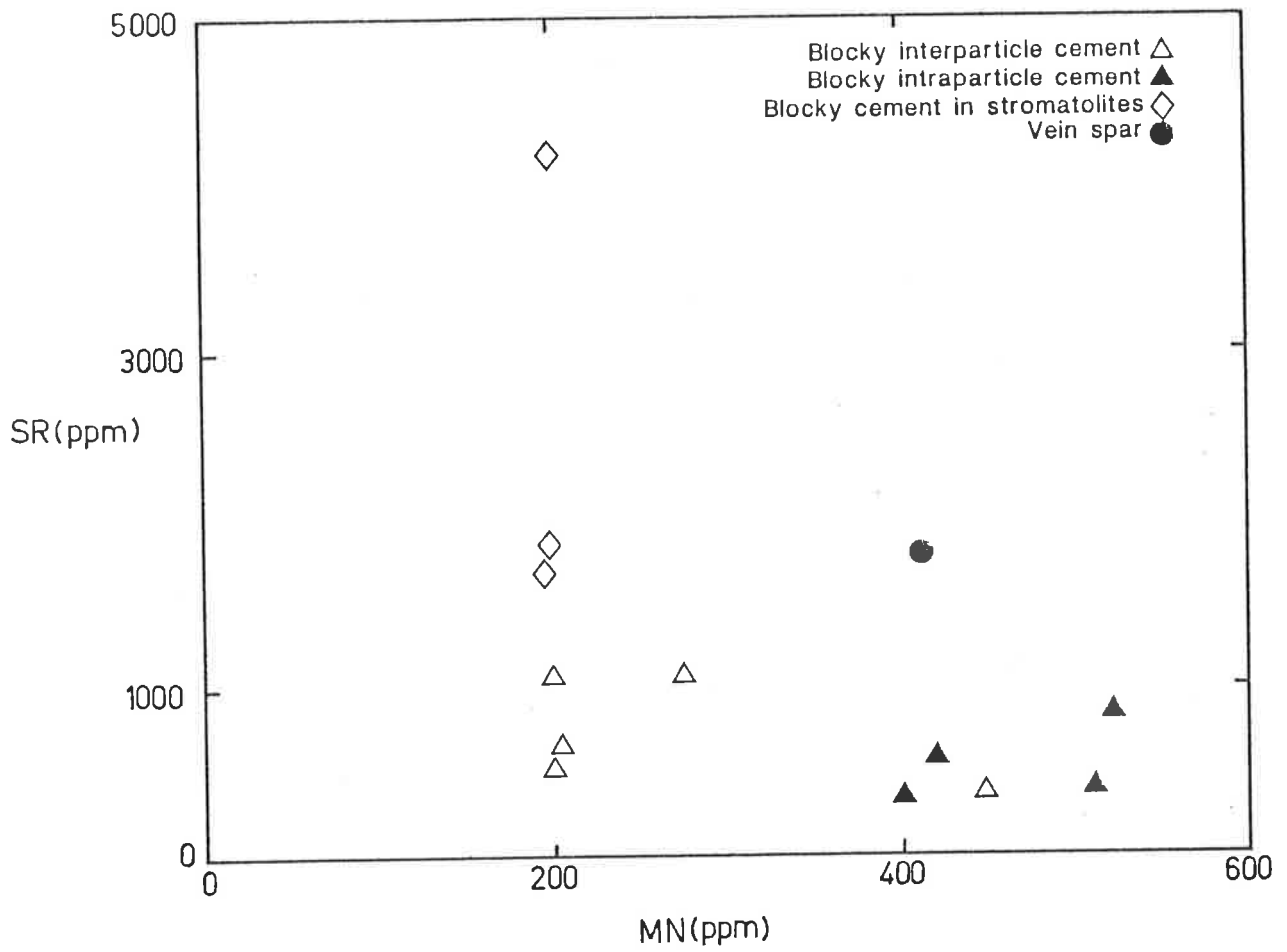20 individual microprobe analyses.

FIG.3.16: Trace element chemistry of ooids from the Late
Precambrian Balcanoona Formation, showing Sr vs Fe plot.
Each plotted sample represents the mean of between 10 to
20 individual microprobe analyses.
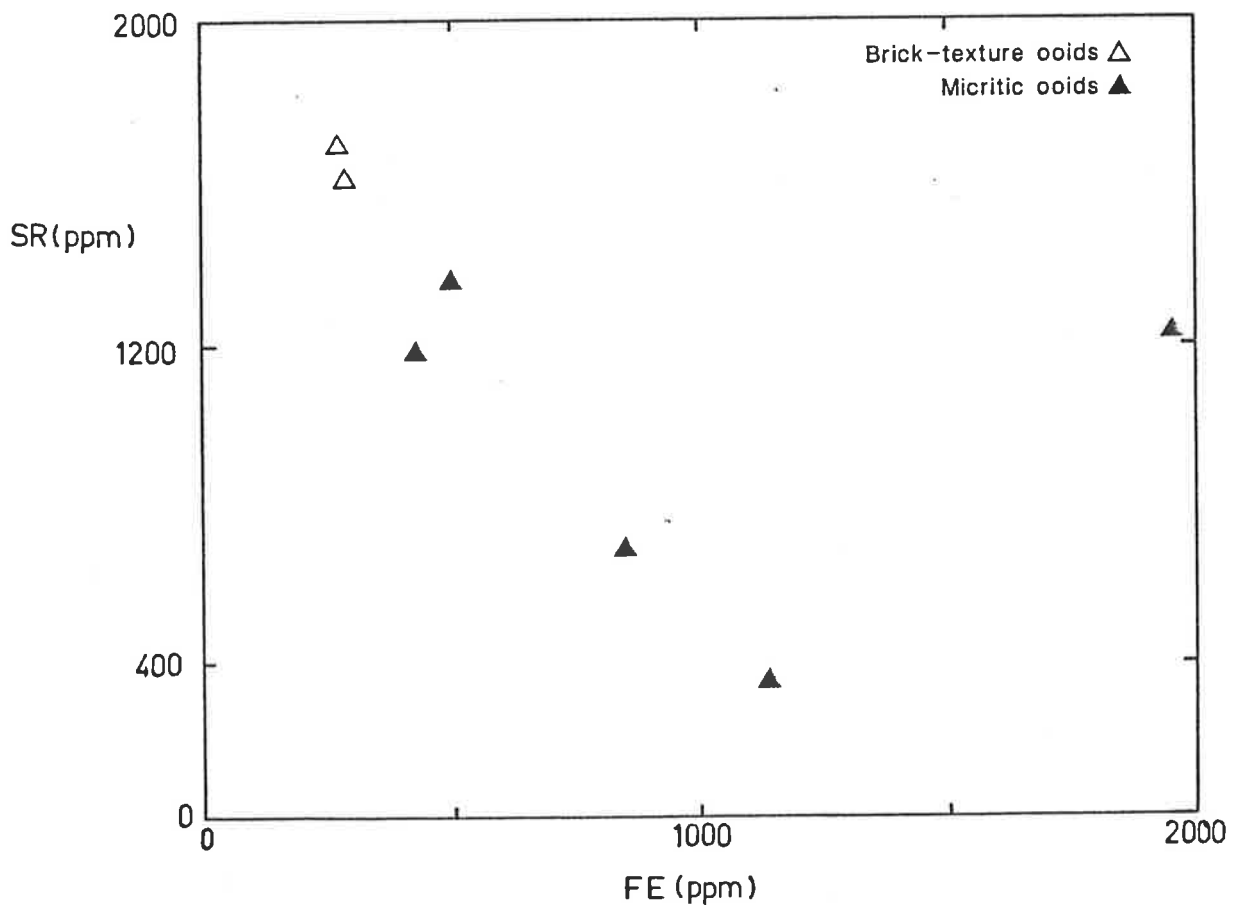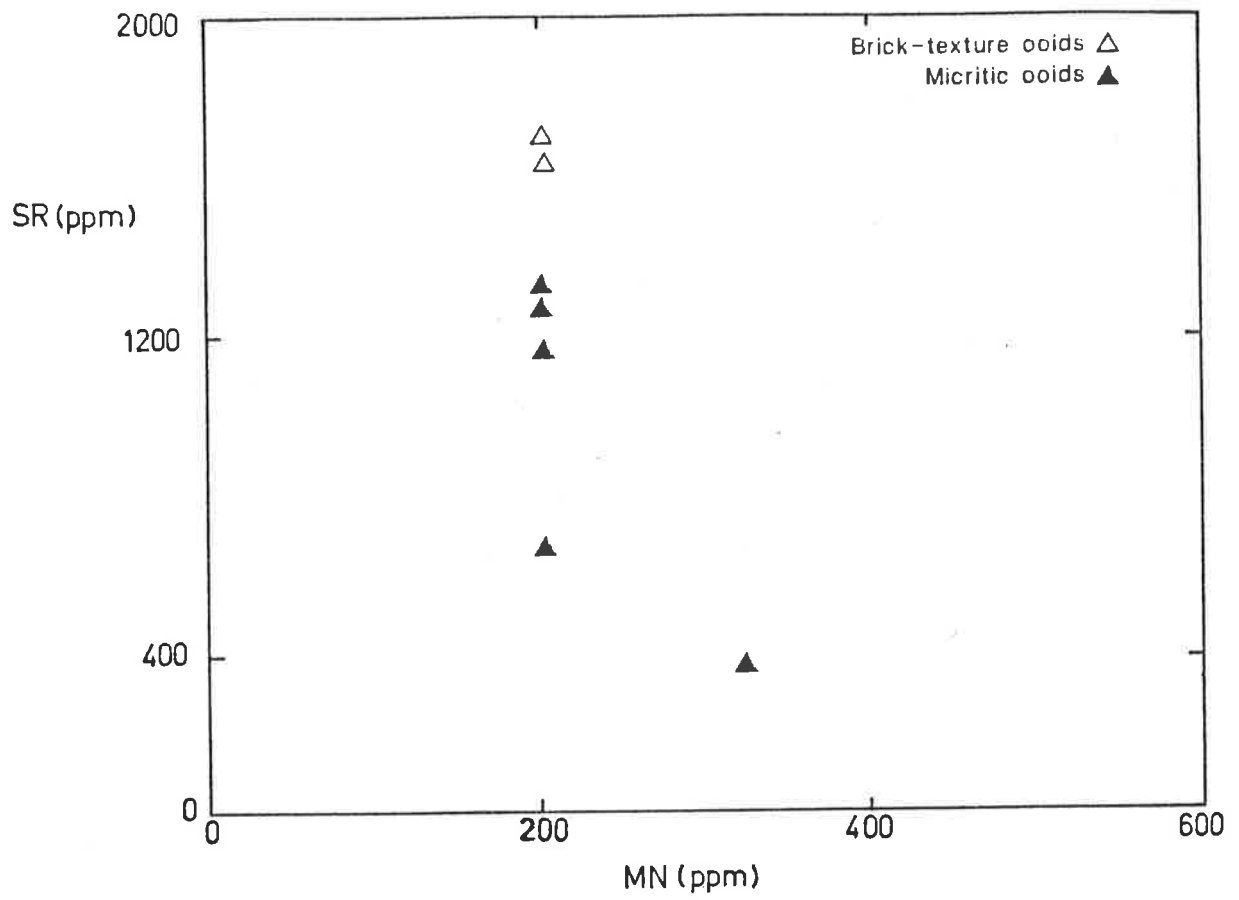
FIG.3.17: Trace element chemistry of ooids from the Late Precambrian Balcanoona Formation, showing Sr vs Mg plot. Each plotted sample represents the mean of between 10 to 20 individual microprobe analyses.
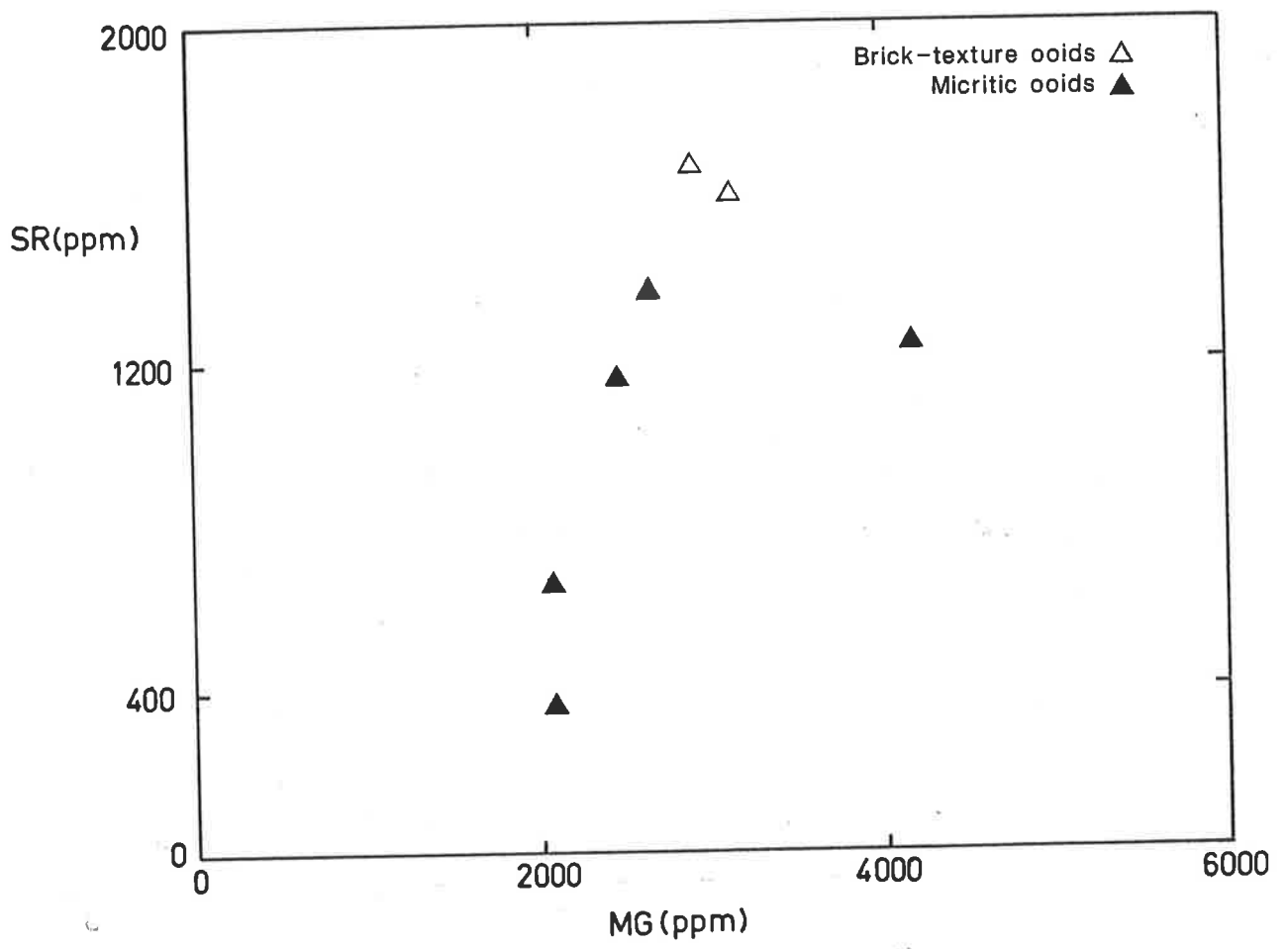
FIG.3.18: Trace element chemistry of cements from the Late
Precambrian Balcanoona Formation, showing Sr vs Mn plot.
Each plotted sample represents the mean of between 10 to
20 individual microprobe analyses.

FIG.3.19: Trace element chemistry of cements from the Late
Precambrian Balcanoona Formation, showing Sr vs Fe plot.
Each plotted sample represents the mean of between 10 to
20 individual microprobe analyses.

Blocky interparticle cement △
Blocky intraparticle cement ▲
Blocky cement in stromatolites ◇
Vein spar ●

SR(ppm)

5000

3000

1000

0

0        200        400        600

MN(ppm)

Blocky interparticle cement △
Blocky intraparticle cement ▲
Blocky cement in stromatolites ◇
Vein spar ●

SR(ppm)

5000

3000

1000

0

0        2000        4000        6000

FE(ppm)

FIG.3.20: Trace element chemistry of cements from the Late
Precambrian Balcanoona Formation, showing Sr vs Mg plot.
Each plotted sample represents the mean of between 10 to
20 individual microprobe analyses.
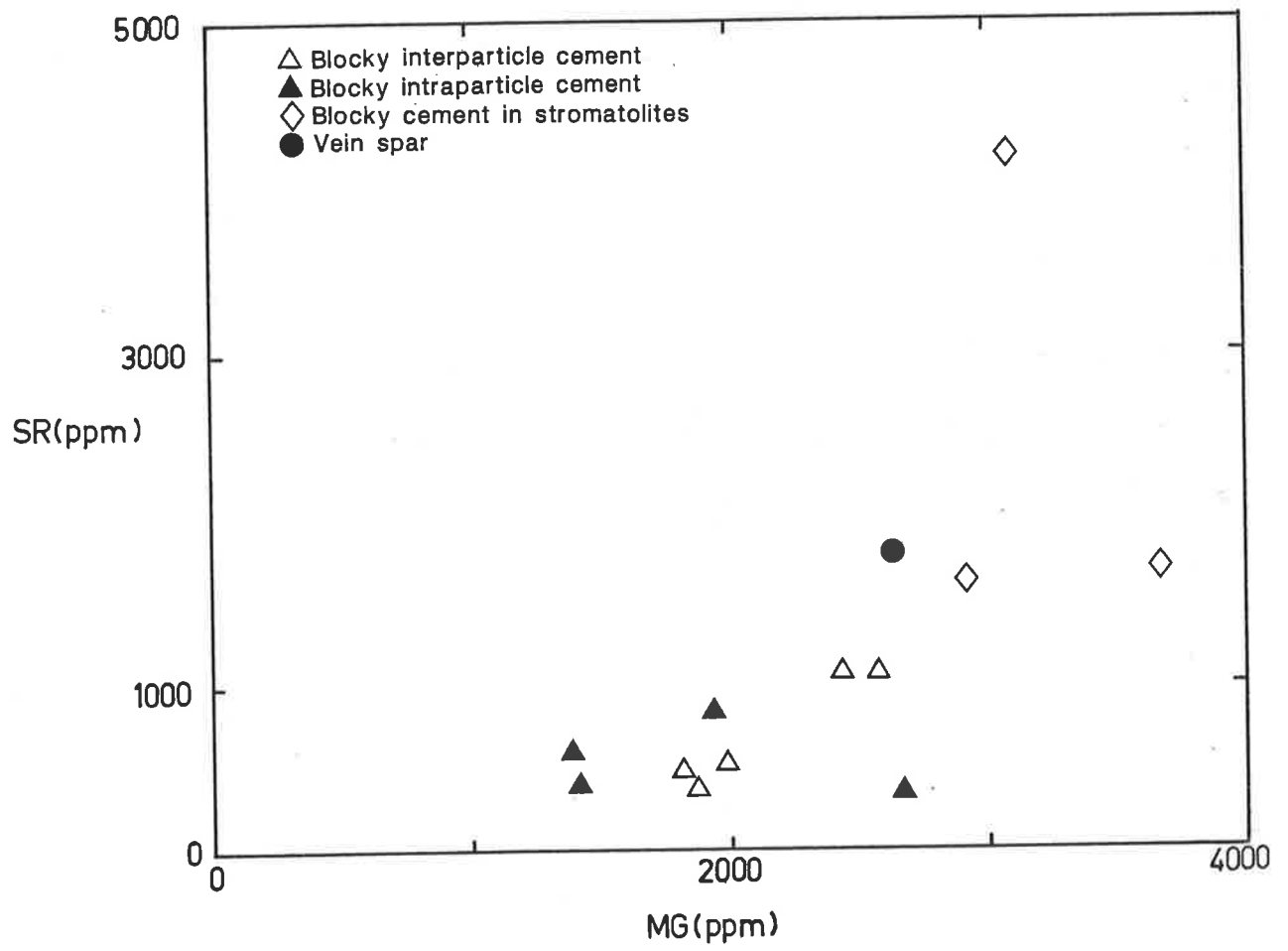
FIG.3.21: STABLE ISOTOPE DATA OF THE BALCANOONA FORMATION

| Sample | Description | Del O18 | Del C13 |
|---|---|---|---|
| **OOIDS** | | | |
| MV64 | Micritic fabric | -12.07 | 8.40 |
| MV61 | " | -10.64 | 8.28 |
| MV66 | " | -11.59 | 8.98 |
| MV65 | " | -8.95 | 1.00 |
| **CEMENTS** | | | |
| MV64 | Blocky interparticle calcite | -6.54 | 7.16 |
| MV66 | " | -7.13 | 8.79 |
| MV62 | " | -4.68 | 9.10 |
| MV65 | " | -7.84 | 5.61 |
| MV64 | Blocky intraparticle calcite | -11.96 | 4.83 |
| MV66 | " | -10.60 | 6.21 |
| MV62 | " | -13.19 | 4.83 |
| **BOUNDSTONE** | | | |
| MV41 | Laminar stromatolite | -12.39 | 3.07 |
| MV43 | " | -11.73 | 3.58 |
| **WHOLE ROCK** | | | |
| MV45 | dolomicrite | -3.76 | 2.96 |
| MV43 | " | -8.92 | 3.79 |

FIG.3.22: Oxygen and carbon isotope plot of the Late
Precambrian Balcanoona Formation. Line joining samples
refers to analyses from within the same sample.

BALCANOONA (STURTIAN)

$\delta^{13}C\,(PDB)$

$\delta^{18}O\,(PDB)$

-18    -12    -6
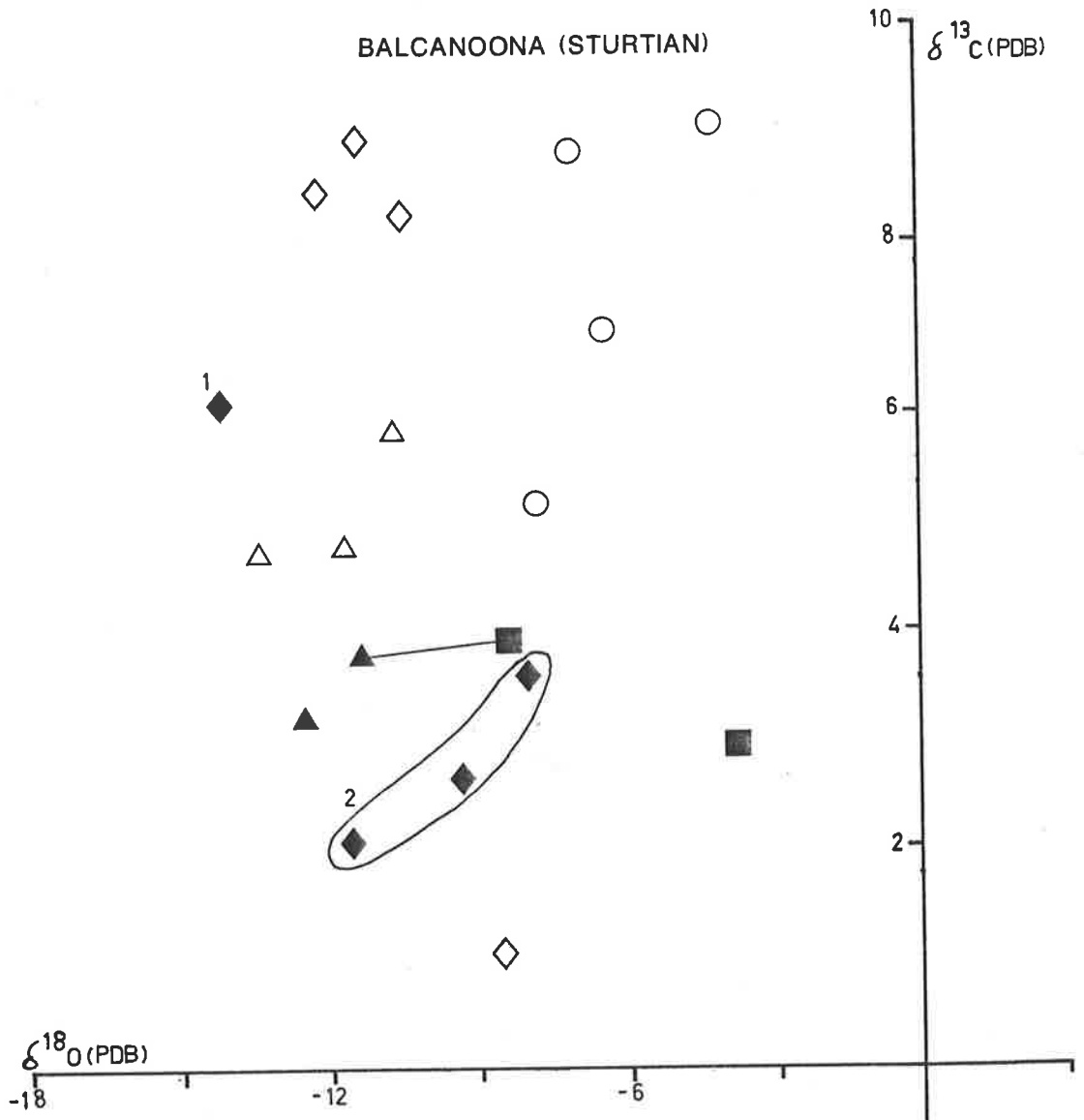
◇ Ooids
○ Blocky interparticle cement
△ Blocky intraparticle cement
■ Dolomite
▲ Stromatolite
◆¹ Schidlowski et al. (1975)
◆² Veizer and Hoefs (1976)

# CHAPTER FOUR

## LATE PRECAMBRIAN WONOKA FORMATION

### 4.1: INTRODUCTION

The Late Precambrian (Ediacaran) Wonoka Formation is part of the Wilpena Group of sediments within the Adelaide Geosyncline. The Wilpena Group comprises two major coarsening upwards, regressive tectono-sedimentary cycles, and the Wonoka Formation represents part of the upper cycle. In the Central Flinders Ranges the Wonoka Formation begins with basal siliclastic turbidites and shales followed by distal carbonate turbidites and storm resedimented carbonates [Haines 1986]. This sequence is capped by intertidal to supratidal carbonates. On a regional scale, the Wonoka Formation facies development indicatesa deepening to the northeast.

The topmost intertidal to supratidal carbonates comprise thin bedded, grey to black micritic and peloidal limestones as well as ooid grainstones. Occasionally stromatolite horizons are developed. This topmost carbonate unit has been named as the Mayo Limestone Member and is 26 m thick at its type section at Brachina Gorge [Haines 1986]. The upper part of the Mayo Limestone Member is a thin, buff coloured, fine-grained dolomite. Samples for this study were collected from the oolites of the Mayo Limestone Member at Brachina and Bunyeroo Gorge (Fig.4.1).

### 4.2: PETROGRAPHY

### 4.2.1: OOIDS

The ooids of the Wonoka Formation display a range of fabrics and include micritic ooids, brick-texture ooids,

neomorphic spar ooids, half-moon or leached ooids and superficial ooids with radial structures. The diameter of the ooids varies from 0.2mm to 2.8mm with a mean of 1.8mm. The ooids are generally spherical although some of the larger ooids tend to have elongate shapes. Intraclasts and cortoids are found associated with the ooids.

Micritic Ooids:

Ooids with micritic fabrics comprise micritic to microsparitic cortical layers with sparry nucleii (Fig.4.2). In some micritic ooids only a vague cortical layering can be discerned. Most of the cores of these micritic ooids have recrystallized to sparry calcite and selective dolomitization of these cores is common. The dolomite within these ooids forms anhedral to subhedral crystal mosaics and occasionally has totally replaced the micritic ooids (Fig.4.11). The micritic ooids, therefore commonly appear as superficial ooids with thin micritic envelopes and dolospar cores.

Brick-texture Ooids:

These ooids have cortical layers of sparry calcite comprising crystals with characteristic tabular or brick-like shapes (Figs.4.5 & 4.6). These individual calcite crystals of the cortex have a preferred tangential orientation and are confined within well defined cortical layers. The nucleus of some of these ooids consists of a mosaic of blocky calcite spar. These brick-texture ooids normally attain larger sizes than the other ooids and reach 2.8mm in diameter.

Neomorphic Spar Ooids:

Some ooids have cortices of neomorphic spar which is pseudopleochroic with a light and dark brownish appearance (Figs.4.8 & 4.9). The margin of this neomorphic spar normally

63

defines the concentric cortical layers. This neomorphic spar
can be coarser, and cross-cut cortical laminae, with relics
of the concentric cortical layers preserved within it. Some
of the component crystals forming the outermost cortical
layers in these neomorphic spar ooids encroach upon
interparticle areas. Occasionally this neomorphic spar fabric
forms composite ooids. The cores of the neomorphic spar ooids
are commonly selectively dolomitiz ed. Spalled cortices and
stylolites are normally associated with these dolomitized
ooids (Fig.4.10).

Half-moon Ooids:

Ooids with partially leached interiors, forming sparry
calcite upper halves and micritic or microsparitic lower
halves, termed half-moon ooids, are common in some
grainstones (Fig.4.7). The shapes of these ooids are normally
elongate and together with the brick-texture ooids, comprise
the largest ooid diameters recorded (2.8mm). The sparry
calcite upper halves of these ooids have typical pore-filling
textures, with increasing crystal size away from pore
margins. The cortical envelope in these half-moon ooids has a
micritic fabric.

Micritic Ooids with Radial Texture:

Ooids with radial calcite cortices and micritic nucleii
were found in some grainstones (Figs.4.12 & 4.13). The radial
texture is defined by areas of brownish calcite spar,
interspersed with micritic areas. Transecting the radial
texture are vague concentric bands. The thickness of these
radial envelopes are much less than the ooid diameter,
resulting in superficial ooids. Ooids with such radial
fabrics are rare and constitute less than 1% of the ooid

population.

## 4.2.2: CEMENTS

Two major cement types were recorded, a bladed fringing cement and a blocky, equant cement. Both these cement types are not always present within a specific ooid grainstone. Dolomite occurs commonly as a replacement of the cores of micritic and neomorphic spar ooids.

Bladed Fringing Cement:

Commonly cementing the ooids and the intraclasts are relatively thin crusts of bladed calcite cements (Figs.4.3 & 4.4). The calcite crystals have prismatic shapes and are normally turbid compared to the later stage clear blocky calcites. These bladed fringe cements are absent from ooid grainstones with brick-texture and neomorphic spar ooids.

Blocky, Equant Cement:

These cements occur both as interparticle and intraparticle pore-fillings. As interparticle cements, they can form a mosaic of equant or granular calcite cement or coarse single calcite crystals. The later type is common in ooid grainstones with bladed fringing cements, where it occludes remaining pore-space (Fig.4.2). In ooid grainstones with brick-texture and coarse pseudospar ooids, the blocky, equant cement is the sole interparticle diagenetic component. In these cases, individual calcite crystal boundaries extend into and encompass the cortical layers of these ooids. As intraparticle cements, the blocky cements occur as void-fillings within half-moon or leached ooids and in recrystallized nucleii of ooids (Fig.4.7).

65

## 4.3: TRACE ELEMENT CHEMISTRY

The trace element chemistry was determined from 14 separate components involving a total of 140 to 280 individual microprobe analyses.

### 4.3.1: OOIDS

The trace element chemistry of the 3 major ooid fabrics; micritic ooids, brick-texture ooids and neomorphic spar ooids was determined. There was no clear distinction between the various ooid types based on their trace element chemistry (Figs.4.14 to 4.17). However, Fe and Mn content of the micritic ooids tended to be higher than in the brick-texture and neomorphic spar ooids (Figs.4.15,4.16). The Fe content in the micritic ooids ranged from about 800 ppm to 2600 ppm and the Mn content from 340 ppm to 1000 ppm. The Fe and Mn content of the brick-texture and neomorphic spar ooids ranged from 400 ppm to 450 ppm and 270 ppm to less than 200 ppm respectively. Both the Sr and Mg content of the various ooid fabrics overlapped; Sr ranged from 220 ppm to a high of 650 ppm and Mg from 1000 ppm to 3500 ppm (Fig.4.17).

### 4.3.2: CEMENTS

As in the ooids, both the bladed cements and the blocky cements could not be distinguished based on their trace element concentrations (Figs.4.18 to 4.20). The Sr content of the bladed fringing cements was below the detection limit on the microprobe (160 ppm). The blocky cements, with one exception, had Sr content varying from less than detection limit to about 700 ppm. The exception being the blocky interparticle cement associated with brick-texture ooids. These blocky cements have Sr content of about 2000 ppm and

low amounts of Mg, Mn and Fe. The highest Mn content is recorded by the blocky intraparticle cements (900-1300 ppm). Some of the blocky interparticle cements also have high Mn content, although they had a larger range (360-1100 ppm). Both the bladed cements and the blocky cements are non-ferroan with Fe content ranging from 220 ppm to 1700 ppm.

## 4.4: OOID INTERPRETATION

The presence of both brick-texture and neomorphic spar ooids implies the presence of aragonitic precursors [Assereto and Folk 1976; Sandberg 1985]. Such ooid fabrics were also described from the Balcanoona and Trezona Formations (sections 3.4 and 2.4). Unlike the calcitized fabrics in the Balcanoona and Trezona Formation ooids however, the ooid fabrics in the Wonoka Formation have low Sr contents. This suggests that the diagenetic alteration of the originally aragonitic ooids in the Wonoka Formation resulted in greater leaching and loss of Sr. This could possibly be related to the presence of a dolomitization phase in the Wonoka Formation, being absent from the previously described Late Precambrian units. Ooids in the Wonoka Formation suffered selective dolomitization, possibly during the late burial stage. This late recrystallization of the ooids could have resulted in the removal of any high Sr concentrations that may have been preserved otherwise.

It is interesting to note the presence of strontium rich blocky interparticle calcite cements associated with brick-texture ooid fabrics. There was no evidence of any extensive dolomitization within these brick-textured ooid grainstones. The brick-textured ooids also had higher Sr contents compared

to the neomorphic spar ooids. The above observations would seem to suggest that the presence of a late dolomitization phase may have caused the lack of preservation of any high Sr precursor signature.

The interpretation of the micritic and radial ooid fabrics remains problematic. The ambiguous genesis of micritic ooids was mentioned in the previous sections describing the Balcanoona and Trezona Formations (sections 3.4 and 2.4). The radial ooid fabrics are unusual in that they were not observed from the other two Late Precambrian units studied. The radial fabric occurs as envelopes on micritic grains and has similarities with the radial ooid fabrics described from the Early Cambrian of this study as well as from previous studies (section 5.4). It differs from them however, since it forms only superficial type ooids. Such radial ooid fabrics have been interpreted as having calcitic precursors [Sandberg 1975]. The lack of any texturally disruptive recrystallization, i.e. coarse calcite mosaics, within these radial ooids precludes the possibility of an aragonitic precursor [Sandberg 1985]. It is inferred that these radial ooids in the Wonoka Formation also had calcitic precursors, but they comprise only about 1% of the ooid population.

4.5: CEMENT INTERPRETATION

The isopachous crust of bladed cements are well developed in ooid grainstones with micritic ooids. In grainstones with half-moon ooid fabrics, these early bladed cements are preserved but not as well developed and defined. No such bladed cement fringes were observed in grainstones

with brick-texture and neomorphic spar ooids. Bladed fringing calcite cements can occur in a range of diagenetic environments from marine phreatic to mixing zones to meteoric phreatic [Longman 1980; James and Choquette 1983]. Their bladed crystal morphology and turbid appearance may suggest Mg-rich marine waters but pore-water composition can sometimes have no bearing on the resulting crystal shape [Braithwaite 1979; Kendall and Broughton 1980; James and Ginsburg 1979; Warme and Schneidermann 1983]. The bladed fringing cements have negligible Sr and low Mg contents, and lower Mn and Fe compared to the later blocky calcite cements. It is inferred that these bladed cements probably reflect precipitation in shallow subsurface meteoric phreatic environments.

The later blocky calcite precipitates that form the dominant interparticle cement type as well as occurring as intraparticle cements in ooid molds, probably formed in the deeper subsurface phreatic environment. They have higher amounts of Fe and Mn compared to the bladed cements. These blocky, coarse and sometimes poikilotopic calcites with ferroan compositions are common for cements associated with subsurface brines [Meyers 1974; Grover 1983; Moore and Druckman 1981].

An unusual feature of some of the blocky calcite cements is their strontium-rich chemistry. Their Mn and Fe content is very low suggesting limited modification with meteoric pore-waters [Brand and Veizer 1980]. Such calcite cements were earlier described from both the Balcanoona and Trezona Formations (section 3.5 and 2.5). They could represent precipitates from Sr enriched pore-waters, since they are

associated with calcitized brick-texture ooids, or are themselves products of aragonite-calcite transformation. The latter possibility is unlikely since it is not supported by textural evidence [Sandberg 1983]. Their genesis is discussed in section 7.4 of the concluding chapter.

## 4.6: OXYGEN AND CARBON ISOTOPES

The few samples analysed for stable isotopes revealed carbon isotope compositions varying from 1.89 permil to -0.75 permil. The oxygen isotopes recorded a range from -7.15 permil to -11.55 permil (Figs.4.21,4.22). Unlike the stable isotope data from the other units, the Wonoka Formation oxygen and carbon isotope compositions are from whole rock analysis of ooid grainstones. Therefore a reliable assessment of the oxygen and carbon isotopic composition of the marine waters during Wonoka Formation (Ediacaran) time is not possible. Nonetheless, given that the carbon isotope composition is less prone to alteration during diagenesis compared to the oxygen isotope [Magaritz 1983; Meyers and Lohmann 1985], the whole rock carbon signature is probably close to the original marine value.

Compared to the carbon signatures of the Balcanoona and Trezona Formations, the Wonoka Formation values are of intermediate range; between the high positive values of the Balcanoona and the negative values of the Trezona. Admittedly the range of carbon isotope compositions within the Balcanoona and Trezona Formations are large, due to contributions from light organic carbon. Even in the Wonoka Formation there is indication of light carbon contribution to the marine carbon signature as revealed by plotted data

(Fig.4.22) in the study by Veizer and Hoefs [1976]. The samples for the present study were carefully chosen taking care to avoid subaerial exposure levels, noted by Haines [1986] in the Wonoka Formation. This accounts for the heavier carbon isotope signatures.

In spite of this diagenetic alteration, there is a real and significant difference in the carbon isotope compositions of the Late Precambrian units studied. From a high in the Balcanoona Formation with it's heavy carbon isotope composition, the carbon isotope trend shows a marked drop to small positive and negative values in the Trezona (Marinoan) and Wonoka (Ediacaran) Formations. The possible implications of this trend and it's comparision with other Late Precambrian sequences is discussed in section 7.5 of the concluding chapter.

## 4.7: SUMMARY

The presence of brick-texture and neomorphic spar ooids within the Wonoka Formation oolites suggest non-skeletal aragonite precipitation during Ediacaran (Wonoka) times. Together with the ooid fabric data from both the Sturtian Balcanoona and Marinoan Trezona Formations described earlier, it suggests that non-skeletal aragonite precipitation occurred during deposition of all three Late Precambrian limestone units studied.

Strontium-rich blocky calcites were recorded in ooid grainstones with calcitized ooid fabrics. This relationship between calcitizied ooids and strontium-rich calcite cements was also observed in the Trezona Formation.

The carbon isotope signature available from the Wonoka

71

Formation was from whole rock analyses and defines a comparatively small field, varying from about 2 permil to - 0.75 permil. This was significantly different from the carbon isotope composition of the Balcanoona and Trezona Formations.

FIG.4.1: Location map of the Bunyeroo and Brachina Gorge

sample areas of the Late Precambrian Wonoka Formation

(Based on Parachilna 1:250,000 sheet).

LAKE TORRENS

BLINMAN

BRACHINA
GORGE

BUNYEROO
GORGE

CAMBRIAN    DIAPIR

PRECAMBRIAN

0          25 km
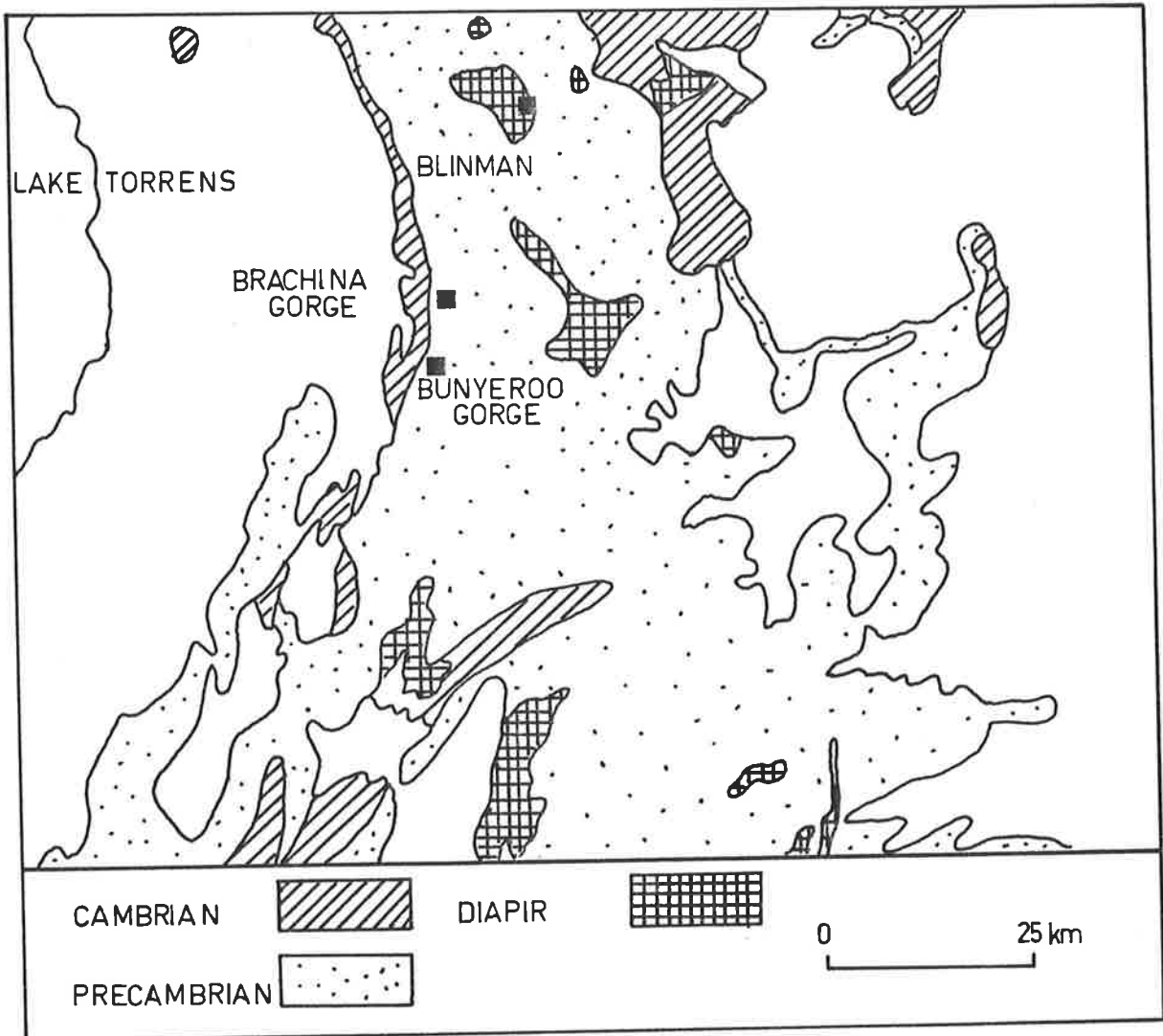
FIG.4.2: Micritic ooids with sparry centers and bladed fringing cement. The cortical layers in the ooid are not well developed. The blocky equant cement represents the pore occluding stage of cementation. Field of view is 4.4mm.

FIG.4.3: Bladed fringing cement enveloping a peloid grain. Remaining pore space is occupied by coarsely crystalline calcite cement. Field of view is 4.4mm.

FIG.4.4: Same view as figure 4.3 but under cross polars. Note optical continuity of coarsely crystalline calcite cement occluding pore center. Field of view is 4.4mm.
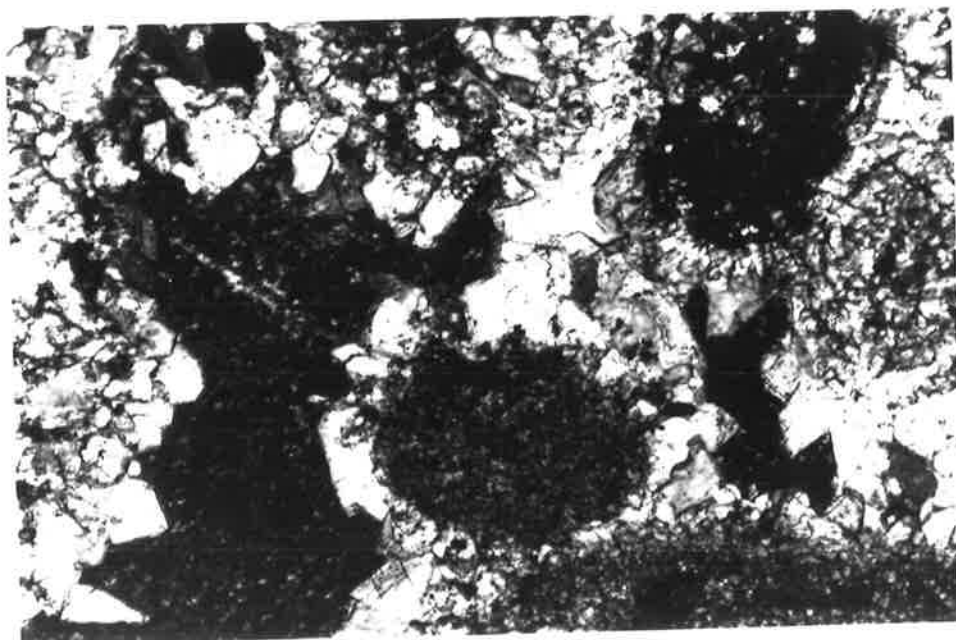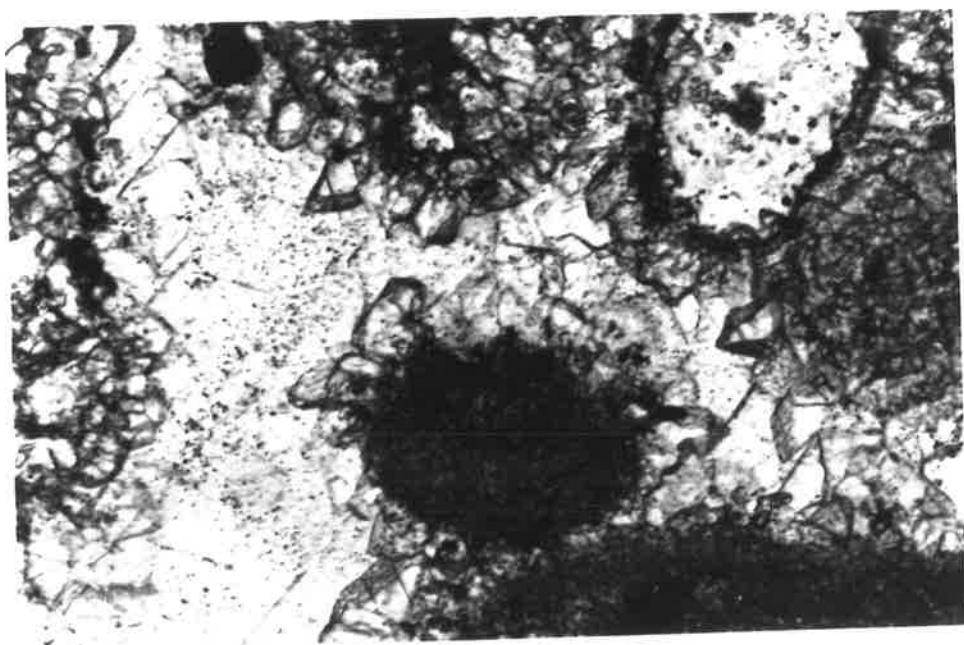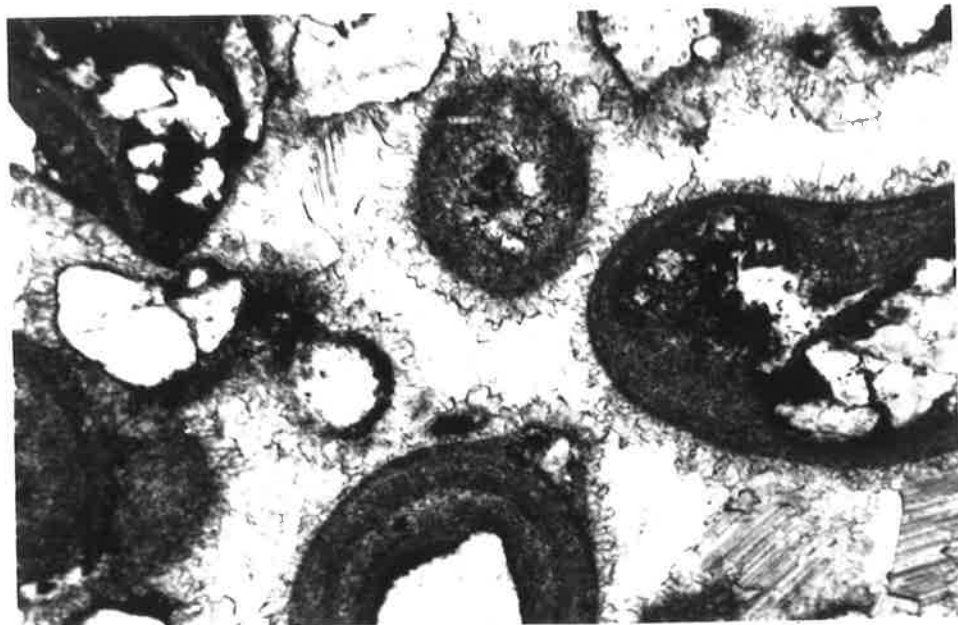
FIG.4.5: Brick-texture ooids with some ooid cores
recrystallized to sparry calcite mosaics. Concentric
cortical layers are developed around indistinct nucleii.
The interparticle cement is a blocky calcite mosaic with
high Sr content. Field of view is 4.4mm.

FIG.4.6: Close up of brick texture ooid showing the
concentric cortical layers and indistinct nucleus. Field
of view is 1.1mm.

FIG.4.7: Half-moon ooid fabrics with sparry tops and
micritic bottoms. The interparticle cement is a blocky
calcite mosaic. Calcite veins transect some elongate
micritic ooids at right. Field of view is 4.4mm.
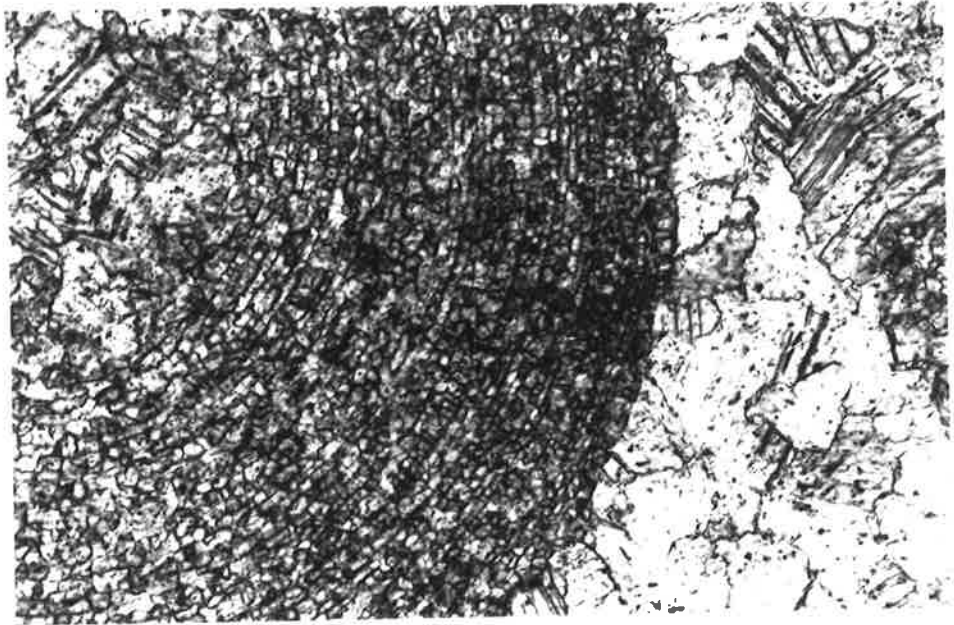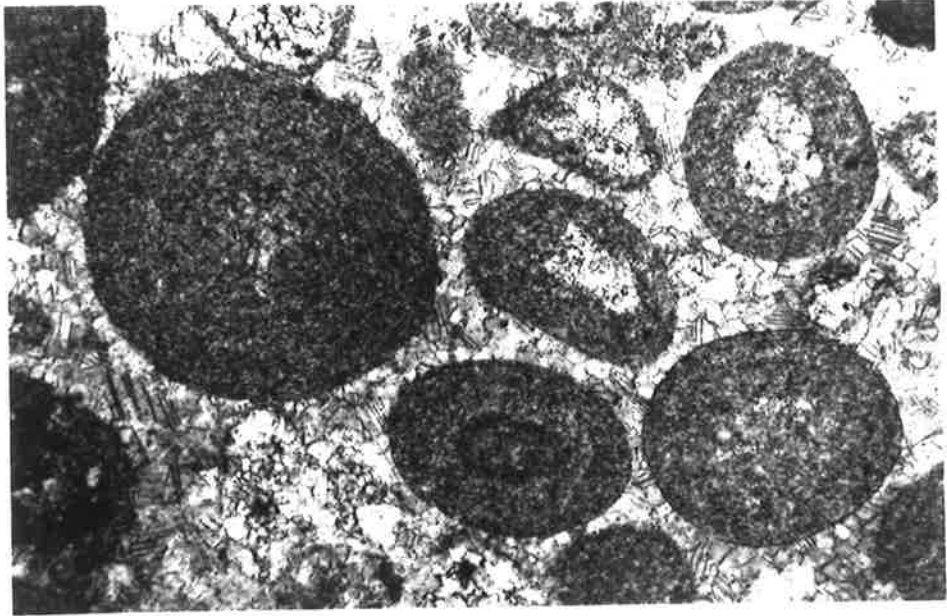
FIG.4.8: Neomorphic spar ooids with characteristic
brownish appearance. Some of the ooid cores are
dolomitiz ed. Interparticle area has a blocky equant
calcite cement. Field of view is 4.4mm.

FIG.4.9: Neomorphic spar ooid with relic concentric
cortical layers and brownish appearance. Field of view is
1.1mm.

FIG.4.10: Neomorphic spar ooids forming compound ooids and
having dolomitiz ed cores and disrupted by stylolites.
Field of view is 4.4mm.
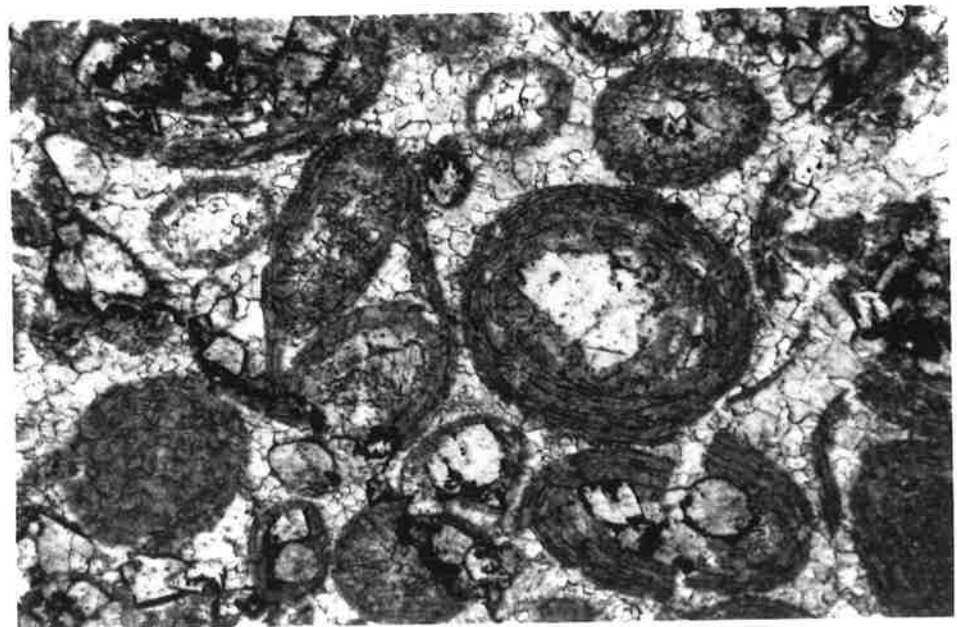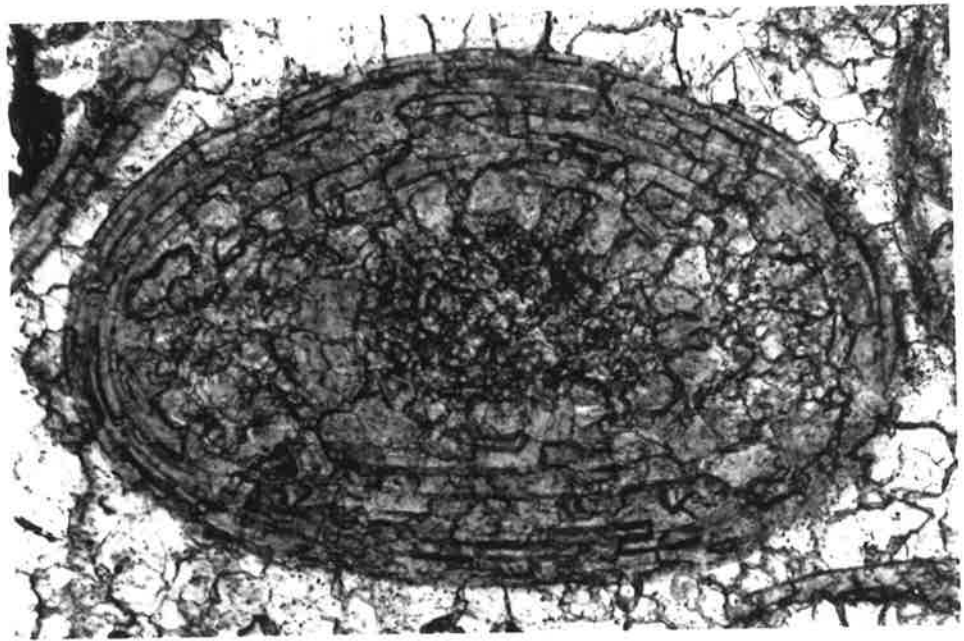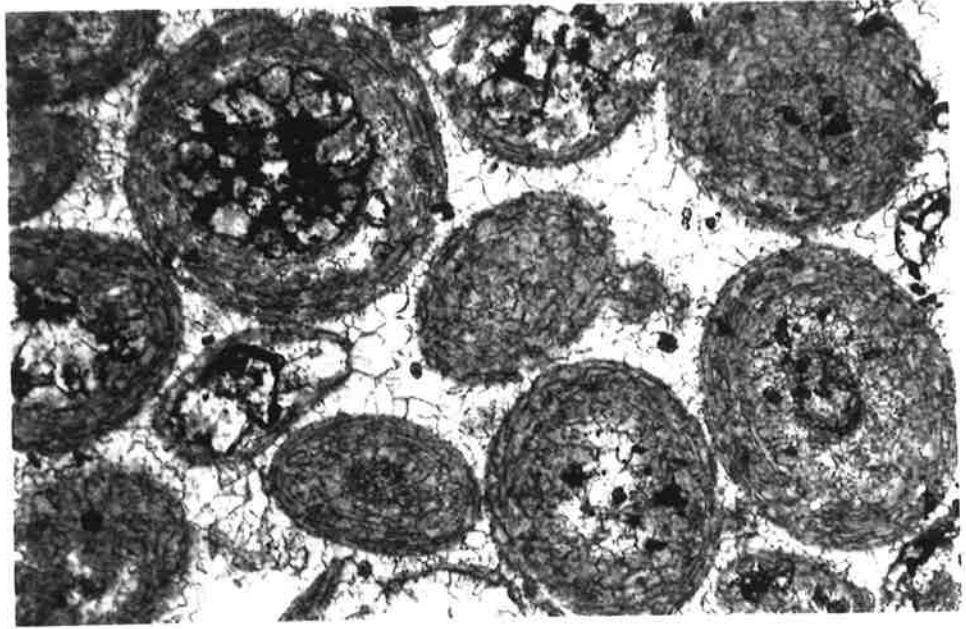
FIG.4.11: Micritic ooids selectively replaced by dolomite.
Field of view is 4.4mm.

FIG.4.12: Micritic ooids with thin radial fabric
envelopes. Field of view is 4.4mm.

FIG.4.13: Close-up of radial fabric from ooids in figure
4.12. Note rim of bladed cement. Field of view is 1.1mm.
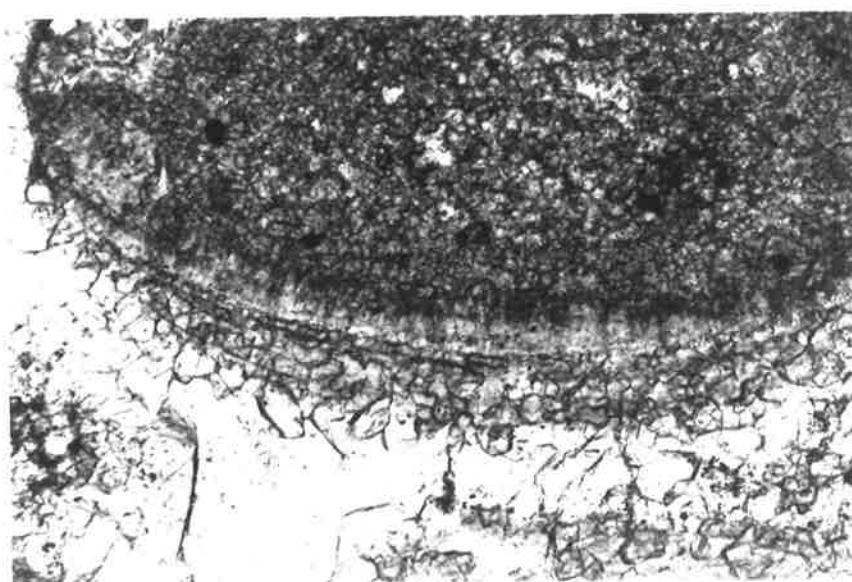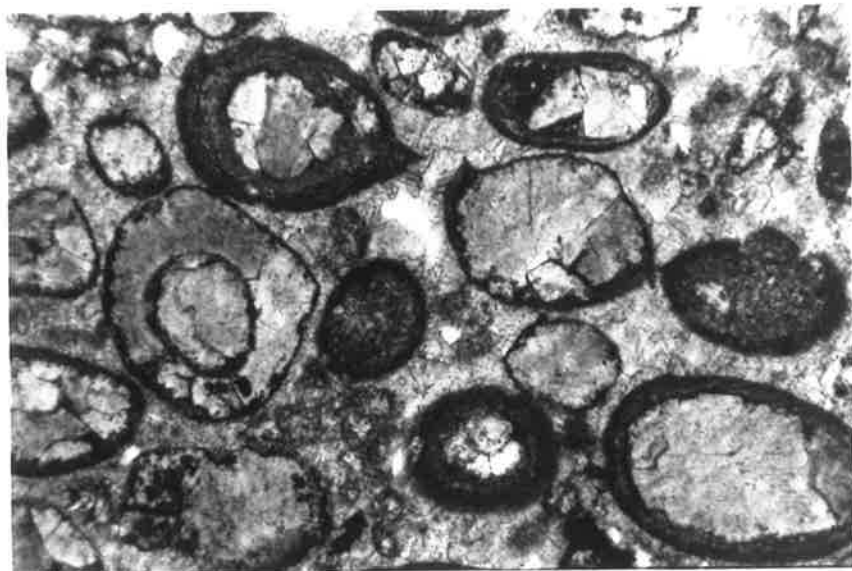
FIG.4.14: Trace element data of Wonoka Formation components. Reported values represent the means of between 10 and 20 microprobe analyses. Values in brackets refer to two standard deviation from mean [2d].

| Sample | Description | Sr (ppm) | Mg (ppm) | Mn (ppm) | Fe (ppm) |
|---|---|---|---|---|---|
| **OOIDS** | | | | | |
| MH7 | Brick-texture | 652 (140) | 2490 (567) | 274 (105) | 421 (180) |
| WK34 | Neomorphic spar | 281 (128) | 1025 (170) | b.d. | 463 (201) |
| SB19 | Micritic | 271 (130) | 1396 (254) | 418 (416) | 1030 (393) |
| BU2 | " | 221 (80) | 1813 (430) | 965 (590) | 2633 (1152) |
| BU29 | " | 588 (202) | 3521 (218) | 340 (212) | 820 (487) |
| **CEMENTS** | | | | | |
| SB19 | Bladed | b.d. | 1795 (1963) | 362 (187) | 523 (268) |
| MH7 | Blocky inter-particle | 2183 (1324) | 1465 (412) | b.d. | 389 (527) |
| WK34 | " | 382 (279) | 1092 (609) | 360 (379) | 244 (174) |
| BU29 | " | b.d. | 3409 (423) | 884 (90) | 1738 (223) |
| BU29 | " | 733 (281) | 3686 (921) | 1132 (701) | 221 (245) |
| BU29 | Blocky intra-particle | 117 (48) | 4760 (1243) | 978 (131) | 1292 (284) |
| BU2 | " | b.d. | 676 (371) | 1341 (862) | 864 (243) |
| **DOLOMITE** | | | | | |
| WK34 | Dolospar | b.d. | 4.33* (2200) | 3127 (1633) | 1.38* (970) |
| SB19 | " | b.d. | 4.20* (3100) | 4900 (2400) | 9700 (2700) |

* Weight percent Mg.

FIG.4.15: Trace element chemistry of ooids from the Late
Precambrian Wonoka Formation, showing Sr vs Mn plot.
Each plotted sample represents the mean of between 10 to
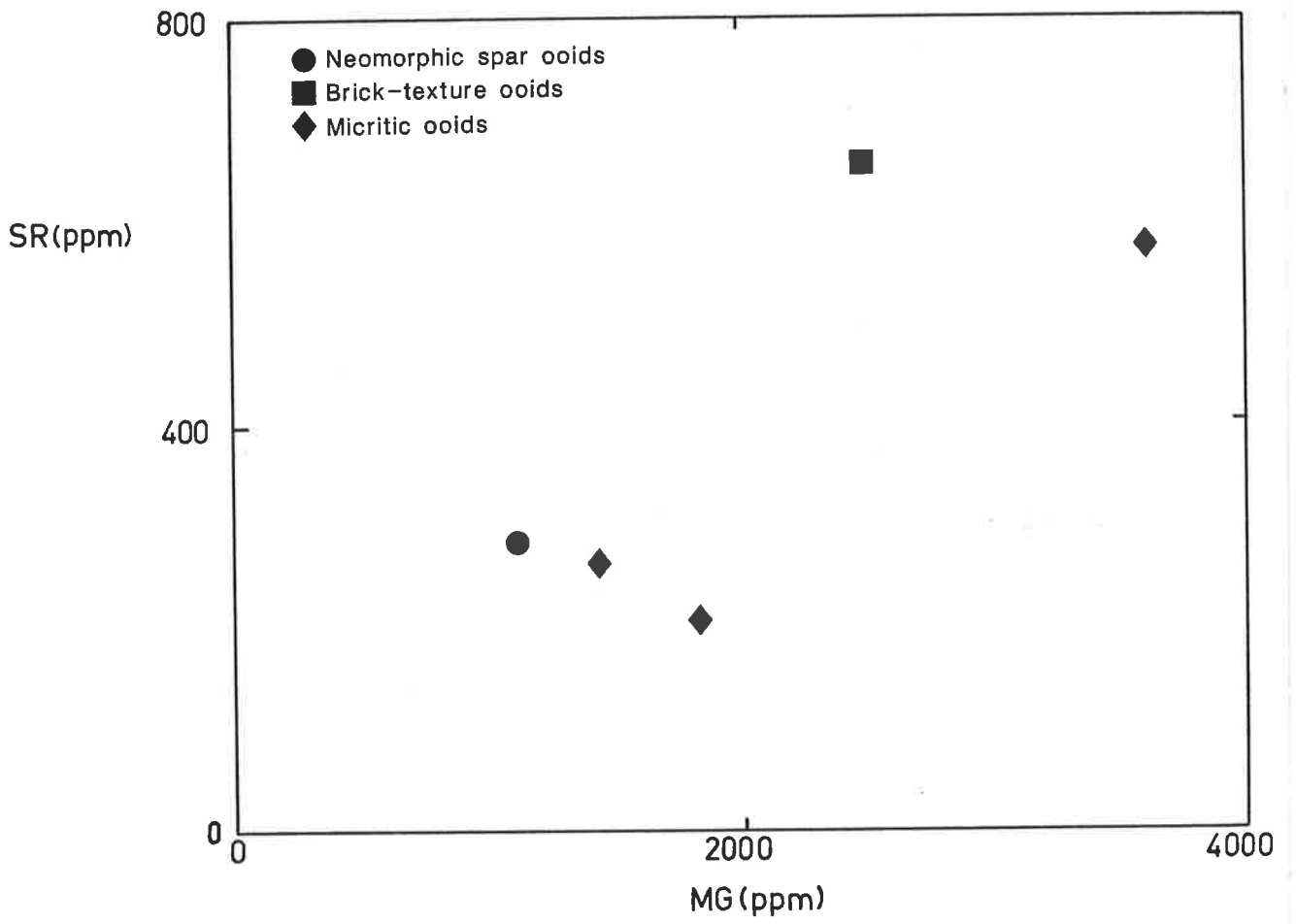20 individual microprobe analyses.

FIG.4.16: Trace element chemistry of ooids from the Late
Precambrian Wonoka Formation, showing Sr vs Fe plot.
Each plotted sample represents the mean of between 10 to
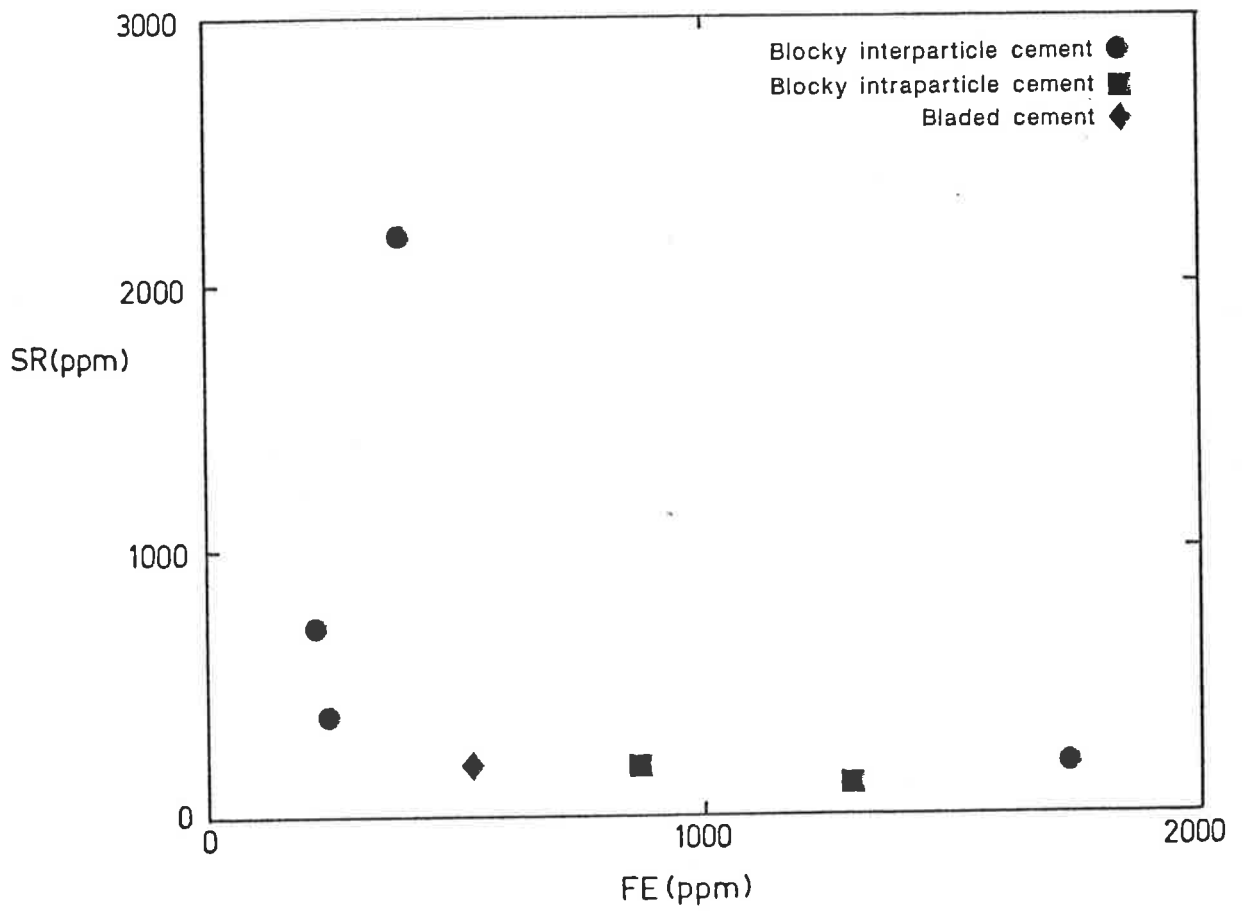20 individual microprobe analyses.
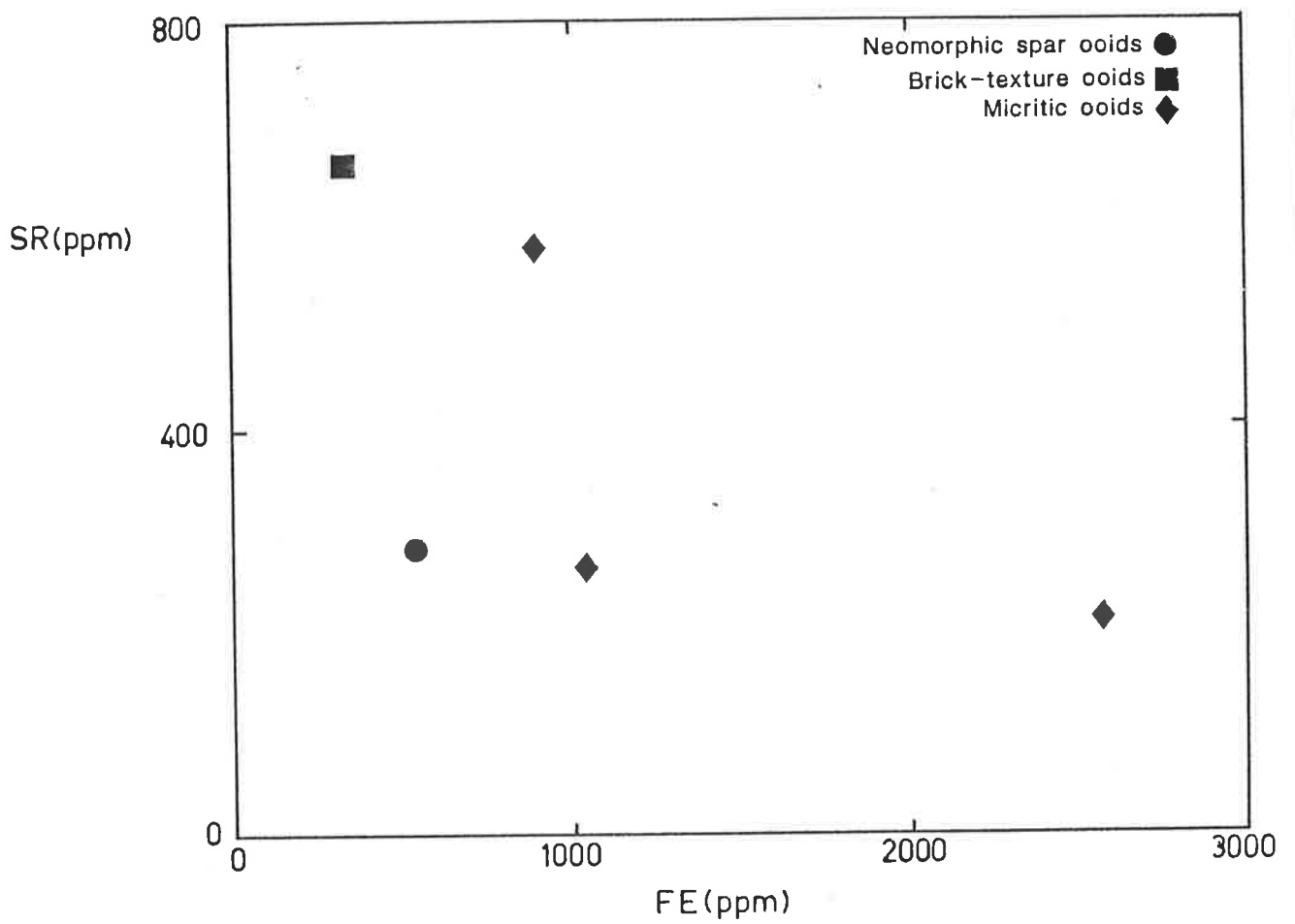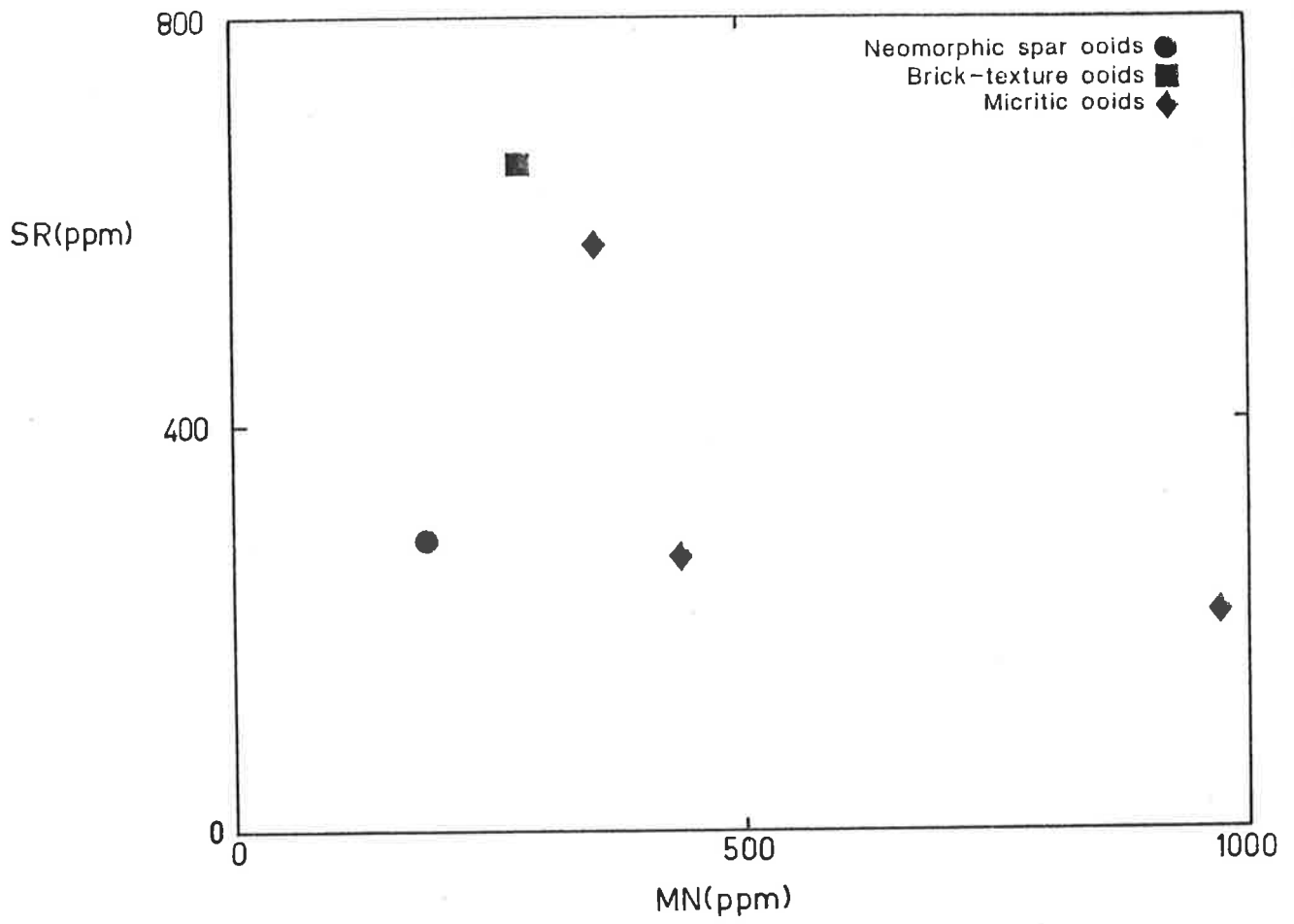
FIG.4.17: Trace element chemistry of ooids from the Late Precambrian Wonoka Formation, showing Sr vs Mg plot. Each plotted sample represents the mean of between 10 to 20 individual microprobe analyses.
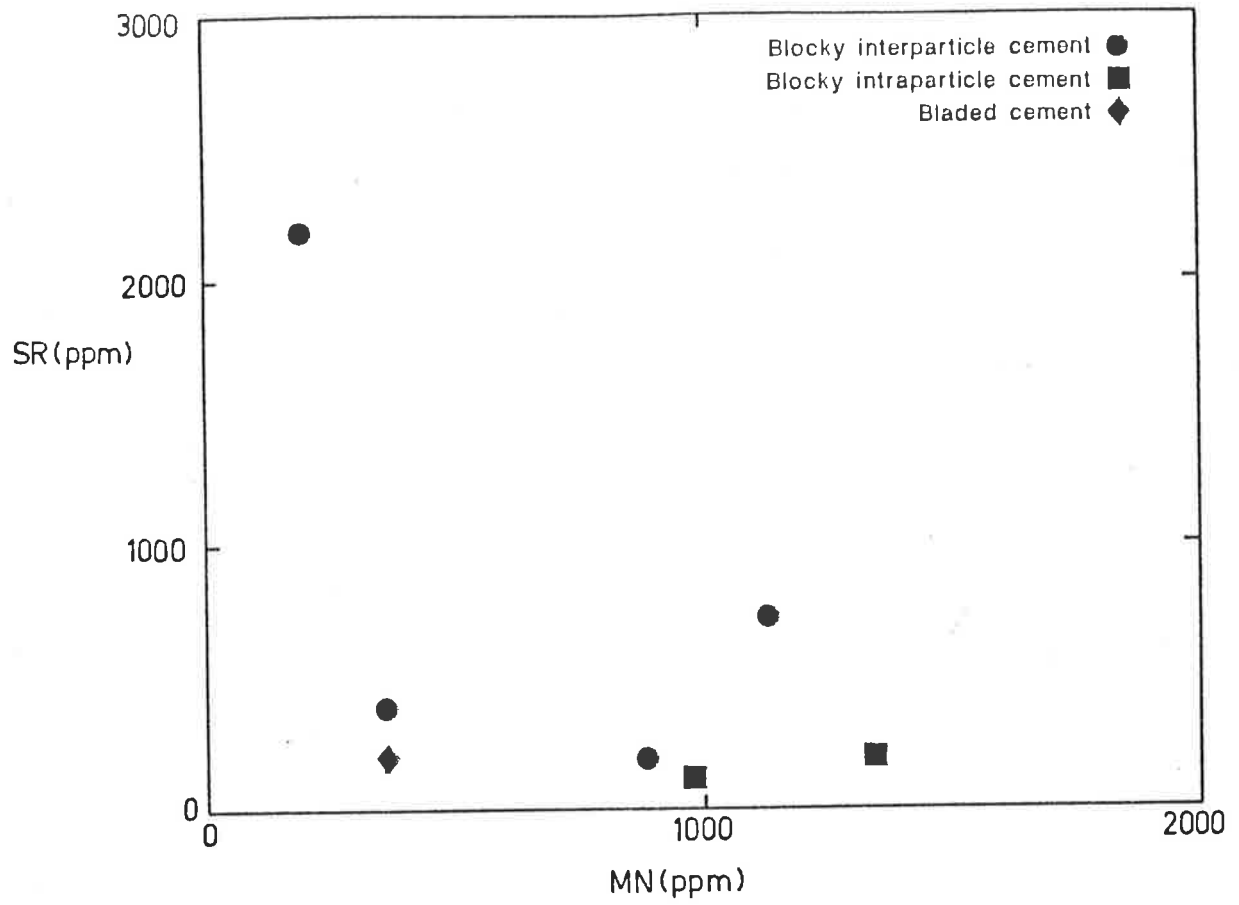
FIG.4.18: Trace element chemistry of cements from the Late
Precambrian Wonoka Formation, showing Sr vs Mn plot.
Each plotted sample represents the mean of between 10 to
20 individual microprobe analyses.

FIG.4.19: Trace element chemistry of cements from the Late
Precambrian Wonoka Formation, showing Sr vs Fe plot.
Each plotted sample represents the mean of between 10 to
20 individual microprobe analyses.

FIG.4.20: Trace element chemistry of cements from the Late
Precambrian Wonoka Formation, showing Sr vs Mg plot.
Each plotted sample represents the mean of between 10 to
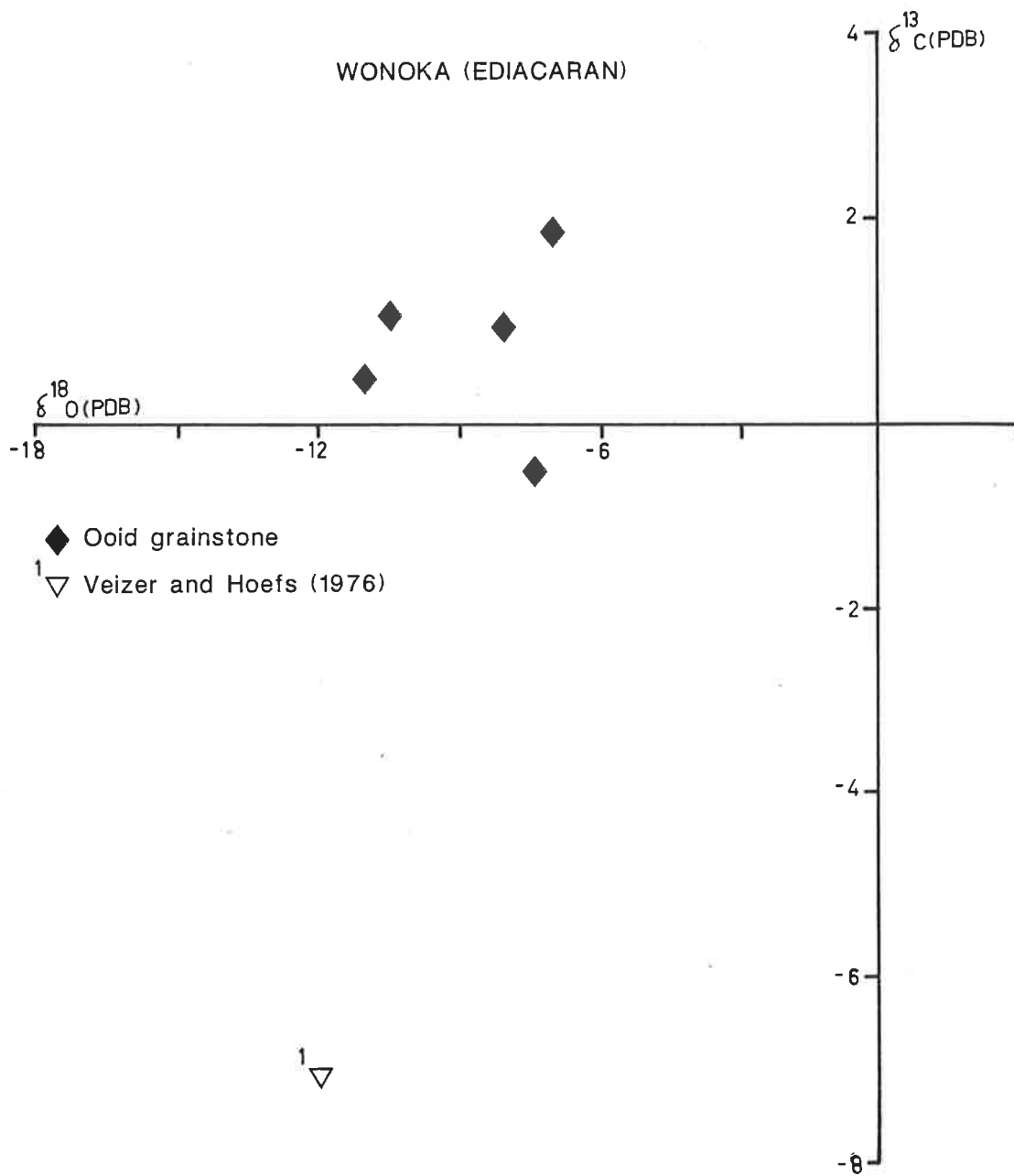20 individual microprobe analyses.
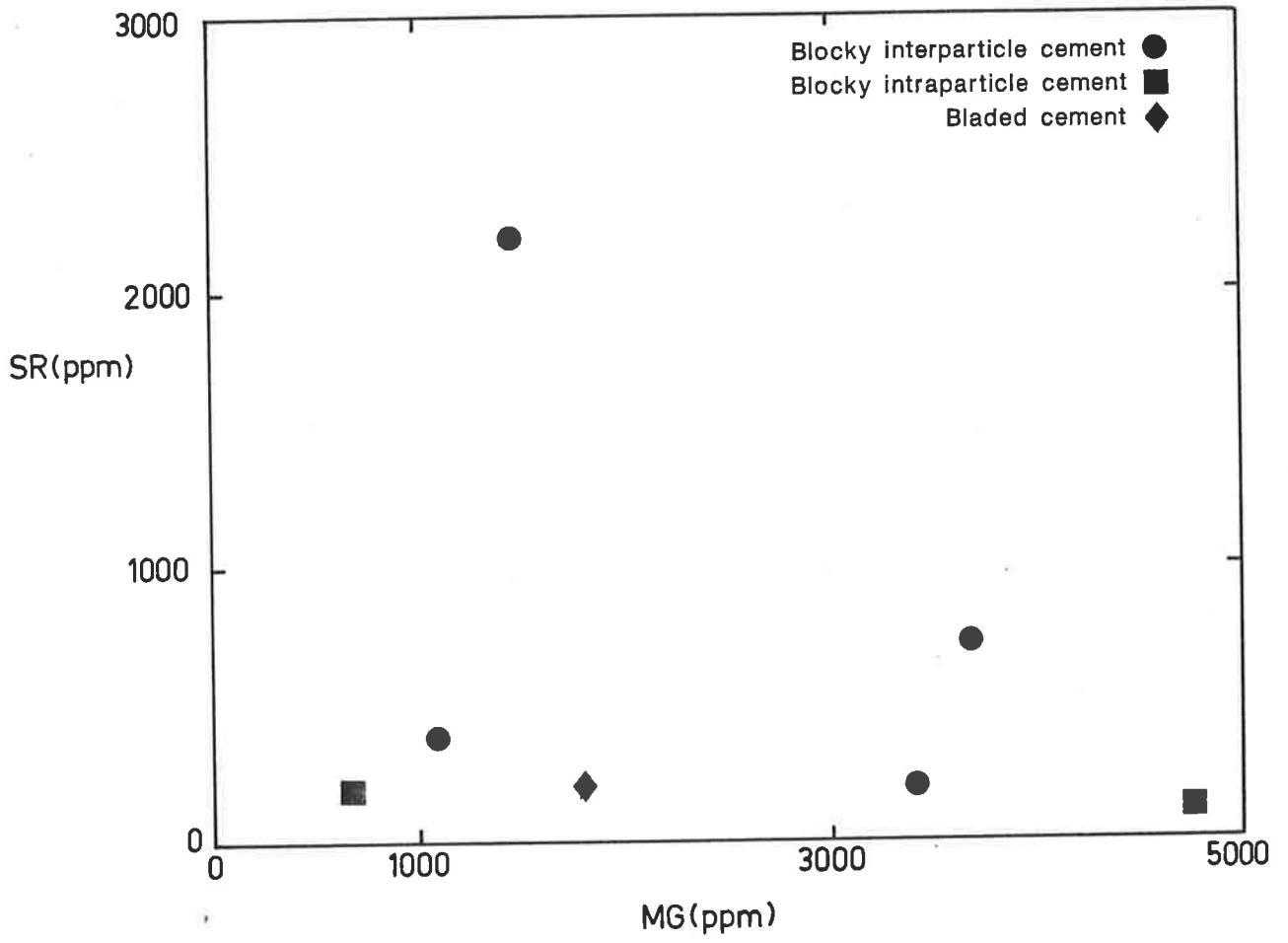
FIG.4.21: STABLE ISOTOPE DATA OF THE WONOKA FORMATION

| Sample | Description | Del O18 | Del C13 |
|--------|-------------|---------|---------|
| **WHOLE ROCK** | | | |
| BU29(1) | Ooid grainstone | -8.19 | 0.99 |
| BU29(2) | " | -11.55 | 0.55 |
| SB19 | " | -10.50 | 1.07 |
| WK34 | " | -7.15 | 1.89 |
| BU2 | " | -7.57 | -0.75 |

FIG.4.22: Oxygen and carbon isotope plot of the Late
Precambrian Wonoka Formation. Analysis is of whole rock
samples.

WONOKA (EDIACARAN)

# CHAPTER FIVE

## EARLY CAMBRIAN WILKAWILLINA LIMESTONE

### 5.1: INTRODUCTION

The Early Cambrian carbonates of the Adelaide
Geosyncline broadly constitute four major stratigraphic
units: the Wilkawillina and Parara Limestones (Ten Mile
Creek), the Ajax Limestone (Mt. Scott Ranges) and the
Andamooka Limestone (Stuart Shelf), as described mainly by
Daily [1956;1972] and Johns [1968]. The Early Cambrian
carbonates can be subdivided into smaller, mapable units
which represent different lithofacies over a regional scale.
The recognition and study of these facies have resulted in
the establishment of new stratigraphic subdivisions; the
Woodendinna Dolomite and the Wirrapowie Limestone constitute
two such recently proposed units [ Haslett 1975].

Cambrian sedimen ∽tion commenced with the Uratanna
Formation, which was deposited on the disconformable surface
of the underlying Pound Quartzite [Daily 1973]. The overlying
clastics of the Parachilna Formation record  the first
widespread Cambrian sedimentation. Carbonate sedimentation
began after the Parachilna Formation clastics, and formed the
transgressive Ajax, Wilkawillina, Parara and Andamooka
Limestones. During late Early Cambrian times there was some
uplift and erosion of the carbonates in some areas, and this
was followed by clastic sedimentation of the Billy Creek
Formation. Carbonate sedimentation commenced again during the
Middle Cambrian with the Wirrealpa and Aroona Creek
Limestones. Sedimentation within the Adelaide Geosyncline
terminated with the clastics of the Lake Frome Group, the

73

uppermost unit being of probable Early Ordovician age [Thomson et al. 1976].

The unit of relevance to the present study is the Wilkawillina Limestone. Haslett [1976] recognised a number of lithological types within this formation: ooid and skeletal grainstones, stromatolite/intraclast mudstones, archeocyathid/algal boundstones, mud-cracked dolomite and calcareous shales. The focus of the present study was on the ooid and skeletal grainstones which constitute a major part of the Wilkawillina Limestone at the Ten Mile Creek type section and are also developed in the Wirrealpa Hill area (Fig.).

As stated in Haslett [1976] the ooid and skeletal grainstone units are developed in the central and western Flinders Ranges. Areas south and west of the Wirrealpa Hinge Zone (line of present day outcrops of Blinman, Wirrealpa and Frome Diapirs) have thick units of ooid and skeletal grainstones, in contrast to the mudstone and wackestone facies of the areas to the north of this hinge zone.

The ooid grainstones studied come dominantly from the Wirrealpa Hill area and the skeletal grainstones from the Ten Mile Creek sections (Fig.5.1). The ooid units have a range of depositional fabrics from grainstones to pack stones and wackestones and vary from light to dark colour. Minor amounts of detrital quartz sand occur with some of the ooids. Archeocyathid fragments are the major components in the skeletal grainstones together with occasional remains of brachiopods and hyolithids. Calcareous algae are fairly common in these skeletal grainstones and can be also found within large cavities which are occluded with thick rinds of white

74

or pale coloured fibrous calcite cements.

## 5.2: PETROGRAPHY

### 5.2.1: OOIDS

Unlike the Late Precambrian units described in previous chapters, the Early Cambrian ooid grainstones consists dominantly of radial ooids. There are, however, various other associated fabrics which result in the generation of different types of ooids. These include radial-concentric ooids, micritic ooids, compound ooids, ooids with eccentric nucleii, broken ooids and ooids with spalled cortices.

Radial Ooids:

These are the predominant ooid type and consist of cortices with radial calcite structures (Figs.5.2 & 5.3). The radial calcite structure is outlined by micritic inclusions and can make-up the whole ooid without any discernible nucleus. Where there is a nucleus present, it is commonly micritic and similar to the associated micritic intraclast. Within these radial ooids there are normally faint concentric micritic bands transecting the radial structure. The radial calcite is non-ferroan and optically continous. The radial calcite cortex can be very thin in some ooids, occurring as an envelope around a micritic core. Although commonly occurring as grainstones, some radial ooids are found within micritic limestones (Fig.5.7).

Radial-Concentric Ooids:

These ooids have a cortex of concentric micritic layers (Figs.5.5 & 5.6). However,these concentric micrite layers have intervening layers of radial calcite, resulting in a cortex of alternating light and dark layers. The nucleus is

generally micritic, although occasionally it comprises a sparry calcite mosaic. In some radial ooids the peripheral parts of the cortex have a micritic envelope resulting in a radial-concentric structure (Fig.5.8). The thickness of this outer micritic envelope varies but is never the dominant component in these radial-concentric ooids and in some ooids it is incompletely developed.

Micritic Ooids:

In places, scattered amongst the other ooids, are found ooids with a vague internal structure and consisting totally of micrite (Fig.5.9). In some micritic ooids the nucleus can be discerned, being of a darker micrite, others have a micritic envelope with a surrounding fringe of bladed cement.

Compound Ooids:

Aggregates of two or more ooids sometimes occur with radial or micritic envelopes, forming compound ooids (Fig.5.12). Some of these compound ooids consists of broken ooid components.

Ooids with Eccentric Nucleii:

Some ooids have a micritic or radial calcite nucleus within a sparry calcite mosaic (Fig.5.11). These nucleii are eccentrically positioned within the ooids. The sparry calcite mosaic has a micrite envelope and two cement generations can be observed within the sparry mosaic.

Broken and Spalled Ooids:

Ooids with spalled envelopes and broken ooid fragments are common in the ooid grainstones (Figs.5.6 & 5.9). The ooids are closely packed with pressure solution contacts and large number of interooid contacts (Figs.5.4 & 5.13).

## 5.2.2: CEMENTS

There are essentially four types of cements within the Early Cambrian limestones; radiaxial fibrous calcite cements, fibrous isopachous cements, bladed fringing cements and blocky or granular cements. Of these only the radiaxial fibrous calcite cements are synsedimentary, whereas the others are postsedimentary. Some ooid grainstones have been extensively dolomitiz ed and were not investigated in the present study (Fig.5.10).

Radiaxial Fibrous Cement (RFC):

This cement constitutes the major pore-filling component in the archeocyatha reef facies and occurs as thick rinds of banded or laminated sparry crust within cavities (Fig.5.16). It consists of a mosaic of bladed or fibrous sparry calcite. The sparry calcite can be clear, with sharp and irregular boundaries and increasing in crystal size away from the pore-walls. Conversely, it can be a distinctly banded, inclusion-rich fibrous calcite rind with no discernible crystal boundaries. Both types display sweeping extinction and are generally iron-poor. Patches of iron-rich blocky calcite mosaics do occur occasionally within these radiaxial fibrous calcite cements. These cements can occur within open cavities or in the interspaces of branching algal structures within such cavities (Figs.5.14 & 5.15).

Fibrous Isopachous Cement:

This cement seems to be restricted to the internal cavities of archeocyathids and forms isopachous rims around micritic elements of the archeocyatha skeleton (Fig.5.17). The calcite normally has a brownish appearance, in contrast to the later clear blocky calcites occluding the pore-spaces

(Figs.5.18 & 5.19).

Bladed Fringing Cement:

This is a common cement type in the ooid grainstones and
represents the earliest cement generation. Prismatic crystal
terminations are normally present and a gradation from
inclusion-rich phases to inclusion-free phases exists
(Figs.5.20, 5.21 & 5.22). The bladed cement is non-ferroan,
like the radiaxial fibrous and fibrous isopachous cements.

Blocky Calcite Cement:

This cement comprises a clear, equant calcite mosaic and
is typically ferroan (Fig.5.19 & 5.20). It represents the
pore-occluding stage of cementation in most cavities and also
occurs in calcite veins and fracture fills.

5.3: TRACE ELEMENT CHEMISTRY

A total of 43 separate components involving 430 to 830
individual microprobe analyses were used in the generation of
the trace element data.

5.3.1: OOIDS

In contrast to the ooids from the late Precambrian units
described in earlier sections, the early Cambrian ooids have
much lower Sr contents. The chemistry of the two major ooid
fabrics, radial and micritic, are very similar in their Sr
and Mg contents (Figs.5.23 to 5.26). The Sr content of both
ooid types range from about 200ppm to 900ppm and the Mg
content from 1500ppm to 2900ppm. Micritic ooids tend to have
a slightly higher Mn and Fe content compared with associated
radial ooids (Fig.5.24,5.25). There is however, a large range
in Mn and Fe content of the ooids; Mn content ranging from
less than detection limit on the probe (195ppm) to 660ppm,

78

and Fe content from about 200ppm to 1300ppm. There is no correlation between the Sr content and the Mn or Mg content. The Fe and Sr plot however, defines a positive correlation (Fig.5.25 ).

The relationship between the Sr and Mn, and Sr and Fe contents reveals trends unlike those normally expected during diagenesis with meteoric waters [Brand and Veizer 1980; Veizer 1983]. There is no increase in the Mn and Fe content of the ooids with decreasing Sr content. This could be accounted for if there was a lack of any meteoric pore-water alteration or from the lack of preservation of any such meteoric alteration due to overprinting by later diagenetic events i.e. burial diagenesis. The increase in the Sr content with increasing Fe could result from burial diagenetic modification and recrystallization of the ooids. Some recent studies have shown that pore-waters can be enriched in Sr under burial diagenetic conditions [Prezbindowski 1985; Baker et al. 1982].

5.3.2: CEMENTS

The trace element chemistry of 3 groups of cements, i.e. radiaxial fibrous cements, bladed/prismatic cements and blocky cements was determined under the microprobe and the results plotted. The trace element chemistry of the cement groups does not define any distinct fields and has large overlaps (Figs.5.27 to 5.32).

The radiaxial fibrous cements has Sr concentrations ranging from about 200ppm to 500ppm, with the Sr concentration decreasing with increasing Mn (Fig.5.27). The Mn concentration has a large variation, ranging from below

the detection limit ( 200ppm ) to 1400ppm. In comparision the range of Fe concentration is smaller, varying from below detection limit ( 200ppm ) to 600ppm (Fig.5.28). The radiaxial fibrous cements have the highest Mg concentration amongst the cements, the maximum measured being 1.23 wt% Mg (Fig.5.29). This high Mg concentration has a correspondingly low Mn and Fe concentration ( <200ppm ). Concentrations as low as 1900ppm Mg are also found in the radiaxial fibrous cements.

The bladed/prismatic cements record some of the highest Sr concentrations ( 1800ppm ) although it generally ranged from 250ppm to 500ppm. The Mn concentration of these cements is very low (Fig.5.27) and defines a small range ( <200ppm to 300ppm ). Although the Fe concentration is also generally low (Fig.5.28), some cements have quite high values ( 1300ppm ). The Mg concentration varied from between 1900ppm to 2500ppm (Fig.5.29).

The blocky cements have a large range of Mn and Fe concentrations, both ranging from < 200ppm to 1500ppm (Fig.5.30,5.31). Their Sr concentration varies from 250ppm to 800ppm. The Sr vs Mn plot reveals a negative correlation for the blocky cements. The Mg concentration of these cements ranges from as low as 1500ppm to a maximum of 3500ppm (Fig.5.32).

5.4: OOID INTERPRETATION

Previous work on these Early Cambrian ooid grainstones consisted mainly of a brief description on their field occurrence and petrographic textures by Haslett [1976, p.40-43]. Haslett recognised two dominant types of ooids, the dark

80

coloured radial ooids and the light coloured micritic ooids. He noted that the dark-coloured radial ooids were associated with low energy sediments and the light-coloured micritic ooids with high energy sediments. The dark colour of the radial ooids was attributed to finely dispersed organic carbon. Such radial calcite ooids are not recorded from the late Precambrian units, except for some rare radial type ooids in the Wonoka Formation (section 4.2.1). A brief overview of previous studies and current understanding of such radial calcite ooids is presented before interpreting the ooid fabrics from the present study.

RADIAL OOID FABRICS AND PRECURSOR MINERALOGY

In spite of the voluminous literature on ooids and their conditions of formation, the details of ooid fabric genesis remain far from resolved. The generation of radial fabrics in ooids have been considered to be both depositional and diagenetic. This has come about mainly from a lack of proper understanding of the genesis of radial fabrics in ooids and from the assumption that the Bahamas-type ooid environments are representative of ancient ooid forming environments. Recent reassesment of modern ooid formation and their diagenetic fabrics indicates that radial ooid textures can be of primary origin, being precipitated as calcitic ooids [ Sandberg 1975 ].

As far back as Sorby [1879], the radial cortical texture of ooids was considered to have been an originally calcitic precipitate. However, this study was forgotten and became buried in the flood of studies on ooids emanating from the Bahamas and Persian Gulf regions [Illing 1954; Newell,Purdy &

Imbrie 1960; Loreau and Purser 1973]. These studies showed that modern marine ooids have an aragonite mineralogy and generate dominantly tangentially oriented crystal fabrics in their cortices. Modern marine aragonite ooids with radial fabrics are restricted to quieter waters and hypersaline lakes [ Davies and Martin 1976; Loreau and Purser 1973; Sandberg 1975; Kahle 1974]. The radial fabrics in ancient ooids were then explained as diagenetic alterations of aragonitic ooids. Bathurst [1971] envisaged a process of inversion of primary aragonite to calcite, thus preserving the details of radial texture. Others suggested that the organic coatings normally associated with ooids may have acted as templates for growth of radial calcite crystals [Shearman et al. 1970]. With aragonite dissolution these organic coatings formed the framework within which voids occurred. The voids are later filled with the radial calcite crystals.

Almost 100 years after Sorby, Sandberg's [1975] landmark paper questioned the validity of accepting modern marine analogs as representative of ancient carbonate precipitation. He discounted the earlier views that Great Salt Lake radial ooids are replacements of originally aragonitic ooids. The large radial rays in these ooids were actually aragonitic rather than calcitic, as previously thought [Kahle 1974]. Kahle proposed that this radial texture could be the result of an aragonite-aragonite transformation process. Sandberg [1975] broadly agreed with Kahle's findings but concluded that radial texture in ooids was generated by precipitation of originally calcitic crystals. He disagreed with the possibility of an aragonite-aragonite transformation. Using

the findings of various other workers and the behaviour of skeletal aragonitic components during diagenesis, he concluded that those ancient non-skeletal grains ( i.e. ooids ) that preserve fine texture must be originally calcitic. Aragonite transformation produces coarse calcite textures, with destruction of any fine precursor texture. Occasionally aragonite inclusions occur within these coarse neomorphic calcites, as well as relics of the precursor fabric. Both these observations seem to suggest the lack of a void stage during aragonite-calcite transformation, thus invalidating Shearman et al.'s [1970] ideas on radial ooid fabrics.

Mg calcite ooids are absent from modern normal marine environments. Relic calcitic ooids have been found in the Great Barrier Reef area and in the Amazon Shelf [ Marshall and Davies 1975; Milliman and Barreto 1975]. Mixed aragonitic-calcitic ooids have been studied from Baffin Bay with radial calcitic fabrics and tangential aragonitic fabrics [ Land, Behrens and Frishman 1979 ]. Radial ooids have been successfully synthesized in the laboratory using organic solutions and unagitated waters [ Davies et al.1978 ]. There are, however, radial ooid structures being generated in inorganic environments such as thermal springs and spherulites in the laboratory [ see Simone 1981 ]. The water chemistry presumably has some control on the radial fabric of aragonitic ooids [ Lippmann 1973]. Radial fabrics in ooids are therefore not unequivocally of organic origin.

An inorganic control, namely the degree of turbulence or transport mechanism may have an effect on the resulting fabrics of ooids [ Heller, Komar and Pevear 1980; Medwedeff and Wilkinson 1983 ]. Heller et al. [1980] proposed a

hyrodynamic interpretation for the radial and concentric fabrics of their ooids. Radial ooids were found to be smaller in size and dominantly experienced suspension transport. Concentric ooids on the other hand were of a larger size and had their originally radial fabric modified by abrasion during bed-load transport. Medwedeff and Wilkinson [1983] noted a progressive change in the cortical fabrics of their ooids from large radial laths to stubby radial laths to equant nannograins with increasing banding density. They noted no difference in the fabric of small ooids of either aragonitic or calcitic mineralogy. Large calcitic ooids, however, had equant nannograined cortical layers whereas large aragonitic ooids had random to tangential cortical layers.

Whilst it might be possible to be fairly confident about the original calcitic mineralogy of radial ooids, the original Mg content of these calcitic precursors is normally difficult to interpret. Richter [1983] has argued that the calcitic precursor of the radial ooids was probably Mg calcite. He based this on the replacement of radial ooids by ferroan calcite and their dichotomous behaviour compared with associated aragonite shells. The preservation of precursor fabrics during diagenesis of these ooids suggest paramorphic replacement during diagenesis.

Recent studies of ancient ooids have appeared suggesting a primary nature for the radial texture in ooids. Wilkinson and Landing [1978] demonstrated the primary nature of the radial texture in their ooids by the relationship between dissolution and compaction. The primary nature of radial textures in early Cretaceous ooids was suggested by Simone

[1972] and D' Argenio et al. [1975]. Precambrian ooids with inferred primary radial calcitic ooids have also been reported [ Tucker 1984 ].

In the present study the radial calcite ooids are also interpreted to be primary calcitic precipitates. The occurrence of syntaxial rims of bladed calcite cements enveloping some of these radial ooids and the dichotomous behaviour of radial calcite nucleii,as well as the envelopes of sparry calcite mosaics in some bimineralic ooids supports the interpretation of a calcitic mineralogy for these ooids.

A primary calcitic mineralogy for these radial calcite ooids would be consistent with their low Sr content, since calcitic precursors have a much lower original Sr content compared to aragonitic ones. However, such trace element data in isolation are not conclusive evidence of precursor mineralogy since low Sr content could also result form diagenetic alteration of aragonitic components. However, diagenetic alteration of aragonitic precursors would not generate such fabric retentive textures as observed in the radial calcite ooids [Sandberg 1985].

Based on the non-ferroan nature of the radial calcite ooids, a low Mg-calcite mineralogy may be suggested as the precursor, since replacement of high Mg-calcite precursors would result in ferroan calcites [Richter 1983; Richter and Fuchtbauer 1978]. Such an interpretation assumes a diagenetic environment with a supply of $Fe^{2+}$ ions. It is quite possible to produce non-ferroan calcite replacements of high Mg-calcites in an $Fe^{2+}$ ion free environment. The presence of high Mg content in the radial calcite ooids may have supported an original high Mg-calcite mineralogy, as

suggested by the high Mg content of some of the RFC cements
(section 5.5). However, the absence of such high Mg content
does not discount the possibility of an original high Mg-
calcite mineralogy. Thus it would seem that with the
available evidence an interpretation of the original Mg
content of the radial ooid calcitic precursors is not
possible.

The micritic fabrics of ooids is not a reliable
indicator of precursor mineralogy, as already discussed in
earlier sections on the late Precambrian ooids (sections 2.4,
3.4 and 4.4).

5.5: CEMENT INTERPRETATION

The syn-sedimentary radiaxial fibrous calcite cements
(RFC) associated with archeocyatha reef facies are
interpreted to have had a calcitic ( high Mg calcite or low
Mg calcite ) precursor. Fabric evidence suggests retention of
original precursor textures and a lack of calcitization
fabrics. Such cements have been reported from numerous
Paleozoic reef carbonates [ Kendall and Tucker 1973; Krebs
1969; Davies 1977; Walls et al. 1979; Kendall 1985 ]. Earlier
views on the genesis of these cements regarded them as
replacements of acicular aragonite or high Mg calcite
precursors [ Kendall and Tucker 1973 ]. Also the lack of any
evidence of calcitic cements with the textures of RFC in
modern marine settings negated their existence as primary
precipitates in ancient ocean waters.

Recent studies have revealed that these RFC cements
could represent primary precipitates [ Kendall 1985 ]. Stable
isotope data provide  constraints on their genesis and
suggest a non-replacement origin for the RFC cements [ Hudson

and Coleman 1978; Walls et al. 1979 ]. The occurrence of both RFC and fasicular optic calcite (FOC) cements in aragonitic Pleistocene limestones as well as in other ancient carbonates implies a possible difference in genesis [ Sandberg 1985; Kendall 1977; Chafetz 1979 ].

The retention of high Mg concentrations within some of the RFC cements of the present study suggests a possible high Mg calcite precursor. The high Mg concentration probably represents limited recrystallization events and limited alteration in meteoric pore-waters, as shown by the low Mn and Fe content of some of these cements. Presumably the high Mg calcite-low Mg calcite transformation took place with loss of Mg and retention of precursor textures, representing a paramorphic replacement type process.

The fibrous isopachous cements are a common cement type in marine environments and are interpreted to represent marine phreatic precipitates in the present study. Their high Mg content suggests that they probably were originally Mg-calcite precipitates. An aragonitic precursor for these cements would not be consistent with the fabric evidence, since it's diagenetic alteration would result in a fabric destructive calcite mosaic.

Bladed fringing cements could represent either meteoric or marine phreatic precipitates. In the present study they formed syntaxial rims around radial calcite ooids, suggesting an original calcitic mineralogy. It is quite likely that these bladed cements formed in meteoric pore-waters, with low Sr and Mg content, with local enrichment in Sr possibly from dissolution of aragonitic components. Such high Sr content in cements have also been noted from the late Precambrian

limestone units described in previous chapters.

The blocky calcite cements are interpreted to be meteoric phreatic precipitates with some of the very coarsely crystalline and poikilitic cements of interparticle areas being possibly of deep burial genesis. There is evidence of compaction and pressure solution in these ooid grainstones (Fig.X). The large scatter in the Fe and Mn content of these blocky cements suggest pore-waters with variable composition and/or Eh conditions.

## 5.6: OXYGEN AND CARBON ISOTOPES

A total of 25 samples were analysed for oxygen and carbon isotope compositions. The C-O plot of the early Cambrian carbonates defines a field that is fairly distinct from the Balcanoona Formation and has an overlap with the Trezona and Wonoka Formations (Figs.5.33 to 5.35). As in the late Precambrian units, there is a large scatter in oxygen and carbon isotope compositions. The carbon isotope composition varies from -7.35 permil to 3.0 permil and the oxygen isotopes from -6.85 permil to -18.40 permil. Analysis of homogeneous components, namely ooids, stromatolites and micrites tends to indicate a bimodal carbon isotope distribution with carbon isotope values around 0 permil and - 6.0 permil. The oxygen isotopes for both populations remains the same, ranging from -8.70 permil to -14.0 permil.

The carbon isotope composition of the RFC cements has a large scatter from -5.15 permil to 0.9 permil (Fig.5.35). The depleted carbon isotope compositions are recorded by RFC cements associated with pisoliths from a karstic subaerial exposure surface. The carbon isotopes of RFC cements in

cavities and interparticle voids not associated with the subaerial exposure surface cluster around 0 permil, representing normal carbon isotope compositions. The depleted carbon isotopes indicate input from organic carbon sources. Such trends are recorded from subaerial exposure surfaces in Pleistocene carbonates [Allan and Matthews 1977; 1982; Videtich and Matthews 1980], due to the involvement of soil gas $CO_2$ in the pore-waters during meteoric diagenesis. The presence of such depleted carbon isotope compositions within the subaerial diagenetic components in the early Cambrian could suggest involvement of similar phenomenon. Evidence for soil gas contributions causing depleted carbon isotope signatures have been reported from rocks as old as the middle Proterozoic [Beeunas and Knauth 1985]. Therefore, isotopic evidence from the present early Cambrian section and the study of Beeunas and Knauth [op cit.] seems to suggest the existence of a biologically active soil zone much earlier than the oldest known fossilized land plants of Upper Silurian age [Chaloner 1970].

Some of the other samples recording depleted carbon signatures were far removed from this subaerial exposure surface and had no features suggesting exposure. They have however, a dark, euxinic character resulting presumably from organic carbon. Presumably the presence of this organic carbon may have resulted in the formation of the depleted carbon isotope signatures during diagenesis. This can result from processes of organic decay and by bacterial activity [Hodgson 1966; Irwin et al.1977], whereby isotopically light $CO_2$ is produced and incorporated into the bicarbonate of pore-waters.

An alternative explanation for the depleted carbon isotope signature of samples not associated with the subaerial exposure surface would involve fluctuations in the sea-water TDC (total dissolved inorganic carbon) isotopic composition. Rapid fluctuations in the carbon isotope composition of sea-water bicarbonate have been inferred from studies of carbon isotope profiles across the Precambrian-Cambrian boundary [Magaritz et al.1986; Tucker 1986]. Within the basal Cambrian, shifts in the carbon isotopes of approximately 4 permil have been recorded from only 50m of section [Magaritz et al.1986]. Due to inadequate sampling, such rapid carbon isotope shifts in the early Cambrian could not be detected in the present study. In addition, the objectives of the present study were to assess major and broader scale isotopic and mineralogical variations spaning a larger time interval from the Late Precambrian (Sturtian) to the early Cambrian.

The oxygen isotope composition of some of the samples are unusually light (max.-18.40 permil). These light oxygen isotope compositions indicate equilibration with pore-waters at higher temperatures of burial and/or with lighter isotopic compositions. Burial diagenetic features are common in some of the ooid grainstones, with over-compacted grain to grain contacts, poikilitic cements and pressure solution seams. The ooids, micrites and ooid grainstones record much lighter oxygen isotope compositions than the radial fibrous cements. Ooids and micrites, being essentially depositional components comprising a fine grain size, will tend to equilibrate much more easily and readily with increasing burial compared to the coarser grained and comparatively stable early diagenetic

radial fibrous cements. Dickson and Coleman [1980] recorded much lighter oxygen isotope compositions for their lime muds compared to skeletal components and attributed this to the fact that lime mud progressed much further along an equilibration path due to it's finer grain size.

The increasingly light oxygen and heavy carbon isotopic composition trend recorded by the stromatolite, micrite and ooid and ooid grainstone samples could be explained in terms of increasing burial and rock/water interaction (Fig.5.34). With progressive equilibration associated with rock/water interactions under burial conditions, the oxygen isotope composition becomes lighter and the carbon isotopes approach rock compositions.

In contrast, the radiaxial fibrous cements have an almost invariant oxygen isotope trend and a large scatter in the carbon isotopes. The oxygen isotope composition of the radiaxial fibrous cements ranged from -7.94 to -9.05 permil, with the oxygen isotopes of the radial fibrous cements associated with pisoliths from the subaerial exposure level being marginally lighter (-8.02 to -9.05 permil).

Such high variability in the carbon isotope composition and relatively unchanged oxygen isotopes can result from progressive rock/water interaction in an open diagenetic system [Meyers and Lohmann 1985]. Meteoric waters, being depleted in both heavy oxygen and carbon isotopes compared to the coeval marine waters, will result in precipitation of calcites with depleted isotopic compositions during meteoric diagenesis. The highly variable carbon isotope signature and the invariant oxygen isotopes of the radiaxial fibrous cements probably represents this diagenetic alteration in an

open system. The similarity in the oxygen isotope compositions of the types of radiaxial fibrous cements, those in pisoliths and those in interparticle voids and cavities, suggest that the pore-waters involved in the diagenetic stabilization of the marine radiaxial fibrous cements were isotopically similar to those involved in the genesis of radiaxial fibrous cements in pisoliths associated with the karst surface. The implies that the oxygen isotope composition of the marine radiaxial fibrous cements is not representative of marine water composition but has been affected by meteoric waters. The oxygen and carbon isotope composition of radiaxial fibrous cements from the early Cambrian of Canada [James and Klappa 1983] are ploted for comparision. The marine radiaxial fibrous cements from the present study are more depleted in the oxygen isotopes compared to the Canadian cements, probably because of it's greater diagenetic alteration.

5.7: SUMMARY

Petrographic evidence from the oolites of the early Cambrian Wilkawillina Limestone reveal the presence of non-skeletal aragonite precipitation in some of the ooids. Ooids with inferred aragonitic precursors occur as sparry ooid molds. However, unlike the late Precambrian limestones described earlier, the early Cambrian ooids have dominantly radial calcite fabrics, which are inferred to represent primary calcitic precipitates. The presence of bimineralic ooids is indicated by eccentrically displaced nucleii with radial calcite fabric within an envelope of sparry calcite mosaic. The chemistry of the radial calcite ooids, with it's

92

low Sr and Mg content supports the textural evidence for a calcitic precursor but it's original Mg content is not known.

The carbon isotope composition of these limestones recorded very large range of values from -7.35 to 3.0 permil. This large scatter in the carbon isotopes is the result of either light carbon isotope contributions from a biologically active subaerial environment and breakdown of organic carbon during diagenesis or fluctuations in the carbon isotopic composition of sea-water TDC. Definite subaerial exposure features associated with some of the depleted carbon isotope signatures offer a partial explanation but not all the depleted carbon signatures are attributable to this phenomenon. One needs to resort to the possibility of organic carbon oxidation or fluctuating sea-water TDC.

Oxygen isotope composition of some samples is very light and probably resulted from burial diagenetic alteration and equilibration. The oxygen isotope signatures of the marine radiaxial fibrous cements record the heaviest values but have nonetheless been affected by meteoric diagenesis and are therefore not representative of the marine water isotopic composition.

FIG.5.1: Location map of the Ten Mile Creek (Wilkawillina Gorge) and Wirrealpa sample areas of the Early Cambrian Wilkawillina Limestone (Based on Parachilna 1:250,000 sheet).

LAKE TORRENS

BLINMAN

WIRREALPA

TEN MILE
CREEK

CAMBRIAN     DIAPIR

PRECAMBRIAN

0        25km
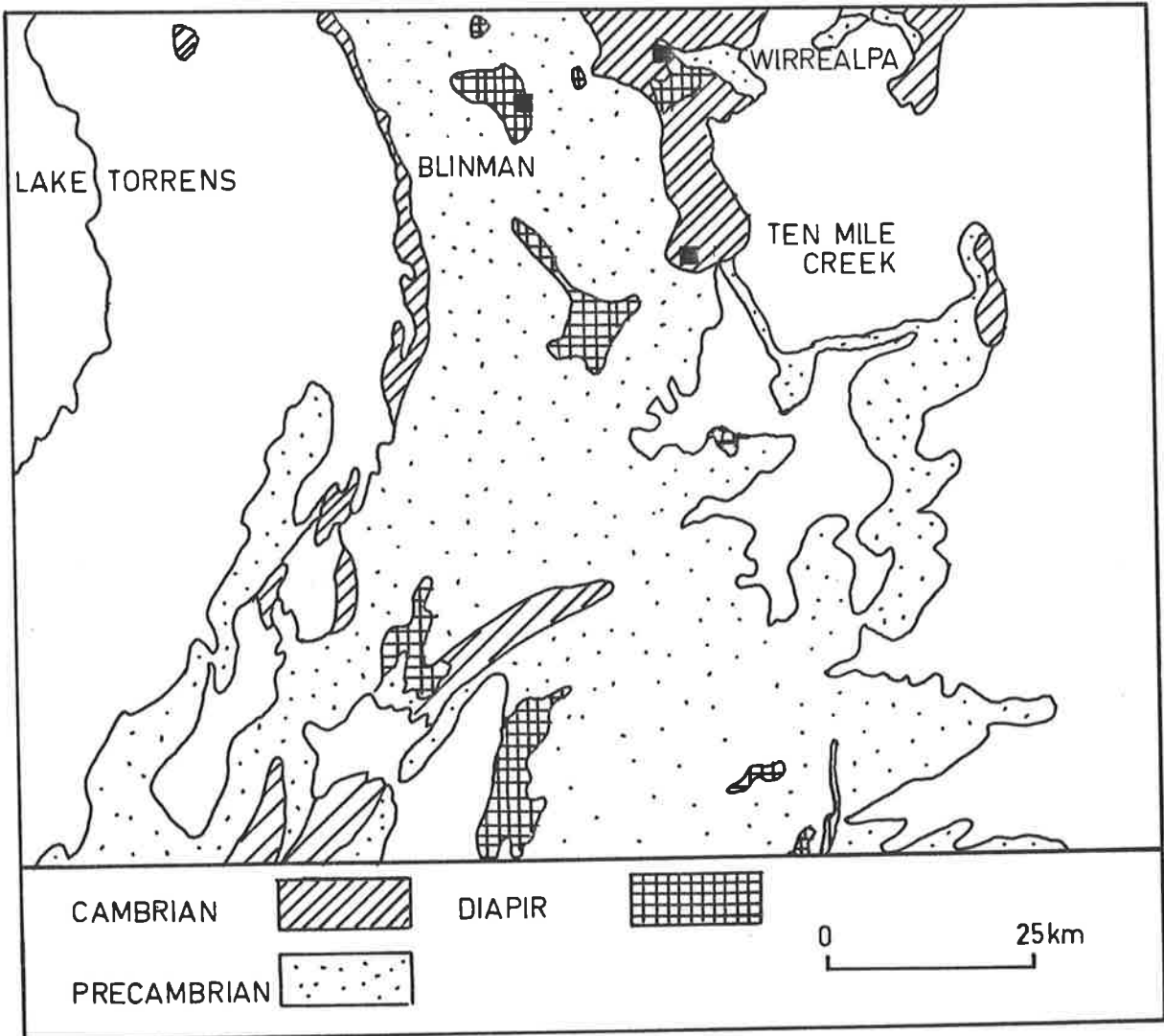
FIG.5.2: Ooid grainstone with radial ooids and intraclast.
Some of the radial ooids have micritic nucleii. Note
highly compacted fabric of grainstone. Field of view is
4.4mm.

FIG.5.3: Close-up of radial ooid with micritic nucleus and
faint concentric bands transecting the radial fabric of
the cortex. Field of view is 1.1mm.

FIG.5.4: Highly compacted radial ooid grainstone with some
sutured interooid contacts. Some interparticle areas have
coarsely crystalline poikilotopic calcite cement. Field of
view is 4.4mm.
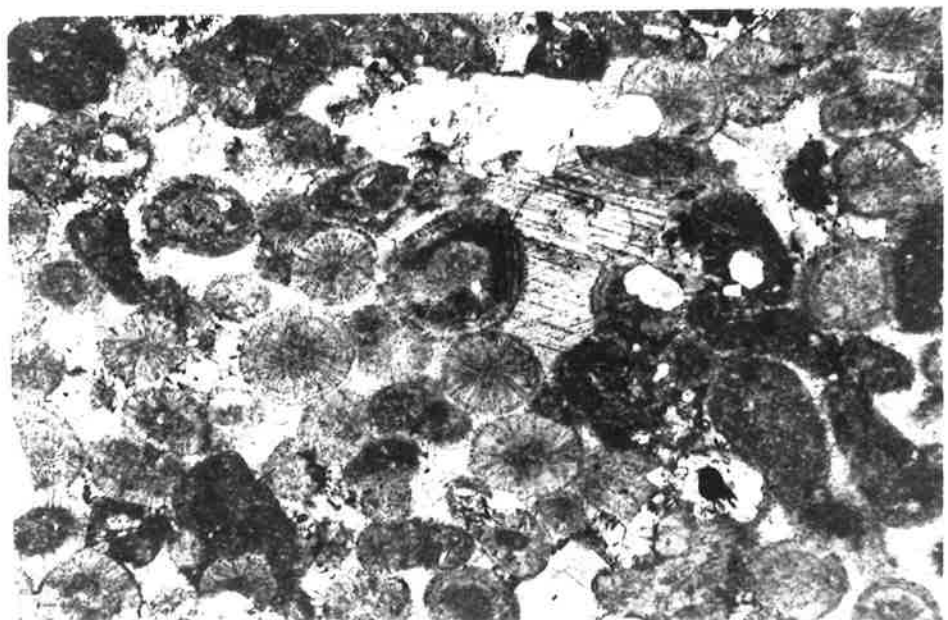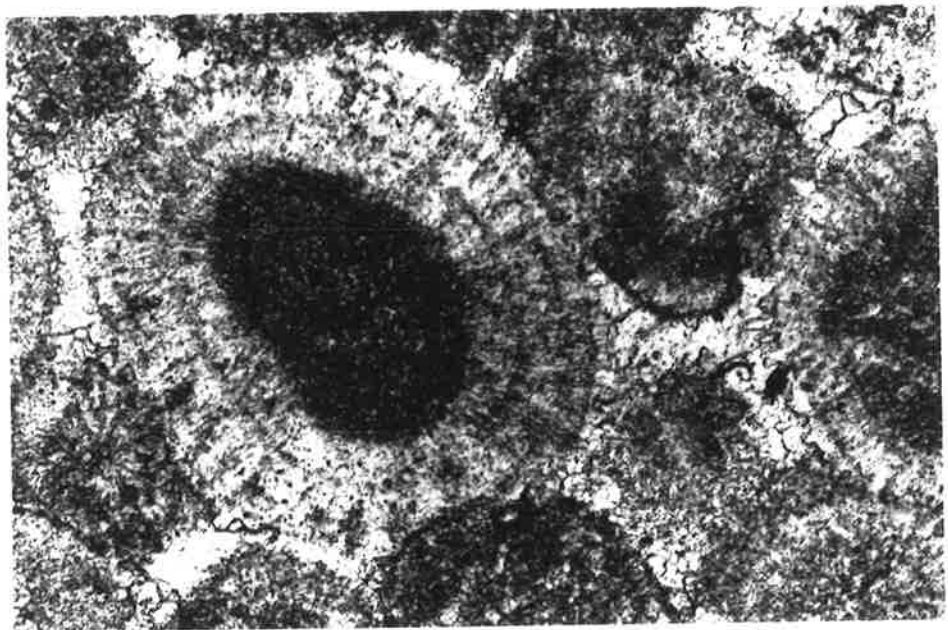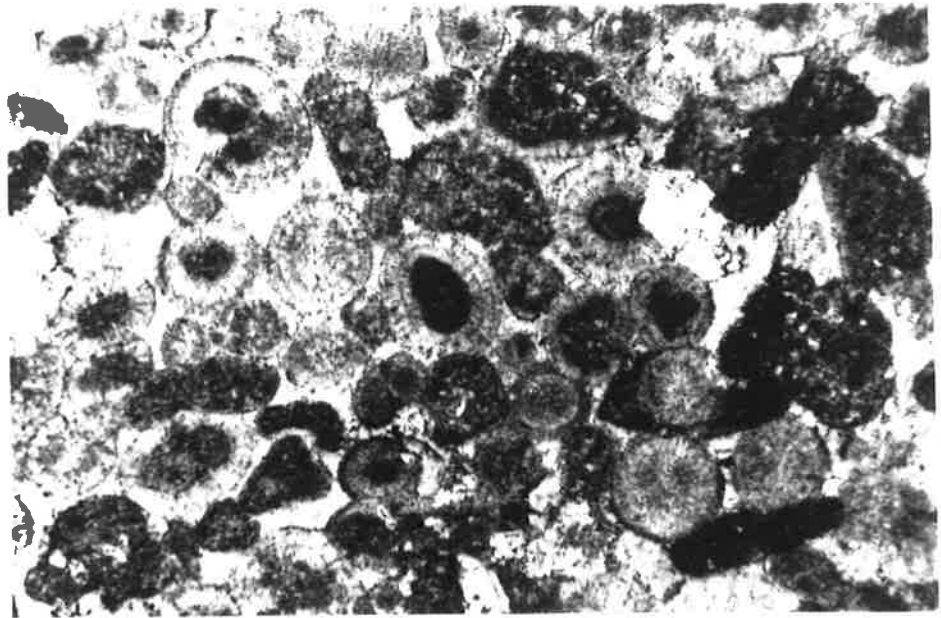
FIG.5.5: Radial-concentric ooids with alternating radial and micritic fabrics. Note intraclasts of broken radial ooids. Field of view is 4.4mm.

FIG.5.6: Radial-concentric ooids with broken and abraded cortices. Field of view is 4.4mm.

FIG.5.7: Radial ooids in a micritic limestone with a few detrital quartz grains. Field of view is 4.4mm.
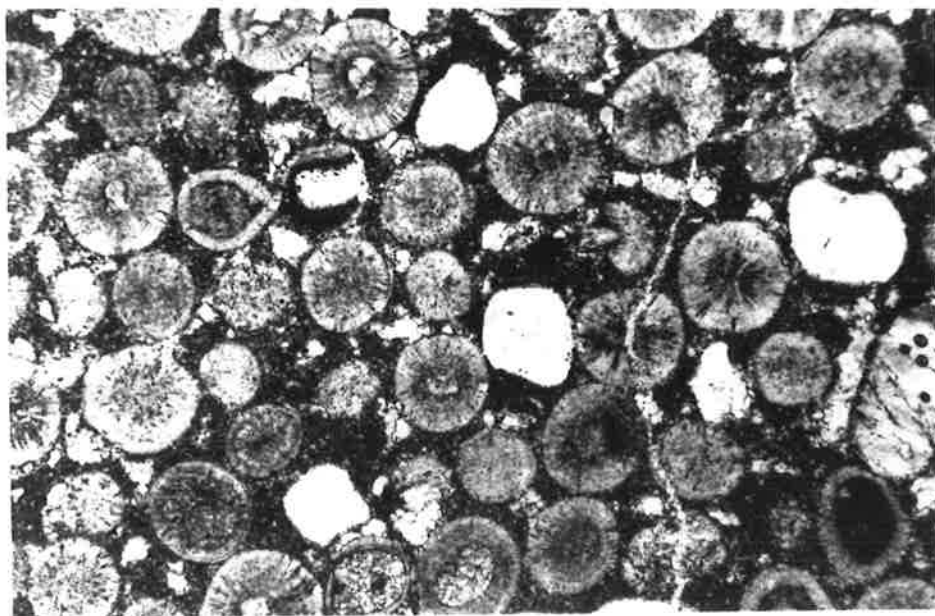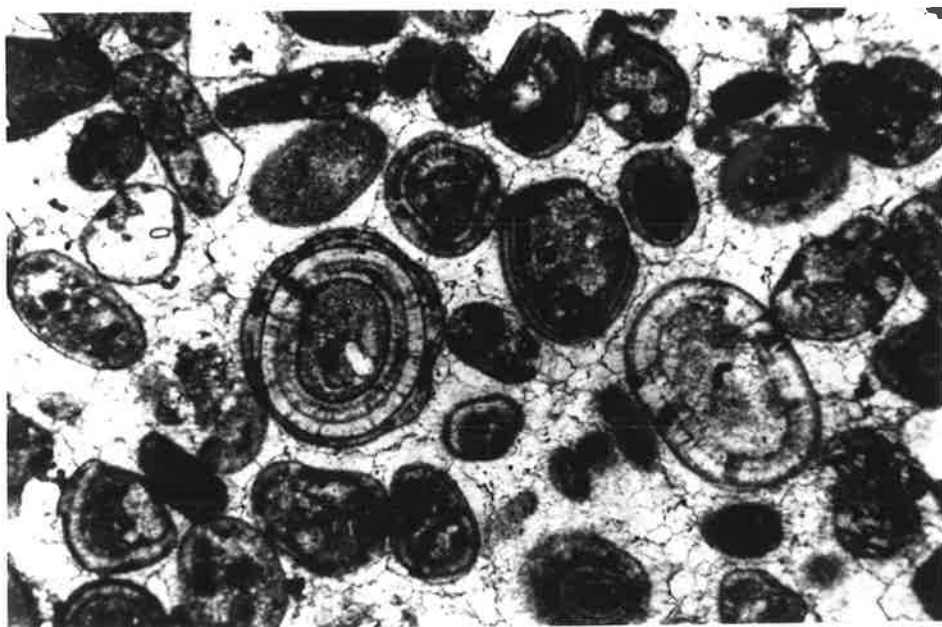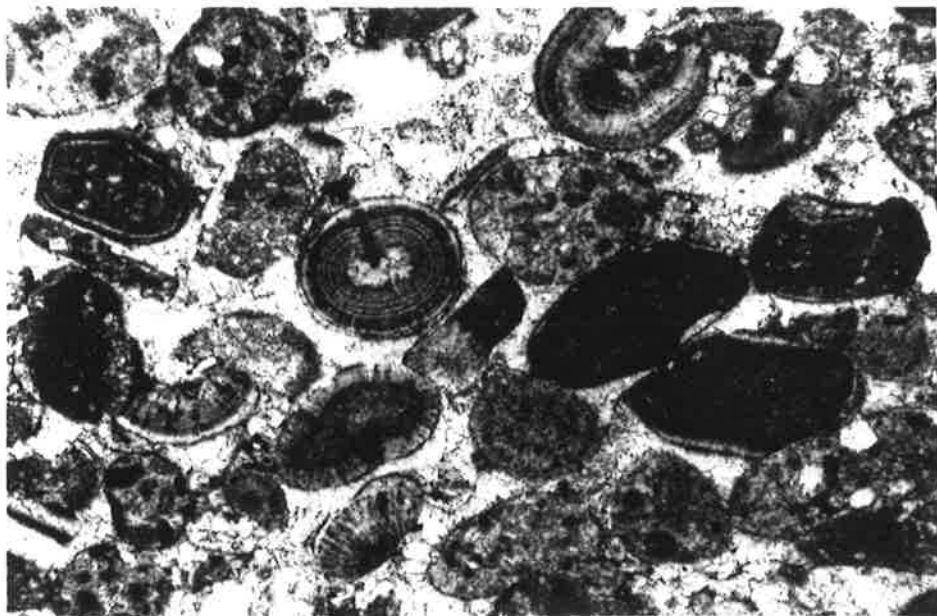
FIG.5.8: Radial and radial-concentric ooids with occasional spalled cortices. Note presence of sparry ooid molds on the right. Field of view is 4.4mm.

FIG.5.9: Micritic ooids with spalled cortices and selective dolomitization of ooid cores. Field of view is 4.4mm.

FIG.5.10: Dolomitized ooid grainstone with dolomite in interparticle areas. Field of view is 4.4mm.
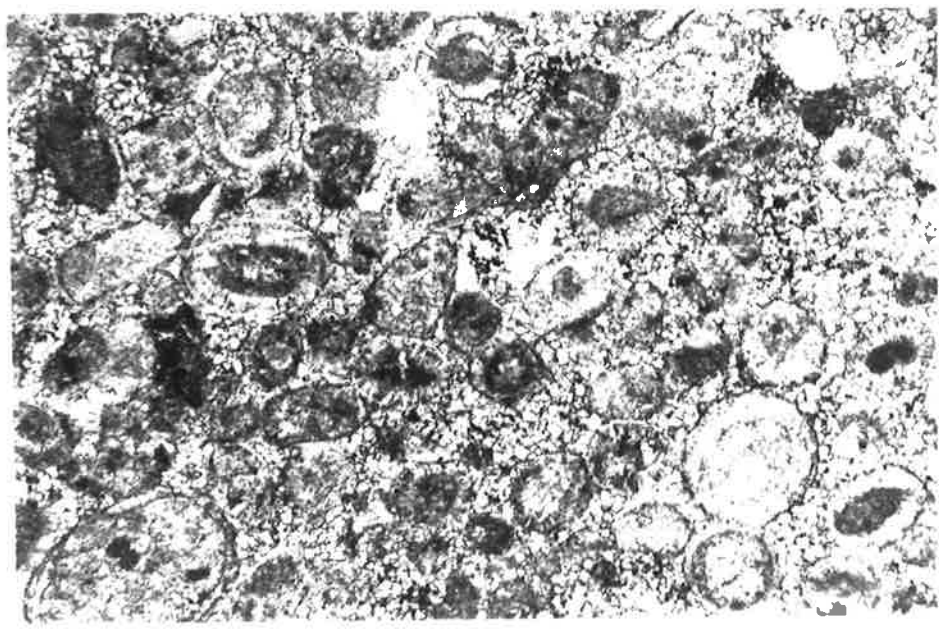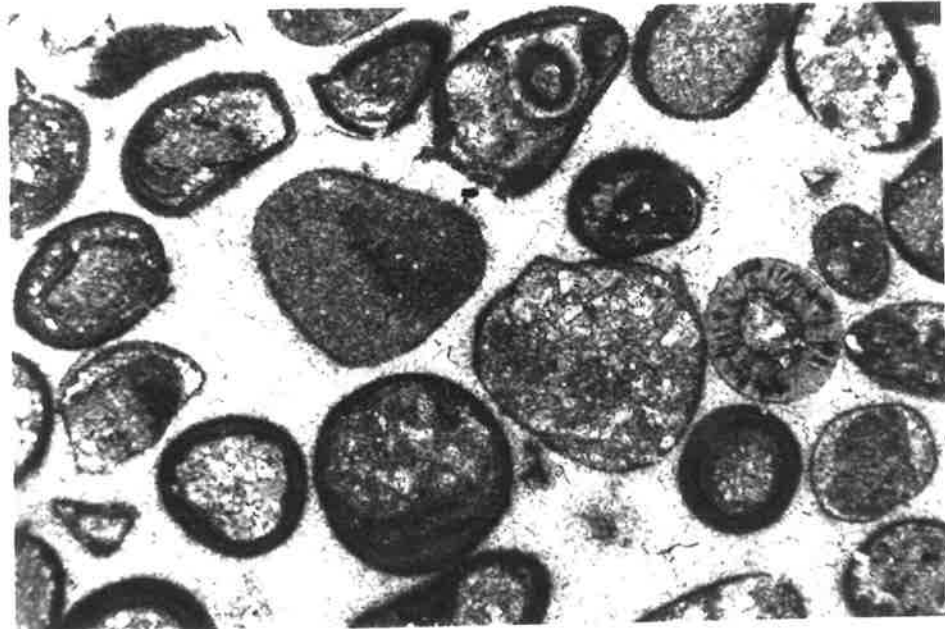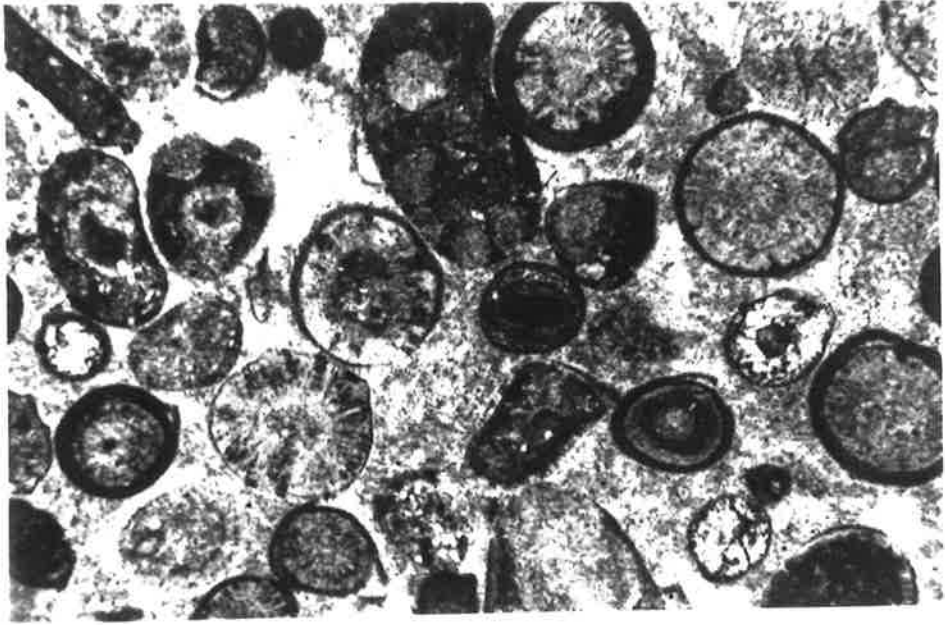
FIG.5.11: Ooids with eccentric nucleii of radial ooids.
Crossed polars. Field of view is 4.4mm.

FIG.5.12: Radial-concentric ooids forming compound ooids.
Many of the radial ooids are broken and abraded. Field of
view is 4.4mm.

FIG.5.13: Highly compacted ooid grainstone with radial and
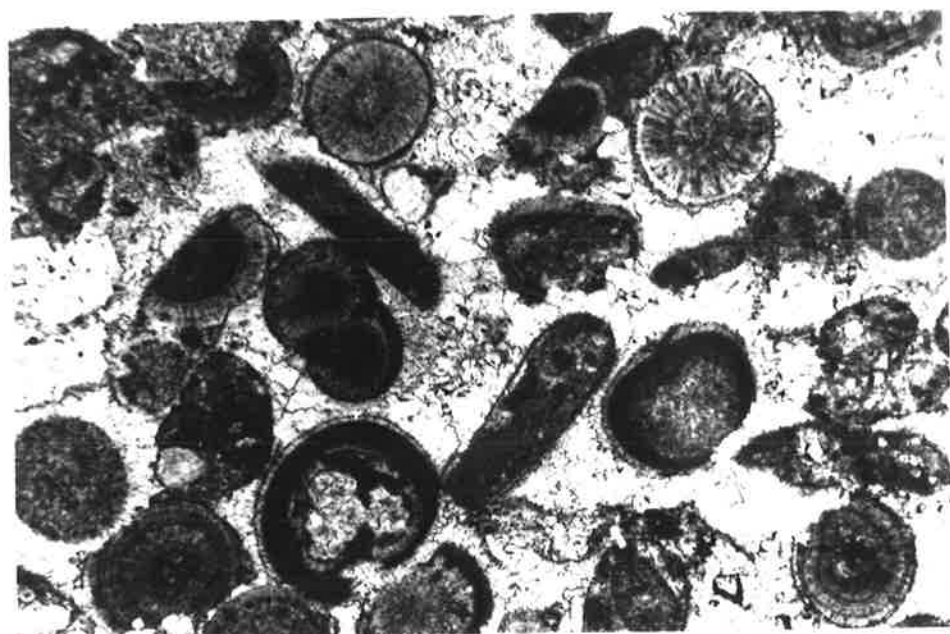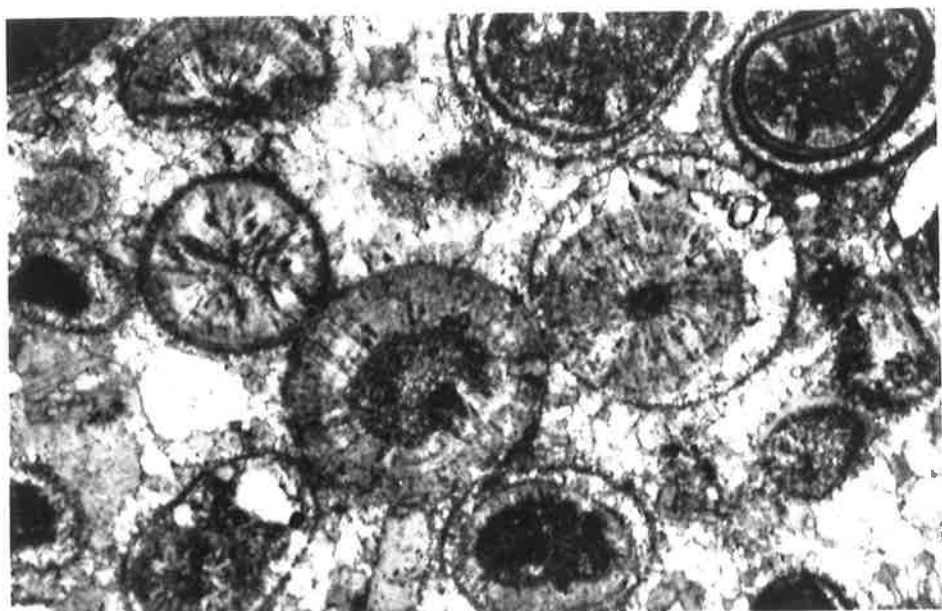micritic ooids. Field of view is 4.4mm.
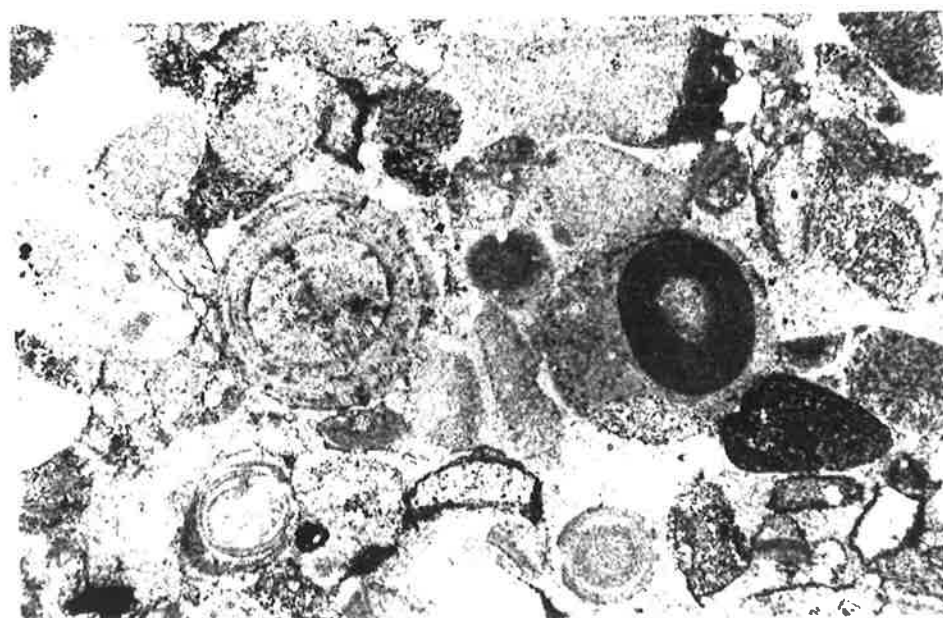
FIG.5.14: Radiaxial fibrous calcite cement filling a cavity with branching algal colony. Field of view is 4.4mm.

FIG.5.15: Archeocyathid cavity cemented with radiaxial fibrous calcite. Field of view is 4.4mm.

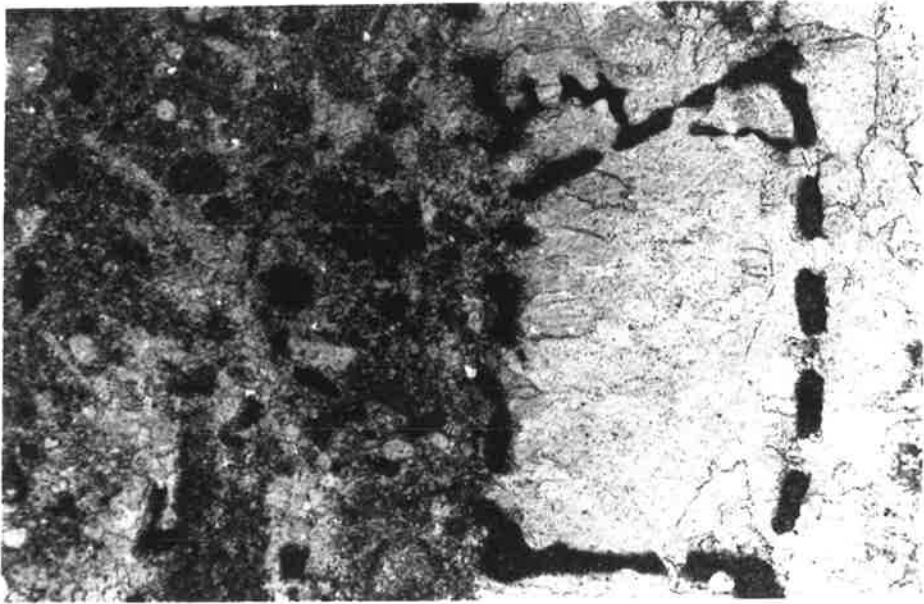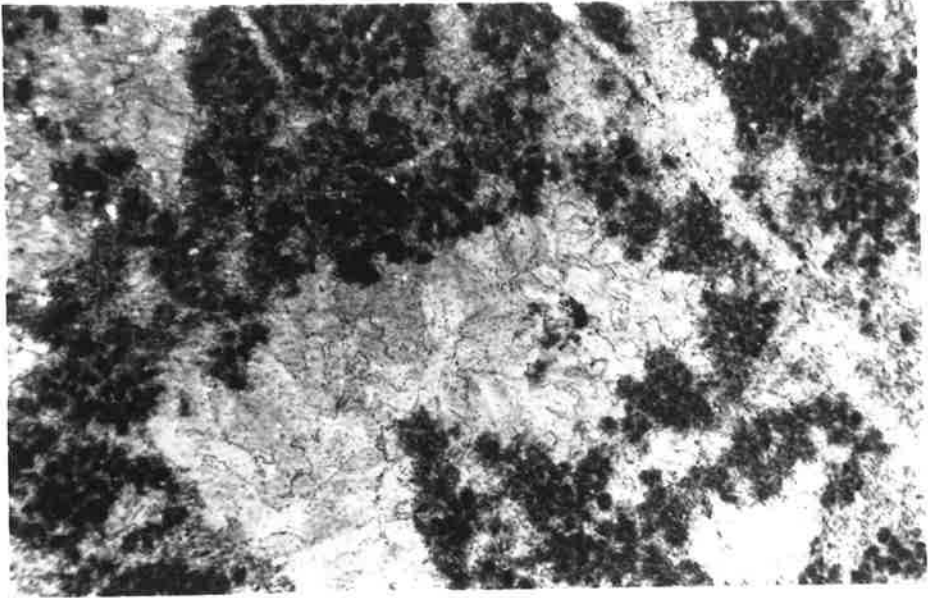FIG.5.16: Radiaxial fibrous calcite cement occupying a cavity. Crossed polars. Field of view is 4.4mm.

FIG.5.17: Fibrous isopachous cement fringing archeocyathid
skeleton. Pore centers occupied by blocky calcite cement.
Field of view is 4.4mm.

FIG.5.18: Fibrous isopachous cement fringing micritic
archeocyathid skeleton. Field of view is 1.1mm.

FIG.5.19: Fibrous calcite cement grading to blocky calcite
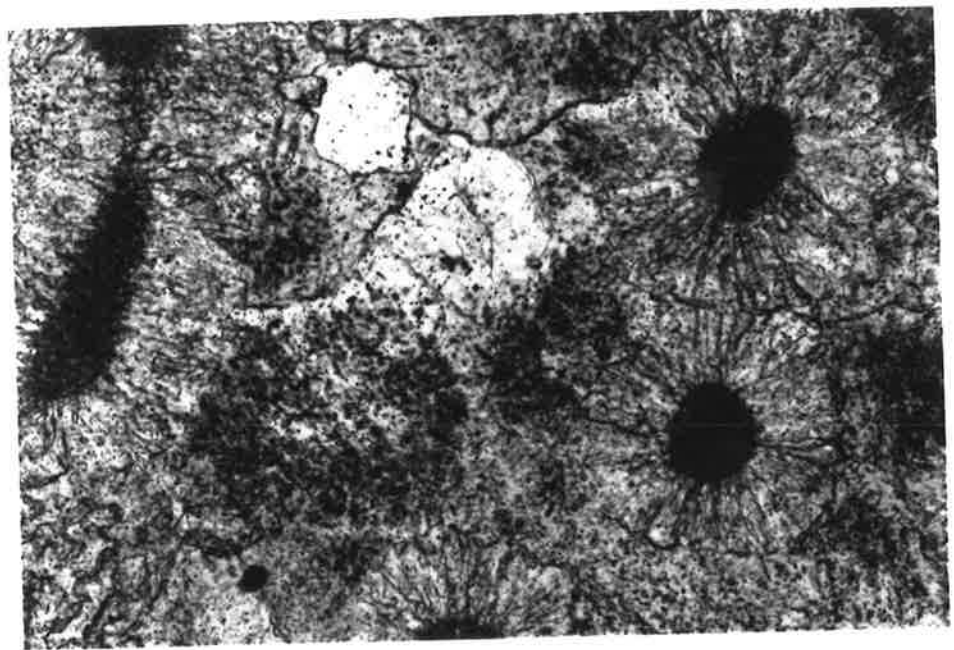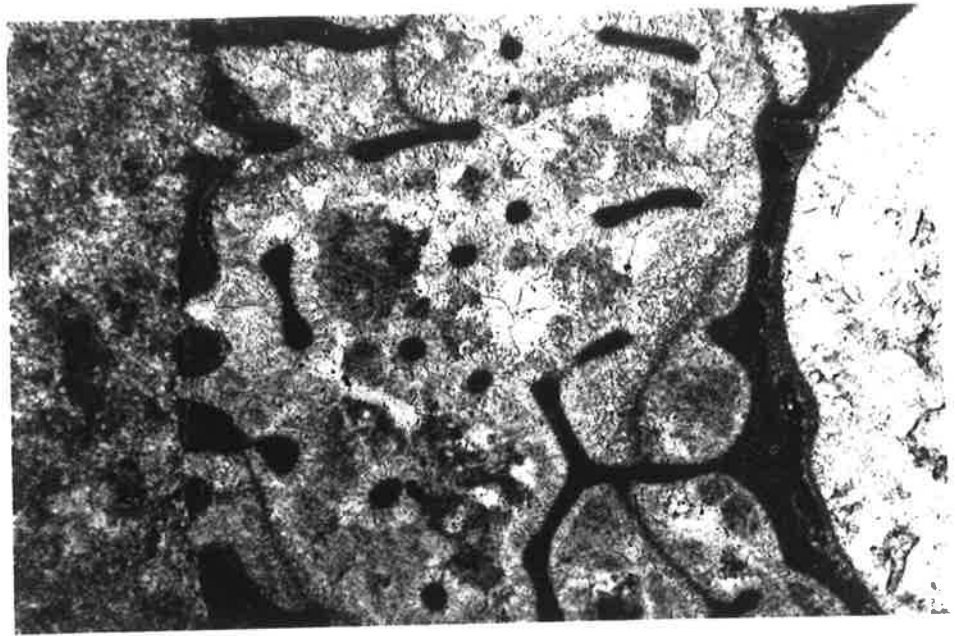cement within archeocyathid cavity. Field of view is
1.1mm.

FIG.5.20: Ooid grainstone with radial-concentric ooids and two generations of interparticle cements. The bladed inclusion rich fringing cement grades into clear blocky calcite cement. Field of view is 4.4mm.

FIG.5.21: Close-up of bladed inclusion rich cement grading into clear blocky cement. Field of view is 1.1mm.

FIG.5.22: Bladed fringing cement in an ooid grainstone. Field of view is 1.1mm.
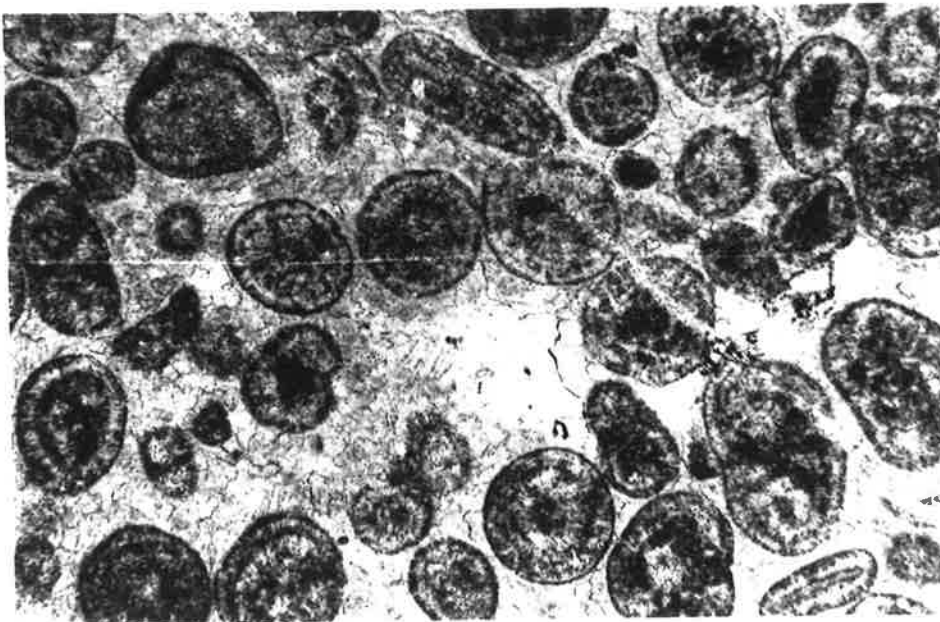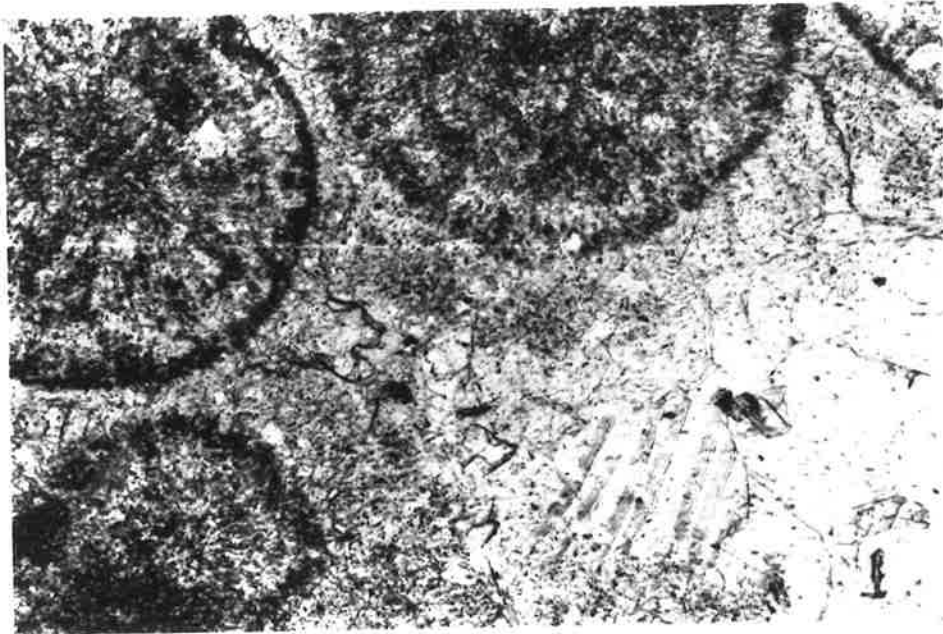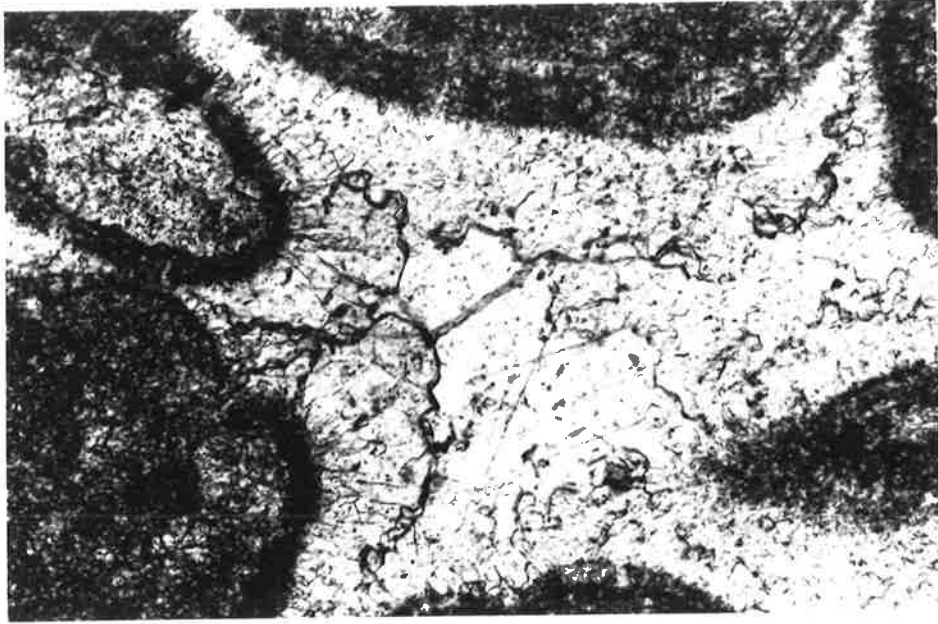
FIG.5.23: Trace element data of the Wilkawillina Limestone
components. Reported values represent means of between 10 and
20 microprobe analyses. Values in brackets refer to two
standard deviation from mean (2d).

| Sample | Description | Sr(ppm) | Mg(ppm) | Mn(ppm) | Fe(ppm) |
|--------|-------------|---------|---------|---------|---------|
| **OOIDS** | | | | | |
| COW5 | Radial fabric | 620 (80) | 1790 (160) | 180 (120) | 1190 (290) |
| COW4 | " | 250 (60) | 1530 (40) | b.d. | 430 (140) |
| COW10 | Micritic | 739 (214) | 2574 (154) | 603 (139) | 1318 (208) |
| COW1 | " | 231 (80) | 1810 (1074) | 665 (360) | 614 (678) |
| LC4 | " | 913 (173) | 1625 (1152) | 323 (65) | 1046 (410) |
| COW6 | " | 420 (150) | 1700 (254) | 450 (175) | 1050 (545) |
| COW5 | " | 620 (30) | 1770 (10) | 260 (70) | 1210 (180) |
| COW3 | " | 390 (180) | 1810 (170) | 190 (110) | 670 (730) |
| COW4 | " | 290 (50) | 1610 (200) | 300 (120) | 700 (350) |
| COW9 | " | 407 (20) | 2887 (145) | 355 (130) | 911 (820) |
| CWG15 | " | 207 (50) | 2144 (290) | 361 (116) | 204 (138) |
| **CEMENTS** | | | | | |
| CWG19 | Radiaxial fibrous cement (RFC) | 312 (64) | 2375 (854) | 347 (297) | b.d. |
| CWG13 | " | 161 (120) | 1745 (1268) | 1390 (1364) | 190 (252) |
| CWG7(1) | " | 553 (218) | 1.23* (6360) | b.d. | b.d. |
| CWG7(2) | " | 302 (54) | 5870 (5560) | 241 (5) | b.d. |
| LCK | " | 214 (108) | 1721 (1970) | 463 (535) | 568 (630) |

| Sample | Description | Sr(ppm) | Mg(ppm) | Mn(ppm) | Fe(ppm) |
| --- | --- | --- | --- | --- | --- |
| CWG8 | Radiaxial fibrous cement | 415 (95) | 4222 (2690) | 232 (150) | 468 (165) |
| CWG3 | " | 384 (70) | 3571 (2648) | b.d. | b.d. |
| COW4 | Blocky cement | 220 (200) | 1530 (360) | b.d. | b.d. |
| CWG8 | " | 218 (25) | 1069 (285) | 1557 (1426) | 1027 (1260) |
| COW9 | " | 307 (130) | 2312 (754) | 439 (130) | 798 (370) |
| COW10 | " | 602 (250) | 2140 (930) | 590 (290) | 1310 (750) |
| COW5 | " | 470 (80) | 1350 (480) | b.d. | 420 (60) |
| COW3 | " | 210 (170) | 1400 (390) | b.d. | b.d. |
| CWG7 | " | 820 (102) | 2129 (620) | b.d. | b.d. |
| COW6 | " | 394 (174) | 1541 (970) | b.d. | 278 (260) |
| COW1(1) | " | 223 (40) | 3364 (2632) | 1234 (256) | 1463 (1401) |
| COW1(2) | " | 380 (306) | 1087 (522) | 924 (1271) | 317 (624) |
| COW2 | " | 323 (198) | 1886 (630) | b.d. | 276 (388) |
| COW8 | " | 790 (600) | 2344 (1093) | 441 (32) | 554 (167) |
| COW10 | Bladed cement | 510 (140) | 2650 (410) | 200 (70) | 1290 (390) |
| COW5 | " | 1790 (1210) | 2180 (640) | b.d. | b.d. |
| COW3 | " | 400 (20) | 1790 (220) | b.d. | b.d. |
| CWG15 | " | 165 (50) | 2440 (514) | 352 (257) | 144 (115) |

| Sample | Description | Sr(ppm) | Mg(ppm) | Mn(ppm) | Fe(ppm) |
|--------|-------------|---------|---------|---------|---------|
| **MICRITE** | | | | | |
| CWG3 | | 223 (51) | 1832 (251) | 309 (94) | 156 (133) |
| CWG19 | | 250 (85) | 1796 (720) | 682 (468) | 169 (117) |
| CWG7 | | 273 (67) | 2091 (216) | 590 (160) | 381 (90) |
| COW2 | | 104 (40) | 1407 (395) | 154 (104) | 2075 (853) |
| COW1 | | 201 (30) | 1599 (183) | 372 (163) | 1382 (326) |
| **DOLOMITE** | | | | | |
| COW9(1) | Dolospar | 240 (96) | 11.35* (321) | 2072 (1334) | 946 (537) |
| COW9(2) | " | 122 (72) | 11.91* (1250) | 2339 (721) | 1.16* (4310) |
| COW8 | " | 185 (100) | 10.66* (4500) | 763 (220) | 1.17* (4600) |
| COW8 | Dolomicrite | 156 (60) | 10.27* (5052) | 769 (156) | 1.17* (3644) |

* Weight percent Mg.

FIG.5.24: Trace element chemistry of ooids from the early Cambrian Wilkawillina Limestone, showing Sr vs Mn plot. Each plotted sample represents the mean of between 10 and 20 individual microprobe analyses. Line joining samples refers to analysis from within the same sample.

FIG.5.25: Trace element chemistry of ooids from the early Cambrian Wilkawillina Limestone, showing Sr vs Fe plot. Each plotted sample represents the mean of between 10 and 20 individual microprobe analyses. Line joining samples refers to analysis from within the same sample.
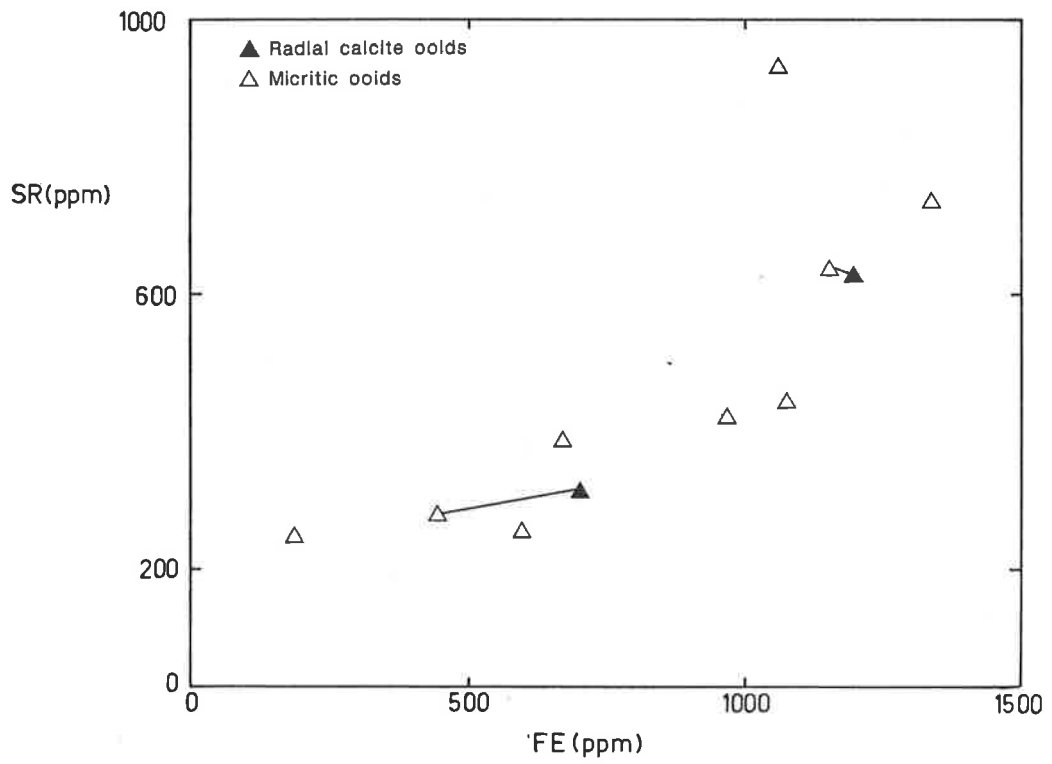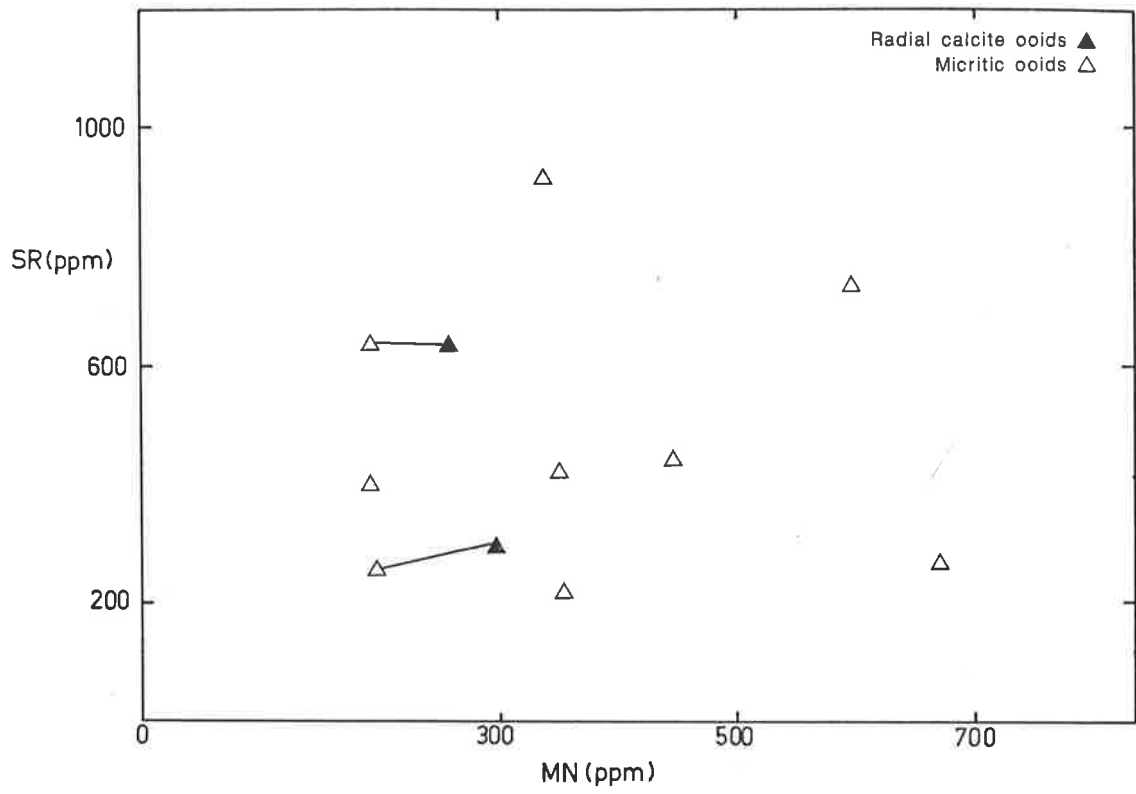
FIG.5.26: Trace element chemistry of ooids from the early
Cambrian Wilkawillina Limestone, showing Sr vs Mg plot.
Each plotted sample represents the mean of between 10 and
20 individual microprobe analyses. Line joining samples
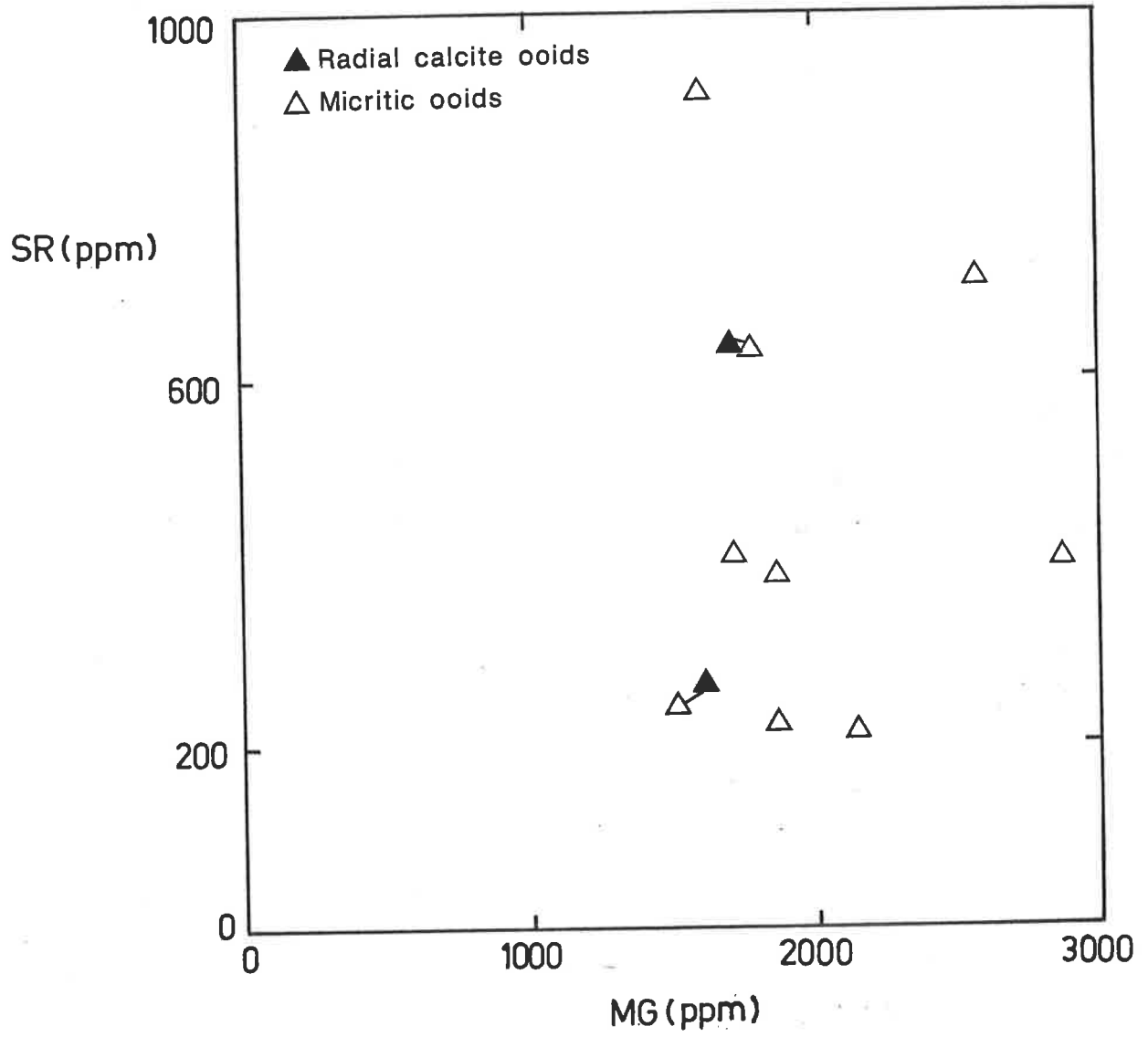refers to analysis from within the same sample.

FIG.5.27: Trace element chemistry of fibrous and bladed cements, showing Sr vs Mn plot. Each plotted sample represents the mean of between 10 and 20 individual microprobe analyses.

FIG.5.28: Trace element chemistry of fibrous and bladed cements, showing Sr vs Fe plot. Each plotted sample represents the mean of between 10 and 20 individual microprobe analyses.
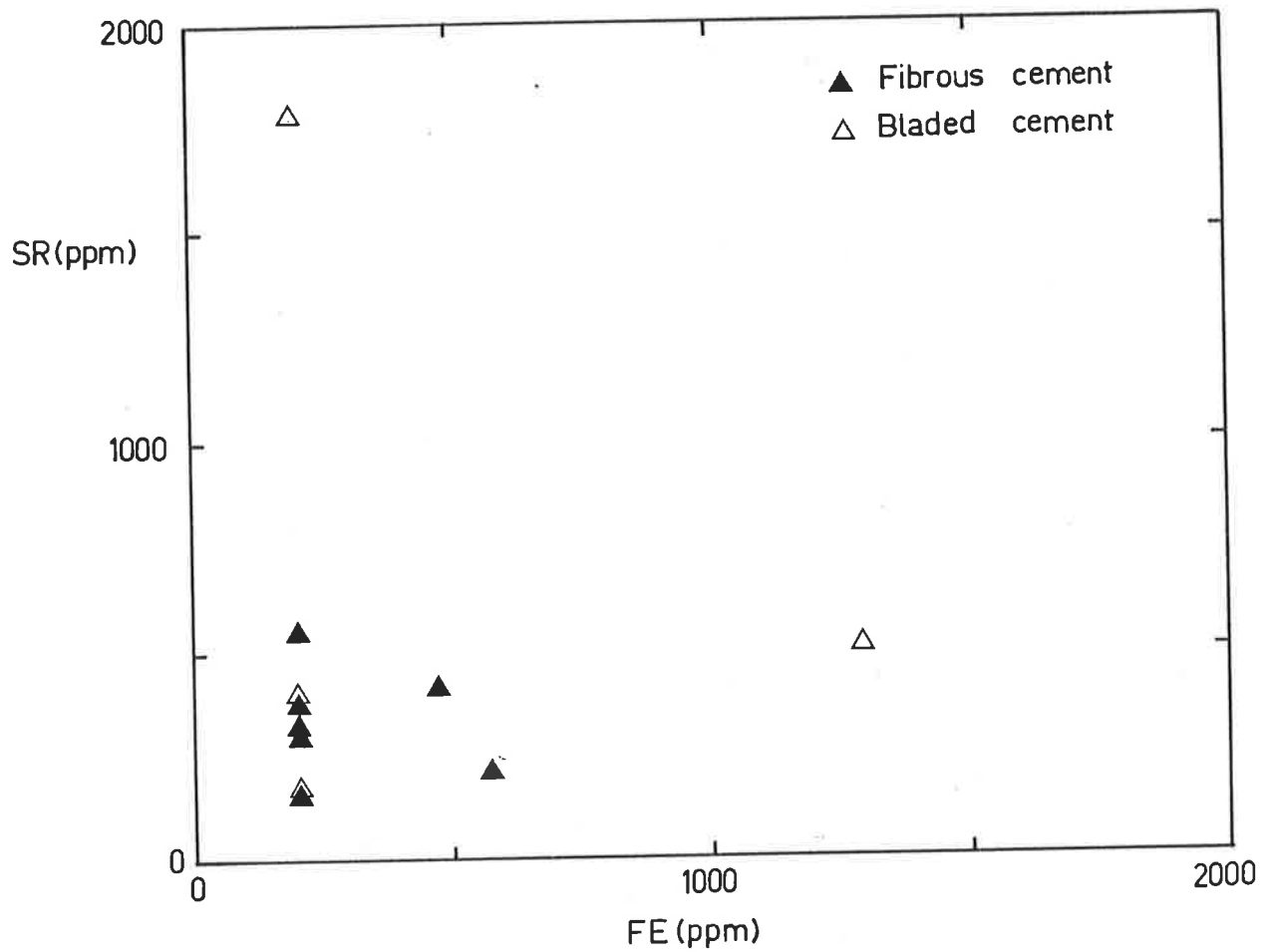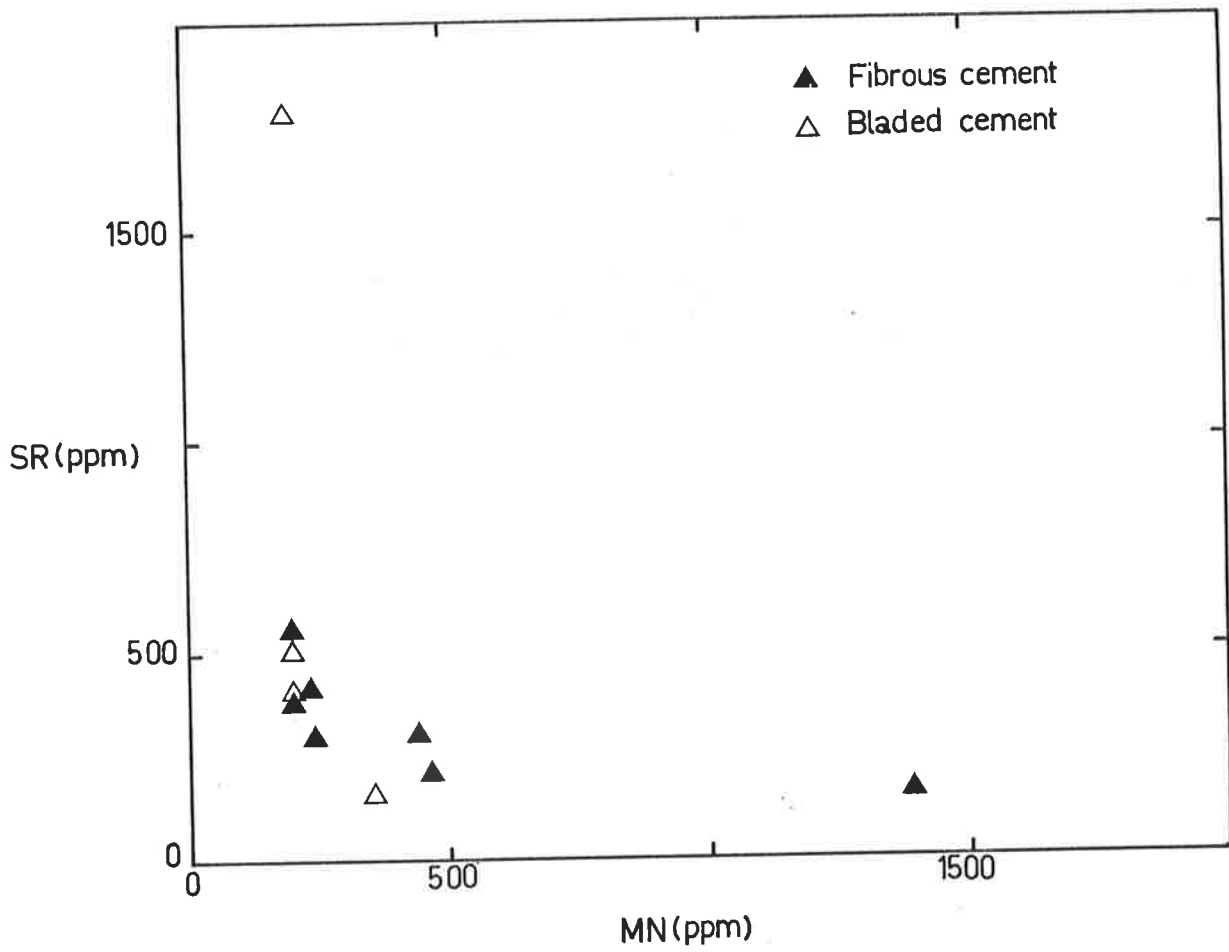
FIG.5.29: Trace element chemistry of fibrous and bladed cements, showing Sr vs Mg plot. Each plotted sample represents the mean of between 10 and 20 individual microprobe analyses.

FIG.5.30: Trace element chemistry of blocky equant cement, showing Sr vs Mn plot. Each plotted sample represents the mean of between 10 and 20 individual microprobe analyses.

FIG.5.31: Trace element chemistry of blocky equant cement, showing Sr vs Fe plot. Each plotted sample represents the mean of between 10 and 20 individual microprobe analyses.
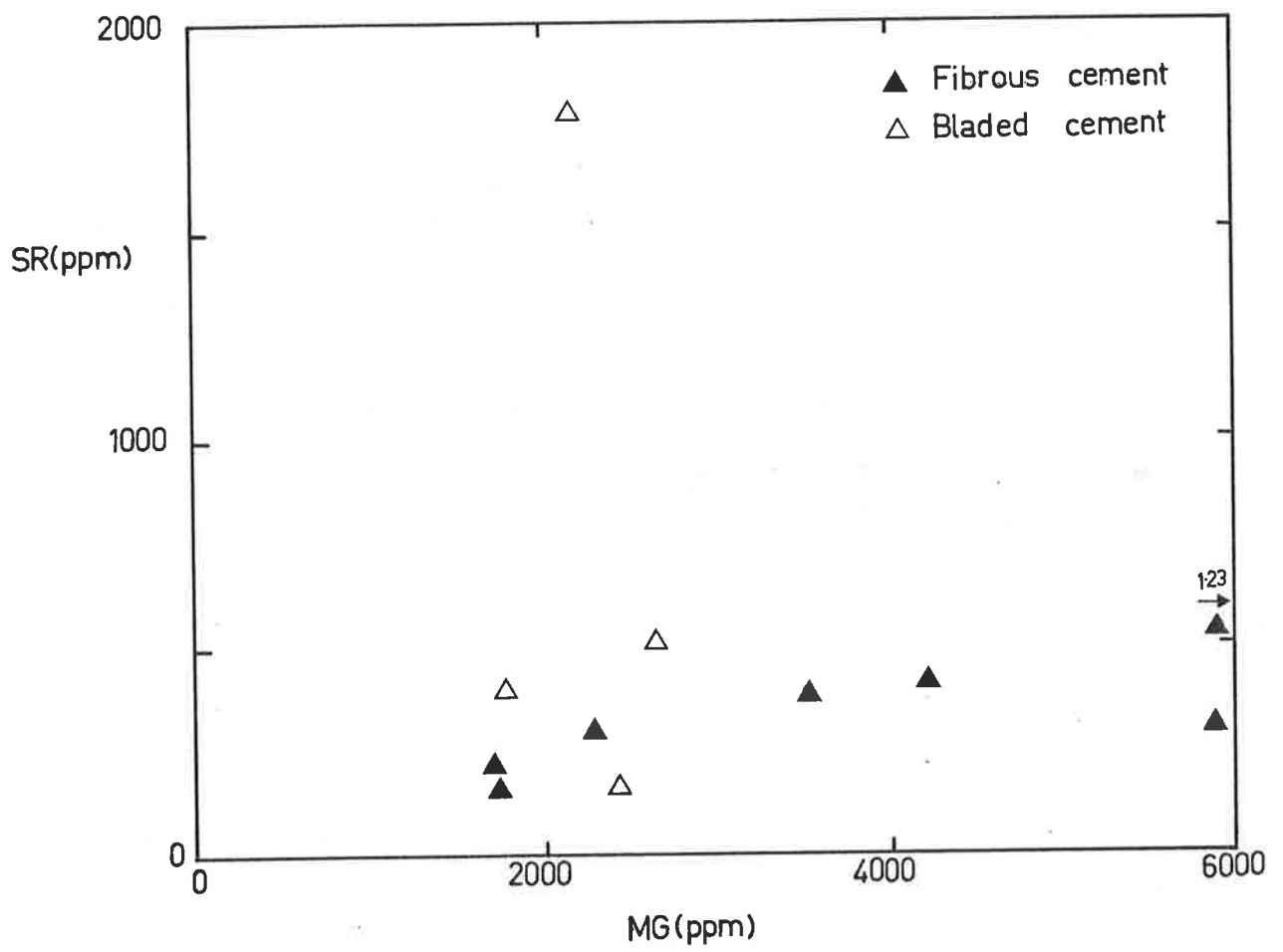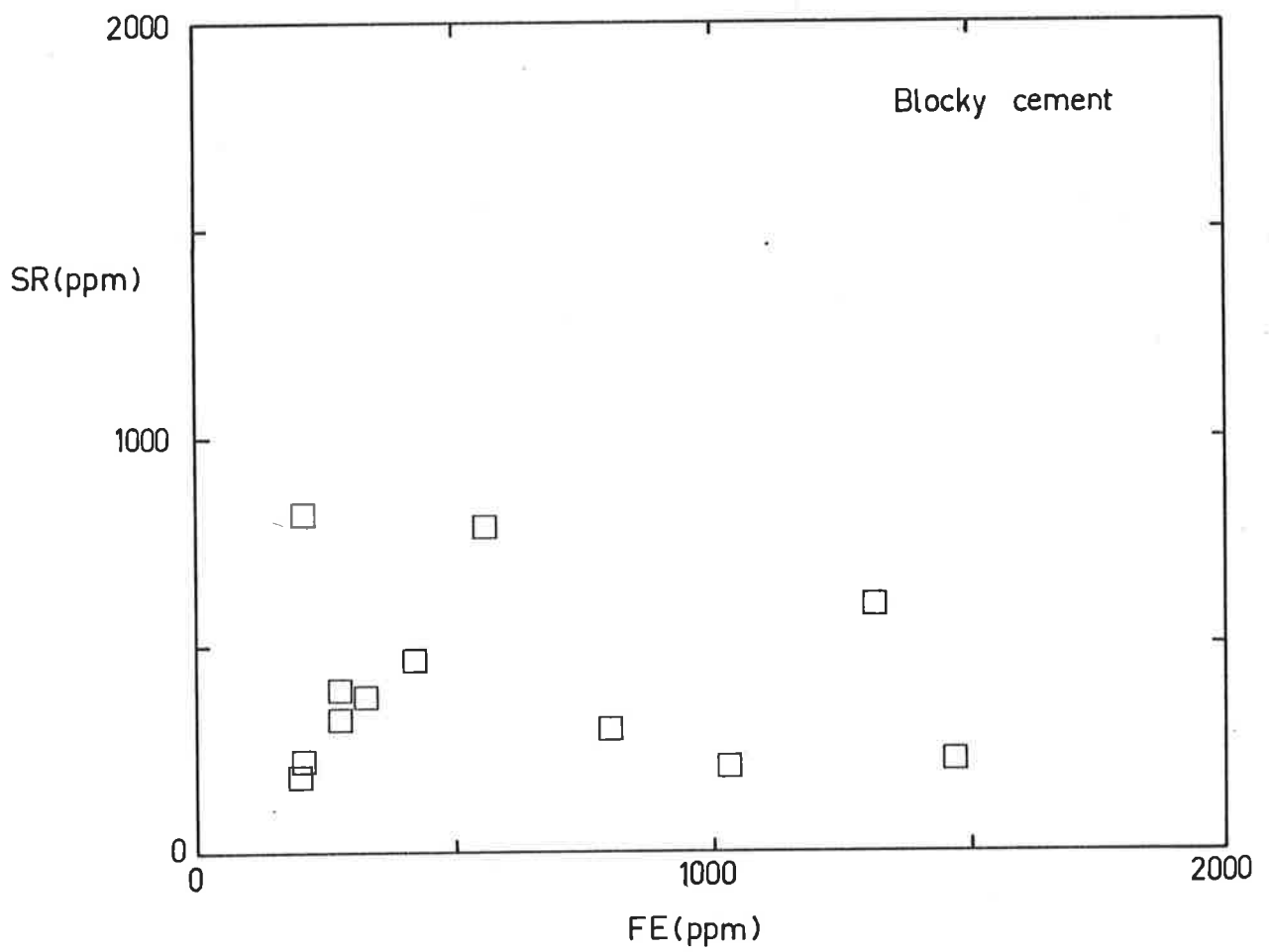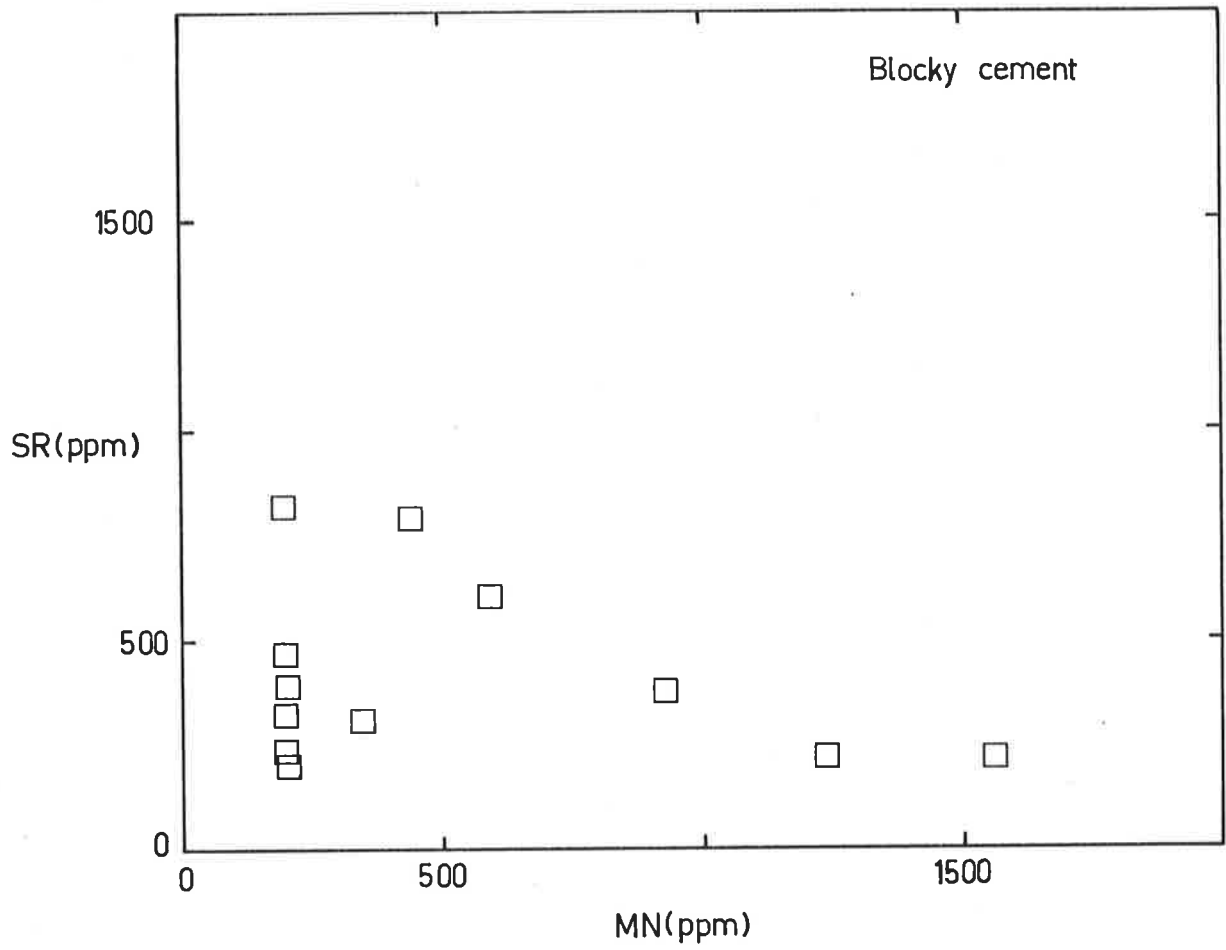
Blocky cement

Blocky cement

FIG.5.32: Trace element chemistry of blocky equant cement, showing Sr vs Mg plot. Each plotted sample represents the mean of between 10 and 20 individual microprobe analyses.
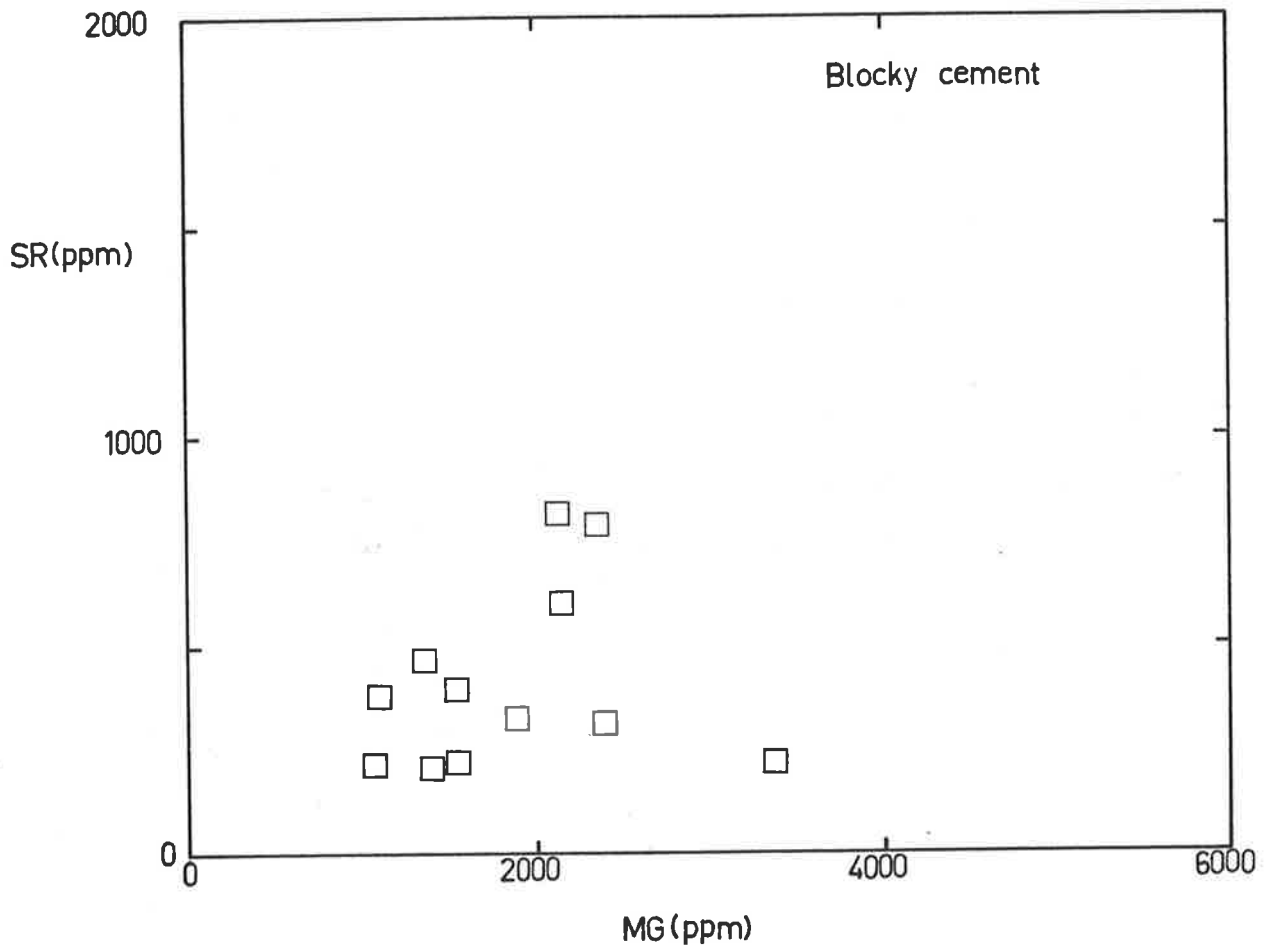
## FIG.5.33: STABLE ISOTOPE DATA OF THE WILKAWILLINA LIMESTONE

| Sample | Description | Del O18 | Del C13 |
|---|---|---|---|
| **OOIDS** | | | |
| COW6 | Micritic fabrics | -11.84 | -0.39 |
| COW10 | " | -18.38 | -2.44 |
| LC4 | " | -9.82 | 0.28 |
| | | | |
| **CEMENTS** | | | |
| CWG19 | Radiaxial fibrous cement (RFC) | -11.51 | 0.37 |
| CWG13 | " | -7.91 | 0.93 |
| CWG7(1) | " | -8.00 | 0.65 |
| CWG7(2) | " | -8.77 | -2.98 |
| CWG7(3) | " | -7.99 | 0.67 |
| CWG3 | " | -7.94 | 0.06 |
| LCK(1) | RFC in pisoliths | -9.05 | -2.81 |
| LCK(2) | " | -8.02 | -5.15 |
| LCK(3) | " | -8.31 | -4.19 |
| | | | |
| **WHOLE ROCK** | | | |
| CWC7 | Ooid grainstone | -13.51 | -5.05 |
| CWG1 | " | -6.85 | 3.03 |
| COW9 | " | -14.93 | -4.14 |
| COW7 | " | -17.13 | -3.82 |
| COW10 | " | -17.13 | -2.36 |
| | | | |
| **MICRITE** | | | |
| CWG3 | | -8.69 | 0.04 |
| CWC8 | | -12.31 | -6.58 |
| CWC10 | | -10.47 | -5.90 |
| CWG19 | | -14.13 | 0.06 |

| Sample | Description | Del O18 | Del C13 |
|--------|-------------|---------|---------|
| **DOLOMITE** | | | |
| COW9 | Dolospar | -7.95 | -1.44 |
| COW7 | " | -14.47 | -3.25 |
| | | | |
| **BOUNDSTONE** | | | |
| CWC7 | | -8.70 | -7.35 |

FIG.5.34: Oxygen and carbon isotope plot of the early Cambrian Wilkawillina Limestone. Line joining samples refers to analyses from within the same sample.

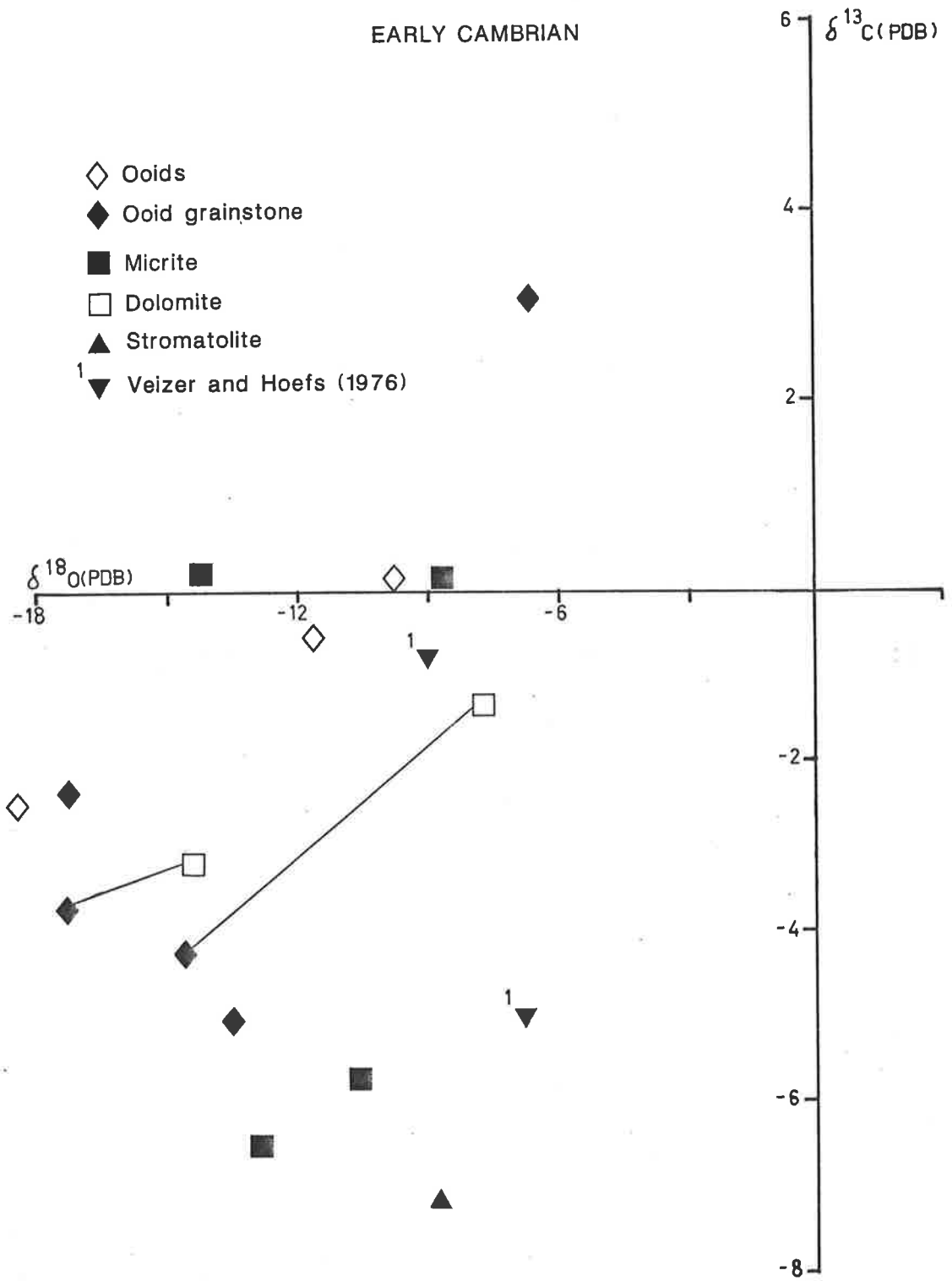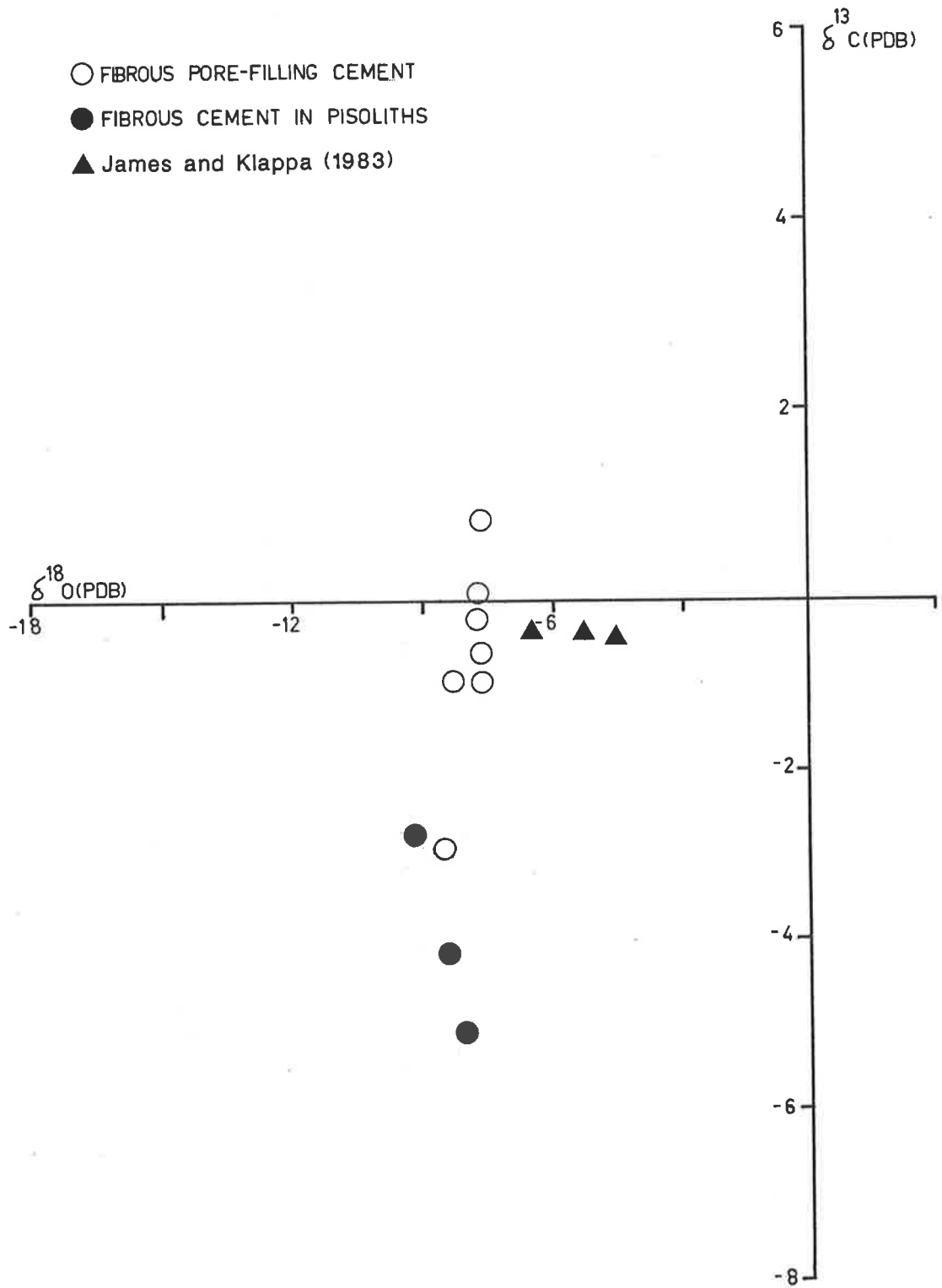EARLY CAMBRIAN

◇ Ooids
◆ Ooid grainstone
■ Micrite
□ Dolomite
▲ Stromatolite
[1] ▼ Veizer and Hoefs (1976)

$\delta^{13}C$(PDB)

$\delta^{18}O$(PDB)

FIG.5.35: Oxygen and carbon isotope plot of the early
Cambrian Wilkawillina Limestone fibrous cements.

# CHAPTER SIX
## STRONTIUM ISOTOPES

### 6.1: INTRODUCTION

The 87Sr/86Sr ratios have been used by various workers in their study of carbonates [Veizer and Compston 1976; Veizer et al. 1983; Burke et al. 1982]. The aim of these studies has been to determine temporal variations in the chemistry of oceans and the resulting carbonate rocks. The present investigation of the strontium isotopes of the Late Precambrian and early Cambrian carbonates was undertaken with two objectives in mind. Firstly, it was decided to study the behaviour of strontium isotopes during carbonate diagenesis. There have been very few studies of this nature in the past. The studies of Stueber et al.[1984] and Moore [1985], employing 87Sr/86Sr isotopic ratios, have demonstrated their potential in carbonate diagenetic work. Secondly, using the results of their diagenetic behaviour, an attempt is made to infer the original 87Sr/86Sr isotopic ratio of marine waters.

A logical next step in the construction of an accurate and reliable 87Sr/86Sr seawater curve would be the refinement of trends established thus far [Burke et al.1982; Koepnick et al.1985]. The Phanerozoic 87Sr/86Sr curve has already undergone some changes since the establishment of these secular trends [ compare Peterman 1970; Burke et al. 1982; Koepnick et al.1985]. The availability of a well defined 87Sr/86Sr seawater curve has potential as a dating tool and would be of immense value in areas where paleontological data are scarce or lacking altogether (eg.Late Proterozoic). In the refinement of the 87Sr/86Sr curve,

selection criteria of samples is of critical importance. The present study demonstrates the potential of one such approach by selecting samples that have the greatest potential of retaining the original 87Sr/86Sr value. Veizer et al.[1983] employed essentially the same approach except their analysis was done with whole rock samples. The possibility of contamination of original 87Sr/86Sr by non-carbonates and later diagenesis can be a problem and was clearly demonstrated [Veizer et al. 1983,Fig.I]. The approach advocated in the present study involves analysing individual components for trace element concentrations and 87Sr/86Sr ratios.

The strontium isotopic ratio derived from such an approach would presumably be able to account for later diagenetic modification of the original ratio. A comparision can then be made between the strontium ratios derived from this study and those obtained from whole rock analysis from the same stratigraphic levels by previous studies [Veizer and Compston 1974].

The 87Sr/86Sr isotopic composition of modern seawater is fairly constant at about 0.7090 and appears to be well-mixed and uniform [Veizer and Compston 1974, Table 1; Burke et al.1982]. Continental fresh-waters however, show a large variation ranging from 0.704 to 0.740. This is largely controlled by the type of source rocks in it's drainage areas, with igneous plutonics having high radiogenic contributions and therefore elevated 87Sr/86Sr ratios. The elevated 87Sr/86Sr ratios result from an increased contribution by radiogenic 87Sr generated by B decay from 87Rb. Continental fresh waters flowing through shield areas

tend to have a fairly high 87Sr/86Sr ratio (0.7160 from Table 2 in Veizer and Compston 1974). Volcanic rocks of basaltic composition have low 87Sr/86Sr ratios ranging from 0.702 to 0.706. The 87Sr/86Sr isotopic composition of marine carbonates varies from 0.7065 to 0.7090. It was initially postulated that with increasing geologic age the 87Sr/86Sr ratio of seawater would show an increase [Wickman 1948]. However, this has not been supported by later studies, which show fluctuations in the 87Sr/86Sr ratio of seawater through geologic history [Peterman et al.1970; Veizer and Compston 1974,1976; Burke et al.1982].

In general most secondary diagenetic processes that affect carbonate sediments tend to either increase the 87Sr/86Sr isotopic ratio or leave it unchanged [Veizer and Compston 1974,p.1464]. During early diagenesis, under the influence of marine waters, the strontium isotopic ratio of the precursor carbonate and seawater is assumed to remain essentially the same since the time lapsed between sedimentation and early diagenesis is relatively small. During dissolution of the precursor, Sr is strongly partitioned into the solution due to it's small partition coefficient (0.05 to 0.14) and therefore the reprecipitated diagenetic calcite would retain the strontium isotopic ratio of it's precursor. Only after completion of bulk transformation of calcium carbonate to diagenetic low Mg calcite will the meteoric 87Sr/86Sr ratio be preserved in subsequent late diagenetic calcites. During flushing by these continentally derived meteoric waters the strontium isotopic ratio changes appreciably enough to record elevated 87Sr/86Sr ratios. Modification of the strontium isotope ratios is

possible by interaction with associated clays and non-carbonates, especially during burial. However, some studies have shown this to be unlikely or negligible [Dasch 1969; Biscaye and Dasch 1971]. No strontium isotopic equilibration appears to occur between clay minerals and seawater as distinct strontium isotope ratios of both fossils and clays were recorded by Peterman et al. [1970]. Moreover, unlike carbon and oxygen isotopes, strontium isotopes do not undergo any fractionation, and are not affected by temperature changes. Therefore the interpretation of strontium isotopic data is comparatively easier and probably more reliable.

The approach used in this study involved the analysis of mainly the ooid and cement components. The components were petrographically studied, then analysed for trace element concentrations and 87Sr/86Sr isotope ratios. Details of sample preparation and measurement of strontium isotopes are given in Appendix Three . This study was not intended to be an extensive investigation of the strontium isotope behaviour across the Precambrian-Cambrian boundary. Rather only two stratigraphic units were picked, one from the Late Precambrian and the other from the early Cambrian, and the results are basically a refinement of already published data [Veizer and Compston 1974]. Between the two units, the Late Precambrian Trezona Formation and the early Cambrian Wilkawillina Limestone, the Trezona Formation was selected for detailed work with only a few analyses from the Wilkawillina Limestone. The results from this study will demonstrate the potential use of an integrated approach utilising petrographic, trace element and isotopic data to make better and more reliable interpretations.

## 6.2: SAMPLE SELECTION AND LIMITATIONS

The ooids selected from the Trezona Formation had type IV, V and VII ooid fabrics (section 2.4) and included both the small and large ooids. The selection of these ooids was governed by their comparatively unaltered nature and relative ease of separation and isolation using the technique described in Appendix Three. In spite of these precautions, it is possible that there were some secondary diagenetic components included within the ooid samples. The most probable source of this diagenetic component is the sparry center of the ooids which could not be identified during separation. The sparry ooid fabrics (type I,II,X) were not sampled because using the available technique, it was not possible to distinguish between sparry ooids and the enclosing sparry cements. It was also not possible to drill out such small areas (0.1mm) due to limitations in the drilling equipment.

As far as possible, cements separated for strontium isotope analysis were those associated with the above sampled ooids. Fenestral cements of blocky ferroan calcite were selected since they represented the final diagenetic phase of cementation. Also included were samples of vein calcite and stromatolites. Amongst the interparticle cements, the poikilotopic type E cement (section 2.5) samples are of composite nature and include peloidal grains and ooids. It was not possible to separate these grains from the cements. Interparticle cement samples may have had minor amounts of early fringing cements incorporated during separation but they form a negligible fraction of such samples.

## 6.3: PETROGRAPHY

Since the study concentrated mainly on the oolite units the major components described are ooids and associated cements. Some stromatolite samples were also included in the analysis. Detailed description of the ooid and cement fabrics of the Trezona Formation and the Wilkawillina Limestone are found in Chapters 2 and 5 respectively, and only a limited number of samples were included. The ooids from the Trezona Formation, described as type IV,V and VII fabrics in section 2.4, are dominantly micritic. The cements had type B,C and E fabrics. In the Wilkawillina Limestone samples, the ooids had radial ooid fabrics and the cements comprised blocky calcites similar to the type C cements of the Trezona Formation. The geochemical results from the Late Precambrian Trezona Formation are presented and discussed first followed by those from the early Cambrian Wilkawillina Limestone.

## TREZONA FORMATION
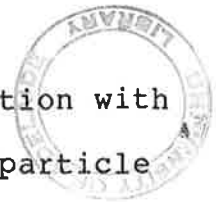
## 6.4: TRACE ELEMENT CHEMISTRY

The Sr and Mn concentration of the various components was utilised in studying the chemical diagenetic trends. There is a large variability in both the Sr and Mn concentrations (Figs.6.1,6.2). Sr content varies from 3450ppm to less than 200ppm (detection limit of microprobe). Analysis of these low Sr components during the course of strontium isotope determination gave values of 130ppm Sr. Mn concentration ranges from between 2095ppm to approximately 200ppm. The trace element concentrations of the components are tabulated in Figure 6.1. A cross-plot of Sr and Mn reveals a negative correlation (Fig. 6.2).

99

The ooids fall into two broad groups based on their Sr and Mn compositions; the high Sr/low Mn group and the low Sr/ high Mn group. The cements or sparry components show the greatest range of Sr and Mn concentrations. The vein calcite and fenestral cements are generally much higher in Mn and lower in Sr compared to the interparticle cements. Some of the interparticle cements have Sr concentrations in excess of 3000ppm.

Texturally, the ooids comprise micritic and microsparitic calcite with some ooid cortices being recrystallized to coarser sparry calcite. Such ooids have lower Sr and higher Mn contents. The ooids with high Sr content (1300-1900ppm) are relatively unaltered and comprise dark grey concentric cortical layers of micrite. Such elevated Sr concentrations have been documented from ancient ooids of Eocene and Pennsylvannian age [Brand and Veizer 1983,Table 5].

Based on equilibrium concentration of Sr in different carbonate mineralogies, these high Sr ooids may have had aragonitic precursors [Brand and Veizer 1983]. There is however lack of sound textural evidence to support this interpretation. If these high Sr ooids were originally aragonitic, then their diagenesis would produce either calcitized fabrics or oomolds of sparry calcite from dissolution and reprecipitation of the aragonitic ooids. Such fabrics are displayed by type I,II and X fabrics (Chapter 2). Conversely if these ooids represent original calcitic precipitates, then their diagenesis would still preserve the original micritic texture. However, the present Sr content of these ooids would indicate little loss of Sr during

diagenesis. These high Sr ooids are found in association with aragonite replacement fabrics and also high Sr interparticle cements (section 2.5). It is possible that during diagenesis the pore-waters would have been enriched in Sr and consequently recrystallization in such an environment could produce elevated Sr content. Exactly how the diagenetic environment was able to remain "closed" for Sr is unclear.

The large range in Sr and Mn concentrations of the cements is probably a reflection of the type of diagenetic environment in which they formed. The interparticle cements represent earlier diagenetic precipitates than the cements in fenestrae and veins. Presumably during early stages of diagenesis, the influence from meteoric waters was minimal and the entrapped pore-waters had a marine character, with the precipitating cements controlled by marine precursor chemistry, thus the low Mn and high Sr content. Nevertheless, the very high Sr content of some of these cements is problematic and discussed in section 7.4. The source of the Sr was probably from an aragonite precursor. Contributions from the non-carbonate fraction are considered unlikely in view of the low amount of residue (5%), and the mild acid digestion used during analysis. Moreover, these high Sr cements have also been examined under the microprobe and reveal that the Sr is in the calcite cements and not in any inclusions or non-carbonates.

The late diagenetic fenestral and vein calcites have trace element concentrations suggesting precipitation from pore-waters of meteoric or burial origin. Such pore-waters are normally enriched in Mn and Fe and depleted in Sr. The vein calcite has an unusually high amount of Mn and probably

represents the influence of reducing pore-waters under the burial environment.

## 6.5: STRONTIUM ISOTOPES

Most of the components analysed for 87Sr/86Sr isotope ratios fall within a fairly narrow range (0.7071-0.7080), with the exception of the fenestral calcite (0.7105). There is a strong positive correlation between the 87Sr/86Sr ratios and the Sr content (Fig.6.4). The relationship between Mn concentration and strontium isotopes is less well defined, but in general high Mn concentration results in slightly elevated 87Sr/86Sr ratios (Fig.6.3). In all the samples analysed for strontium isotopes the Rb content averaged 10ppm with the maximum being 20ppm in the stromatolites. Therefore no corrections were made for contributions to the strontium isotopes by Rb decay since these were exceedingly small.

The "primary" components have a narrow range of 87Sr/86Sr ratios and Mn concentration compared to the "secondary" components (Fig.6.3). There is an increase in the 87Sr/86Sr ratios of the late diagenetic components. This large variability in strontium isotopes of the secondary components is probably a manifestation of input from radiogenic 87Sr sources in the form of either continental waters during meteoric diagenesis or non-carbonate residual silicates or clays. As outlined in the introduction, such diagenetic modifications result in an increase in the original strontium isotope ratios. With progressively increasing 87Sr/86Sr ratios, the Sr content of the components decreases. Morrow and Mayers [1978] showed that early diagenesis generally does not reduce the Sr content below

102

400ppm. Late diagenesis reduces the Sr content to between 100-200ppm but requires very large volumes of meteoric pore-waters. In the present study most of the carbonate components had greater than 400ppm Sr and the 87Sr/86Sr ratio ranged from 0.7071-0.7080. However, once the Sr content falls below 200ppm, the 87Sr/86Sr becomes exceedingly large (0.7105). Blocky calcites with such radiogenic strontium ratios occur as void fills in fenestrae. The components most likely to record the original strontium isotope signature would be the ooids and components with high Sr concentrations. Originally calcitic components, which have low Sr contents, can also record original strontium isotope ratios if relatively unaltered. Therefore, not all low Sr components are unsuitable for determination of original strontium isotopic ratios. Those components most likely to do so can be selected after determining the chemical diagenetic trends of the various components [Brand and Veizer 1980]. Based on this reasoning then, some of the ooids, boundstones and strontium rich cements probably record the original 87Sr/86Sr ratio (Fig.6.4).

Interestingly,the high Sr cement (type E,Chapter 2) shows an inversion of the normal chemical diagenetic trend as established by Brand and Veizer [1980]. During diagenesis by meteoric pore-waters micritic components alter into sparry components with a fall in Sr and increase in Mn content. The high Sr cements could represent a strong marine influence on their chemistry. Therefore, these cements probably retained the original strontium isotope ratios.

Veizer et al. [1983] in their study of 87Sr/86Sr variations in Proterozoic carbonates, reported high Sr

contents from some of their South African samples. These include the carbonates of the Cango and Malmesbury Formations, which had Sr contents varying from 639ppm-1729ppm. Their Nama System carbonates had even higher Sr contents ranging from 515ppm-3084ppm. They suggested that these high Sr carbonates represents alterations of originally aragonitic carbonates under semi-closed environments. Their 87Sr/86Sr values were therefore inferred to be representative of the original marine values.

The 87Sr/867Sr ratio of the primary components and strontium rich cements and, by inferrence, the Late Precambrian marine waters is found to be close to 0.7071. This is lower than the previously published range of 0.7074-0.7077 from this stratigraphic level [Veizer et al.1983,Table 5]. Their higher ratio was of total carbonate and therefore contributions from non-carbonate fractions as well as from diagenetic events may have resulted in their slightly elevated ratios. In any case the 87Sr/86Sr ratio during the Late Precambrian was at a low before the increase in the early Cambrian (0.7085-0.7093).

6.6:STRONTIUM ISOTOPE DIAGENETIC TRENDS

To study the variation in 87Sr/86Sr and its evolution in pore-waters during diagenesis, samples were obtained of the various diagenetic phases within individual samples. These consisted essentially of grains or an early diagenetic component and a late diagenetic component and are referred to as component pairs. The plot of the 1/Sr vs 87Sr/86Sr shows the progressive radiogenic character of the later diagenetic components (Fig.6.4). The linear relationship between the Sr

content and the 87Sr/86Sr suggests that there was variable
mixing between two types of pore-waters, radiogenic low Sr
pore-waters and non-radiogenic high Sr pore-waters [Faure
1977]. The 87Sr/86Sr values of the ooids presumably represent
the original marine isotopic composition, as inferred
earlier. The interparticle cements have slightly higher
87Sr/86Sr values, derived from later pore-waters of more
radiogenic composition. Later pore-waters acquired a more
radiogenic composition and lower Sr content, probably from
detrital clays and silicates. In one of the rare studies
using strontium isotopes for carbonate diagenetic
investigations, Stueber et al.[1984] found that their highly
radiogenic brines were derived from detrital clays,micas and
K-feldspars of an adjoining basinal unit. They believed a
major portion of their Sr content in the brines was derived
from the marine interstitial waters, being largely
contributed by the dissolution and recrystallization of
aragonite.

In the present study the evidence seems to indicate that
the ooids stabilised early in marine waters thereby retaining
the 87Sr/86Sr composition of Late Proterozoic seawater. The
later interparticle cements acquired a more radiogenic
87Sr/86Sr ratio, with some post-interparticle cements having
extremely elevated 87Sr/86Sr ratios. The exception to this
trend of progressively higher 87Sr/86Sr values with
diagenesis is the type E cement. This cement could have been
an early diagenetic product formed before any significant
burial and under an essentially closed to semi-closed
chemical environment. The elevated Sr content could have been
either from an aragonitic precursor or from the dissolution

105

of aragonitic grains, evidence of which is found in associated ooid grainstones (section 2.4 and 2.5). The strontium isotopic composition of these pore-waters and the resulting cements would essentially be that of the original marine waters during Late Proterozoic (Marinoan) times.

## 6.7: WILKAWILLINA LIMESTONE

The early Cambrian Wilkawillina Limestone radial ooids fall into the low Sr,high Mn group (Fig.5.24). As discussed in Chapter Five, section 5.4, radial ooids are inferred to represent original calcite precipitates [Sandberg 1975]. Their Sr content is much lower than those from the Trezona Formation ooids. Moreover these radial ooids are non-ferroan, possibly indicating relatively stable mineralogy which resisted change by diagenetic pore-waters. Former high Mg calcite components are recognised by their replacement with ferroan calcites [Richter and Fuchtbauer 1978]. However, presence of non-ferroan calcites does not necessarily rule out a high Mg calcite mineralogy. Indeed, if alteration took place in a diagenetic environment that lacked iron in solution (eg. vadose zone ) then the replacement of high Mg calcite components would generate non-ferroan calcites. An original calcitic precursor would result in low Sr contents for the replacement products, since it had a much lower Sr content originally (1000-2000ppm).

Therefore, based on the textural and geochemical data the original mineralogy of these radial ooids was either calcite or Mg calcite. In either case these originally calcitic (calcite or Mg calcite) ooids would have been relatively stable components, and have therefore possibly

retained the original 87Sr/86Sr values of the ambient seawater. Some of the micritic ooids have very high Sr contents, suggesting stabilization or recrystallization in pore-waters with strong marine influence. Recent studies have indicated that diagenetic calcites can be fairly stable and once precipitated undergo little change by subsequent diagenesis [Sandberg and Hudson 1977]. It is argued therefore that the ooids in the early Cambrian are reasonable indicators of original 87Sr/86Sr ratio of seawater during that period. The 87Sr/86Sr value of the ooids range from 0.7085-0.7093 (Fig.6.1). This falls within the range of 0.7089-0.7094 obtained by Veizer and Compston [1974].

6.8: STRONTIUM ISOTOPE SECULAR TRENDS

As mentioned in the introduction, the strontium isotopic ratio of seawater depends on three major sources. These are the sialic rocks,with 87Sr/86Sr that averages 0.720; mafic volcanics with values averaging 0.704; marine carbonates and sulfates that average 0.708 [Faure et al. 1965; Faure and Powell 1972]. Since tectonics controls to a large extent the types and areal extent of these three sources, it follows that the 87Sr/86Sr secular trend is tectonically controlled. Large contributions of high ratio Sr from sialic sources causes high 87Sr/86Sr values while large contributions of low ratio Sr from mafic volcanics results in low 87Sr/86Sr values. Sources of Sr from marine carbonates and sulfates, although forming a major component does not affect the 87Sr/86Sr composition of seawater since it has a narrow range of 0.7068-0.7091.

Tectonic changes affect a whole range of other factors

which can have a bearing on variations in the 87Sr/86Sr values of seawater. Some of these include changes in sea-levels, variations in lithologic composition of the crust exposed to weathering, volcanic activity, sea-floor spreading rates, continental flooding and configuration and topographic relief of the continents [Koepnick et al.1985]. Variations in climate and paleo-oceanographic conditions are possible related factors. Although broad trends in the 87Sr/86Sr variations of seawater can be correlated to tectonic phenomenon, the combined effect of these factors can make direct tectonic interpretations for portions of the curve difficult.

Numerous studies have appeared over the years dealing with secular variations of the 87Sr/86Sr of marine waters through geologic history [Peterman et al.1970; Dasch and Biscaye 1971; Veizer and Compston 1974;1976; Faure et al.1978; Burke et al.1982]. With the exception of Veizer and Compston [1976], who looked at Precambrian carbonates, the others are based on the Phanerozoic record. The Phanerozoic record of 87Sr/86Sr of seawater has fluctuated with periods of increasing and decreasing values occurring rapidly in certain times in the past (Fig.6.5). This trend seems to continue into the Precambrian (Fig.6.6), although the data is probably not as reliable as for the Phanerozoic.

The main sources of error in obtaining an accurate curve of 87Sr/86Sr are uncertainty in age estimation of samples and the effect of diagenesis on the original ratio. In the case of Precambrian samples these errors are accentuated due to lack of fine resolution in age estimation and the greater degree of diagenetic modification suffered by the samples.

Nevertheless these studies are based on large numbers of data over wide geographic areas and their results are broadly in agreement with one another.

Systematic rises in the marine 87Sr/86Sr ratio, like that in the Cenozoic, have been attributed to a relative decrease in the contribution of low ratio Sr from oceanic sources and an increased contribution from high ratio Sr from continental sources. This can result from a decrease in oceanic ridge volumes and spreading rates [Pitman 1978] or an increase in continental orogenic activity and erosion of high ratio Sr source terrains [Palmer and Elderfield 1985]. The relatively low 87Sr/86Sr values for the Cretaceous occurred at a time of the continued break-up of Pangea and development of oceanic spreading centers and oceanic ridge systems [Hays and Pitman 1973; Pitman 1978]. This would have caused an increase in the contribution of low ratio Sr from oceanic sources and a decreased supply of high ratio Sr from continental sources. Not all changes in the 87Sr/86Sr curve can be correlated with tectonic events. The Aptian and Turonian are times of 87Sr/86Sr changes and occur during low sea-level stands [ Cooper 1977; Vail et al.1977; Hallam 1984]. The 87Sr/86Sr curve is at a minima at these times. The increased continental exposure at these times does not record any increase in the 87Sr/86Sr values of seawater. This suggests a complex interplay of tectonic,climatic and eustatic factors. Broad patterns in the 87Sr/86Sr of seawater can therefore be correlated to tectonic phenomenon. Superimposed on these broad tectonically influenced first-order cycles are secondary and minor cycles that probably are a result of a variety of factors including tectonic,climatic

and eustatic.

The Precambrian portion of the 87Sr/86Sr seawater curve has been defined to some extent by studies of Veizer and Compston [1976] and Veizer et al. [1983]. The resulting curve records a broad pattern of maxima and minima in 87Sr/86Sr values probably representing the influence of major tectonic events during the Precambrian (Fig.6.6). Veizer and Compston [1976] attributed these fluctuations to the dominance of ensimatic and ensialic source areas during the Archean and Proterozoic respectively. The existence of a "mantle event" at around 900±50Ma is suggested as the reason for the 87Sr/86Sr minima at this interval [Veizer et al.1983]. One of the problems involved with the Precambrian carbonates is poor stratigraphic resolution compared to the Phanerozoic and the large sample intervals used in previous studies (300Ma in Veizer and Comimposton 1976). Therefore secondary and minor fluctuations in the curve are not resolvable. In effect therefore the Precambrian section of the 87Sr/86Sr curve of seawater is probably a first order cycle analogous to the broad trend of the Phanerozoic minus the secondary fluctuations.

In order to produce a detailed curve for the Precambrian, additional sampling and an improved sample selection criteria are required. The results of this study demonstrate the large variability in 87Sr/86Sr possible within individual samples due to diagenesis (Fig.6.4). Therefore selection of samples that are most likely to retain the original 87Sr/86Sr value is critical in constructing an accurate curve. This becomes especially important in this stratigraphic interval between the Late Proterozoic and the

Cambrian since there is a rapid increase in the 87Sr/86Sr of seawater. In terms of the behaviour of the 87Sr/86Sr curve, the Late Proterozoic-Cambrian transition is analogous to the Early Cretaceous-Recent transition (Figs.6.5 & 6.6). The possible reasons for the rise of the 87Sr/86Sr values for the Early Cretaceous-Recent transition have already been elucidated above. A comparision between the 87Sr/86Sr curve of the Phanerozoic and sea-level changes shows a broad correlation between a rise in sea-level and increase in 87Sr/86Sr of seawater. However the secondary fluctuations do not correlate with any sea-level changes. The rapid rise in the 87Sr/86Sr ratio during the Late Carboniferous appears to have taken place during a time when sea-levels were falling and approaching a low sea-level stand. This reinforces the earlier idea of a complex interplay between tectonic, climatic and eustatic factors on the 87Sr/86Sr of seawater.

By analogy with the Phanerozoic, the rapid rise in 87Sr/86Sr for the Late Proterozoic-Lower Cambrian recorded in this study and in previous ones could be the result of the rise in sea-level during this interval. The Late Proterozoic interval investigated in this study occurs in the Marinoan and is stratigraphically above the Sturtian (Fig.1.2). Both these intervals record glacigene sediments and suggest a time of low sea-levels. The intervening sediments record essentially shallow water sedimentation in the form of carbonates with occassional basinal shales indicating a deepening with minor eustatic shifts in sea-level. In global terms this stratigraphic interval has evidence of glaciation over a wide geographical area [Hambrey and Harland 1983]. Following this low sea-level stand there was a rise in sea-

111

level to a maxima sometime in the Cambrian. There is a correlation then of a rise in sea-level with the increase in the 87Sr/86Sr.

A combination of tectonic and sea-level changes between the Late Proterozoic (Marinoan) and the early Cambrian of the Adelaide Geosyncline may have caused the increase in the 87Sr/86Sr of seawater. A low sea-level with rift type tectonics indicates small areal extent of flooded continental rocks and increased supply of volcanic sources thereby leading to a low 87Sr/86Sr value for seawater. A higher sea-level with large areal extent of continental flooding increased supply of high ratio Sr leading to high 87Sr/86Sr despite the contributions of low ratio Sr from sea-floor spreading.

## 6.9: SUMMARY

A study of strontium isotopes in carbonates was undertaken to understand their trend during diagenesis and thereby better define the original strontium isotope ratio. The strontium isotope analysis was confined mainly to the late Precambrian Trezona Formation with a few analyses from the early Cambrian Wilkawillina Limestone.

A strong negative correlation exists between the Sr content and the 87Sr/86Sr ratio of the Late Precambrian Trezona Formation components. Some micritic ooids and the strontium rich cements recorded low, non-radiogenic 87Sr/86Sr ratios, which are inferred to represent the original marine isotopic composition. This 87Sr/86Sr ratio is 0.7071 and is lower than the previously obtained ratio of 0.7074-0.7077 by Veizer et al.[1983]. The late diagenetic components recorded

high, radiogenic 87Sr/86Sr ratios ranging from 0.7074-0.7105. Such radiogenic ratios probably resulted from diagenetic alteration and precipitation from either continentally derived meteoric waters or radiogenic subsurface brines modified by interaction with non-carbonates. The 87Sr/86Sr ratio of the early Cambrian carbonates is much higher, ranging from 0.7085-0.7093.

The rapid rise in the 87Sr/86Sr ratio for the late Precambrian-Cambrian portion of the curve requires reliable and accurate determination of the original marine 87Sr/86Sr ratio. The use of an integrated textural, trace element and strontium isotope study, as demonstrated above, is therefore essential in establishing a reliable 87Sr/86Sr record for possible marine strontium isotope chronostratigraphic use. This rapid increase in the 87Sr/86Sr ratio during the late Precambrian to Cambrian transition is probably related to a global rise in sea-level and the initiation of continental rifting during the Cambrian.

FIG.6.1: Trace element chemistry and 87Sr/86Sr ratios of
selected Trezona Formation and Wilkawillina Limestone samples.

TREZONA FORMATION (LATE PRECAMBRIAN):

| Sample | Description | Mn(ppm) | Sr(ppm) | 87Sr/86Sr |
|---|---|---|---|---|
| **OOIDS** | | | | |
| TB5 | Micritic | 775 | 710 | 0.7076 |
| TBG17 | " | 200 | 1300 | 0.7072 |
| TBG17 | " | 130 | 1900 | 0.7072 |
| TB4 | " | 600 | 450 | 0.7080 |
| TB6 | " | 280 | 1840 | 0.7072 |
| **BOUNDSTONES** | | | | |
| TB2 | | 200 | 2580 | 0.7071 |
| TBG9 | | 200 | 610 | 0.7075 |
| **MICRITE** | | | | |
| TB5 | Interparticle micrite | 931 | 410 | 0.7080 |
| **CEMENTS** | | | | |
| TG6 | Poikilotopic | 120 | 3450 | 0.7072 |
| TB6 | Blocky inter-particle | 190 | 980 | 0.7074 |
| TBG17 | " | 1070 | 870 | 0.7075 |
| TGC3 | Fenestral | 470 | 360 | 0.7080 |
| TG6 | " | 420 | 130 | 0.7105 |
| TBG16 | Blocky vein spar | 2095 | 280 | 0.7080 |

WILKAWILLINA LIMESTONE (EARLY CAMBRIAN):

| Sample | Description | Mn(ppm) | Sr(ppm) | 87Sr/86Sr |
|--------|-------------|---------|---------|-----------|
| OOIDS | | | | |
| COW4 | Radial calcite | 250 | 230 | 0.7093 |
| COW6 | Micritic | 450 | 370 | 0.7090 |
| LC4 | " | 200 | 2630 | 0.7085 |
| CEMENTS | | | | |
| COW6 | Blocky inter-particle | 250 | 410 | 0.7087 |

FIG.6.2: Sr vs Mn plot of Trezona Formation components analysed for strontium isotopes.
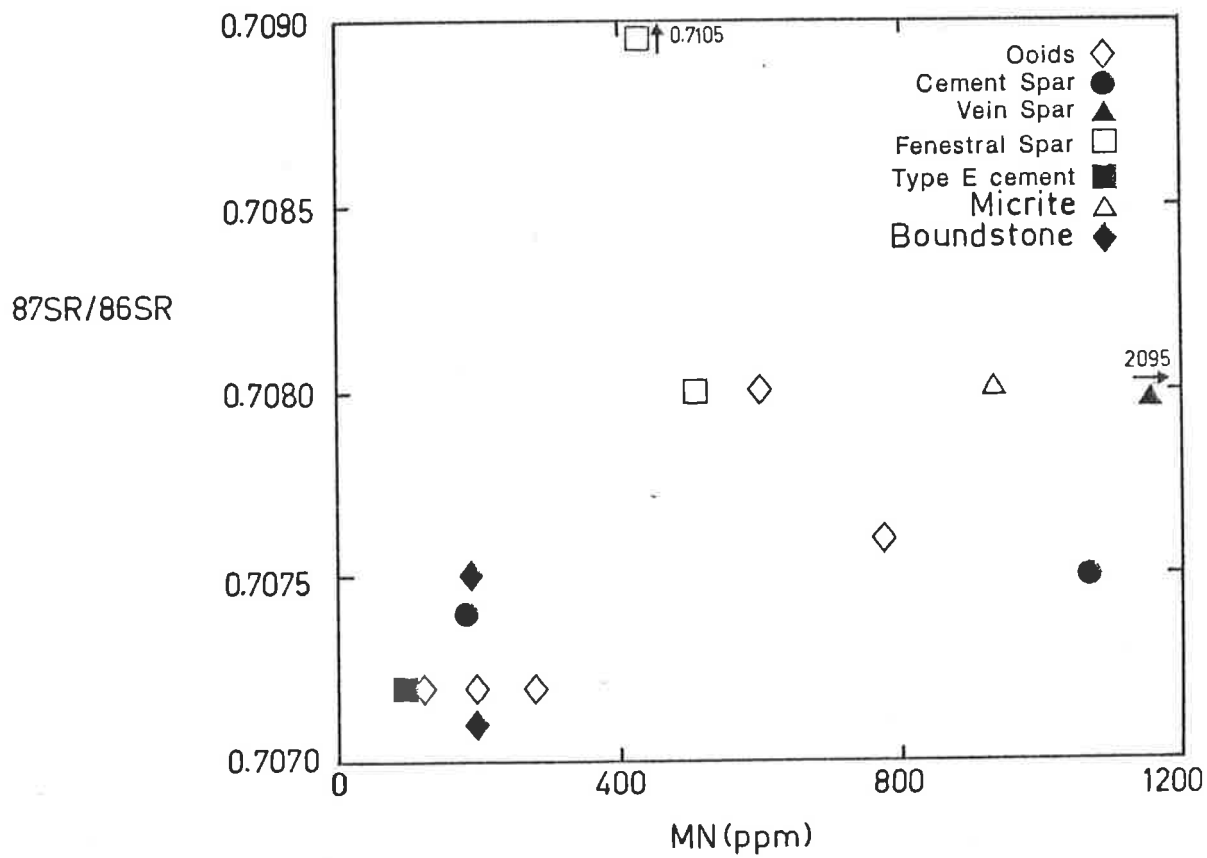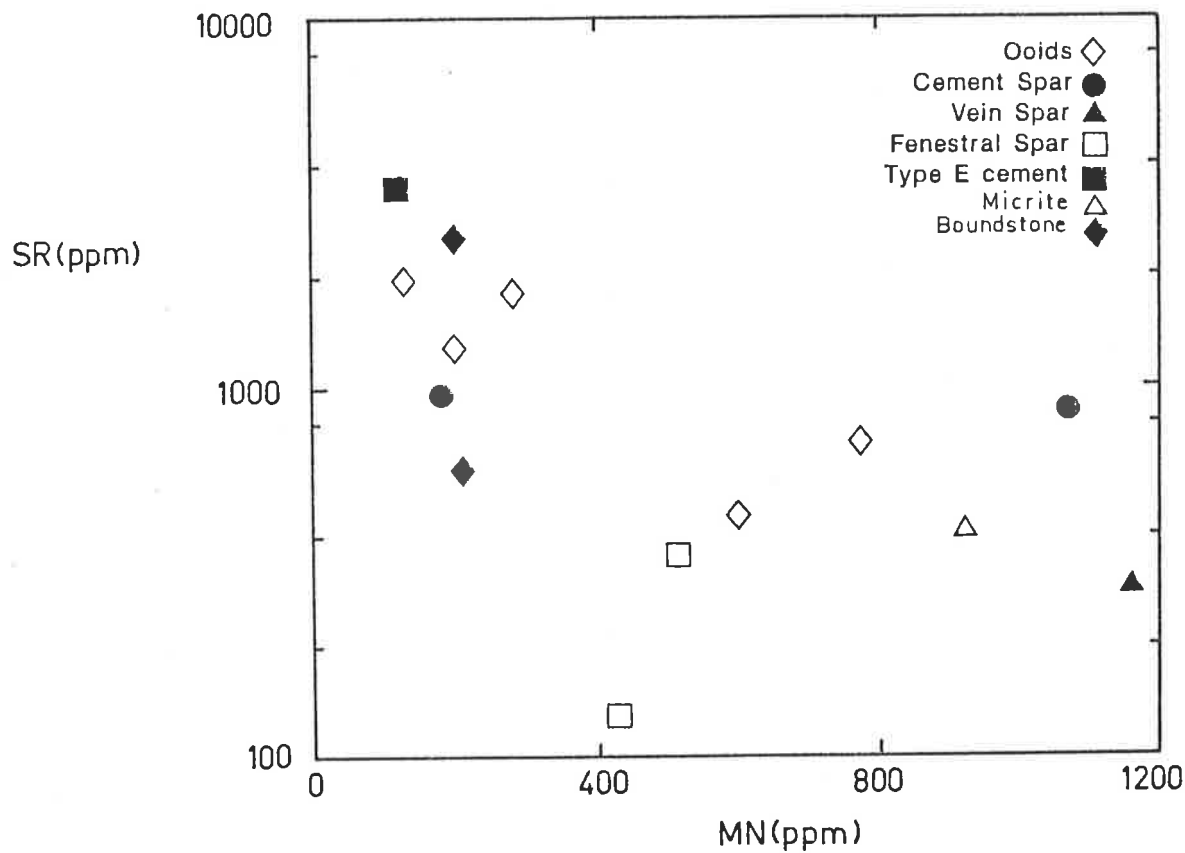
FIG.6.3: 87Sr/86Sr vs Mn plot of Trezona Formation components.

FIG.6.4: 1/Sr vs 87Sr/86Sr plot of Trezona Formation
components.
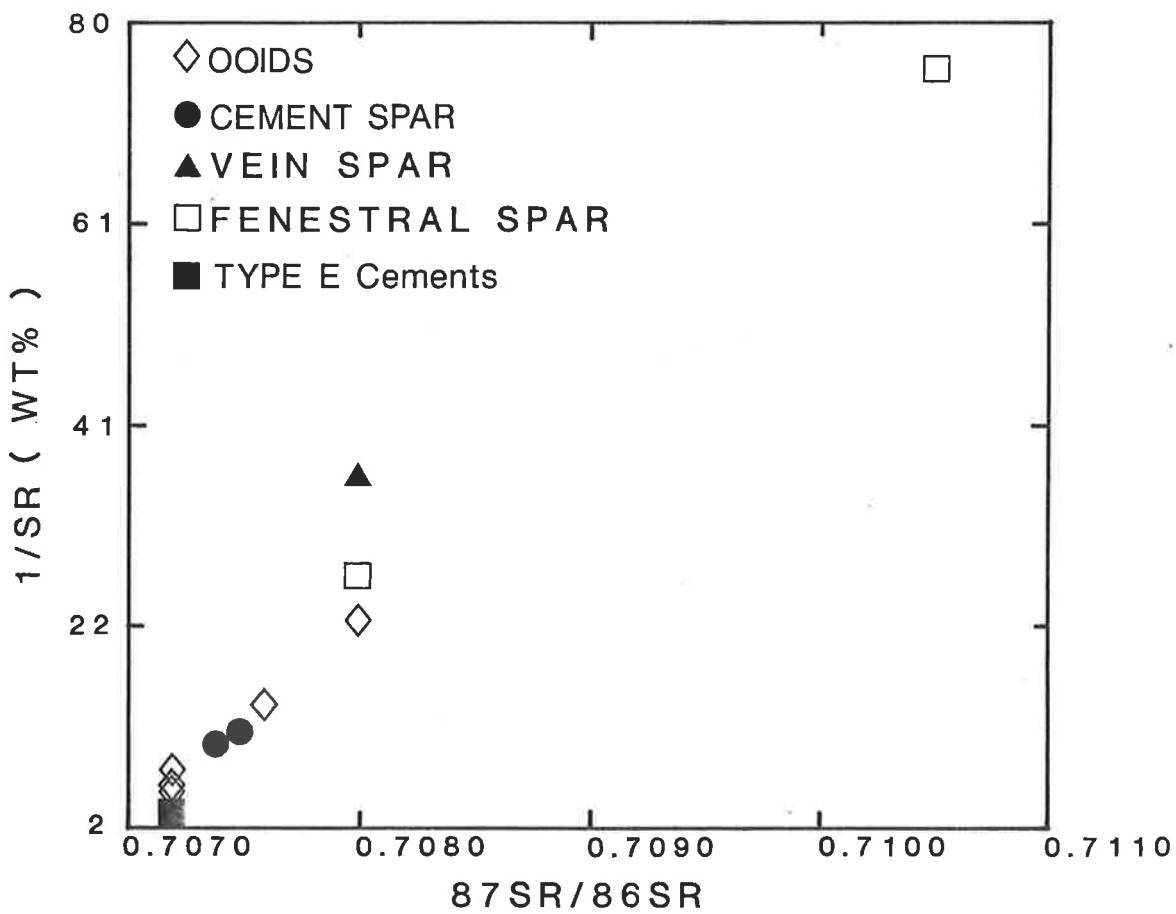
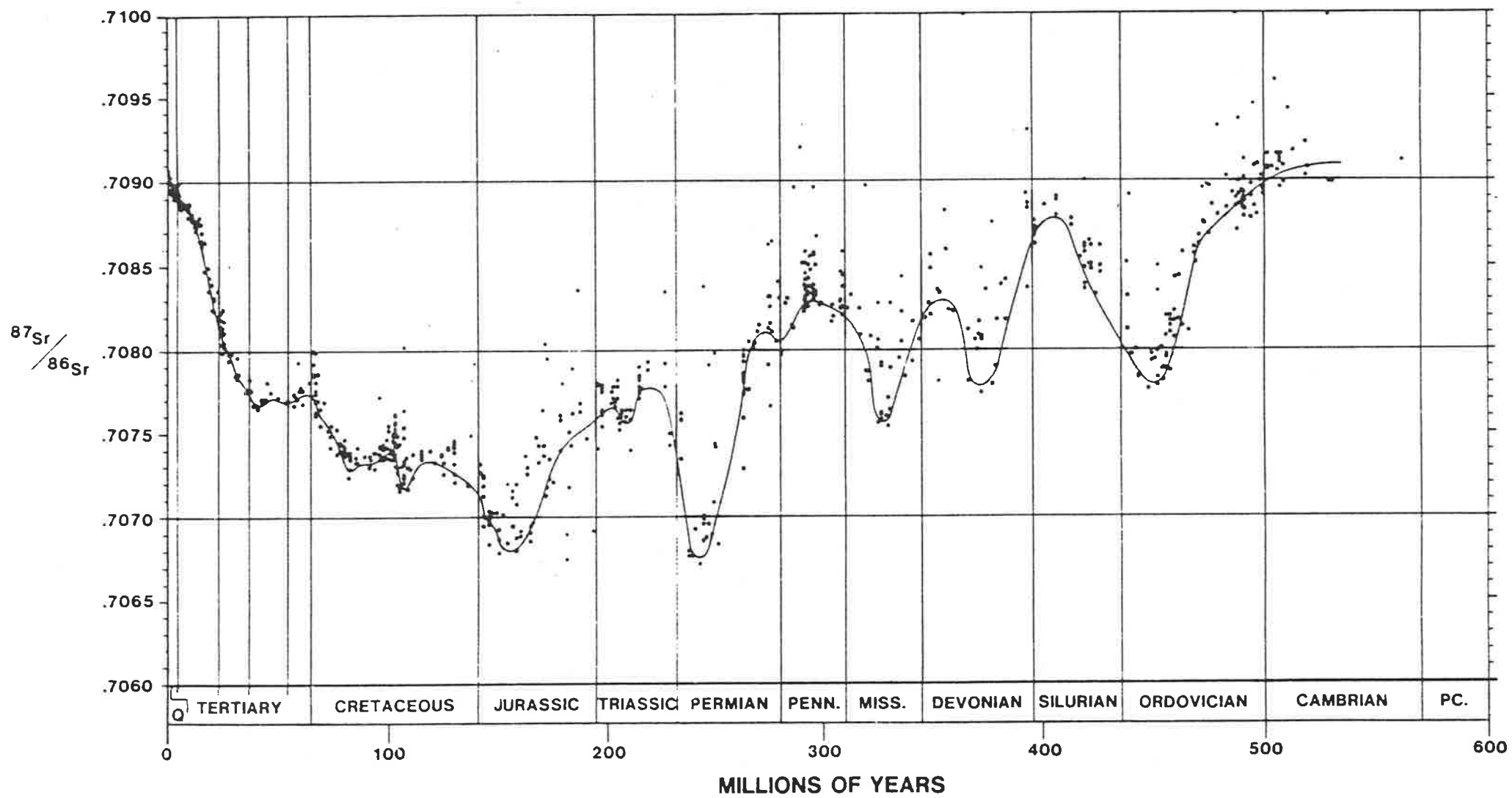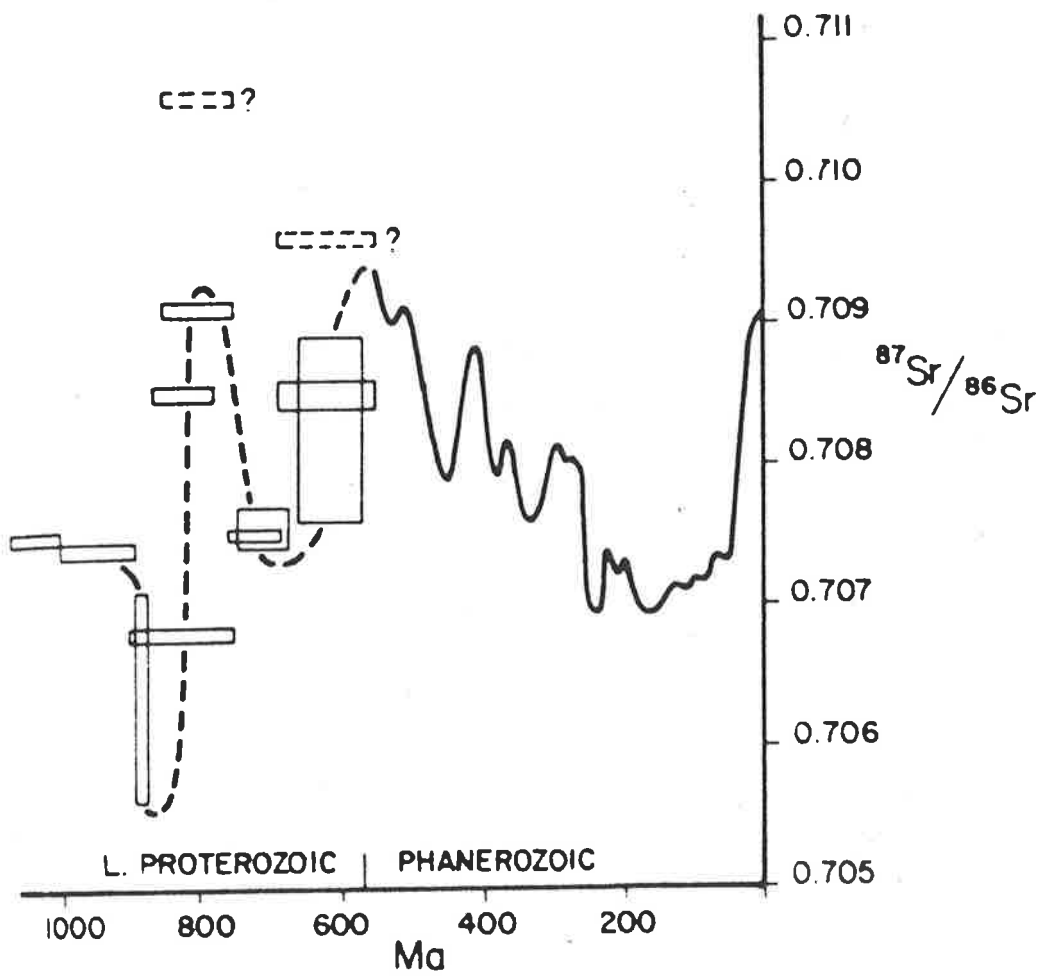FIG.6.5: 87Sr/86Sr secular variation curve of marine carbonates within the Phanerozoic (After Burke et al.1982).

FIG.6.6: Extension of the 87Sr/86Sr secular variation
curve into the Proterozoic (After Veizer et al.1983).

# CHAPTER SEVEN

## LATE PROTEROZOIC AND EARLY CAMBRIAN MARINE CARBONATES

### 7.1: INTRODUCTION

As reviewed in the Introduction in Chapter One, recent studies have suggested that carbonate precipitation in ancient environments may have been markedly different from that of the present day [Sandberg 1975; 1983; Tucker 1982]. Furthermore Late Proterozoic and early Cambrian earth history represents a critical period and carbonates deposited during that time have acheived added importance. Sauk sequence carbonates (Late Proterozoic to mid-Ordovician) have thus been included as one of the major projects requiring global study [Knoll 1986].

Within the Phanerozoic an oscillating trend in non-skeletal carbonate mineralogy has been proposed by Sandberg [1983] based on ooid and cement textures. This trend was related to tectonics and pCO2 levels [Mackenzie and Piggot 1981] and climatic variations [Fischer 1981; 1983]. Data on the late Precambrian to early Cambrian transition in non-skeletal carbonate mineralogy is scarce and therefore the timing of this shift is not known. Some recent studies on late Precambrian ooids and their textures indicate that this was a period of non-skeletal aragonite precipitation [Tucker 1984; 1985]. In addition Fairchild [1986] has both textural and geochemical evidence for aragonite precipitation within the Vendian carbonates of Spitsbergen and East Greenland.

The findings from the above and present study should aid us in clarifying the shift in aragonite vs calcite precipitation mentioned above. The nature of the trend in

114

non-skeletal carbonate mineralogy in the late Precambrian and early Cambrian of the Flinders Ranges is discussed below as is the occurrence of unusually large ooids and strontium-rich blocky calcite cements.

As well as trends in non-skeletal carbonate mineralogy, the Phanerozoic marine carbonate record has periods of abnormal or anomalous carbon isotope composition [Scholle and Arthur 1980; Holser et al.1986;]. Carbon isotopic data from the late Proterozoic is scarce and represents large temporal episodes. Veizer and Hoefs [1976] studied both oxygen and carbon isotopic variations and found a shift to heavier carbon values in the Precambrian. Later studies have confirmed this generally heavier carbon isotope signature of late Proterozoic carbonates [Knoll et al.1986 and refs. therein]. The carbon isotope record from the late Proterozoic of the Flinders Ranges also shows a shift to heavy carbon values from normal and depleted ones. The results are discussed below and compared with carbon profiles from other late Proterozoic sequences.

## 7.2: NON-SKELETAL MINERALOGY TRENDS

Reiterating the point made in the introductory chapter, ever since the appearance of Sandberg's [1975] study on ooid textures and precursor mineralogy, there has been a need to reassess the doctrine " the present is the key to the past ". Based on textural studies of ooids, cements and bioclasts a number of criteria for the identification of aragonitic precursors have been proposed [Sandberg 1985]. Applying these textural and geochemical criteria to the carbonate rock record, an oscillating trend in non-skeletal mineralogy was

established for the Phanerozoic [Sandberg 1983] (Fig.7.1).

The present study on some late Proterozoic and early Cambrian oolites of the Adelaide Geosyncline points to non-skeletal aragonite precipitation from the late Proterozoic Sturtian to the early Cambrian (Fig.7.2). Supporting textural and geochemical evidence has been presented in earlier chapters. The point of interest is the appearance of radial calcite ooids in the early Cambrian, possibly suggesting that non-skeletal calcite precipitation may have been initiated at this time. It is quite possible that some of the micritic ooids, which were present in all the oolites studied, could have had a calcitic precursor. However, available evidence does not allow a reliable interpretation of their precursor mineralogy to be made. The idea of the initiation of non-skeletal calcite mineralogy during the early Cambrian does seem plausible, since the Cambrian presumably marked the begining of an " aragonite-inhibiting " episode [Sandberg 1983]. The late Proterozoic period appears to have had non-skeletal aragonite and possibly high-Mg calcite precipitation, not unlike the present day environments. Calcitic (presumably low-Mg calcite) precursors probably only made an appearance in the early Cambrian. The ooid fabric and chemistry from the present study together with studies by Tucker [1983; 1984; 1986] supports an inference of primary aragonite precipitation during the Late Proterozoic. Evidence for the presence of high-Mg calcite precursors during the late Proterozoic was noted by Fairchild [1986], in the form of radial fibrous calcite cements in the Vendian carbonates of East Greenland and Svalbard.

Factors controlling aragonite vs calcite precipitation

are not clearly understood. The first-order cycles of aragonite and calcite phases proposed for the Phanerozoic are presumably controlled by tectonic and climatic effects, with the accompanying changes in atmospheric PCO2 [Mackenzie and Piggot 1981; Fischer 1981], and possibly Mg/Ca ratios [Sandberg 1975; Mottl and Holland 1978; Wilkinson and Given 1986 and refs. therein]. Using available data on marine ooids and cements, Wilkinson and Given [1986] proposed some chemical constraints on the occurrence of aragonite or calcite phases in the rock record. Tectonism, sea-level changes and atmospheric PCO2 levels are clearly factors of major importance in controlling the type of carbonate phase being precipitated.

Possibly, the transition from an aragonite precipitating period during the late Proterozoic to an aragonite plus calcite precipitating period during the early Cambrian, as recorded in the Flinders Ranges, is due to a change in the types of tectonic and climatic regime operating during these two periods. The late Proterozoic was a period of generally low sea-levels, with the presence of major glacial events, resulting in low atmospheric PCO2. Such conditions presumably favoured aragonite precipitation (Mackenzie and Piggot's 1981 emergent mode). During the early Cambrian, the major glaciations had retreated, sea-levels rose and major rifting of continents began, causing atmospheric PCO2 to rise and favouring calcite precipitation (their submergent mode).

Such cycles in carbonate phases represents only broad, first-order events and smaller scale variations in carbonate mineralogy do occur. In present-day marine waters, ooids with both calcitic and aragonitic cortical layers have been

117

reported [Land, Behrens and Frishman 1979] and such
bimineralic ooids have been recorded from the rock record
[Wilkinson, Buczynski and Owen 1984; present study]. A
relationship between the energy level and carbonate
mineralogy has been noted in ooids, with aragonitic ooids
predominant in high energy settings and calcitic ooids in low
energy settings. Apparently the rate of reactant supply at
the growth site, namely supply of carbonate ions, can control
the type of carbonate mineralogy precipitated [Given and
Wilkinson 1985]. High carbonate ion supply [high energy
settings] favours aragonite precipitation and low carbonate
ion supply [low energy settings] favours calcite
precipitation. The factors controlling the precipitation of
one carbonate phase over the other are probably fairly subtle
and small changes in the microenvironment can cause shifts in
the carbonate phase.

## 7.3: LARGE OOID SIZE

Unusually large diameter ooids [max.16mm] were recorded
from the Marinoan Trezona Formation (Fig.7.2) and have also
been recognised from other late Precambrian units [Radwanski
and Birkenmajer 1977]. Whilst large ooid sizes do occur
within the Phanerozoic, they are commonly found in restricted
or lacustrine and hypersaline facies and are unusual in
normal marine facies. Modern Bahamian shoals have a maximum
ooid size of 1mm [Newell et al.1960] with larger sizes being
confined to coastal and sabkha settings in the Persian Gulf
[Loreau and Purser 1973; Shinn 1973]. The size attained by an
ooid is presumably the result of a balance between
precipitation and abrasion [Bathurst 1968]. The type of

transport mechanism can also determine the size as well as the fabric of the resulting ooid [Heller et al.1980]. Radwanski and Birkenmajer [1977] explain their large ooid size (average 10mm) to the profuse precipitation of carbonate, resulting possibly from a difference in chemistry of Precambrian marine waters.

The reasons for such large ooid sizes are purely of a speculative nature at present and their proper understanding requires a detailed study. Nonetheless, two points of possible significance to the problem of large ooid size are raised here. Firstly, the lack of metazoan browsers during the late Precambrian implies that a larger ecological niche was available for blue-green algal or cyanobacterial colonisation [Garret 1970; Awramik 1971]. Whilst there may not be any direct biological involvement in ooid genesis, and indeed none was observed in the present study, indirectly the activity of blue-green algae may have resulted in a marine chemistry conducive to faster carbonate precipitation rates and attainment of larger ooid size. In present day carbonate environments, such conditions only exist in hypersaline environments and it is in these environments that large ooids are produced. Secondly, within the late Proterozoic there was apparently an increase in the diversity of microplankton during the late Riphean and early Vendian [Vidal and Knoll 1982]. It is within this time interval that the ooids of the Marinoan Trezona Formation and those studied by Radwanski and Birkenmajer [1977] occur. Is it possible that such a bloom of microplankton could have indirectly resulted in ooids with large diameters being produced? The later diversification of microplankton during early Cambrian times recorded by Vidal

and Knoll [1982] did not generate large ooid sizes possibly because of their ecological restriction by the grazing and browsing activity of the recently evolved metazoans. More studies on such large ooid occurrences and an understanding of the controls on ooid size in present day environments is needed before an adequate explanation for such large ooid sizes is forthcoming.

7.4: STRONTIUM-RICH BLOCKY CEMENTS

The initial concentration of Sr in a carbonate depends on it's precursor mineralogy; being about 10000 ppm in aragonite, 1000-3000 ppm in Mg calcites and 1000-2000 ppm in calcites. During diagenesis by meteoric pore-waters, the concentration of Sr and Na in the precursor carbonate decreases and that of Fe and Mn increases [Brand and Veizer 1980; Veizer 1983]. Therefore the majority of calcites produced during diagenesis i.e. dLMC, have Sr content of a few hundred ppm [Kinsman 1969; Morrow and Mayers 1978]. The decrease of Sr during diagenesis is due to the distribution coefficient for Sr being much less than unity and the lower concentration of Sr in meteoric waters compared to marine waters. Depletion in Sr however, can also occur in carbonates that have no evidence of recrystallization in meteoric waters and presumably can take place in marine waters [Katz et al.1972; Land 1979,1980].

Ancient limestones have a wide range of Sr concentrations, with suggestions of a weakly bimodal distribution. Bausch [1968] noted that his reef complex limestones have Sr contents of between <100 ppm and 400 ppm. The basinal limestones on the other hand had higher Sr contents ranging from 500 ppm to 3000 ppm. Such a facies

related bimodal distribution of Sr was also recorded by Veizer and Demovic [1973,1974]. They distinguished two major groups of Mesozoic limestones; low Sr limestones with a mode of 100-250 ppm, comprising light coloured algal bank and reef facies and high Sr limestones with a mode of 600-700 ppm, comprising dark coloured, deep-sea and lagoonal facies. The distribution of Sr in the above limestones may have been strongly influenced by the porosity and permeability of the sediments. A strong porosity control on the Sr content of limestones was suggested by Morrow and Mayers [1978]. Shelf-edge grainstones, for instance, will tend to undergo greater amount of Sr leaching than their lagoonal mudstone equivalents. The porosity controls the "open" vs "close" nature of the diagenetic alteration [Pingitore 1976; Veizer 1983]. The occurrence of strontium rich diagenetic calcites (>1000 ppm Sr) in limestones is therefore unusual. This is especially so if they occur as interparticle calcite cements in grainstones, with their high initial porosities. They have also been recorded from Phanerozoic limestones [Mayall 1986; Moore 1985] and late Proterozoic limestones [Fairchild 1986; Tucker 1983; 1986].

Such strontium rich blocky calcites were described from all the Late Precambrian units in the present study (Figs.7.2 & 7.4). Within the Balcanoona Formation blocky calcites with anomalous Sr content occur as interparticle calcite cements in the ooid grainstones and also as sparry laminae in stromatolites. In the Trezona Formation, high Sr content is found in the interparticle blocky calcites and in light coloured, sparry laminae within a laminated limestone facies. The Wonoka Formation has ooid grainstones with strontium rich

interparticle calcite cements. Based on their occurrence, the strontium rich blocky calcites in this study could be divided into two groups; those associated with grainstones and those associated with mudstones/boundstones.

## 7.4.1: STRONTIUM-RICH GRAINSTONE CEMENTS

The possibility of an aragonitic precursor for these strontium rich blocky calcites is not supported by textural evidence since these void-fill precipitates show no evidence of any calcitized or neomorphic fabrics [Sandberg 1985]. An external source for the high Sr, possibly from Sr enriched brines, seems unlikely since there are no Sr-rich mineralogies, eg. celestite, associated with the cements. Moreover, an external source for the Sr rich pore-waters would have to explain the occurrence of such Sr rich cements at various stratigraphic levels in the Late Precambrian of the Flinders Ranges.

All of the ooid grainstones with strontium rich blocky calcites occurring as interparticle cements have ooids with calcitized fabrics. This suggests a possible relationship between the high Sr content and the presence of aragonitic precursors. The pore-waters that generated these high Sr calcite cements may have been enriched in Sr from the dissolution and alteration of the aragonitic ooids [Halley and Harris 1979; Moore 1985]. However, the mechanism or process responsible for generation of such high Sr concentrations in a water-rock system that presumably had high initial porosity is not understood. Moreover, the neomorphic spar of these calcitized ooids has a high Sr content, suggesting retention of most of the original Sr in

the precursor.

## 7.4.2: STRONTIUM-RICH MUDSTONE/BOUNDSTONE CEMENTS

These blocky calcites occur in the Balcanoona and Trezona Formations and have higher concentrations of Sr than the blocky calcites associated with grainstones described above. Within the Balcanoona Formation, such strontium-rich blocky calcites form light coloured laminae in stromatolites. There are no included grains within this calcite mosaic, unlike the cements from the Trezona Formation described below. Occasionally, there are calcite veins transecting these sparry laminae and these also have high Sr contents. This suggests a late diagenetic origin for these strontium-rich calcites, possibly under burial conditions with calcite precipitation from Sr enriched brines. The source of the Sr is unclear and could possibly be from associated aragonitic components.

Strontium rich calcites from the Trezona Formation occur within dark coloured laminae in a laminated limestone facies interpreted as quiet water lagoonal or deep subtidal deposits. The calcites in these dark layers described as poikilotopic calcite cements in Chapter Two, were recorded by Tucker [1983; 1986] from other late Proterozoic limestones. He recognised ooids and problematic grains referred to as spheroids within coarse calcite mosaics which were brownish in colour and pseudopleochroic.

The high Sr content of these calcites was attributed to burial diagenetic stabilization of aragonitic components in marine derived pore-waters. The fabric of these cements are very unusual and quite unlike the pore-filling precipitates

described in section 7.4.1. One possible inference is that these strontium-rich blocky calcites represent calcitized products of an original pore-filling aragonite cement. However, Sandberg [pers.comm.] is of the opinion that such an interpretation is unreasonable. He bases his argument on the fact that such pore-filling aragonite cements are rare anywhere in the Phanerozoic. So, given the possible difference in chemistry of Precambrian marine waters, it is difficult to argue that during the Precambrian, in contrast to the entire Phanerozoic, intergranular pores were totally aragonite filled. Furthermore, even if such cements were calcitized aragonitic precursors, there are no relic structures present in them.

Tucker [1986] recognised ooids within these strontium-rich blocky calcites that had calcitized neomorphic fabrics, suggesting an original aragonitic mineralogy. In the present study, the enclosed ooids did not display any clear evidence of calcitization and occur as relics within the coarse calcite mosaics. Thus, although the textural data in the present study does not seem to have typical aragonite replacement features [Sandberg 1985 and pers.comm.], the unusual fabric of these cements together with it's high Sr content suggest a possible aragonite precursor.

## 7.5: CARBON ISOTOPE TRENDS

The carbon isotope composition of marine carbonates provides information on the source of carbon. Modern marine waters represent a well mixed carbon reservoir, with carbon isotope values (Del C13) around 0 permil. Minor variations do occur in non-marine waters and depend on various factors

including exchange with atmospheric CO2, input of dissolved carbonate in ground-waters, photosynthesis and CO2 production during organic matter decomposition [Fritz and Poplawski 1974]. Modern marine carbonates have a range of carbon isotope compositions between 0 permil and 4 permil and ancient limestones range from -2 permil to 2 permil [Hudson 1977]. Organic derived CO2 causes large shifts in the normal range of isotopic compositions of natural carbonates, since organic carbon is greatly depleted in C13.

The carbon isotope profile of the late Proterozoic and early Cambrian carbonates in the Flinders Ranges is marked by a positive carbon excursion in the Sturtian Balcanoona Formation, with normal and depleted carbon isotope values for the Marinoan Trezona and Ediacaran Wonoka Formations and the early Cambrian Wilkawillina Limestone (Fig.7.2). Such carbon isotope profiles have been obtained in recent studies of late Proterozoic and early Cambrian carbonates [Tucker 1986; Knoll et al.1986]. In the Moroccan section, Tucker [1986] recorded a heavy carbon isotope signature within a dolomite unit that is probably close to the Riphean/Vendian boundary (Fig.7.5). A smaller positive carbon excursion was recorded within the early Cambrian carbonates. Although stratigraphic control in the Moroccan section is poor, the positive carbon isotope excursion at the probable Riphean/Vendian boundary can be broadly correlated to the positive carbon isotope signature of the Sturtian Balcanoona Formation. Both these positive carbon excursions occur in carbonates that overlie glacial sediments; Sturtian glacials in the Flinders Ranges and Tiddiline Formation glacials in Morocco. The Flinders Ranges section has a second younger glacial unit representing the

Marinoan glaciation developed above the Trezona Formation and is of probable Vendian age. The carbon isotope signature of the Trezona Formation is a depleted one , similar to the depleted values in the Vendian Serie Lie de Vin of the Moroccan section.

Knoll et al. [1986] recorded positive carbon isotope signatures for the dominant part of the late Proterozoic sections in East Greenland and Svalbard (Fig.7.6). Excursions to normal and depleted carbon isotope values occurred at various stratigraphic levels. Within the context of the Flinders Ranges, the negative carbon isotope excursion at the level of the Vendian glacials in the East Greenland and Svalbard sections is interesting. These Vendian glacials could be correlated with the Marinoan glacials in the Flinders Ranges and in both sections there is a negative excursion in the carbon isotope signature of carbonates at this stratigraphic level (Figs.7.2 & 7.6). The positive carbon isotope signature of the Balcanoona Formation would correlate with the generally positive carbon isotope signature of the late Riphean part of the East Greenland and Svalbard sections. The carbon isotope trend across the Precambrian-Cambrian boundary in the Siberian Platform also recorded positive excursions from normal and depleted signatures [Magaritz et al. 1986]. This carbon isotope trend cannot be correlated with the Flinders Ranges due to a lack of carbonates of comparable age.

There is however, broad aggreement in the carbon isotope profiles of the Moroccan, East Greenland and Svalbard late Proterozoic and early Cambrian carbonate sections with those of the Flinders Ranges.

The variation in the carbon isotope signatures observed above are mainly the result of changes in the Corg/Ccarb ratio. The present day carbon isotope signature of ~ 0 permil is the result of a Corg/Ccarb ratio of 1:4. Variations in this ratio in the past would have caused changes in the carbon isotope composition of the total dissolved inorganic carbon (TDC) in marine waters. The carbon isotope composition of marine carbonates reflects this TDC isotopic signature. Variations in the carbon isotope composition of marine TDC and therefore of the marine carbonate can be brought about by changes in biological productivity in marine waters [Broecker 1982], changes in vertical circulation of marine waters [Brass, Southam and Peterson 1982] and fractional preservation of organic carbon on the sea-floor caused by expansion and contraction of the oxygen minimum layer [Scholle and Arthur 1980]. Increased preservation of organic carbon can result from either increased productivity or expansion of the oxygen minimum layer, causing heavy or positive carbon isotope composition in the TDC and resulting carbonates. Such positive carbon isotope signatures have been related to oceanic anoxic events (OAEs) in the Phanerozoic carbonate record [Scholle and Arthur 1980].

The positive carbon isotope excursions recorded from the carbonates of the late Proterozoic and early Cambrian have been attributed dominantly to increased biological productivity [Tucker 1986; Magaritz et al. 1986]. Since the Precambrian-Cambrian period represents a time of evolution of metazoans and radiation of microplankton, these events presumably caused changes in the Corg/Ccarb ratio and the ensuing carbon isotopic composition. Apart from changes in

biological productivity, a change in the vertical circulation pattern of marine waters by glaciations can also have an effect on the carbon isotope composition. Knoll et al. [1986] noted that the return to normal and depleted carbon isotope compositions from positive signatures within their late Proterozoic sections coincided with the major Eocambrian glaciations. The presence of a global glacial regime would have increased vertical circulation in marine waters thereby causing a reduction in the burial of organic carbon. The resulting carbon isotope composition would have depleted or normal marine values. A buildup of atmospheric oxygen during the period from 700 to 800my was proposed by Knoll et al. [1986]. This would then have caused the depleted carbon isotope signatures in the latest Vendian due to very high oxygen pressures and an aggressive environment.

Within the Adelaide Geosyncline the association of ironstones with the lower Sturtian glacials indicates high oxygen levels and/or increased circulation in marine waters. This association of iron-rich or red, oxidised facies with glacials is also noted during the upper Marinoan glaciation. Prior to the deposition of the Marinoan glacial unit, sedimentation in the underlying Trezona Formation consisted of characteristic red carbonate facies within what until then had been dark grey euxinic type sediments. Possibly the approach of the Marinoan glaciation and the probable presence of ice-caps during Trezona Formation deposition [Jenkins 1986] caused increased oxygenation of marine waters. This resulted in depleted carbon isotope compositions due to the destruction and reduced burial of organic carbon. Hsu et al. [1985] noted a negative carbon isotope trend caused by

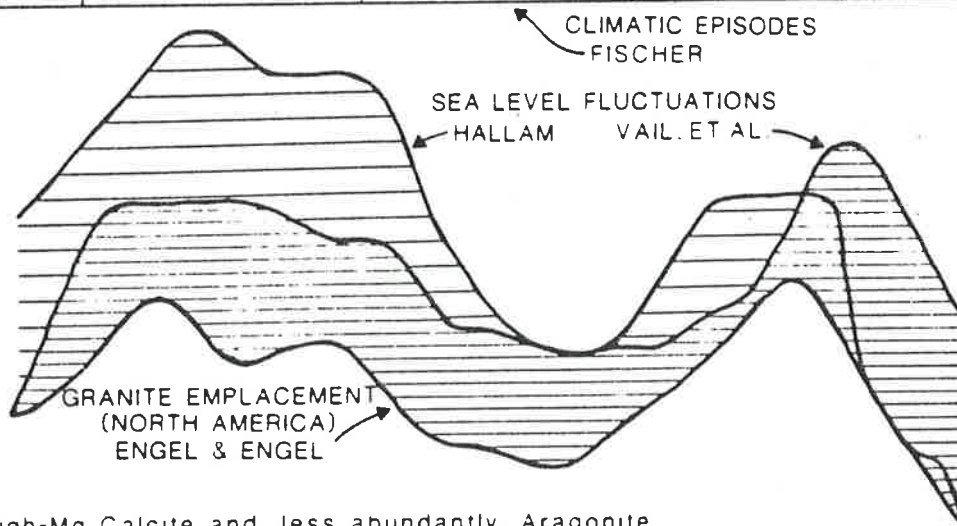destruction of biological productivity and buildup of C12.

Conversely, the Balcanoona Formation carbonate sedimentation occurred during an essentially interglacial period of high sea-levels and reduced vertical circulation. The resulting lower level of oxygenation caused increased organic carbon burial and a positive or heavy carbon isotope signature.

The similarities in the carbon isotope profile of the late Proterozoic and early Cambrian sections from the Adelaide Geosyncline with those from East Greenland, Svalbard and Morocco indicates a possible global change in the carbon isotopic composition of marine carbonates. Factors that may have caused this trend include the late Proterozoic glaciations and the initiation of rifting of continents during the early Cambrian [Ziegler et al. 1979; Bambach 1980].

FIG.7.1: Variation in non-skeletal carbonate mineralogy within the Phanerozoic and its relations to sea-level changes, tectonism and climate (After Sandberg 1983).

"Aragonite Threshold"
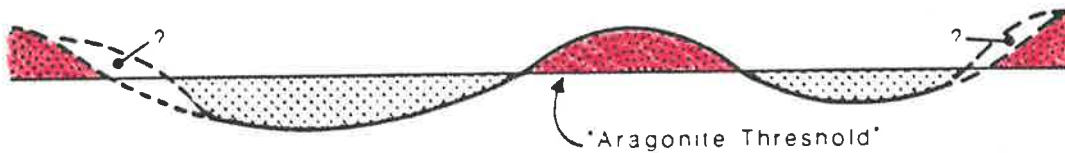
| PC | CAM. | ORD. | SIL | DEV | CARB. | PER. | TR | JUR. | CRET. | CEN. |
|----|------|------|-----|-----|-------|------|----|------|-------|------|
| ICEHOUSE | | GREENHOUSE | | | ICEHOUSE | | | GREENHOUSE | | ICE |

CLIMATIC EPISODES
— FISCHER

SEA LEVEL FLUCTUATIONS
— HALLAM       VAIL. ET AL.

GRANITE EMPLACEMENT
(NORTH AMERICA)
ENGEL & ENGEL

High-Mg Calcite and, less abundantly, Aragonite

Calcite: Mg content generally lower, increasing toward 'Threshold'

FIG.7.2: Summary of variations in non-skeletal carbonate
mineralogy, ooid size, strontium content of cements and
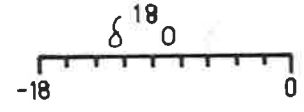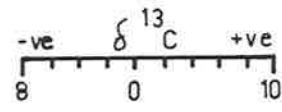oxygen and carbon isotope compositions within part of
the Adelaidean sequence of the Flinders Ranges as
determined by this study.
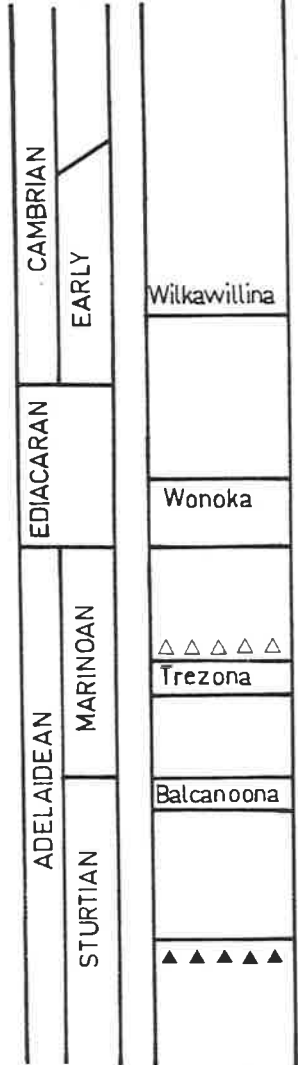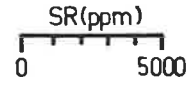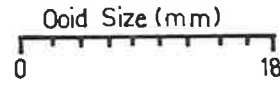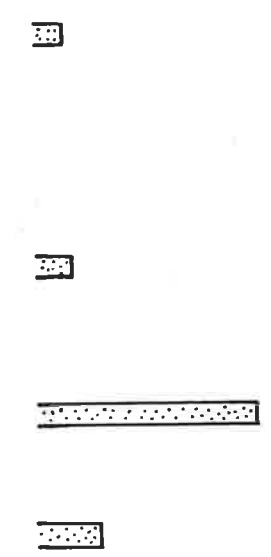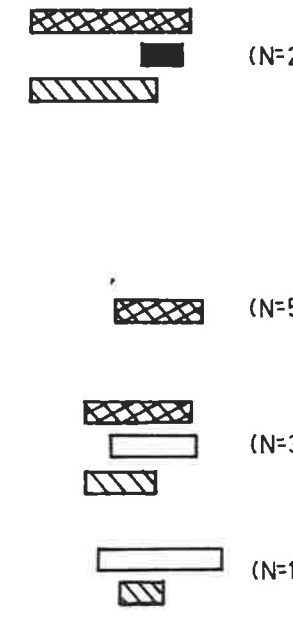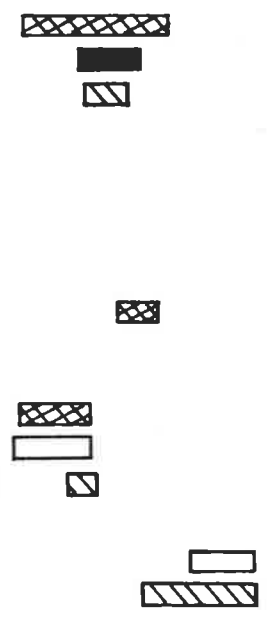
FIG.7.3: A composite plot of Sr vs Mn content of ooids
from the Late Precambrian and early Cambrian units
studied.

FIG.7.4: A composite plot of Sr vs Mn content of
interparticle cements from the Late Precambrian and early
Cambrian units studied.
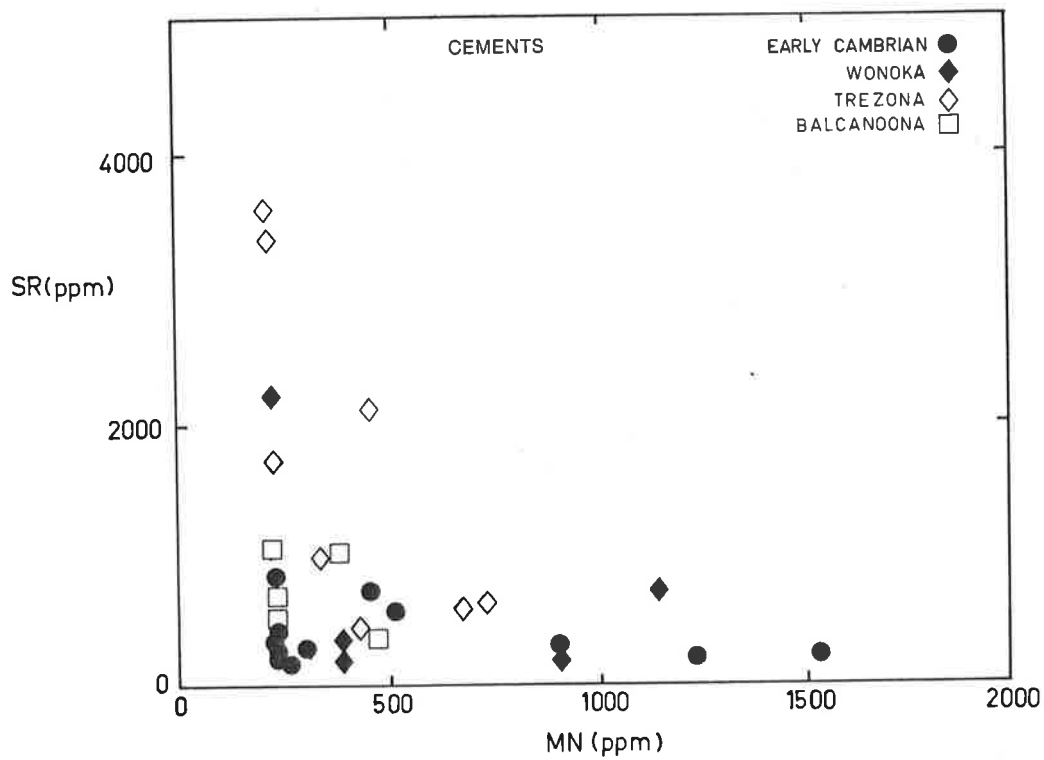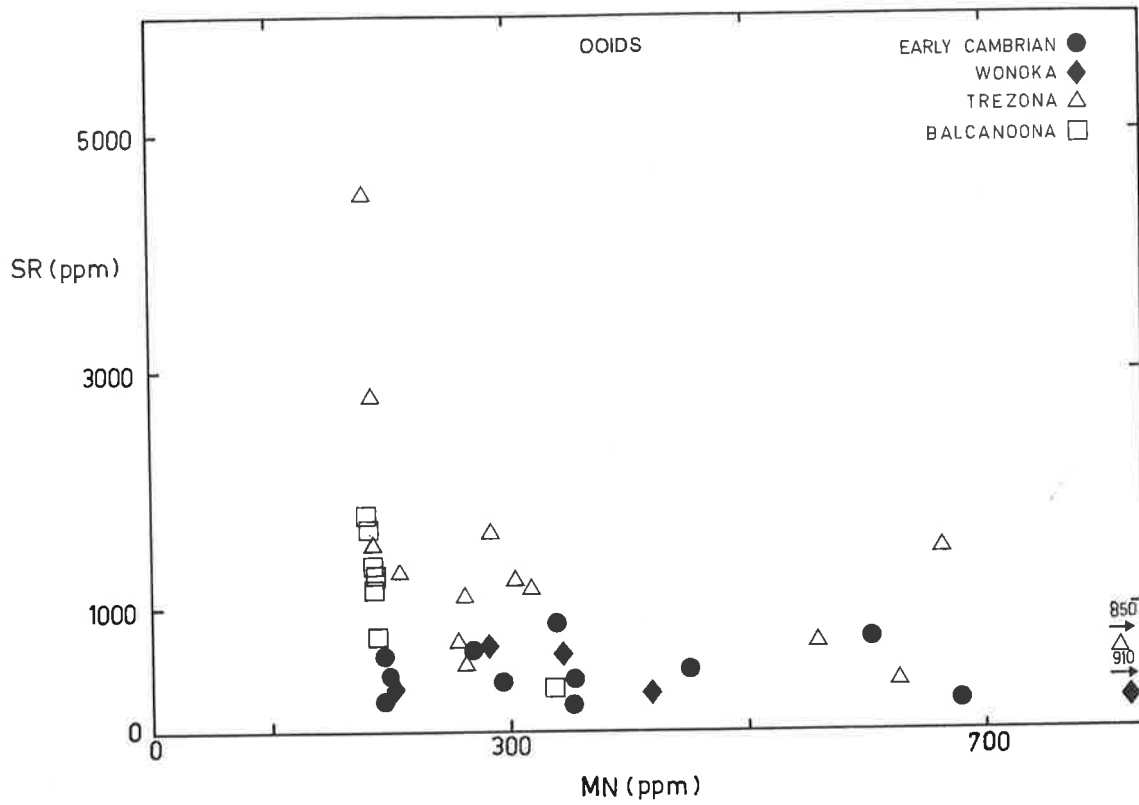
FIG.7.5: Carbon isotope profile within the Late Precambrian and Cambrian carbonate sequence of Morocco (After Tucker 1986).(Closed symbols, dolomites; open symbols, limestones).

Serie
Schisto
Calcaire

Transition
Beds

Calcaire
Superieur

Serie Lie de Vin

Upper

Middle

Lower

Dolomie
Inferieur

First trilobites

1,500
1,400
1,300
1,200
1,100
1,000
900
800
700
600
500
400
300
200
100
0
100
metres

-5  -4  -3  -2  -1  0  1  2  3  4  5  6  7

$\delta^{13}C$
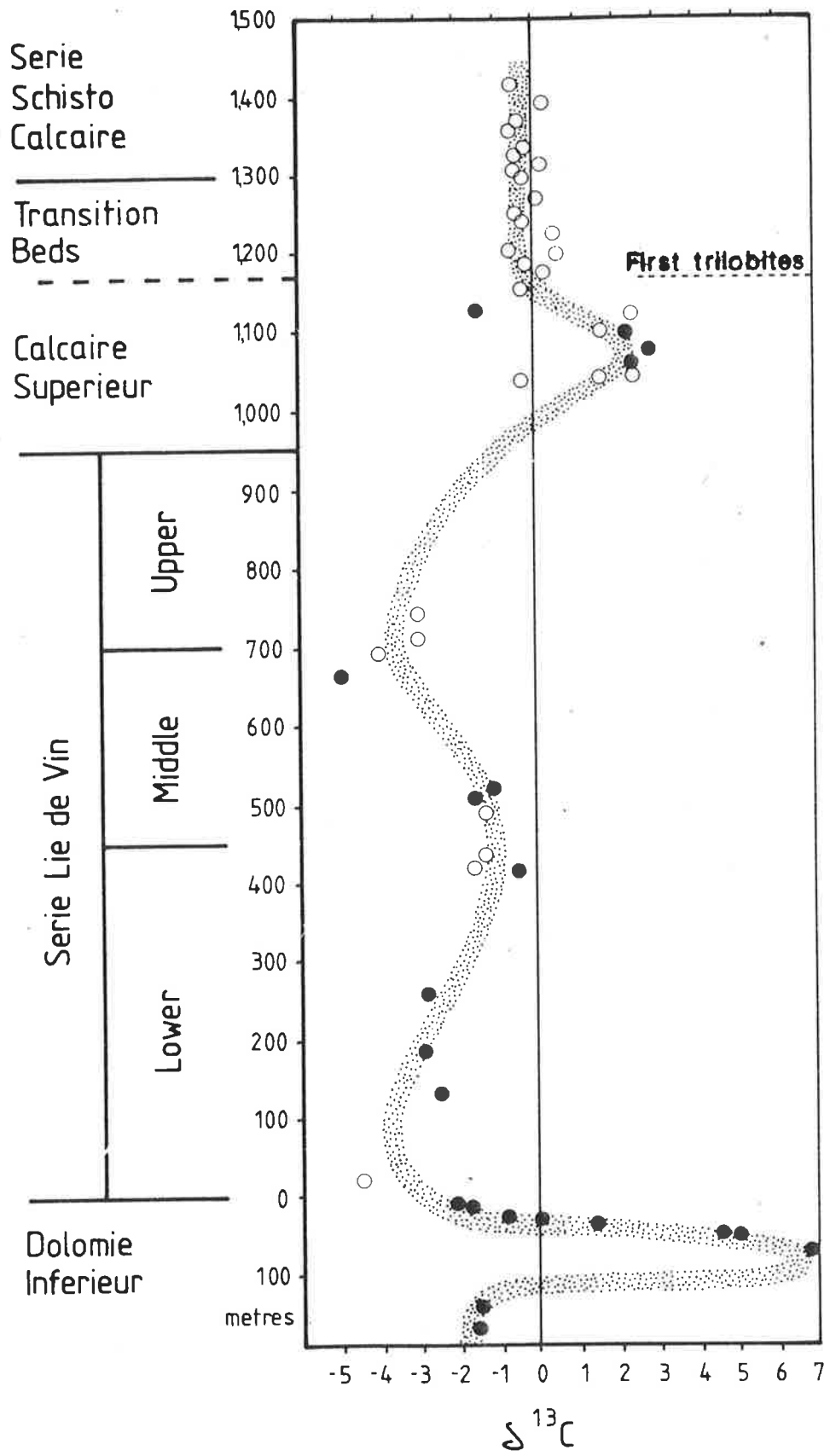
FIG.7.6: Carbon isotope profile within the Late Proterozoic carbonate sequence of Svalbard and East Greenland (After Knoll et al.1986). The Late Precambrian Trezona Formation in the present study correlates with stratigraphic position number 2 on the figure. (Squares, samples with <0.2 mg C per g sample; triangles, samples with <10% carbonate (as calcite); filled symbols, samples with 26.5% $\leq$ e $\leq$ 30.5%, where e refers to the isotopic fractionation between carbonate and organic carbon).
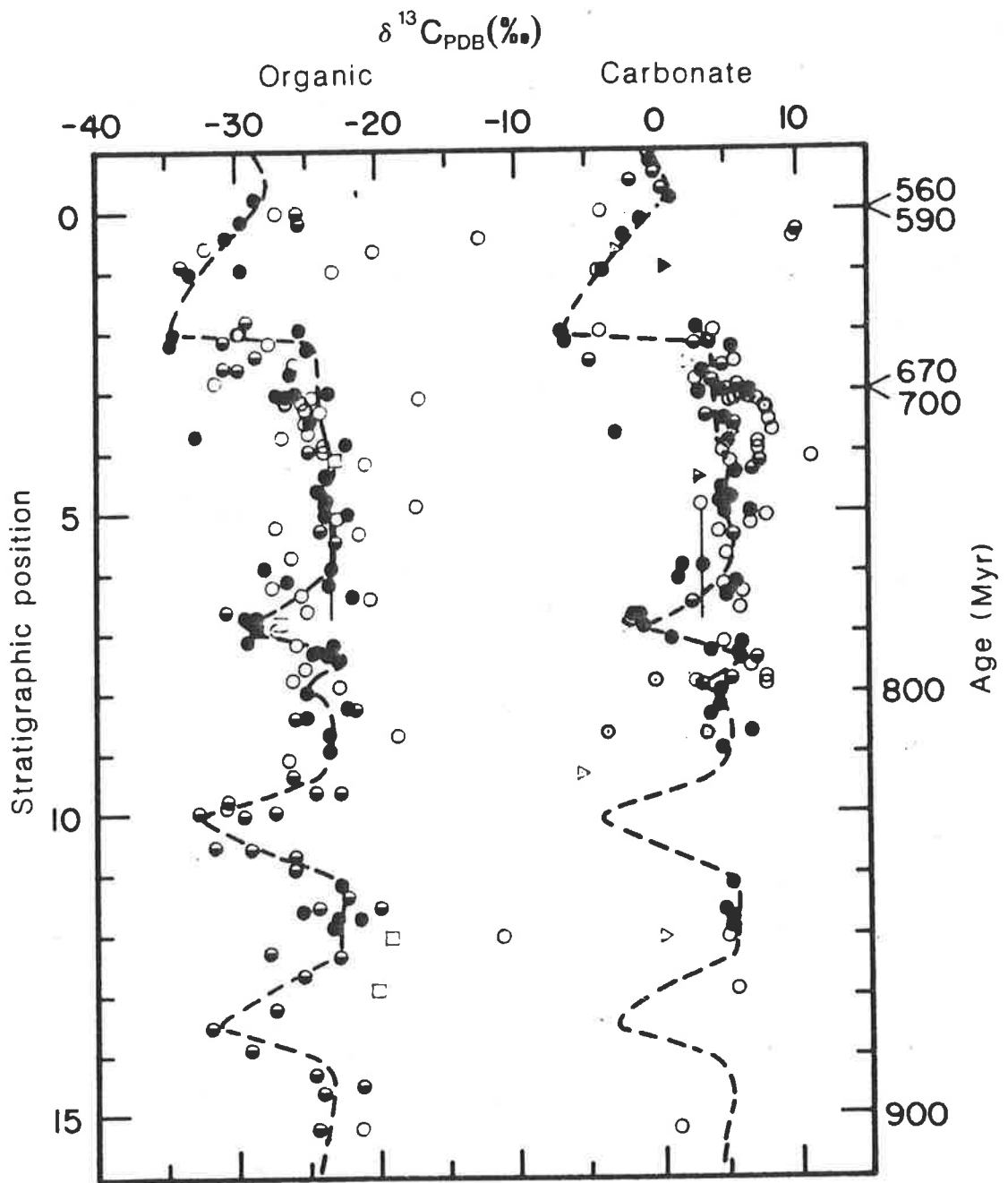
# CHAPTER EIGHT
## CONCLUSIONS

One of the aims of the this study was to understand the nature of non-skeletal carbonate precipitation within some Late Precambrian and early Cambrian limestones. Petrographic analysis of the late Proterozoic Balcanoona, Trezona and Wonoka Formations and the early Cambrian Wilkawillina Limestone of the Adelaidean in the Flinders Ranges was therefore undertaken. The late Proterozoic units represent carbonate deposition during Sturtian (Balcanoona), Marinoan (Trezona) and Ediacaran (Wonoka) times.

Detailed petrographic study of the oolite units from these formations show that ooids with definite aragonite replacement textures occur in both the Late Precambrian and Early Cambrian units. These include neomorphic spar ooids, brick-texture ooids and ooid molds. Evidence for possible bimineralic ooids, i.e. with aragonitic and calcitic cortical layers, is present in all the units studied and include half-moon ooid fabrics and ooids with eccentrically displaced nucleii. Ooids with calcitic precursor mineralogy, i.e. radial calcite ooids, only appear in the Early Cambrian. Micritic ooids are ubiquitous and their precursor mineralogy is difficult to interpret. Very large ooid sizes (maximum diameter, 16mm) are recorded from the Marinoan Trezona Formation. The appearance of definite calcitic precursors in the early Cambrian may reflect the change in tectonic and climatic regimes that probably occurred during this time. Globally, the late Proterozoic represents a period of low sea-levels with glacial events and the early Cambrian a period of rising sea-level and transgressions together with

the rifting of continents. This change in environments may have induced an increase in the atmospheric $PCO_2$ levels in the early Cambrian, which resulted in the precipitation of calcitic mineralogies.

Supporting geochemical evidence for aragonite precipitation is recorded in the ooids and some cements. Electron microprobe analyses record unusually high Sr concentrations (1000–4500 ppm Sr) in some ooids and cements from the Late Precambrian units. Some of the cements occur as blocky interparticle cements in ooid grainstones associated with calcitiz ed ooids. Others occur as blocky calcite mosaics within sparry laminae of stromatolites or laminated limestones. Most of these strontium rich blocky calcite cements do not have the classical calcitization fabrics and their genesis remains uncertain. Some of these strontium rich (poikilotopic) cements, have neomorphic fabrics and could represent calcitized products. This latter cement type has also been reported from late Proterozoic carbonates in California and south Norway.

A second major aim of this thesis was to determine the precursor chemistry of marine waters during the Late Precambrian-early Cambrian interval. This involved mainly the oxygen and carbon isotope chemistry of the limestones, although the $^{87}Sr/^{86}Sr$ ratio in some of the carbonate units was also obtained. Strontium isotope analysis revealed a large range of $^{87}Sr/^{86}Sr$ ratios for the Late Precambrian Trezona Formation marine limestones. However, based on trace element data it is inferred that the original marine $^{87}Sr/^{86}Sr$ during Trezona Formation time was 0.7071, lower than the previously obtained value of 0.7074 to 0.7077. The

early Cambrian had higher 87Sr/86Sr ratios, varying from 0.7085 to 0.7093.

The carbon isotope signature within each of the above units has a large scatter. However, there is a real and significant difference in the carbon signatures of some of the units. Carbon isotope analyses indicate a heavy carbon signature in the Sturtian Balcanoona Formation with a decrease to small positive or negative values in the Marinoan, Ediacaran and Early Cambrian. Depleted carbon signatures were recorded from the Marinoan and Early Cambrian diagenetic components. This carbon shift is broadly correlated with those recorded from other Late Proterozoic carbonate sequences in East Greenland, Svalbard and Morocco. The Sturtian-Marinoan carbon isotope shift may have been due to glacially induced changes in oxygenation levels, causing changes in the $C_{org}/C_{carb}$ ratio. Unlike the carbon isotopes, oxygen isotopes of the Late Precambrian and Early Cambrian units studied had a more or less constant range of values and did not reveal any discernible trend.

The Precambrian-Cambrian boundary in the present study did not reveal any significant changes apart from the appearance of definite calcitic precusors. A major shift in the stable isotope chemistry of shallow marine environments seems to have occurred during the late Precambrian with the occurrence of anomalous carbon isotope compositions recorded in this and previous studies. More complete and detailed carbon isotope profiles are required from this and other late Proterozoic sequences to enable a reconstruction of global environmental history during this crucial interval.

# APPENDIX ONE

## ELECTRON MICROPROBE ANALYSIS

Samples selected for microanalysis were polished and carbon coated. A total of 175 thin sections were studied, out of which 95 were selected for electron probe analysis. Quantitative determination of trace element compositions of carbonate components was done on an automated JEOL 733 Superprobe electron microprobe analyser. The trace elements analysed were Ca,Mg,Fe,Mn,Sr and Na.

The operating conditions used were 15 KV accelerating voltage ,30uA beam current and a 10-20um beam diameter. Details on the procedure, including detection limits are listed in Table 1 . The data was processed on line using modified JEOL software based on JASTRAN, with full ZAF corrections. From the list of analyses, the distribution of Sr, Mg, Mn and Fe were plotted and interpreted.

Details of quantitative analysis using the JEOL 733 Superprobe microanalyser.

Accelerating voltage= 15 KV.　　　　Beam current=0.3000E-07[A]

| Element | Channel | Xal | Peak [mm] | Bgd+ [mm] | Bgd- [mm] | Detection limits [ppm] |
|---------|---------|-----|-----------|-----------|-----------|------------------------|
| CA | 2 | PET | 107.565 | 5 | 5 | 205 |
| MG | 1 | TAP | 107.515 | 5 | 5 | 70 |
| FE | 3 | LIF | 134.625 | 5 | 5 | 248 |
| MN | 3 | LIF | 146.150 | 5 | 5 | 195 |
| SR | 1 | TAP | 74.605 | 4 | 4 | 160 |
| NA | 1 | TAP | 129.475 | 5 | 5 | 90 |

No. of unknown sequences= 3

| Seq.No. | Element [s] | Peak time [sec] | Background time [sec] |
|---------|-------------|-----------------|-----------------------|
| 1 | Mg, Ca, Fe | 40 | 20 |
| 2 | Na, Mn | 80 | 30 |
| 3 | Sr | 80 | 40 |

The raw microprobe data is stored as computer output files and was too voluminous to be presented in the thesis but is available from the Department of Geology and Geophysics, University of Adelaide. Only microprobe analyses that had totals from 99% to 101% was used and therefore the total number of individual microprobe analyses used for any one component varied from 10 to 20 analyses points. The data generated from the microprobe analyses was collated and tabulated and is presented in the text.

# APPENDIX TWO

## OXYGEN AND CARBON ISOTOPE DETERMINATION

Samples analysed for stable oxygen and carbon isotope compositions included both whole rock as well as individual component samples of ooids and cements. Individual components were extracted from polished slices using a hand-held drill. About 20mg of sample was then reacted with 100% phosphoric acid at 25$^o$C for 24hrs in the case of calcite samples and 36hrs for dolomite samples. The CO2 gas generated was collected and its isotopic composition determined.

Measurement of isotopic ratios was done on a Micromass 602 mass-spectrometer and the commonly employed correction procedures were followed before obtaining a final Del value [ Craig 1957 ]. The isotopic ratios were expressed as "Del" values permil (parts per thousand) calculated with respect to the international standard (PDB) for both oxygen and carbon stable isotopes.

$$Del(x) = \frac{( Rx - Rstd )}{Rstd} \times 1000$$

where Rx = Isotopic ratio of sample (180/160 or 13C/12C).

Rstd = Isotopic ratio in the standard.

# APPENDIX THREE

## STRONTIUM ISOTOPE MEASUREMENT

Sample Preparation:

The samples selected for Sr isotope analysis were initially crushed to approximately 10 mesh size and the components hand separated under a binocular microscope. Any composite type component grains were rejected. Approximately 0.1g of the separated samples were then reacted with 0.1N HCL and left to react overnight. The samples were then centrifuged and the solutions decanted, leaving behind minor residues. A mixed spike of 85Rb + 84Sr was added and the Rb and Sr separated by passing through ion exchange columns using 1.0N and 2.5N HCL.


Isotope Measurement:

The Sr isotope measurements were done using a modified Thomson TSN 206 S mass spectrometer with a 30 cm radius of curvature, a Cary 401 vibrating reed electrometer, automatic peak switcher and a Hewlett Packard 5326 B digital voltmeter. All 87Sr/86Sr ratios were normalised to 8.3752 for 88Sr/86Sr. Twenty-four replicate analysis of the Eimer and Amend Sr standard gave 0.7080348±0.0000371 (2d).

The contribution of radiogenic strontium by 87Rb decay was neglected since the initial batch of 12 samples analysed had very low Rb concentration (0.5ppm). No correction was therefore made to the measured 87Sr/86Sr ratios for in situ radiogenic enrichment.

# REFRENCES

Allan, J.R. and Matthews, R.K.,1977, Carbon and oxygen isotopes as diagenetic and stratigraphic tools: Data from surface and subsurface of Barbados, West Indies: Geology, v.5, p.16-20.

Allan, J.R. and Matthews, R.K.,1982, Isotope signatures associated with early meteoric diagenesis: Sedimentology,v.29, p.797-818.

Anderson, T.F. and Arthur, M.A.,1983, Stable isotopes of oxygen and carbon and their application to sedimentologic and paleoenvironmental problems. In: Stable Isotopes in Sedimentary Geology, SEPM Short Course 10, Dallas, 1-1 to 1-151.

Assereto,R.,and Folk,R.L.,1976, Brick-like texture and radial rays in Triassic Pisolites of Lombardy, Italy: Sed.Geology,v.16,p.205-222.

Awramik,S.M.,1971, Precambrian columnar stromatolite diversity: reflection of metazoan appearance: Science, v.174, p.825-827.

Baker,P.A.,Gieskes,J.M.and Elderfield,H.,1982, Diagenesis of carbonates in deep-sea sediments- evidence from Sr/Ca ratios and interstitial dissolved Sr2+ data: Jour.Sed.Petrology,v.52, p.71-82.

Bambach,R.K.,Scotese,C.R.and Ziegler,A.M.,1980, Before Pangea: The geographies of the Palaeozoic world: Am.Sci., v.68,p.26-38.

Bathurst,R.G.C.,1968, Precipitation of ooids and other aragonite fabrics in warm seas. In: Recent Developments in Carbonate Sedimentology in Central Europe (ed.G.Muller and G.M.Friedman), Springer, Berlin, p.1-10.

Bathurst,R.G.C.,1971, Carbonate sediments and their diagenesis: Amsterdam, Elsevier,620p.

Bathurst,R.G.C.,1975, Carbonate sediments and their diagenesis: Amsterdam, Elsevier, 2nd ed. 658p.

Beeunas, M.A. and Knauth, L.P.,1985, Preserved stable isotopic signature of subaerial diagenesis in the 1.2-b.y. Mescal Limestone, central Arizona: Implications for the timing and development of a terrestrial plant cover: Bull.Geol.Soc.Am. v.96, p.737-745.

Biscaye,P.E. and Dasch,J.E.,1971, The rubidium,strontium-isotope system in deep-sea sediments: Argentine Basin: J.Geophys.Res., v.76, p.5087-5096.

Braithwaite,C.J.R.,1979, Crystal textures of recent fluvial pisolites and laminated crystalline crusts in Dyfed, South Wales: Jour. Sed. Petrology, v.49,p.181-194.

Brand,U.,and Veizer,J.,1980, Chemical diagenesis of a multicomponent carbonate system-1: Trace elements: Jour.Sed.Petrology,v.50,p.1219-1236.

Brand, U. and Veizer, J.,1981, Chemical diagenesis of a multicomponent carbonate system -2: Stable isotopes: J.sedim.Petrol.v.51, p.987-997.

Brand,U.,and Veizer,J.,1983, Origin of coated grains: Trace element constraints: In: Coated Grains (ed. T.M.Peryt), Springer, Berlin, p.9-25.

Bricker,O.P.,1971, Carbonate Cements: John Hopkins Univ.
    Studies in Geology No.19, 376p.

Burke, W.H., Denison, R.E., Hetherington, E.A., Koepnick,
    R.B.,Nelson, H.F. and Otto,J.B.,1982, Variation of sea-
    water 87Sr/86Sr throughout Phanerozoic time:
    Geology,v.10, p.516-519.

Carozzi,A.V.,1963, Half-moon oolites: Jour.Sed.Petrology,
    v.33, p.633-645.

Chafetz,H.S.,1979, Petrology of carbonate nodules from a
    Cambrian tidal inlet accumulation, Central Texas:
    Jour.Sed.Petrology, v.49, p.215-222.

Chaloner,W.G.,1970, The rise of the first land plants:
    Biological Reviews, v.45, p.353-377.

Chowdhury,A.N.and Moore,C.H.,1986, Diagenesis and
    dolomitization of Upper Smackover grainstones: East
    Texas Shelf (abstr): Abstr. 12th Int.Sedim.Congr.,
    Canberra, Australia, 1986, p.59.

Coats,R.P.,1965, Diapirism in the Adelaide Geosyncline:
    J.Aust.Petrol.Explor.Assoc., v.1965, p.98-102.

Coats,R.P.and Blisset,A.H.,1971, Regional and economic
    geology of the Mount Painter Province: Bull.geol.Surv.
    S.Aust., v.43, p.1-426.

Compston,W.,Crawford,A.F.and Bofinger,V.M.,1966, A
    radiometric estimate of the duration of sedimentation in
    the Adelaide Geosyncline, South Australia: J.Geol.Soc.
    Aust., v.13, p.229-276.

Conley,C.D.,1977, Origin of distorted ooliths and pisoliths:
    Jour.Sed.Petrology,v.47,p.554-564.

Cooper,J.A.and Compston,W.,1971, Rb-Sr dating within the Houghton Inlier, South Australia: J.Geol.Soc.Aust., v.17, p.213-219.

Cooper,J.A.,1975, Isotopic datings of the basement cover boundaries within the Adelaide "Geosyncline". In: Proterozoic Geology, Abstr. 1st Aust.Geol.Conv., Adelaide, 1975, Geol.Soc.Aust., p.12.

Cooper,M.R.,1977, Eustacy during the Cretaceous: it's implications and importance: Palaeogeogr. Palaeoclimatol.Palaeoecol., v.21, p.165-208.

Craig, H.,1957, Isotopic standards for carbon and oxygen and correction factors for mass spectrometer analysis of carbon dioxide: Geochim. cosmochim. Acta, v.12, p.133-149.

Craig, H.,1965, The measurement of oxygen isotope paleotemperatures. In: Stable Isotopes in Oceanographic Studies and Paleotemperatures (Ed. by E.Tongiorgi): pp. 3-24. Consiglio Nazionale delle Ricerche, Pisa.

D'Argenio,B.,De Castro,P.,Emiliani,C.and Simone,L.,1975, Bahamian and Apenninian limestones of identical lithofacies and age: Bull.Am.Assoc.Pet.Geol., v.59, p.524-530.

Daily,B.,1956, The Cambrian in South Australia: In: El Sistema Cambrico, Su Paleogeografia Y El Problema De Su Base (ed.Rodgers,J.), Int.geol.Cong., 20th Sess., Mexico, 2: p.91-147.

Daily,B.,1972, Aspects of carbonate sedimentation in the Cambrian of South Australia: Abstr. Joint Specialists Meetings, Canberra, Geol.Soc.Aust., C10-14.

Daily,B.,1973, Discovery and significance of basal Cambrian Uratanna Formation, Mount Scott Range, Flinders Ranges, South Australia: Search, v.4, p.202-205.

Dansgaard, W.,1964, Stable isotopes in precipitation: Tellus, v.16, p.436-468.

Dasch,J.E.,1969, Strontium isotopes in weathering profiles, deep-sea sediments and sedimentary rocks: Geochim.cosmochim. Acta., v.33, p.1521-1552.

Dasch,J.E. and Biscaye,P.E.,1971, Isotopic composition of strontium in Cretaceous-to-Recent pelagic foraminifera: Earth.Planet.Sci.Lett., v.11, p.201-204.

Davies,G.R.,1977, Former magnesian calcite and aragonite submarine cements in Upper Paleozoic reefs of the Canadian Arctic: A summary: Geology, v.5,p.11-15.

Davies,P.J.and Martin,K.,1976, Radial aragonite ooids, Lizard Island, Great Barrier Reef, Queensland, Australia: Geology, v.4, p.120-122.

Davies,P.J.,Bubela,B.and Ferguson,J.,1978, The formation of ooids: Sedimentology, v.25, p.703-730.

Dickson,J.A.D. and Coleman,M.L.,1980, Changes in carbon and oxygen isotope composition during limestone diagenesis: Sedimentology,v.27, p.107-118.

Dravis,J.,1979, Rapid and widespread generation of recent oolitic hardground an a high energy Bahamian platform, Eleuthera Bank, Bahamas: Jour.Sed.Petrology,v.49,p.195-208.

Emiliani, C.,1966, Isotopic paleotemperatures: Science, v.154, p.851-857.

Epstein,S.,1959, The variations of the 18O/16O ratio in nature and some implications. In: Researches in geochemistry (Ed. P.H.Abelson), Wiley, New York, p.217-240.

Fairbanks, R.G. and Matthews, R.K.,1978, The marine oxygen
 isotope record in Pleistocene coral, Barbados, West Indies:
 Quat. Res.v.10, p.181-196.

Fairchild,I.J.,1986, Palaeoclimatology, palaeoenvironments and
 diagenesis of late Precambrian carbonates from Spitsbergen
 and East Greenland (abstr): Abstr. 12th Int.Sedimentological
 Congress, Canberra, Australia, 1986, p.99.

Fanning,C.M.,Ludwig,K.R.,Forbes,B.G.and Preiss,W.V.,1986,
 Single and multiple grain U-Pb zircon analyses for the Early
 Adelaidean Rook Tuff, Willouran Ranges, South Australia:
 Geol.Soc.Aust., Abstr.No. 15, 8th Aust.Geol.Convention,
 Adelaide, 1986, p.71-72.

Faure,G.,Hurley,P.M. and Powell,J.L.,1965, The isotopic
 composition of strontium in surface water from the North
 Atlantic Ocean: Geochim.cosmochim.Acta., v.29, p.209-220.

Faure,G. and Powell,J.L.,1972, Strontium Isotope Geology:
 Springer, New York, N.Y., 188p.

Faure, G.,1977, Principles of Isotope Geology, New York, John
 Wiley & Sons, 464p.

Faure,G.,Assereto,R. and Tremba,E.L., 1978, Sr isotope
 composition of marine carbonates of Middle Triassic to Early
 Jurassic age, Lombardic Alps, Italy: Sedimentology, v.25,
 p.523-543.

Fischer,A.G.,1981, Climatic oscillations in the Biosphere. In:
 Biotic Crises in Ecological and Evolutionary Time
 (ed.M.Nitecki), Acad.Press, p.103-131.

Folk,R.L.,and Land,L.S.,1975, The Mg/Ca ratio and salinity: two
 controls over crystallization of dolomite:
 Amer.Assoc.Petroleum Geologists,Bull. v.59,p.60-69.

142

Friedman,G.M.,1964, Early diagenesis and lithification in carbonate sediments: Jour.Sed.Petrology, v.34, p.777-813.

Fritz,P.and Poplawski,S.,1974, 18O and 13C in the shells of freshwater molluscs and their environments: Earth.planet.Sci.Lett., v.24, p.91-98.

Garrels,R.M.and Christ,C.L.,1965, Solutions, Minerals and Equilibria: Harper Row, New York, 450p.

Garrett,P.,1970, Phanerozoic stromatolites: noncompetitive ecologic restriction by grazing and burrowing animals: Science, v.169, p.171-173.

Given,R.K.,and Wilkinson,B.H.,1985,Kinetic control of morphology, composition, and mineralogy of abiotic sedimentary carbonates: Jour.Sed.Petrology,v.55,p.109-119.

Gross,M.G.,1964, Varitions in the 18O/16O and 13C/12C ratios of diagenetically altered limestones in the Bermuda Islands: Jour.Geol., v.72, p.170-194.

Grotzinger,J.,and Read,J.F.,1983, Evidence for primary aragonite precipitation, lower Proterozoic (1.9Ga) Rocknest dolomite, Wopmay orogen, Northwest Canada: Geology,v.11, p.710-713.

Grover,G.,Jr.,1983, Paleoaquifer and deep burial related cements defined by regional cathodoluminescent patterns, Middle Ordovician carbonates, Virginia: Amer.Assoc.Petroleum Geologists Bull., v.67, p.1275-1303.

Haines,P.W.,1986, Sedimentology and palaeontology of the Late Precambrian Wonoka Formation, Flinders Ranges, South Australia: Ph.D. thesis (Unpubl), University of Adelaide.

Hallam,A., 1984, Pre-Quaternary sea-level changes: Annu.Rev. Earth.Planet.Sci., v.12, p.205-243.

Halley,R.B.,and Harris,P.M.,1979, Fresh-water cementation of a 1000-year-old oolite: Jour.Sed.Petrology,v.49,p.969-988.

Hambrey,M.J.and Harland,W.B.,1981, Earth's Pre-Pleistocene Glacial Record: Cambridge University Press, Cambridge.

Haslett,P.G.,1975, The Woodendinna Dolomite and Wirrapowie Limestone- two new lower Cambrian Formations, Flinders Ranges, South Australia: Trans.R.Soc.S.Aust., v.99, p.211-220.

Haslett,P.G.,1976, Lower Cambrian stratigraphy and sedimentology, old Wirrealpa Springs, Flinders Ranges, South Australia: University of Adelaide, Ph.D. thesis (Unpubl).

Hays,J.D. and Pitman,W.C., 1973, Lithospheric plate motion, sea-level changes and climatic and ecological consequences: Nature, v.246, p.16-22.

Heller,P.L.,Komar,P.D.and Pevear,D.R.,1980, Transport processes in ooid genesis: Jour.Sed.Petrology, v.50, p.942-952.

Hodgson,W.A.,1966, Carbon and oxygen isotope ratios in diagenetic carbonates from marine sediments: Geochim.cosmochim.Acta., v.30, p.1223-1233.

Holser,W.T.,Magaritz,M.and Clark,D.L.,1986, Carbon-isotope stratigraphic correlations in the late Permian: Am.Jour.Sci., v.286, p.390-402.

Hudson, J.D.,1977, Stable isotopes and limestone lithification: J.geol.Soc.Lond.v.133, p.637-660.

Hudson,J.D.and Coleman,M.L.,1978, Submarine cementation of the Scheck Limestone conglomerate (Jurassic, Austria): Isotopic evidence: N.Jb.Geol.Palaont.Mh., v.1978, p.534-544.

Hsu,K.,Oberhansli,H.,Gao,J.Y.,Shu,S.,Haihong,C.and Krahenbuhl,U.,1985, "Strangelove ocean" before the Cambrian explosion: Nature v.316, p.809-811.

Illing,L.V.,1954, Bahamian calcareous sands: Bull.Am.Assoc.Pet. Geol., v.38, p.1-95.

Irwin, H., Curtis, C.D. and Coleman, M.L.,1977, Isotopic evidence for source of diagenetic carbonates formed during burial of organic-rich sediments: Nature, v.269, p.209-213.

James,N.P.,and Ginsburg,R.N.,1979, The seaward margin of Belize barrier and atoll reefs: International Association of Sedimentologist Special Publication No.3,199p.

James,N.P.,and Klappa,C.F.,1983, Petrogenesis of early Cambrian reef limestones, Labrador, Canada: Jour.Sed.Petrology,v.53, p.1051-1096.

James,N.P.,and Choquette,P.W.,1983,Diagenesis 6. Limestones-The sea floor diagenetic environment: Geoscience Canada,v.10,p.162-180.

Jenkins,R.J.F.,1981, The concept of an "Ediacaran Period" and its stratigraphic significance in Australia: Trans.R.Soc.S.Aust., v.105, p.179-194.

Jenkins,R.J.F.,1986, The early environment: In: Animal Life without Oxygen, C.Bryant (Ed.), Croom Helm, Neatherlands, (in press).

Johns,R.K.,1968, Geology and mineral resources of the Andamooka-Torrens area: Bull.Geol.Surv.S.Aust., v.41, p.7-103.

Kahle,C.F.,1974, Ooids from Great Salt Lake, Utah, as an analogue for the genesis and diagenesis of ooids in marine limestones: Jour.Sed.Petrology, v.44, p.30-39.

Katz,A.,Sass,E.,Starinsky,A.and Holland,H.D.,1972, Strontium behaviour in the aragonite-calcite transformation: An experimental study at 40-98C: Geochim.cosmochim.Acta., v.36, p.481-496.

Katz,A.and Matthews,A.,1977, The dolomitization of CaCO3: an
experimental study at 252-295 C: Geochim.cosmochim.Acta.,
v.41, p.297-308.

Keith,M.L.and Weber,J.N.,1964, Carbon and oxygen isotopic
composition of selected limestones and fossils:
Geochim.cosmochim.Acta., v.28, p.1787-1816.

Kendall,A.C.,1977, Fascicular-optic calcite: a replacement of
bundled acicular carbonate cements: Jour.Sed.Petrology,
v.47, p.1056-1062.

Kendall,A.C.,1985, Radiaxial fibrous calcite: A reappraisal:
In: Carbonate Cements, Schneidermann,N.,and
Harris,P.M.,(eds.),Society of Economic Paleontologist and
Mineralogist Special Publication No.36,p.59-77.

Kendall,A.C.and Tucker,M.E.,1973, Radiaxial fibrous calcite: a
replacement after acicular carbonate: Sedimentology, v.20,
p.365-389.

Kendall,A.C.,and Broughton,P.L.,1978, Origin of fabrics in
speleothems composed of columnar calcite crystals:
Jour.Sed.Petrology,v.48,p.519-538.

Kettenbrink,E.C.,and Manger,W.L.,1971, A deformed marine
pisolite from the Plattsburg Limestone (Upper Pennsylvanian)
of southeastern Kansas: Jour.Sed.Petrology,v.41,p.435-443.

Kinsman,D.J.J.,1969, Interpretation of Sr2+ concentrations in
carbonate minerals and rocks: Jour.Sed.Petrology,v.39,p.486-
508.

Knoll,A.H.,Hayes,J.M.,Kaufman,A.J.,Swett,K.and Lambert,I.B.,
1986, Secular variations in carbon isotope ratios from Upper
Proterozoic successions of Svalbard and East Greenland:
Nature, v.321, p.832-838.

Knoll,A.H.,1986, Sauk sequence carbonates: The global
sedimentary geology program, Report of an International
Workshop, Fisher Island, Florida, August, 1986.

Koepnick,R.B.,Burke,W.H.,Denison,R.E.,Hetherington,E.A.,Nelson,
H.F.,Otto,J.B. and Waite,L.E., 1985, Construction of the
seawater 87Sr/86Sr curve for the Cenozoic and Cretaceous:
Supporting data: Chemical Geology (Isotope Geoscience
Section), v.58, p.55-81.

Krebs,W.,1969, Early void-filling cementation in Devonian fore-
reef limestones (Germany): Sedimentology, v.12, p.279-299.

Land, L.S., Behrens, E.W.,and Frishman, S.A.,1979, The ooids of
Baffin Bay, Texas: Jour.Sed.Petrology,v.49,p.1269-1298.

Land,L.S.,1980, The isotopic and trace element geochemistry of
dolomite: the state of the art: SEPM Spec.Publ. No.28, p.87-
110.

Lasemi,Z.and Sandberg,P.A.,1983, Recognition of original
mineralogy in ancient micrites: Am.Assoc.Petroleum
Geologists Bull., v.67, p.499-500.

Lemon,N.M.,1985,Physical modelling of sedimentation adjacent to
diapirs and comparision with the Late Precambrian Oratunga
breccia body in the Central Flinders Ranges, South Australia:
A.A.P.G.Bull.v.69,p.1327-1338.

Lippmann,F.,1973, Sedimentary Carbonate Minerals: Springer,
Berlin, 229p.

Lohmann,K.C.,and Meyers,W.J.,1977, Microdolomite inclusions in
cloudy prismatic calcites- a proposed criterion for former
high-magnesium calcites:Jour.Sed.Petrology,v.47,p.1078-1088.

Longman,M.W.,1980, Carbonate diagenetic textures from nearshore
diagenetic environments: Amer.Assoc.Petroleum
Geologists,Bull.,v.64.p.461-487.

147

Loreau,J.P.and Purser,B.H.,1973, Distribution and
    ultrastructure of Holocene ooids in the Persian Gulf. In:
    The Persian Gulf (ed.Purser,B.H.), Springer, Berlin, p.279-
    328.

Lorens,R.B.,1981, Sr,Cd,Mn and Co distribution coefficients in
    calcite as a function of calcite precipitation rate:
    Geochim.cosmochim.Acta. v.45, p.553-561.

Mackenzie,F.T.,and Piggot,J.D.,1981, Tectonic controls of
    Phanerozoic sedimentary rock cycling: Jour.Geol.Soc.London,
    v.138,p.183-196.

Magaritz, M.,1983, Carbon and oxygen isotope composition of
    recent and ancient coated grains. In: Coated Grains (Ed. by
    T.M.Peryt), Springer-Verlag, Berlin, Heidelberg, pp. 27-35.

Magaritz, M., Holser, W.T., and Kirschvink, J.L.,1986, Carbon-
    isotope events across the Precambrian/Cambrian boundary on
    the Siberian Platform: Nature, v.320, p.258-259.

Marshall, J.D.,1981, Zoned calcites in Jurassic ammonite
    chambers: trace elements, isotopes and neomorphic origin:
    Sedimentology, v.28, p.867-887.

Marshall,J.F.and Davies,P.J.,1975, High-magnesian calcite ooids
    from the Great Barrier Reef: Jour.Sed.Petrology, v.45,
    p.285-292.

Martin, G.D., Wilkinson, B.H. and Lohmann, K.C.,1986, The role
    of skeletal porosity in aragonite neomorphism- strombus and
    montastrea from the Pleistocene Key Largo Limestone,
    Florida: J.sedim.Petrol.56, p.194-203.

Mason,M.G.,Thomson,B.P.and Tonkin,D.G.,1978, Regional
    stratigraphy of the Beda Volcanics, Backy Point Beds and
    Pandurra Formation on the southern Stuart Shelf, South
    Australia: South Aust.Geol.Surv.Q.Geol.Notes, v.66, p.1-9.

Mawson,D.and Sprigg,R.C.,1950, Subdivisions of the Adelaide
System: Aust.J.Sci., v.13, p.69-72.

Mayall,M.J.,1986, Deposition and diagenesis of Miocene
limestones, Senkang Basin, Sulawesi, Indonesia (abstr):
Abstr. 12th Int.Sedim.Congr., Canberra, Australia, 1986,
p.205.

Mazzullo,S.J.,1980, Calcite pseudospar replacive of marine
acicular aragonite and implications for aragonite cement
diagenesis: Jour.Sed.Petrology, v.50, p.409-422.

Medwedeff,D.A.and Wilkinson,B.H.,1983, Cortical fabrics in
calcite and aragonite ooids. In: Coated Grains
(ed.T.M.Peryt), Springer, Berlin, p.109-115.

Meyers,W.J.,1974, Carbonate cement stratigraphy of the Lake
Valley Formation, Mississipian, Sacremento Mountains, New
Mexico: Jour.Sed.Petrology, v.44, p.837-861.

Meyers, W.J. and Lohmann, K.C.,1985, Isotope geochemistry of
regionally extensive calcite cement zones and marine
components in Mississippian limestones, New Mexico. In:
Carbonate cements (Ed. by N.Schneidermann & P,M.Harris),
SEPM Spec.Publ.36, pp.223-239.

McIntire,W.L.,1963, Trace element partition coefficients- a
review of theory and application to geology:
Geochim.cosmochim.Acta., v.27, p.1209-1264.

Milliman,J.D.and Barreto,H.T.,1975, Relict magnesian calcite
oolite and subsidence of the Amazon shelf: Sedimentology,
v.22, p.137-145.

Moore,C.H.,1985, Upper Jurassic subsurface cements: A case
history. In: Carbonate cements (Ed. by N.Schneidermann &
P.M.Harris), SEPM Spec.Publ.36, pp.291-308.

Morrow,D.W.and Mayers,I.R.,1978, Simulation of limestone

   diagenesis- a model based on strontium depletion:

   Can.J.Earth.Sci., v.15, p.376-396.

Mottl,M.J.and Holland,H.D.,1978, Chemical exchange during

   hydrothermal alteration of basalt by seawater:

   Geochim.cosmochim.Acta., v.42, p.1103-1115.

Newell,N.D.,Purdy,E.G.and Imbrie,J.,1960, Bahamian oolitic

   sand: J.Geol., v.68, p.481-497.

Palmer,M.R. and Elderfield,H.,1985, Sr isotope composition of

   sea-water over the past 75 Myr: Nature, v.314, p.526-528.

Peterman,Z.E.,Hedge,C.E. and Tourtelot,H.A., 1970, Isotopic

   composition of strontium in sea-water throughout Phanerozoic

   time: Geochim.cosmochim.Acta., v.34, p.105-120.

Pingitore,N.E.,1976, Vadose and Phreatic diagenesis: processes,

   products and their recognition in corals:

   Jour.Sed.Petrology, v.46,p.985-1006.

Pingitore,N.E.,1978, The behaviour of Zn2+ and Mn2+ during

   carbonate diagenesis: Theory and applications:

   Jour.Sed.Petrology,v.48,p.799-814.

Pitman,W.C.,1978, Relationship between eustacy and

   stratigraphic sequences of passive margins:

   Geol.Soc.Am.Bull. v.89, p.1389-1403.

Preiss,W.V.,1971, The biostratigraphy and paleoecology of South

   Australian Precambrian stromatolites: Ph.D. thesis,

   University of Adelaide.

Preiss,W.V.,1977, The biostratigraphic potential of Precambrian

   stromatolites: Precambrian Res., v.5, p.207-219.

Prezbindowski,D.R.,1985, Burial cementation- is it important? A case study, Stuart City Trend, South Central Texas. In: Carbonate cements (Ed. by N.Schneidermann & P.M.Harris), SEPM Spec.Publ.36, pp.241-264.

Radwanski,A.and Birkenmajer,K.,1977, Oolitic/pisolitic dolostones from the Precambrian of south Spitsbergen: their sedimentary environment and diagenesis: Acta.geol.Polonica, v.27, p.1-39.

Rich,M,1982, Ooid cortices composed of neomorphic pseudospar: possible evidence for ancient originally aragonitic ooids: Jour.Sed.Petrology, v.52, p.843-847.

Richter,D.K.,and Fuchtbauer,H.,1978, Ferroan calcite replacement indicates former magnesian calcite skeletons: Sedimentology,v.25,p.843-861.

Richter,D.K.,and Besenecker,H.,1982,Subrecent thermal ooids with tangentially oriented high-Sr aragonite (Tekke Ilica/Turkey): in Peryt,T.,ed.,Coated Grains:Heidelberg, Springer-Verlag,p.154-162.

Richter,D.K.,1983,Calcareous ooids: a synopsis: in Peryt, T.,ed.,Coated Grains:Heidelberg, Springer-Verlag,p.71-99.

Rutland,R.W.R.,1973, Tectonic evolution of the continental crust of Australia. In: Continental Drift, Sea Floor Spreading and Plate Tectonics: Implications to the Earth Sciences (Ed.D.H.Tarling and S.H.Runcorn), Academic Press, London, p.1003-1025.

Rutland,R.W.R.,1977, Proterozoic platforms and mobile belts (Abstr.): 48th ANZAAS Congr. Melbourne.

Rutland,R.W.R.,1981, Structural framework of the Australian Precambrian: In: Precambrian of the Southern Hemisphere, Hunter,D.R. (ed.),p.1-32.

Rutland,R.W.R.,Parker,A.J.,Pitt,G.M.,Preiss,W.V.and
Murrel,B.,1981, The Precambrian of South Australia: In:
Precambrian of the Southern Hemisphere, Hunter,D.R. (ed.),
p.309-360.

Sandberg,P.A.,1975, New interpretation of Great Salt Lake ooids
and of ancient non-skeletal carbonate mineralogy:
Sedimentology,v.25,p.673-702.

Sandberg,P.A.,and Hudson,J.D.,1983, Aragonite relic
preservation in Jurassic calcite-replaced bivalves:
Sedimentology,v.30,p.879-892.

Sandberg,P.A.,1983, An oscillating trend in Phanerozoic non-
skeletal carbonate mineralogy: Nature,v.305,p.19-22.

Sandberg,P.A.,1985, Aragonite cements and their occurrence in
ancient limestones: in Carbonate Cements, Schneidermann,N.,
and Harris,P.M. (eds.),Society of Economic Paleontologists
and Mineralogists Special Publication No.36,p.33-58.

Schneidermann,N.,1970, Genesis of some Cretaceous carbonates in
Israel: Israel Jour.Earth Sci., v.19, p.97-115.

Schidlowski,M.,Eichmann,R.and Junge,C.E.,1975, Precambrian
sedimentary carbonates: Carbon and oxygen isotope
geochemistry and implications for the terrestrial oxygen
budget: Precambrian Res. v.2,p.1-69.

Scholle,P.A.and Arthur,M.A.,1980, Carbon isotope fluctuations
in Cretaceous pelagic limestones: Potential stratigraphic
and petroleum exploration tool: Am.Assoc.Petroleum
Geologists Bull., v.64, p.67-87.

Shackelton, N.J. and Kennett, J.P.,1975, Paleotemperature history of the Cenozoic and the initiation of Antarctic glaciation: oxygen and carbon isotope analyses in DSDP sites 277, 279, and 281. In: Kennett, J.P. & Houtz, R.E., eds., Initial Reports of the Deep-Sea Drilling Project, XXIX, U.S. Govt. Printing Office, Washington, v. XXIX, pp. 743-755.

Shearman,D.J.,Twyman,J.,and Karimi,M.Z.,1970, The genesis and diagenesis of oolites: Geol.Assoc.Proc., v.81, p.561-576.

Simone,L.,1972, Pluristadial ooids in the uppermost Jurassic-Lr.Cretaceous carbonates of the Apennines: 5th Meeting of Carbonate Sedimentologists, Liverpool, 1972.

Simone,L.,1981, Ooids: A review: Earth.Sci.Rev., v.16, p.319-355.

Singh, U.,1986, Ooids and cements from the Late Precambrian of the Flinders Ranges, South Australia: Jour.Sed.Petrology ( in the press ).

Sorby,H.C.,1879, The structure and origin of limestones: Proc. geol.Soc.London, v.35, p.56-95.

Sprigg,R.C.,1952, Sedimentation in the Adelaide Geosyncline and the formation of the continental terrace. In: Sir Douglas Mawson Anniversary Volume (Ed.M.F.Glaessner and R.C.Sprigg), University of Adelaide, p.153-159.

Steinen,R.P.,1978, On the diagenesis of lime mud: Scanning electron microscopic observations on subsurface material from Barbados, W.I.: Jour.Sed. Petrology, v.48, p.1139-1147.

Stueber, A.M., Pushkar, P. and Hetherington, E.A.,1984, A strontium isotopic study of Smackover brines and associated solids, southern Arkansas: Geochim.cosmochim.Acta, v.48, p.1637-1649.

Thomson,B.P.,Coats,R.P.,Mirams,R.C.,Forbes,B.G.,Dalgarno,C.R. and Johnson,J.E.,1964, Precambrian rock groups in the Adelaide Geosyncline: a new subdivision: South.Aust.Geol.Surv.Q.Geol.Notes, v.9, p.1-19.

Thomson,B.P.,1966, The lower boundary of the Adelaide System and older basement relationships in South Australia: J.Geol.Soc.Aust., v.13, p.203-228.

Thomson,B.P.,1969, Precambrian basement cover- the Adelaide System. In: Handbook of South Australian Geology (Ed.L.W.Parkin) South Aust.Geol.Surv., Govt.Printer, Adelaide, p.49-83.

Thomson,B.P.,1970, A review of the Precambrian and lower Palaezoic tectonics of South Australia: Trans.R.Soc.S.Aust., v.94, p.193-221.

Thomson,B.P.,Daily,B.,Coats,R.P.and Forbes,B.G.,1976, Late Precambrian and Cambrian geology of the Adelaide Geosyncline and Stuart Shelf, South Australia: Excursion Guide No.33A, 25th Int.geol.Congr., Sdyney, 1976.

Thomson,B.P.,1980, Geological Map of South Australia, Scale 1:1,000,000. Geol.Surv.South Australia.

Towe,K.and Hemleben,C.,1976, Diagenesis of magnesian calcite: Evidence from miliolacean foraminifera: Geology, v.4, p.337-339.

Tucker,M.E.,1982, Precambrian dolomites: Petrographic and isotopic evidence that they differ from Phanerozoic dolomites: Geology,v.10,p.7-12.

Tucker,M.E.,1983, Sedimentation of organic-rich limestones in the Late Precambrian of Southern Norway: Precambrian Research,v.22,p.295-315.

Tucker,M.E.,1984, Calcitic, aragonitic and mixed calcitic-aragonitic ooids from the mid-Proterozoic Belt Supergroup, Montana: Sedimentology,v.5,p.627-644.

Tucker, M.E.,1986, Carbon isotope excursions in Precambrian/Cambrian boundary beds, Morocco: Nature, v.319, p.48-50.

Tucker,M.E.,1986b, Formerly aragonitic limestones associated with tillites in the late Proterozoic of Death Valley, California: Jour.Sed.Petrology, (in the press).

Vail,P.R., Mitchum,R.M., Todd,R.G., Widmier,J.M., Thompson,S., Sangree,J.B., Bubb,J.N. and Hatlelid,W.G.,1977, Seismic stratigraphy and global changes in sea-level: Am.Assoc.Pet.Geol.Mem. v.26, p.49-212.

Veevers,J.J.and McElhinny,M.W.,1976, The separation of Australia from other continents: Earth.Sci.Rev., v.12, p.139-159.

Veizer,J.and Demovic,R.,1973, Environmental and climatic controlled fractionation of elements in the Mesozoic carbonate sequences of the western Carpathians: Jour.Sed.Petrology, v.43, p.258-271.

Veizer,J.and Demovic,R.,1974, Strontium as a tool for facies analysis: Jour.Sed.Petrology, v.44, p.93-115.

Veizer,J. and Compston,W.,1974, 87Sr/86Sr composition of sea-water during the Phanerozoic: Geochim.cosmochim.Acta, v.38, p.1461-1484.

Veizer,J. and Compston,W.,1976, 87Sr/86Sr in Precambrian carbonates as an index of crustal evolution: Geochim.cosmochim.Acta, v.40, p.905-914.

Veizer, J. and Hoefs, J.,1976, The nature of O18/O16 and
   C13/C12 secular trends in sedimentary carbonate rocks:
   Geochim.cosmochim. Acta, v.40, p.1387-1395.

Veizer,J., Compston,W., Clauer,N. and Schidlowski,M.,1983,
   87Sr/86Sr in Late Proterozoic carbonates: evidence for a
   "mantle" event at ~900Ma ago: Geochim.cosmochim.Acta, v.47,
   p.295-302.

Veizer,J.,1983, Chemical diagenesis of carbonates: Theory and
   application of trace element technique. In: Stable Isotopes
   in Sedimentary Geology, SEPM Short Course No.10, Dallas,
   p.3-1 - 3-100.

Vidal,G,and Knoll,A.H.,1982, Radiations and extinctions of
   plankton in the late Proterozoic and early Cambrian: Nature,
   v.297, p.57-60.

Videtich,P.E.and Matthews,R.K.,1980, Origin of discontinuity
   surfaces in limestones: isotopic and petrographic data,
   Pleistocene of Barbados, West Indies: Jour.Sed.Petrology,
   v.50, p.971-980.

Videtich,P.E.,1985, Electron microprobe study of Mg
   distribution in recent Mg calcites and recrystallized
   equivalents from the Pleistocene and Tertiary:
   Jour.Sed.Petrology,v.55,p.421-429.

Wagner,P.D.and Matthews,R.K.,1982, Porosity preservation in the
   Upper Smackover (Jurassic) carbonate grainstone, Walker
   Creek field, Arkansas: Response of paleophreatic lenses to
   burial processes: Jour.Sed.Petrology, v.52, p.3-18.

Walls,R.A.,Mountjoy,E.W.and Fritz,P.,1979, Isotopic composition
   and diagenetic history of carbonate cements in Devonian
   Golden Spike reefs, Alberta, Canada: Geol.Soc.Am.Bull.,
   Pt.1, v.90, p.963-982.

Walls,R.A.,and Burrowes,G.,1985, The role of cementation in the
   diagenetic history of Devonian reefs, Western Canada: in
   Carbonate Cements, Schneidermann,N.,and Harris,P.M.,(eds.),
   Society of Economic Paleontologist and Mineralogist Special
   Publication No.36,p.185-220.

Walter,L.M.,1985, Relative reactivity of skeletal carbonates
   during diagenesis: Implications for diagenesis: in Carbonate
   Cements, Schneidermann,N.,and Harris,P.M.,(eds.),Society of
   Economic Paleontologist and Mineralogist Special Publication
   No.36,p.3-16.

Walter,M.R.,1976, Stromatolites, (M.R.Walter, ed.), Elsevier,
   Amsterdam.

Wardlaw,N.,Oldershaw,A.,and Stout,M.,1978, Transformation of
   aragonite to calcite in a marine gasteropod: Can.Jour.Earth
   Sci.v.15,p.1861-1866.

Warme,J.E.,and Schneidermann,N.,1983, Patch-reef cementation:
   Holocene of Enewetak Atoll and Jurassic of Morocco [abs.]:
   Amer.Assoc.Petroleum Geologist Bull.,v.67,p.566.

Webb,A.W.,Coats,R.P.,Fanning,C.M.,and Flint,R.B.,1983,
   Geochronological framework of the Adelaide Geosyncline:
   Symposium on the Adelaide Geosyncline-Sedimentary
   environments and tectonic settings, Geological Society of
   Australia abstracts No.10.p.7-9.

Wickman,F.W.,1948, Isotopic ratios: A clue to the age of
   certain marine sediments: J.Geol., v.56, p.61-66.

Wilkinson,B.H.and Landing,1978, "Egg-shell" diagenesis and
   primary radial fabric in calcitic ooids: Jour.Sed.Petrology,
   v.48, p.129-138.

Wilkinson,B.H.,Janecke,S.U.,and Brett,C.E.,1982, Low magnesian calcite marine cements in Mid-Ordovician hardgrounds from Kirkfield, Ontario: Jour.Sed.Petrology,v.52,p.47-57.

Wilkinson,B.H.,Buczynski,C.,and Owen,R.M.,1984, Chemical control of carbonate phases: Implications from Upper Pennsylvanian calcite-aragonite ooids of southeastern Kansas: Jour.Sed.Petrology,v.54,p.932-947.

Wilkinson,B.H.,Owen,R.M.,and Carroll,A.R.,1985, Submarine hydrothermal weathering, global eustasy,and carbonate polymorphism in Phanerozoic marine oolites: Jour.Sed.Petrology, v.55,p.171-183.

Wilkinson,B.H.,Smith,A.L.,and Lohmann,K.C.,1985, Sparry calcite marine cements in Upper Jurassic limestones of southeastern Wyoming:in Carbonate Cements, Schneidermann,N.,and Harris,P.M.,(eds.),Society of Economic Paleontologist and Mineralogist Special Publication No.36,p.169-184.

Wilkinson,B.H.and Given,R.K.,1986, Secular variation in abiotic marine carbonates: constraints on Phanerozoic atmospheric carbon dioxide contents and oceanic Mg/Ca ratios: Jour.Geol., v.94, p.321-333.

Zemann,J.,1969, Crystal chemistry. In: Handbook of Geochemistry v.1 (Ed.K.H.Wedepohl), Springer, Berlin, p.12-36.

Ziegler,A.M,Scotese,C.R.,McKerrow,W.S.,Johnson,M.E.and Bambach,R.K.,1979, Palaeozoic paleogeography: Ann.Rev.Earth Planet.Sci., v.7, p.473-502.

COPY OF PAGE PROOFS OF PUBLICATION IN PRESS WITH THE JOURNAL OF
SEDIMENTARY PETROLOGY.

# OOIDS AND CEMENTS FROM THE LATE PRECAMBRIAN OF THE FLINDERS RANGES, SOUTH AUSTRALIA[1]

U. SINGH
*Department of Geology and Geophysics*
*University of Adelaide*
*Box 498, G.P.O.*
*Adelaide, South Australia, 5001*

ABSTRACT: Both fabric and geochemical evidence suggest that the oolite units of the Late Precambrian Trezona Formation had both aragonitic and calcitic precursors. Ooids inferred to be originally aragonitic occur as ooid molds filled by blocky, ferroan calcite and as calcitized ooids of neomorphic spar. The former are occasionally deformed, forming irregular shapes, and the calcitized ooids have elevated Sr concentration of between 3,000 ppm to 5,000 ppm. Some of the interparticle cements associated with these ooids have high Sr concentrations of between 2,000 ppm–5,000 ppm. The fabrics of these cements include clear calcite mosaics and poikilotopic spar. The precursor mineralogy and genesis of these cements remain uncertain, and various possibilities are evaluated.

The majority of ooids have micritic and microsparitic fabrics with clear, sparry calcite replacing the central cortical parts of the ooids. The precursor mineralogy of these ooids is not interpretable with the confidence of the aragonitic ooids. In some of the micritic ooids the replacing spar has microdolomite inclusions. This might indicate a high-Mg calcite precursor, but the process responsible for the retention and concentration of the Mg is not known. The Sr content of these micritic ooids is between 600 and 1,500 ppm. The micritic ooids invariably have cloudy, bladed to subgranular isopachous cements with Sr content of 800–1,200 ppm.

## INTRODUCTION

It had been widely accepted that the abundant aragonite in Holocene sediments has mirrored the formation of carbonates in the geological past. Beginning with Sandberg (1975), these conventional ideas have increasingly been questioned. His work suggested that carbonate mineralogy through geologic time may not have remained constant, and he concluded that Paleozoic nonskeletal carbonates were mainly calcitic and that aragonite became abundant only in the Cenozoic. Later work by Mackenzie and Piggot (1981) showed essentially similar trends. There was, however, disagreement on the placement of the transition from calcite dominance to aragonite dominance. Sandberg (1975) placed the transition during the early to middle Cenozoic, but Mackenzie and Piggot (1981) placed it during the Carboniferous. However, later work by Sandberg (1983) has suggested a cycle of varying carbonate mineralogies throughout the Phanerozoic.

Tucker (1982) suggested that Precambrian marine waters may have been markedly different from those of the present day, and dominated by primary dolomite precipitation. Such shifts in mineralogy have been attributed to the possible change in the chemistry of the hydrosphere and atmosphere, the evolving biosphere, or a difference in precursor mineralogy.

Recent studies suggest the coexistence of aragonite and calcite nonskeletal components during deposition of ancient carbonates. Studies by James and Klappa (1983), Sandberg (1983), Rich (1982), Wilkinson et al. (1984), Grotzinger and Read (1983), and Tucker (1984) have put forth evidence for the coprecipitation of aragonite and calcite components during carbonate deposition of Precambrian (mid-Proterozoic), Cambrian, Mississippian, and Pennsylvanian age.

The present study is significant for two reasons. First, it looks at a section of ancient oolitic carbonates from which, compared to Phanerozoic ooids, very little is known. Second, it is the first such study of an Australian Precambrian carbonate sequence and should add to our understanding of Precambrian carbonate environments.

## GEOLOGICAL SETTING

The Trezona Formation is part of the Umberatana Group of glacigene and interglacial sediments that forms part of a thick sequence of sedimentary rocks, ranging from Late Precambrian (Adelaidean) to Cambrian in age, that make up the Adelaide "Geosyncline" (Rutland 1981). The glacigene sediments mark both the start and end of sedimentation during this interval of the Adelaidean. Based on radiometric data, the upper (Marinoan) glaciation is estimated to have occurred later than 724 Ma (Webb et al. 1983). The interglacial sediments are dominantly siltstones with local development of shallow-water carbonates formed around diapiric structural highs (Lemon 1985). The Trezona formation is such a sequence of shallow-water carbonates developed in the central Flinders Ranges.

The area chosen for this study is south of Blinman because the Trezona Formation is thickest and best developed here, and the sediments are relatively undeformed. Samples were collected from sections at Werta, Bulls Gap, and Enorama Creek (Fig. 1). The carbonate environments varied from subtidal barrier complexes to lagoonal and intertidal flats with extensive development of stromatolites (Preiss 1971). Ooid shoal bodies occur in all the sections studied, but are best developed adjacent to the diapiric structure at Bulls Gap. The environment of carbonate deposition became increasingly restricted during deposition of the Trezona Formation, and terminated with the onset of glacial and fluvioglacial conditions of the Elatina Formation.
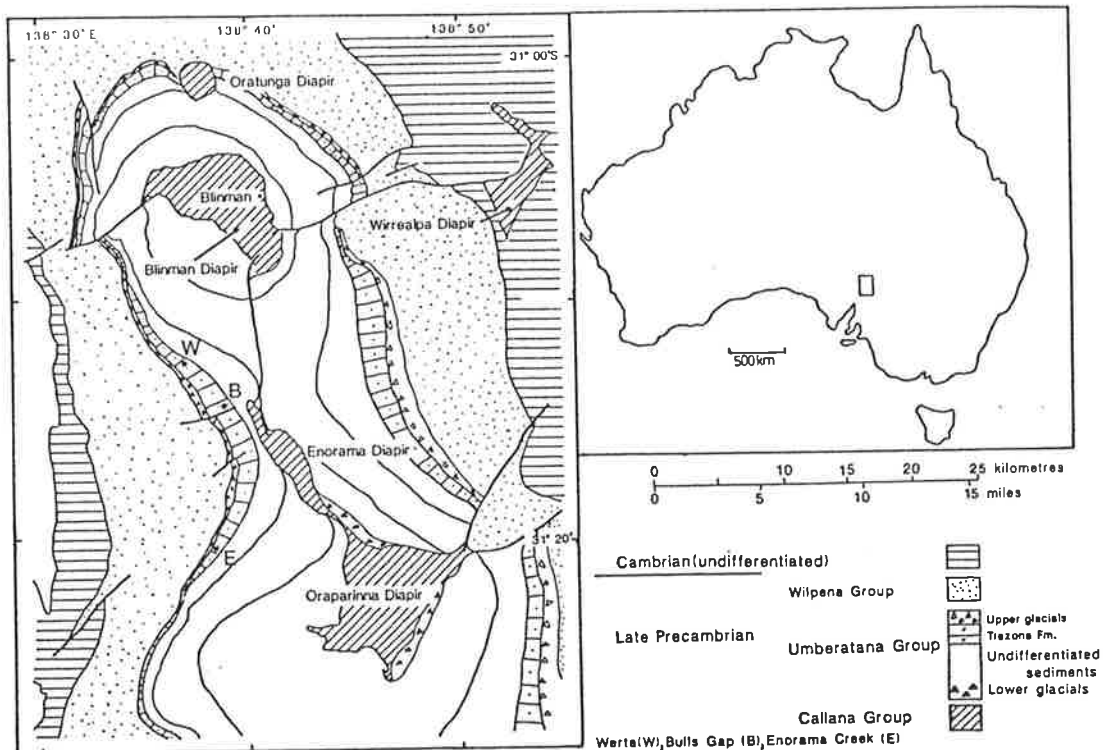
Fig. 1.—Location of study area and sample sites within the Trezona Formation (modified after Lemon 1985). Geology based on South Australia Dept. of Mines and Energy, 1:250,000 Parachilna sheet.

## ANALYTICAL TECHNIQUES

Samples selected for microanalysis were polished and carbon-coated. A total of 55 thin sections were studied, out of which 25 were selected for electron-probe analysis. Quantitative determination of trace-element composi-

TABLE 1.—*Details of quantitative analysis using the JEOL 733 Super-probe microanalyzer*

| Accelerating voltage = 15 kV. | | | | | Beam current = 0.3000E-07 (A) | |
|---|---|---|---|---|---|---|
| Element | Channel | Xal | Peak (mm) | Bgd+ (mm) | Bgd− (mm) | Detection Limits (ppm) |
| Ca | 2 | PET | 107.565 | 5 | 5 | 205 |
| Mg | 1 | TAP | 107.515 | 5 | 5 | 70 |
| Fe | 3 | LIF | 134.625 | 5 | 5 | 248 |
| Mn | 3 | LIF | 146.150 | 5 | 5 | 195 |
| Sr | 1 | TAP | 74.605 | 4 | 4 | 160 |
| Na | 1 | TAP | 129.475 | 5 | 5 | 90 |

Number of unknown sequences = 3

| Seq. No. | Element(s) | Peak Time (sec) | Background Time (sec) |
|---|---|---|---|
| 1 | Mg, Ca, Fe | 40 | 20 |
| 2 | Na, Mn | 80 | 30 |
| 3 | Sr | 80 | 40 |

tions of carbonate components was done on an automated JEOL 733 Superprobe electron microprobe analyzer. The trace elements analyzed were Ca, Mg, Fe, Mn, Sr, and Na.

The operating conditions used were 15 kV accelerating voltage, 30uA beam current, and a 10–20 $\mu$m beam diameter. Details on the procedure, including detection limits, are listed in Table 1. The data was processed on line using modified JEOL software based on JASTRAN, with full ZAF corrections. From the list of analyses, the distributions of Sr, Mg, and Fe were plotted and interpreted.

## BACKGROUND

Calcitic and Mg calcitic components, being relatively stable, retain their original fabrics during diagenesis. Metastable aragonitic components fail to retain any original fabrics during their transformation to stable calcite. Based on the diagenesis of skeletal and nonskeletal aragonitic components, a set of criteria have developed for evaluating original aragonitic mineralogy (Sandberg 1985). These include presence of coarse (relative to original aragonite) calcite mosaics irregularly cross-cutting original structure and containing relic inclusions, presence of aragonite relics, brownish nature of replacement spar, and elevated Sr content of replacement calcites. High-Mg cal-
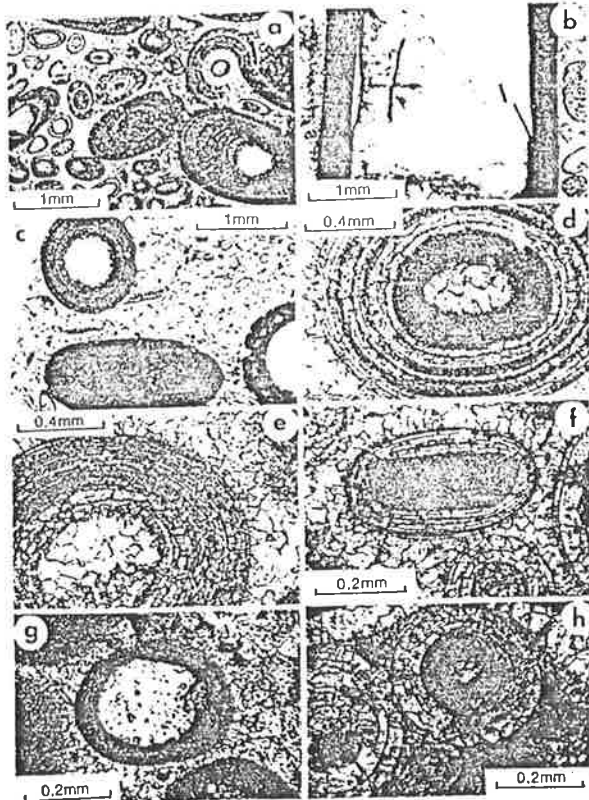
FIG. 2.—a) Both large and small ooids with well-developed micritic-concentric cortical fabrics designated as Type V and VII ooid fabrics. Large ooid in lower right corner has quartz grain with authigenic overgrowths as nucleus. The central cortical parts of some ooids have altered to coarse, blocky ferroan calcite Type C cement of text. b) Large Type V ooid with interior of blocky ferroan calcite and inward collapse of micritic cortical laminations. c) Large Type IV ooids with a "groundmass" of Type II ooids of void-filling calcite. Note asymmetrical shape of large ooid at bottom center. d) Large ooid with both sparry and micritic fabrics and blocky ferroan calcite core designated as Type VI ooid fabrics. e) Type X ooids with cortices of sparry, bricklike fabric made of brownish calcite and clear calcite in interparticle areas and ooid core. These ooid fabrics have elevated Sr content (ref. Fig. 7). f) Coated grain with the sparry bricklike fabric of Type X ooids and micritic nucleus. Associated are Type I ooids of neomorphic spar at bottom right and right. g) Type III ooid fabrics with spar-replaced interior. Note presence of rhomb-shaped inclusions in this replacement spar. h) Type I calcitized ooids of neomorphic spar under crossed nicols. Concentric cortical laminations are preserved as inclusions within the coarse calcite. Microprobe analysis revealed Sr content ranging from 3,000–5,000 ppm.

cite and low-Mg calcite components generally display little change during diagenesis, apart from possible increase in size or loss of Mg. However, recent studies have shown that aragonite has the same solubility as calcite with 12.5 mole % $MgCO_3$ (Walter 1985). The study by Walters (1985) also showed that under certain diagenetic settings, the microstructure can override the mineralogy and aragonite dissolution can precede the less stable Mg calcite. Evaluation of original ooid mineralogy based purely on
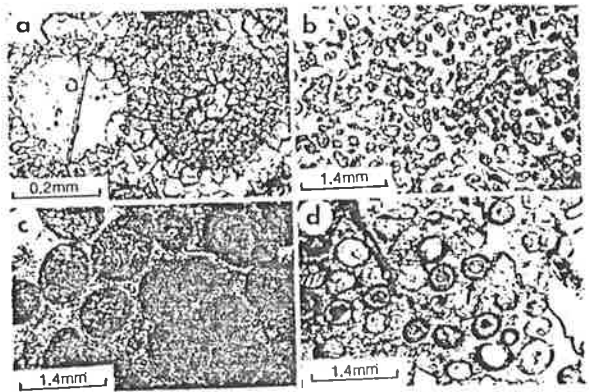


FIG. 3.—(a) Calcitized ooid of brownish calcite (Type I ooid fabric) adjacent to an ooid replaced by blocky ferroan calcite (Type II ooid fabrics). The interparticle cement is of Type B with its elevated Sr content (ref. Fig. 8). b) Type E poikilotopic calcite cement enclosing peloids. This cement has an Sr content between 2,000 and 5,000 ppm. c) Stained acetate peel of Type II and Type X ooid fabrics. The Type II fabrics are ferroan as are the nuclei of the Type X ooids. d) Ooid grainstone comprising Type IX ooids (arrow) and Type IV ooids.

fabric criteria is therefore fraught with uncertainty. A combination of fabric and geochemical data can make this task a little easier.

Chemical diagenetic trends in carbonates have been the subject of a number of studies over the years (e.g., Pingitore 1976, 1978; Brand and Veizer 1980). Based on the above cited studies, it is found that Sr and Na concentrations decrease and Mn and Fe concentrations increase with increasing diagenetic modification. Mg can increase or decrease, depending on the precursor mineral. Magnesium concentration of high-Mg calcite precursors decreases with increasing diagenesis. In spite of diagenesis, carbonate components can still retain some of their original geochemical signatures. This heterogenous distribution of trace elements among the various components is used as an aid in evaluating diagenetic history and precursor mineralogy.

### OOIDS

#### Ooid Fabrics

There is a large range of fabrics and sizes displayed by the ooids. Ooid diameters vary from 0.3 mm to 1.0 mm for the small ooids, and up to 10 mm or more (max. 16 mm) for the large ooids (pisoids). The types of fabrics observed are shown in Figures 2, 3, and 5. The large ooids have nuclei varying from 0.3 mm to 2 mm in diameter, with well-developed, concentric, cortical fabrics of micrite and microspar (Fig. 2a). The interiors of the large ooids are commonly made of clear, blocky ferroan calcite filling a void into which fragments of the micritic cortex sometimes collapsed and were preserved (Fig. 2b). The shapes of these large ooids generally tend to be elongate and asymmetrical, although occasionally spherical and symmetrical ooids are present (Fig. 2, a and c). Some of
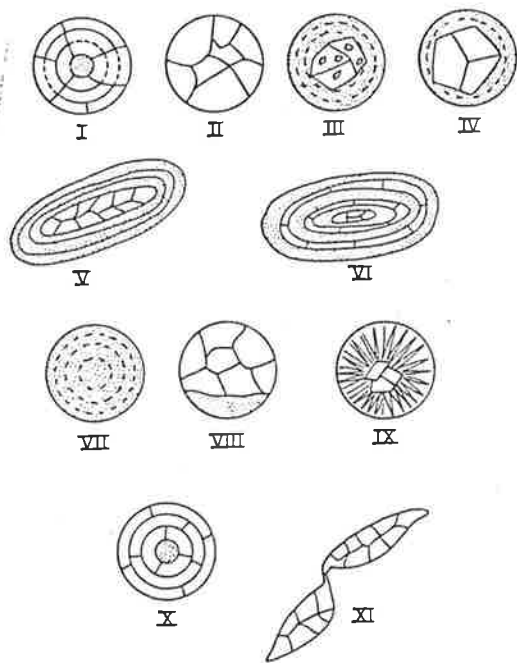
I—Coarse neomorphic spar ooids with relict inclusions

II—Ooid molds with void-filling blocky ferroan calcite

III—Micritic ooids with ferroan calcite cores and microdolomite

IV—Micritic ooids with ferroan calcite cores

V—As type IV but with asymmetrical shapes

VI—Ooids with both sparry brick-like and micrite calcite

VII—Micritic ooids

VIII—Half-moon ooids with micritic floors and void-filling ferroan calcite

IX—Ooids in-filled with drusy calcite mosaics

X—Sparry brick-like calcite ooids

XI—Deformed ooids in-filled with blocky ferroan calcite

FIG. 4.—Summary of various ooid fabrics in the Trezona Formation oolites.

micritic with no discernible cortical laminations. In contrast, some ooids display neomorphic fabrics with sparry cortices of coarse calcite with concentric cortical laminations preserved as inclusions (Fig. 2h). The calcite crystals of these sparry, neomorphic fabrics have a brownish color. Fibrous, nonferroan isopachous calcite mosaics are found infilling some small oomolds and are succeeded by blocky, ferroan calcites at ooid centers (Fig. 3d). Half-moon ooid fabrics with their micritic lower halves and sparry upper halves are present but rare (Fig. 5h). The various ooid fabrics have been summarized in Figure 4. In all ten different ooid fabric types, I to X were identified. The following section on ooid geochemistry makes reference to these ooid types described in Figure 4.

## Ooid Geochemistry

The trace-element chemistry of the various ooid and cement fabrics, when plotted, fall into distinct fields with few overlaps (Figs. 7 and 8). Ooid fabrics of Type I and X have elevated Sr concentrations that are higher by an order of magnitude than Type II, III, and IV fabrics (Fig. 7). Type I fabric has the highest Sr and lowest Mg concentration, with a Fe concentration comparable to the blocky ferroan calcites of Type II fabrics. The sparry Type X ooid fabric has a lower Fe content, similar to that of the micritic Type VII fabric. The trace-element chemistry of Type II, III, and IV fabrics cluster with large overlaps. Broadly, the trace-element chemistry of Type I and that of Types II, III, IV, and VII fabrics represent two end members, while the chemistry of Type X fabrics is intermediate.

## Ooid Fabrics Interpretation

Most of the ooid fabrics have been described by other workers studying Phanerozoic ooids (Sandberg 1975; Wilkinson et al. 1984) and Precambrian ooids (Tucker 1984). Type I ooid fabrics representing calcitized ooids of neomorphic spar, and the bricklike Type X fabrics are inferred to have been aragonitic originally (Fig. 2e and h). In Type I fabrics, the preservation of original, concentric cortical laminae as inclusions implies a neomorphic, fine-scale replacement process. The replacement spar comprises coarse, interlocking calcite crystals and has a brownish coloration. These fabrics have been described by Sandberg (1985) and are typical in calcite replacement of skeletal aragonite. In addition, the Type I ooid fabrics have elevated Sr concentrations, supporting the inference of aragonite replacement.

The Type X fabrics may result from the neomorphic alteration of an aragonite precursor and are identical to those described by Tucker (1984) and Assereto and Folk (1976). These Type X ooid fabrics also have elevated Sr concentrations, although they are not as high as those of the Type I fabrics. In both the Type I and X ooid fabrics, there is preservation of precursor relics, that is, inclusions in Type I fabrics and concentric cortical boundaries in Type X fabrics.

Type I and X ooid fabrics can normally be found within

the cortical layers are sparry and made of equant to subequant calcite crystals with a bricklike fabric (Fig. 2, d and e). Each "brick" in the fabric corresponds to an individual component calcite crystal.

Small ooids have some of the fabrics displayed by the large ooids and some fabrics that are unique. The small ooids are commonly micritic with sparry cores, or they occur as oomolds with blocky, ferroan calcite infills (Figs. 2g and 5b). Some oomolds clearly show an earlier generation of medium-crystalline calcite cement that lines the inner ooid margins and a later generation of coarsely crystalline calcite cement in the ooid centers (Fig. 5b). These spar-filled oomolds also display some irregular shapes with trunk-to-tail elephantine chains (fig. 5f). The sparry calcite of micritic ooid cores has irregularly distributed rhomb-shaped inclusions not found in the clear calcite in oomolds (Fig. 2g). Some small ooids are totally
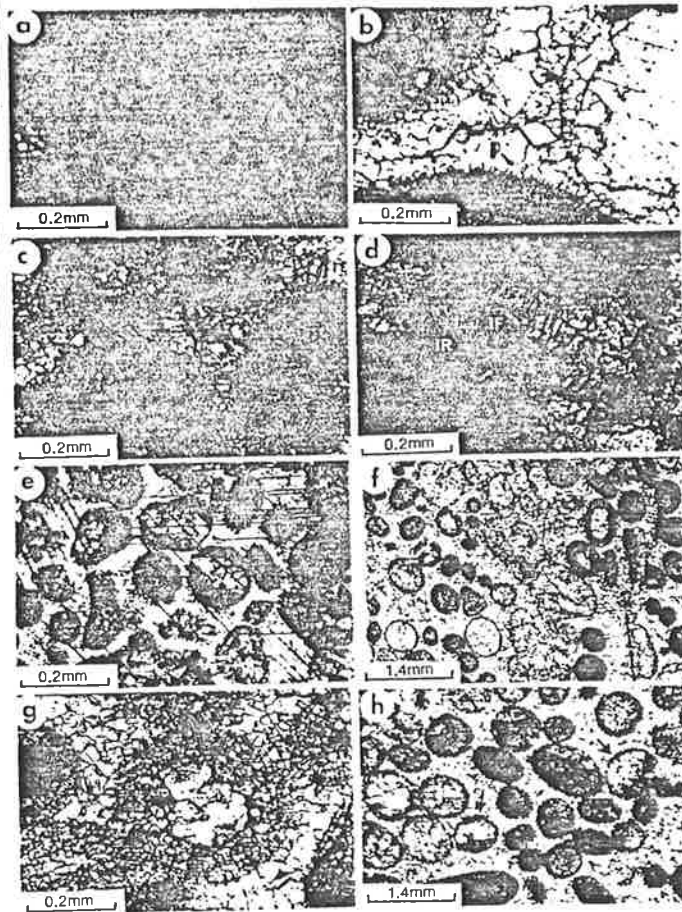
FIG. 5.—a) Acetate peel of Type A fibrous fringing cement and later-generation Type C blocky ferroan calcite cement. b) Interparticle Type B cements with fringe of prismatic (p) cement around ooids Ooid on right has been replaced by blocky ferroan calcite (Type II ooid). c) Sparry Type X ooids with clear Type B nonferroan blocky calcite in interparticle areas. This calcite cement has high Sr concentrations, ranging from 2,000–4,000 ppm. d) Type D calcite cement (IR) progressing into an inclusion-free (IF) phase (generally associated with ooid grainstones having ooid fabrics, suggesting calcitic precursors). e) Similar to Figure 3b, but with higher power objective. f) Distorted ooids with elephantine shapes associated with micritic ooids. g) Calcitized ooid of brownish calcite (Type I) being replaced by clear, blocky ferroan calcite. Note preservation of concentric cortical layers within the brownish calcite. h) Micritic and microsparitic ooids (Type VII) with half-moon ooid fabrics (Type VIII) in some (arrowed).

the same thin section and would therefore have been subjected to the same diagenetic environment. The reasons for generation of such different fabrics under essentially similar diagenetic conditions are unclear. The difference in the Sr content of these two calcitization fabrics may have been a reflection of the degree of interaction between the solution-films at reaction zones (calcitization frons) and the pore waters proper. This concept is explained in Pingitore (1976) and Brand and Veizer (1980). A "closed" diagenetic environment is one brought about by the presence of thin-solution films across diagenetic frons in static-water settings (vadose) (Pingitore 1976). The "open" diagenetic system results in mobile porewater settings (phreatic) where there is a high degree of interaction between the reaction frons and the main pore-

water body. The higher Sr and Fe of Type I ooids compared to Type X ooids would seem to suggest that Type X ooids may have been generated in shallow-meteoric settings and Type I ooids in deep-burial environments. However, Sandberg and Hudson (1983) found no difference in the calcitization fabrics in either of these two environments. Obviously, more empirical work on calcitization fabrics needs to be done.

In some cases ooid fabrics have a composite fabric in which the central cortical parts are composed of blocky ferroan calcite, similar to that of Type II ooids, and the remaining cortical envelope comprises the brownish neomorphic spar of Type I ooids (Figs. 3a and 5g). The chemistry of these two calcite types is also different, with the brownish neomorphic spar falling in the field of Type E

elements and the void-filling, blocky calcites in the field of Type C cements (Fig. 8).

Type II ooid fabrics composed of oomolds filled with clear, blocky ferroan calcite cements represent void-filling calcites (Fig. 5b). The lower Sr content of the Type II ooid fabrics suggest an "open" diagenetic environment. This "open" setting was the result of the voids in the form of oomolds that were subsequently filled by the blocky ferroan calcites. These voids would have had relatively mobile pore-water flow conditions that allowed easy exchange of cations during calcite precipitation (Pingitore 1976). Some of these spar-filled molds are deformed into irregular shapes (Fig. 5f) and are similar to those described by Kettenbrink and Manger (1971) and Conley (1977). They result from the early dissolution of aragonite in ooids and the subsequent collapse during burial. They normally have an outer rim of early calcite cements, thereby retaining the gross shape of the ooid subsequent to deformation.

There are some ooid fabrics that indicate presence of bimineralic cortices, that is, calcite and aragonite. These ooids, called half-moon ooid fabrics, have been interpreted by Carozzi (1963) as resulting from the dissolution of soluble or metastable elements in the ooid cortex and the collapse of the stable elements onto the ooid floor. The remaining cavity was later filled by calcite cement. The half-moon ooids in this study have probably formed in a similar fashion with the dissolution of aragonitic layers in the cortex (Fig. 5h).

Inference of the precursor mineralogy of the micritic and microsparitic Type V, VI, and VII ooid fabrics is problematic. Wilkinson et al. (1985, p.175) found micritic and microsparitic ooid fabrics to be of ambiguous origin. These fabrics can represent original equant calcitic nannograins forming ooid cortices, or micritized aragonitic or calcitic ooids. In view of these two possibilities, Type VI ooid fabrics are interesting. The cortical laminae of the ooids include both sparry, bricklike calcite (equivalent to Type X ooids) and micrite (Fig. 2d). The generation of the micritic cortical fabrics by micritization is unlikely because of the patchy and discontinuous distribution of individual micritic laminae. The sparry fabrics in such ooids have calcites with elevated Sr concentrations similar to the Type X ooid fabrics. The micritic laminae have comparatively lower Sr concentrations of between 600 and 1,500 ppm. Such high-Sr calcites are unlikely to be derived from micritic-calcitic ooids and are normally associated with calcites derived from transformation of aragonites (Assereto and Folk 1976; Davies 1977; Sandberg and Hudson 1983). One possibility is the existence of both calcite and aragonite cortical layers and their alteration to generate the fabrics in Type VI ooids. In such a case the sparry brick fabrics would represent the altered aragonite layers and the micritic fabrics the calcite layers. Alternatively, if these ooids are inferred to have been originally aragonitic, then the micritic and sparry cortical fabrics represent two different replacement products of aragonite. Such ooid fabrics have been described from Pleistocene marine oolites and from hot-spring ooids (Richter 1983; Richter and Besenecker 1982). In these

two settings, tangential-aragonitic ooids occur in various stages of transformation, from partially calcitized to completely calcitized and micritic/microsparitic forms. In both cases an aragonite precursor is inferred, either partially or totally making up the ooids. The bricklike fabric of some cortical layers and their high Sr content are evidence of this. Therefore, while it is not possible to explain adequately the Type VI ooid fabrics, it seems probable that an aragonite precursor had a part in the genesis.

In Type V and VII ooid fabrics, however, there is no such association of sparry and micritic cortical fabrics (Fig. 2a and c). In these two ooid fabrics, no clear evidence exists for determining the precursor mineralogy. The cortices are totally micritic. In both fabrics the micrites have comparatively low Sr concentrations, similar to the micrite in Type VI ooids (600–1,500 ppm). A precursor ooid made up of equant calcitic or Mg calcitic nannograins could generate such a fabric during diagenesis. However, algal micritization of original aragonite or calcite ooids can also generate similar fabrics. The void-filling calcite in some of the Type V ooid cores suggests/dissolution of a metastable element (aragonite) prior to precipitation of the ferroan calcite. In some cases, however, these sparry cores resemble sparry ferroan calcites within micritic cortical areas of similar ooids, possibly formed by aggrading neomorphism during burial diagenesis.

Ooid fabrics of Type III and IV were probably originally calcitic with the replacement spar being the result of aggrading neomorphism of the original micritic fabric. Such an interpretation is supported by the existence of ooids in various stages of neomorphism into spar, from some entirely micritic ooid fabrics to some entirely composed of sparry calcite. The comparatively high-Mg content of these replacement calcites with their microdolomite inclusions suggests Mg-enriched pore waters (Lohmann and Meyers 1977). The source of this Mg could have been intragranular or from external sources. An external source of the Mg is discounted because of the distribution of the microdolomite inclusions. They are confined to the ooids of Type III and IV fabrics. No microdolomite inclusions are found in similar ferroan calcites in interparticle cements. The fabric-specific occurrence of the microdolomite suggests some sort of local source for the Mg, probably a Mg calcite precursor. Also, ferroan calcites are common replacements of Mg calcite precursors (Richter and Fuchtbauer 1978). Lohmann and Meyers (1977) suggested the processes of solid-state exsolution and incongruent dissolution for the formation of microdolomite inclusions in calcite cements.

Solid-state exsolution results in the formation of two stable phases, dolomite and calcite, by solid-state diffusion. This process, however, proceeds at slow rates at diagenetic temperatures and is probably insignificant. Incongruent dissolution involves microscale dissolution of the precursor Mg calcite resulting in Mg enrichment of the solution film. This Mg enrichment presumably requires some sort of closed to semiclosed diagenetic environment. The processes involved and the factors responsible for this closure are not known. It is possible that local microstructural differences may have aided in

the formation of microdolomites and the large variation in Mg observed in these recrystallized ooids. Videtich (1985), in her study of Mg distribution during diagenesis, found that inclusion-rich areas had lower Mg than inclusion-rich areas of recrystallized limestones. This was attributed to the presence of higher microporosity and permeability in inclusion-rich areas and their subsequent faster dissolution-reprecipitation. The Mg-rich, inclusion-free areas, however, might undergo closed-system diagenesis, resulting in the formation of microdolomites. It is not clear which mechanism was responsible for the microdolomite in the present study.

Among the Type III and IV ooids are occasionally found Type IX ooids made up of fibrous calcite mosaics with micritic envelopes. The difference in the fabrics of these associated ooids probably indicates the difference in original mineralogy. The lack of collapse features among these Type IX ooids, despite evidence of pressure solution (Fig. 3d) indicates stabilization before significant burial. The nonferroan calcites of these ooid fabrics suggest absence of burial depths which normally produced ferroan calcites. It is inferred, therefore, that the fibrous calcites of Type IX ooids were formed at shallow depths, probably by dissolution of a metastable component (? aragonite). Their association with Type III and IV ooids implies the existence of both originally calcitic and aragonitic components, with the calcitic being dominant in these oolite units. Type IX ooids form a very small percentage of the total ooid population (less than 5%). The micritic envelopes in the Type IX ooids may have existed as original calcitic envelopes or as micritized aragonitic ooids. The essentially isopachous nature of this cement indicates a vadose type of environment although there was no evidence of vadose interparticle cements. Possibly they were present but have been overprinted by later phreatic cements. The clear ferroan cements found in the centers of some of these Type IX ooids represent the pore-occluding cementation stage during burial.

### CEMENTS

#### Cement Fabrics

Based on fabrics, spatial distribution, and ferroan-nonferroan nature, five different groups of cements are recognized.

*Type A.*—Isopachous, fibrous, fringing cements around depositional grains are nonferroan and record the earliest stage of cementation (Fig. 5a). They are the dominant interparticle cement around ooids and intraclasts in intercolumnar areas of stromatolite biostromes. In the ooid grainstones proper, however, they comprise less than ten percent of the total interparticle cements.

*Type B.*—This cement is also nonferroan and occurs as a bladed to granular form with anhedral crystal shapes. It is the dominant cement in the interparticle spaces (Fig. 5c). It generally has a brownish appearance similar to the calcite in Type I and X ooid fabrics. The shape of these calcites varies from bladed to granular forms (Fig. 5b). Crystals vary from 50–200 $\mu$m in size and are inclusion-



A—Fibrous isopachous cement

B—Non-ferroan equant calcite cement

C—Blocky ferroan calcite cement in oomolds

D—Inclusion rich(IR) subequant calcite cement grading into type C cement

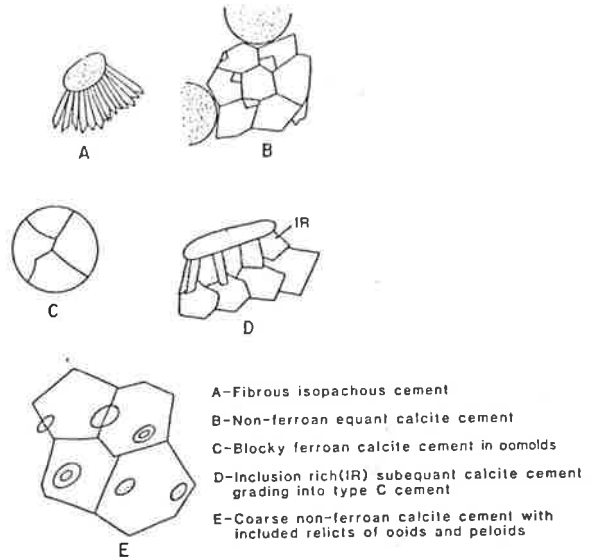E—Coarse non-ferroan calcite cement with included relicts of ooids and peloids

Fig. 6.—Summary of cement fabrics in the Trezona formation oolite

free. In some ooids this cement forms drusy calcite mosaics.

*Type C.*—This cement is a blocky ferroan calcite spar. It is the dominant component filling oomolds (Figs. 2c and g, 5b) and is composed of well-developed, subhedral to euhedral crystals, 1–0.13 mm in size. In interparticle spaces it represents the pore-occluding stage of cementation after Type A or B cements. In ooids with Type III and IV fabrics, the blocky, ferroan calcite has microdolomite inclusions. Blocky calcite is also present in fractures and veins and cross-cuts earlier cement phases. In ooid grainstones with large intraclastic populations fenestral voids are commonly filled with this blocky cement. In such cases the earlier cement is ferroan with nonferroan cement occupying pore centers.

*Type D.*—This cement is typically cloudy subequant or bladed calcite crystals. It is restricted to ooid grainstones that have Type III and IV ooid fabrics (Fig. 5d). This cement is nonferroan when stained but has occasional iron-rich phases within it. In large pores, this cement is followed by the pore-occluding Type C cement.

*Type E.*—This is a coarsely crystalline, nonferroan calcite mosaic containing relict ooids and peloidal grains (Fig. 5e). It has a characteristic brownish appearance similar to the Type B cements. There is no regular spatial relationship between the position of ooids and peloids and the crystal margins of the calcite mosaic. In some cases the peloidal grains occur in centers of calcite crystals, with the calcite resembling syntaxial growths around peloids. In others, the crystal margins cut across the peloids. Unlike the other cement fabrics described thus far, type E cements occur in association with a laminated limestone facies and not with ooid grainstones. This laminated limestone facies consists of alternating dark, micritic layers
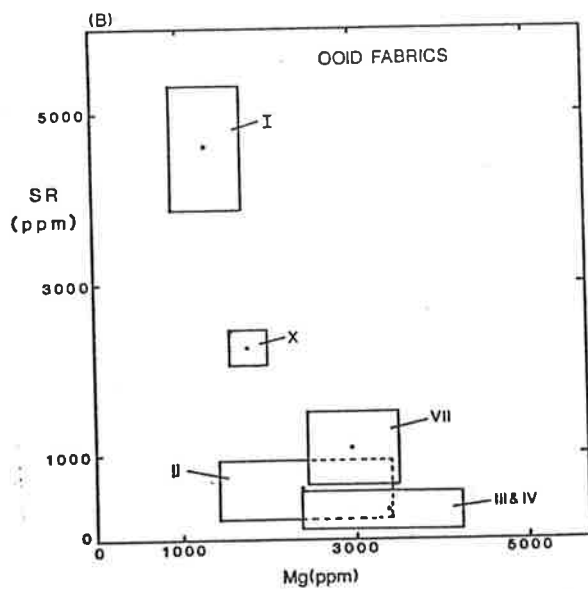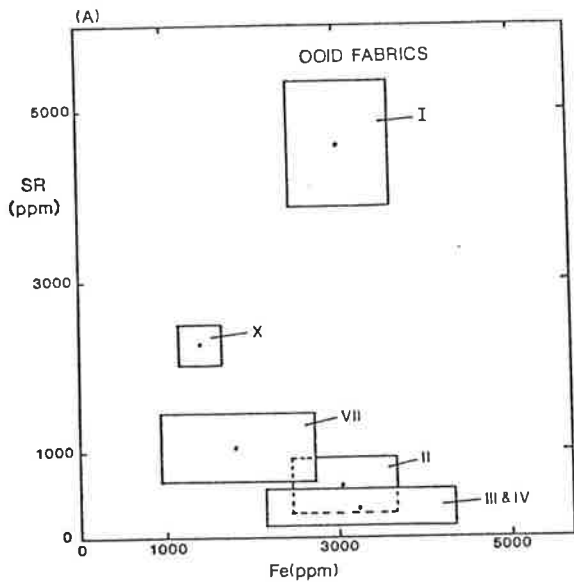
OOID FABRICS

SR (ppm)

5000

3000

1000

0

I

X

VII

II

III & IV

0    1000    3000    5000
Fe(ppm)

(B)

OOID FABRICS

SR (ppm)

5000

3000

1000

0

I

X

VII

II

III & IV

0    1000    3000    5000
Mg(ppm)

(A)

CEMENT FABRICS

SR (ppm)

5000

3000

1000

0

E

B

A

D

C

0    1000    3000    5000
Fe(ppm)

(B)

CEMENT FABRICS

SR (ppm)

5000

3000

1000

0

E

B

A

D

C

0    1000    3000    5000
Mg(ppm)

FIG. 7.—Trace-element chemistry of the various ooid fabrics determined with the electron microprobe. The fields of the ooid fabrics are defined by two standard deviations from the mean (2). The ooid fabric types correspond to those in Figure 4. The number of analyses (N) for each field varied from 10 to 50.
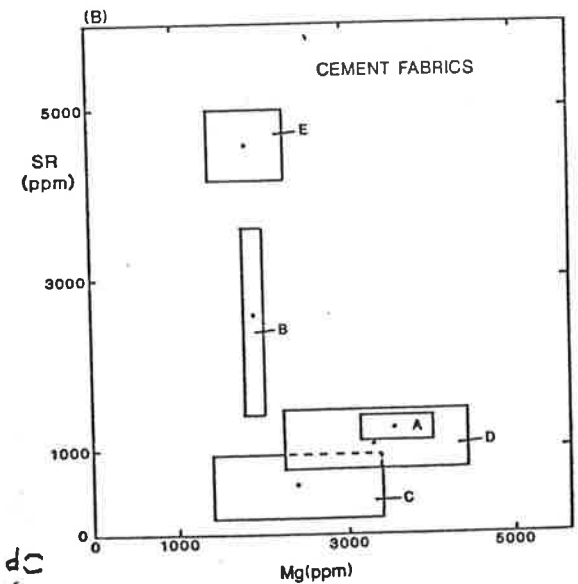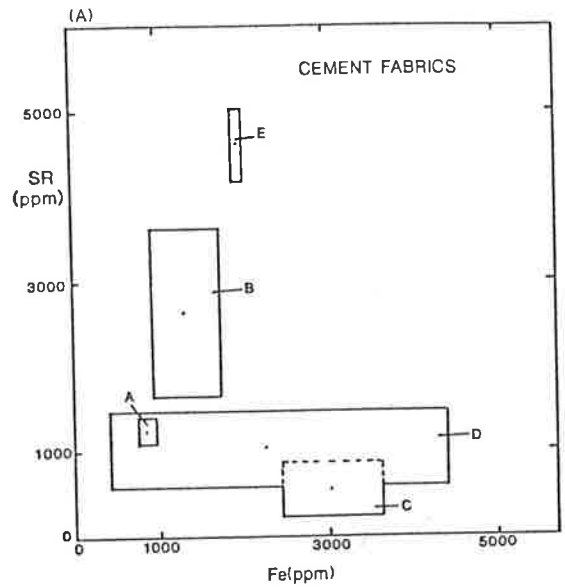
FIG. 8.—Trace-element chemistry of the various cement fabrics determined with the electron microprobe. The fields of the cement fabrics are defined by two standard deviations from the mean (2). The cement fabric types correspond to those in Figure 6. The number of analyses (N) for each field varied from 10 to 50.

and light, sparry layers (Type E cements). The various cement fabrics are summarized in Figure 6.

### Cement Geochemistry

The cements can also be separated into distinct groups based on trace-element chemistry (Fig. 8). Type E cement fabrics, with the highest Sr and lowest Mg concentrations, fall into the same category as Type I ooid fabrics. The similarity of Type C cements to Type II ooid fabrics occurs because the blocky ferroan calcites form the spar-filled Type II ooid fabrics. The Type A fibrous, isopachous cements and the inclusion-rich Type D cements have the same trace-element chemistry, but Type D cements have
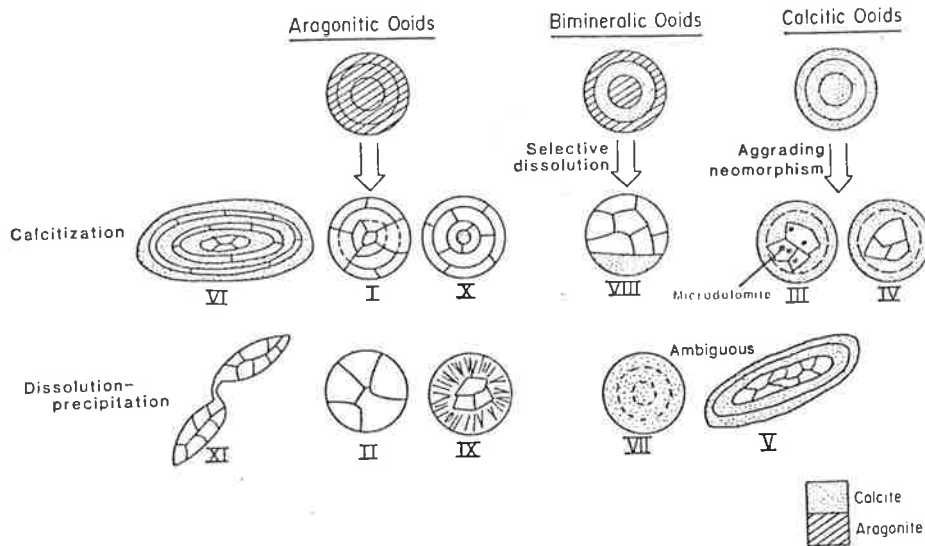
Fig. 9. — Schematic diagram of the inferred original ooid mineralogies and their replacement fabrics.

## Interpretation of Cement Fabrics

The cements associated with the oolite units record a wide range of diagenetic environments, from marine-phreatic to meteoric-phreatic and deep-burial. The Type A cements with their fibrous form and relatively Mg-enriched chemistry are inferred to represent marine-phreatic precipitates. Most modern-day marine cements form isopachous crusts of acicular crystals of aragonite or Mg calcite (Folk and Land 1975; Longman 1980; James and Choquette 1983). Precipitation of the Type A cements seems to be favored in areas of active-water circulation, such as the intercolumnar areas of stromatolitic buildups. The retention of a fibrous fabric and the absence of a coarse calcite replacement fabric tends to discount the possibility of Type A cements having an aragonite precursor. Both its fibrous form and high-Mg content suggest that the precursor was Mg calcite.

Type D cements, with their bladed calcites and inclusion-rich appearance, are also interpreted as marine-phreatic. Geochemically they encompass the field of the inferred marine Type A cements. The large variation in their Mg and Fe contents is due to the presence of these inclusions. These inclusions do not represent microdolomite phases but are trapped solids including clays and iron oxides. Such inclusion-rich calcites of marine origin are described in skeletal grainstones of Devonian reefs (Walls and Burrowes 1985). The clear, blocky, ferroan Type C cements represent the final phase of cementation and probably formed in the deep-phreatic burial environment.

The equant form and relatively clear appearance of the Type B and E cements is commonly interpreted to represent precipitation from meteoric-phreatic waters (Folk and Land 1975) or a result of burial diagenesis. However, such a relationship between crystal habit and pore-water chemistry is not strictly valid. Equant high-Mg calcites are known to form in Holocene shallow-marine environments (James and Ginsburg 1979; Warme and Schneidermann 1983) and fibrous, low-Mg calcites in meteoric-vadose environments (Braithwaite 1979; Kendall and Broughton 1978). Also, equant, blocky calcites are reported to form marine cements in Upper Jurassic (Wilkinson et al. 1985), and Ordovician limestones (Wilkinson et al. 1982).

Type B and E cements, however, have a very high Sr content (2,000–5,000 ppm), which is unlike normal diagenetic calcite cements (400–700 ppm) (Kinsman 1969). Such high Sr calcites have been inferred to represent aragonite replacements in previous studies (Wardlaw 1978; Davies 1977). But the fabrics of both Type B and E cements are unlike those commonly observed during calcitization (Sandberg 1985). Although both the Type E and B cements have high Sr content, Type B cements have a comparatively lower Sr content and are associated with ooid grainstones.

The constraints imposed by the geochemical and fabric data are of opposing nature. The geochemical data point to an aragonite precursor, but this is not supported by the fabric data. If there is an aragonite precursor involved, the fabrics of Type B and E cements certainly do not represent normal aragonite-calcite transformation. Could an aragonite precursor have been responsible in an indirect way for the high Sr content of these cements? The ooid-cement relationship does seem to suggest this for the Type B cements.

### Ooid-Cement Relations

An interesting association of inferred aragonitic ooids with high-Sr cements and calcitic ooids with low or "normal" Sr cements is found in the ooid grainstones. Whenever ooids with aragonite replacement fabrics were present, the interparticle cements were of Type B, described above. Where there was no evidence for the presence of aragonite-replacement fabrics in ooids, the interparticle cement was of Type D. It is common to find oolite units with both calcitic and aragonitic precursor ooids coexisting as well as those with only calcitic precursor ooids. The reasons for shifts in precipitation of Mg calcite and aragonite in sea water are unclear. Situations where both aragonite and Mg calcite are precipitated in modern marine settings as cements and ooids are known (James and Ginsburg 1979; Land et al. 1979). The influence of organics and kinetic controls is possibly important (Given and Wilkinson 1985).

Possibly the coexistence of high-Sr cements with inferred aragonitic ooids may be related to the diagenetic alteration of these ooids. During the transformation of the aragonite ooids, pore waters would have high Sr concentrations, which could then result in the precipitation of high Sr cements similar to the Type B cements. Such elevated Sr concentrations in pore waters have been observed in modern oolites undergoing meteoric diagenesis (Halley and Harris 1979). Obviously, such a diagenetic environment would have to be, essentially, a closed chemical system.

Such an explanation would not explain the Type E cement fabrics, since there is a lack of such aragonite replacement ooids with the Type E cements. The Type E cements are very similar to the calcite laminae fabrics described by Tucker (1983, p. 301–303 and his fig. 8a and b). His cements are also associated with a laminated limestone facies, which is organic-rich. Based on the very high Sr content of his carbonates and the occurrence of ooid grainstones (within the same formation) with aragonite replacement fabrics, he inferred an aragonite precursor for the laminated limestone facies. Tucker (1983) made no mention of any calcitized fabrics or of textural evidence supporting aragonite replacement. While the type B cement fabrics are unlikely to be replacements of aragonite, the Type E cement fabrics certainly are not typical of calcite cements. Although Type E cements are void-filling cements, they do not have the typical features of crystal growth from pore margins and drusy crystal mosaics (Bathurst 1975). With the evidence in hand, a proper interpretation of the genesis of these cements is not possible. Although the geochemical data suggest an aragonite precursor, this is not supported by the textural data. Alternatively, it may be possible that the Type E cement fabrics did have an aragonite precursor and the resulting fabrics are atypical of the commonly observed calcitization fabrics.

### SUMMARY

1) Evidence for the precipitation of aragonite and calcite ooids during the Late Precambrian is found in the Trezona Formation carbonates. The ooids inferred to have been originally aragonitic are made of coarse interlocking mosaics of calcite with a brownish coloration. Some of these coarse replacement calcites have cortical laminations preserved as inclusions. These calcites have elevated Sr concentrations of between 3,000 ppm and 5,000 ppm. The ooids inferred to have been originally calcitic have micritic fabrics, as well as sparry interiors formed by aggrading neomorphism. The spar replacing the micritic ooids has high Mg concentration as well as microdolomite inclusions.

2) The cements associated with the ooids inferred to have been aragonitic have high Sr concentrations, varying from 2,000 ppm to 5,000 ppm. High Sr cements were also found in an associated laminated limestone facies. The genesis and precursors of these high-Sr cements remain unclear but may possibly be aragonitic. In contrast, cements associated with the ooids inferred to have been calcitic have lower Sr concentrations of between 800 and 1,200 ppm.

### REFERENCES

ASSERETO, R., AND FOLK, R. L., 1976, Brick-like texture and radial rays in Triassic Pisolites of Lombardy, Italy: Sed. Geology, v. 16, p. 205–222.

BATHURST, R. G. C., 1975, Carbonate sediments and their diagenesis: Elsevier, Amsterdam, 658 p.

BRAITHWAITE, C. J. R., 1979, Crystal textures of recent fluvial pisolites and laminated crystalline crusts in Dyfed, South Wales: Jour. Sed. Petrology, v. 49, p. 181–194.

BRAND, U., AND VEIZER, J., 1980, Chemical diagenesis of a multicomponent carbonate system-1: Trace elements: Jour. Sed. Petrology, v. 50, p. 1219–1236.

CAROZZI, A. V., 1963, Half-moon oolites: Jour. Sed. Petrology, v. 33, p. 633–645.

CONLEY, C. D., 1977, Origin of distorted ooliths and pisoliths: Jour. Sed. Petrology, v. 47, p. 554–564.

DAVIES, G. R., 1977, Former magnesian calcite and aragonite submarine cements in Upper Paleozoic reefs of the Canadian Arctic: a summary: Geology, v. 5, p. 11–15.

DRAVIS, J., 1979, Rapid and widespread generation of recent oolitic hardground an a high energy Bahamian platform, Eleuthera Bank, Bahamas: Jour. Sed. Petrology, v. 49, p. 195–208.

FOLK, R. L., AND LAND, L. S., 1975, The Mg/Ca ratio and salinity: two controls over crystallization of dolomite: Am. Assoc. Petroleum Geologists Bull. v. 59, p. 60–69.

GIVEN, R. K., AND WILKINSON, B. H., 1985, Kinetic control of morphology, composition, and mineralogy of abiotic sedimentary carbonates: Jour. Sed. Petrology, v. 55, p. 109–119.

*well cited* ( GROTZINGER, J., AND READ, J. F., 1983, Evidence for primary aragonite precipitation, lower Proterozoic (1.9 Ga) Rocknest dolomite, Wopmay orogen, Northwest Canada: Geology, v. 11, p. 710–713.

*in text??*

HALLEY, R. B., AND HARRIS, P. M., 1979, Fresh-water cementation of a 1,000-year-old oolite: Jour. Sed. Petrology, v. 49, p. 969–988.

JAMES, N. P., AND KLAPPA, C. F., 1983, Petrogenesis of early Cambrian reef limestones, Labrador, Canada: Jour. Sed. Petrology, v. 53, p. 1051–1096.

JAMES, N. P., AND GINSBURG, R. N., 1979, The seaward margin of Belize barrier and atoll reefs: International Association of Sedimentologist Special Publication No. 3, 199 p.

JAMES, N. P., AND CHOQUETTE, P. W., 1983, Diagenesis 6. Limestones—the sea-floor diagenetic environment: Geoscience Canada, v. 10, p. 162–180.

KENDALL, A. C., AND BROUGHTON, P. L., 1978, Origin of fabrics in speleothems composed of columnar calcite crystals: Jour. Sed. Petrology, v. 48, p. 519–538.

KETTENBRINK, E. C., AND MANGER, W. L., 1971, A deformed marine pisolite from the Plattsburg Limestone (Upper Pennsylvanian) of southeastern Kansas: Jour. Sed. Petrology, v. 41, p. 435–443.

KINSMAN, D. J. J., 1969, Interpretation of $Sr^{2+}$ concentrations in carbonate minerals and rocks: Jour. Sed. Petrology, v. 39, p. 486–508.

LAND, L. S., BEHRENS, E. W., AND FRISHMAN, S. A., 1979, The ooids of Baffin Bay, Texas: Jour. Sed. Petrology, v. 49, p. 1269–1298.

LEMON, N. M., 1985, Physical modelling of sedimentation adjacent to diapirs and comparison with the Late Precambrian Oratunga breccia body in the Central Flinders Ranges, South Australia: Am. Assoc. Petroleum Geologists Bull., v. 69, p. 1327–1338.

LOHMANN, K. C., AND MEYERS, W. J., 1977, Microdolomite inclusions in cloudy prismatic calcites—a proposed criterion for former high-magnesium calcites: Jour. Sed. Petrology, v. 47, p. 1078–1088.

LONGMAN, M. W., 1980, Carbonate diagenetic textures from nearshore diagenetic environments: Am. Assoc. Petroleum Geologists Bull., v. 64, p. 461–487.

MACKENZIE, F. T., AND PIGGOT, J. D., 1981, Tectonic controls of Phanerozoic sedimentary rock cycling: Jour. Geol. Soc. London, v. 138, p. 183–196.

PINGITORE, N. E., 1978, The behavior of $Zn^{2+}$ and $Mn^{2+}$ during carbonate diagenesis: theory and applications: Jour. Sed. Petrology, v. 48, p. 799–814.

———, 1976, Vadose and Phreatic diagenesis:processes, products and their recognition in corals: Jour. Sed. Petrology, v. 46, p. 985–1006.

PREISS, W. V., 1971, The biostratigraphy and paleoecology of South Australian Precambrian stromatolites [Ph.D. thesis]: University of Adelaide, Australia.

*1982,*
*) rtices*
*of*
*pseudo-*
*sible*
*for*
*originally*
*ooids;*
*Petrology,*
*.843 –*
*847.*

RICHTER, D. K., AND FUCHTBAUER, H., 1978, Ferroan calcite replacement indicates former magnesian calcite skeletons: Sedimentology, v. 25, p. 843–861.

RICHTER, D. K., 1983, Calcareous ooids: a synopsis, *in* Peryt, T., ed., Coated Grains:Heidelberg, Springer-Verlag, p. 71–99.

RICHTER, D. K., AND BESENECKER, H., 1982, Subrecent thermal ooids with tangentially oriented high-Sr aragonite (Tekke Ilica/Turkey), *in* Peryt, T., ed., Coated Grains:Heidelberg, Springer-Verlag, p. 154–162.

RUTLAND, R. W. R., 1981, Structural framework of the Australian Precambrian, *in* Hunter, D. R., ed., Precambrian of the Southern Hemisphere: p. 1–32.

SANDBERG, P. A., 1975, New interpretation of Great Salt Lake ooids and of ancient non-skeletal carbonate mineralogy: Sedimentology, v. 25, p. 673–702.

SANDBERG, P. A., AND HUDSON, J. D., 1983, Aragonite relic preservation in Jurassic calcite-replaced bivalves:Sedimentology, v. 30, p. 879–892.

SANDBERG, P. A., 1983, An oscillating trend in Phanerozoic non-skeletal carbonate mineralogy: Nature, v. 305, p. 19–22.

———, 1985, Aragonite cements and their occurrence in ancient limestones, *in* Schneidermann, N., and Harris, P. M., eds., Carbonate Cements: Soc. Econ. Paleontologists Mineralogists, Spec. Publ. No. 36, p. 33–58.

TUCKER, M. E., 1982, Precambrian dolomites: Petrographic and isotopic evidence that they differ from Phanerozoic dolomites: Geology, v. 10, p. 7–12.

———, 1983, Sedimentation of organic-rich limestones in the Late Precambrian of Southern Norway: Precambrian Research, v. 22, p. 295–315.

———, 1984, Calcitic, aragonitic and mixed calcitic-aragonitic ooids from the mid-Proterozoic Belt Supergroup, Montana: Sedimentology, v. 5, p. 627–644.

VIDETICH, P. E., 1985, Electron microprobe study of Mg distribution in recent Mg calcites and recrystallized equivalents from the Pleistocene and Tertiary: Jour. Sed. Petrology, v. 55, p. 421–429.

WALLS, R. A., AND BURROWES, G., 1985, The role of cementation in the diagenetic history of Devonian reefs, Western Canada, *in* Schneidermann, N., and Harris, P. M., eds., Carbonate Cements: Soc. Econ. Paleontologists Mineralogists Spec. Publ. No. 36, p. 185–220.

WALTER, L. M., 1985, Relative reactivity of skeletal carbonates during diagenesis: implications for diagenesis, *in* Schneidermann, N., and Harris, P. M., eds., Carbonate Cements: Soc. Econ. Paleontologists Mineralogists Spec. Publ. No. 36, p. 3–16.

WARDLAW, N., OLDERSHAW, A., AND STOUT, M., 1978, Transformation of aragonite to calcite in a marine gasteropod: Can. Jour. Earth Sci., v. 15, p. 1861–1866.

WARME, J. E., AND SCHNEIDERMANN, N., 1983, Patch-reef cementation: Holocene of Enewetak Atoll and Jurassic of Morocco [abs.]: Am. Assoc. Petroleum Geologists Bull., v. 67, p. 566.

WEBB, A. W., COATS, R. P., FANNING, C. M., AND FLINT, R. B., 1983, Geochronological framework of the Adelaide Geosyncline: Symposium on the Adelaide Geosyncline-Sedimentary environments and tectonic settings: Geological Society of Australia, Abstracts No. 10, p. 7–9.

WILKINSON, B. H., BUCZYNSKI, C., AND OWEN, R. M., 1984, Chemical control of carbonate phases: implications from Upper Pennsylvanian calcite-aragonite ooids of southeastern Kansas: Jour. Sed. Petrology, v. 54, p. 932–947.

WILKINSON, B. H., OWEN, R. M., AND CARROLL, A. R., 1985, Submarine hydrothermal weathering, global eustasy, and carbonate polymorphism in Phanerozoic marine oolites: Jour. Sed. Petrology, v. 55, p. 171–183.

WILKINSON, B. H., SMITH, A. L., AND LOHMANN, K. C., 1985, Sparry calcite marine cements in Upper Jurassic limestones of southeastern Wyoming, *in* Schneidermann, N., and Harris, P. M., eds., Carbonate Cements: Soc. Econ. Paleontologists Mineralogists Spec. Publ. No. 36, p. 169–184.

WILKINSON, B. H., JANECKE, S. U., AND BRETT, C. E., 1982, Low-magnesian calcite marine cements in Mid-Ordovician hardgrounds from Kirkfield, Ontario: Jour. Sed. Petrology, v. 52, p. 47–57.